NASA/Goddard Space Flight Center
Greenbelt, Maryland

The Constellation X-ray Observatory

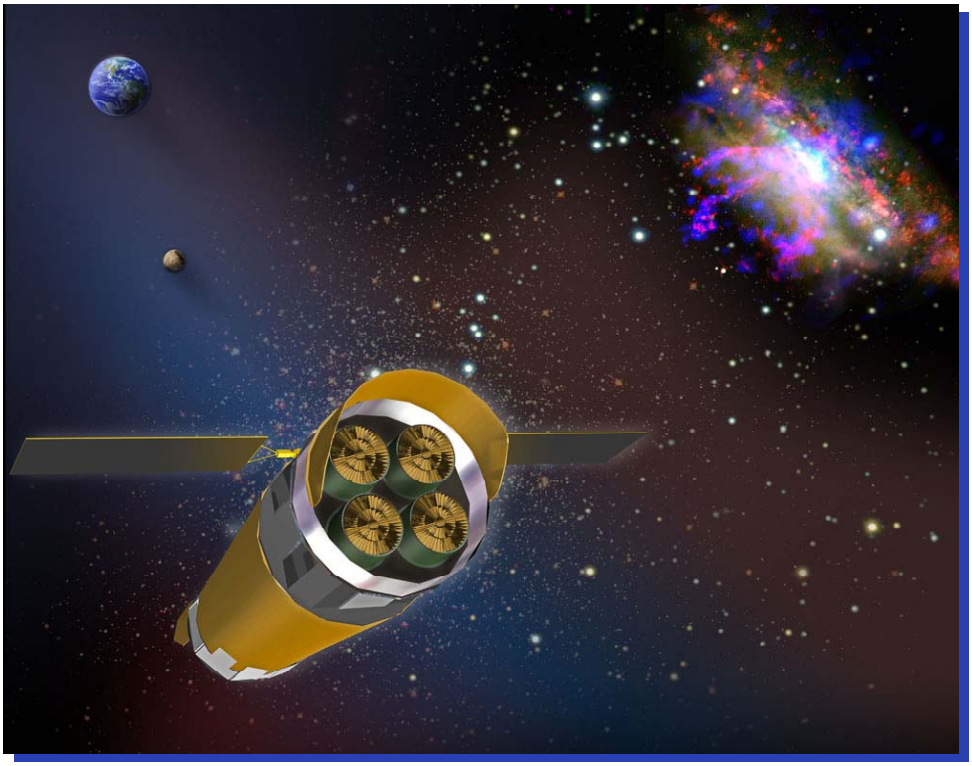

Response to the
NRC Beyond Einstein Program Assessment Committee
Request for Information

January 22, 2007

Key Project Personnel for
The Constellation X-ray Observatory

Project Scientist.....Nicholas White (GSFC)
Project Manager.....Jean Grady (GSFC)
Facility Science Team Chair.....Harvey Tananbaum (SAO)

Deputy Project Scientist.....Ann Hornschemeier (GSFC)
Deputy Project Scientist.....Robert Petre (GSFC)
Mission Scientist.....Jay Bookbinder (SAO)
SAO Science Lead.....Michael Garcia (SAO)

Instrument Scientist.....Jean Cottam (GSFC)
Instrument Scientist.....Suzanne Romaine (SAO)
Instrument Scientist.....Richard Kelley (GSFC)
Mirror Technology Scientist.....Will Zhang (GSFC)

SAO Project Manager.....Bob Rasche (SAO)
SAO Optics Lead.....Paul Reid (SAO)

Mission Systems Engineer.....Gabriel Karpati (GSFC)
Instrument Systems Engineer.....Gary Sneiderman (GSFC)
Project Systems Engineer.....Tom Buckler (GSFC)
Mirror Technology Manager.....Diep Nguyen (GSFC)

TABLE OF CONTENTS

LIST OF FIGURES

LIST OF TABLES

1. SCIENTIFIC OBJECTIVES

Question: Describe the scientific objectives and the measurements required to fulfill these objectives.

RESPONSE

X-ray astronomy requires space-based observatories since the Earth's atmosphere readily absorbs X-rays from astronomical sources. Current X-ray observatories, including the *Chandra* and *XMM-Newton* flagship missions, utilize technology largely developed during the 1980's. The science objectives discussed in this response are achievable as a result of ongoing instrumentation (optics and detectors) development that promises the next quantum leap in capability.

High resolution X-ray spectra from the *Chandra* and *XMM-Newton* grating spectrometers are reaching the level of detail previously obtained in the optical band, demonstrating the power of X-ray spectroscopy but limited by throughput to only a small number of bright X-ray sources. The 0.3 - 10 keV X-ray band contains the inner (K-shell) lines for all of the abundant metals from carbon to zinc as well as many L-shell lines. These atomic transitions provide plasma diagnostics that enable precise characterization of physical conditions in sources. A spectral resolving power of at least 300 is required to separate the density and temperature-sensitive triplet lines of helium-like ions of O, Si and S. In the spectral region between 6 and 7 keV that covers the Fe K complex a resolving power of order 2000 is required to resolve the complex Fe K structure arising in the accretion disks of black holes. Resolving powers of 300-3000 provide absolute velocity measurements ranging from 100-1000 km/s which are found in many astronomical systems.

The throughput of Constellation-X (more than 100 times the throughput of the *Chandra* and XMM high resolution grating spectrometers across the 0.6-10 keV band) along with its high spectral resolution are essential for achieving the four primary science objectives described here:

1. **Black Holes:** Using black holes to test General Relativity (GR) and measuring black hole spin
2. **Dark Energy:** Improving the constraints on the key Dark Energy (DE) parameters by a factor of ten
3. **Missing Baryons:** Unambiguous detection of the hot phase of the Warm-Hot Intergalactic Medium (WHIM) at $z>0$
4. **Neutron Star Equation of State:** Measuring the mass-radius relation of neutron stars to determine the Equation of State (EOS) of ultra-dense matter

In addition, the large increase in capabilities provided by the Constellation X-ray observatory will enable major advances covering all of astrophysics from solar system objects to distant quasars. These science topics are enabled by the mission, but do not create any additional drivers on the performance of the observatory. We list two of these, Evolution of Supermassive Black Holes and Cosmic Feedback as "Non-driving objectives" and also describe a subset of the other science topics in an "Observatory Science" section. We have confined our response to a top-level description of the science objectives that drive the mission requirements (see also Question 4). For more detail, including hundreds of spectroscopic simulations, we refer the BEPAC to our collection of Constellation-X Facility Science Team presentations: [http://constellation.gsfc.nasa.gov/mission/fst/meetings/index.html].

1.1 Constellation-X Science Objective #1 – Black Holes

Using black holes to test General Relativity (GR) and measuring black hole spin

On macroscopic scales, General Relativity (GR) remains our best theory of gravity. For weak gravitational fields, GR has passed precision tests but strong-field tests of GR are more difficult. The lack of a single parameterization/theory for alternatives to GR highlights the need to probe strong-field gravity in as many independent and unbiased ways as possible. Of the known inventory of astrophysical objects, only neutron stars and black holes are strong-gravity entities. Black holes are observationally much simpler objects, having only two parameters: mass and spin. Constraint of black hole spin is a difficult measurement that has been achieved in very few cases.

Ever since the detection of rapid X-ray variability over 20 years ago, it has been clear that X-ray observations of accreting black holes provide a window on the immediate vicinity of the black hole event horizon. The most powerful technique for inner accretion disk studies to date is the study of the broad iron fluorescence line seen in the X-ray spectrum of many accreting black holes (see Figure 1-1). This line is emitted by the surface layers of the thin, Keplerian accretion disks believed to extend nearly down to the event horizon, and possesses a highly broadened and skewed energy profile sculpted by the effects of relativistic Doppler shifts and gravitational redshifts.

A driving Constellation-X science objective is to test General Relativity through observations of material falling into black holes, close to the event horizon where the strong field will dominate the observed properties. In addition Constellation-X will utilize the observed properties of accreting black holes to constrain the growth of black holes by measuring the fundamental parameter of black hole spin.

1.1.1 Measurements for Objective #1 – Black Holes

The most powerful technique for inner accretion disk studies to date is the study of the broad iron fluorescence line seen in the X-ray spectrum of many accreting black holes. Observations by the current generation of X-ray observatories have demonstrated the X-rays are highly variable, indicating that the accretion process is composed of hot spots generated by magnetic reconnection instabilities in the disk, probably analogous to the coronal loops seen above the solar surface. It is expected that the broad iron K lines that are seen with current observatories are made up of many narrower features that are currently smeared out because of insufficient collecting area and spectral resolving power.

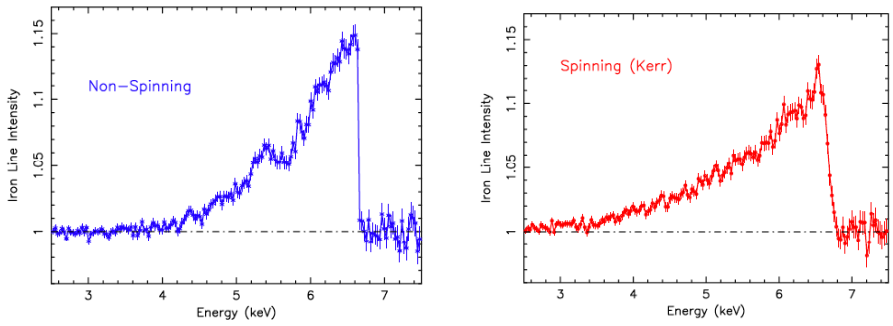

Figure 1-1. Broad Iron K line in MCG-6-30-15

On the right we show a 300 ks Con-X simulation of the broad line expected for an AGN having the parameters measured for MCG-6-30-15 (a nearly maximally spinning black hole). The simulation on the left shows how different the iron line shape appears when the black hole is not spinning.

1.1.1.1 Measurement of Matter and Photon Orbits Using FeK

Constellation-X will add a new dimension – time – to the study of iron lines. Its superior collecting area will enable detection of iron line variability on sub-orbital timescales (minutes to hours). The 6,000 cm^2 collecting area at 6 keV is required to ensure that there are at least 10 AGN targets accessible for these measurements. The fact that observations of the accretion flow can be used to probe the spacetime metric (and hence test GR) follows from the geometric and dynamic simplicity of accretion disks. In the luminous systems that are usable for this study, the accretion flow is in the form of a thin, pancake-like disk of gas orbiting the black hole. Each parcel of gas has an orbit around the black hole that closely approximates a circular test-particle orbit. Deviations from test-particle orbits are due to radial pressure gradients that are typically less than 1% in such thin accretion disks.

Any non-axisymmetry in the emission of the iron line will appear as "arcs" on the time-energy plane, each arc corresponding to an orbit of a given bright region (Figure 1-2). Note that evidence for similar features from outlying regions of the accretion disk (where the orbital timescale is longer and hence the features are easier to detect) has been seen in XMM data for NGC 3516 and Markarian 766. GR makes specific predictions for the form of these arcs, and the ensemble of arcs can be fitted for the mass and spin of the black hole, and the inclination at which the accretion disk is being viewed. The error contours derived from fitting a single track observed by Con-X to derive the radius and spin are shown in Figure 1-2. Many such tracks will be observed and if GR is correct, then each of these tracks will have a form which matches the GR predictions for a given mass, spin and radius. There are two possible scenarios of different track measurements: 1) yielding consistent spin measurements at different radii (consistent with GR) verses 2) a case where the tracks deviate (break down of GR). If the latter were the case, these measurements would provide a framework to examine alternate gravity theories, or extensions to GR.

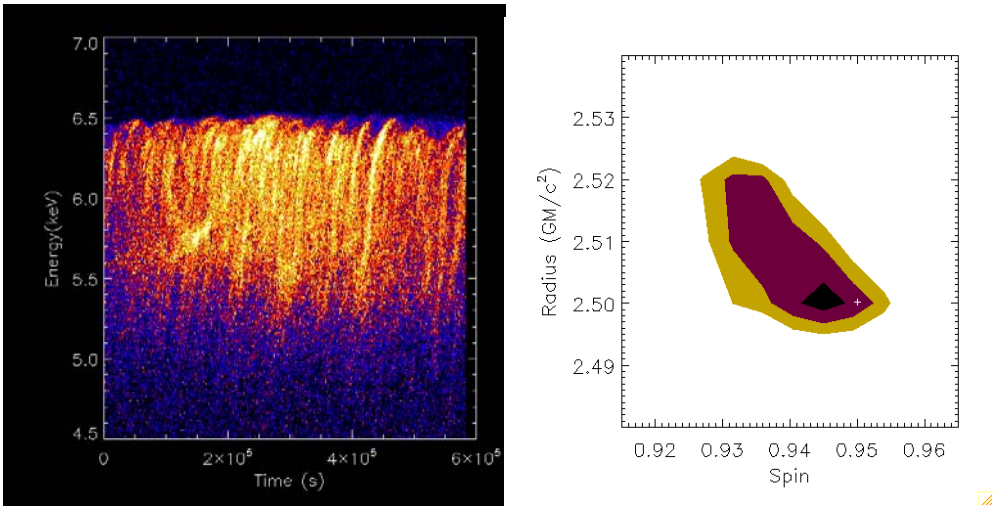

Figure 1-2. Tracking Accretion Disk Structure and Spin Measurements

Left: Con-X simulation of the iron line in the time (x-axis) - energy (y-axis) plane including simulated Poisson noise. The spot is the brightest as it approaches the observer because of relativistic beaming. We assume $M_{BH}=3\times10^7 M_\odot$, disk inclination of 30°, and a flux of 5×10^{-11} erg/s/cm^2 (2-10 keV), typical of a bright Seyfert 1 galaxy. Right: The figure shows the resulting 1, 2, and 3σ confidence contours on black hole spin and hot spot orbital radius that result from a χ^2 comparison of a library of theoretical tracks with simulated data. The small cross shows the actual values. We assumed a circular test-particle orbit at a radius of r=2.5GM/c^2, dimensionless spin parameter a=0.95, and that 10% of the total iron line flux is contained in the orbiting feature. The Kerr metric can be tested by searching for consistency in the black hole mass and spin between fits to multiple individual tracks.

A second kind of iron line variability will occur due to the reverberation (or "light echo") of X-ray flares across the accretion disk. In addition to the simple time-delay caused by the distance between the X-ray source and the accretion disk, the path and travel time of photons close to the black hole is strongly affected by space-time curvature and frame-dragging. A particularly powerful diagnostic is possible with very rapidly rotating black holes: the accretion disk capable of producing line emission extends down to almost the event horizon so we can probe time-delays close to the horizon. These photon paths are responsible for a low-energy, time-delayed "tail" in the GR reverberation transfer function. Direct calculations show that the nature of this tail is insensitive to the location of the X-ray source but is highly sensitive to the space-time metric. Characterizing this tail on the reverberation transfer function provides another powerful test of GR, this time based on photon orbits rather than matter orbits.

Observed reverberation signatures can be compared directly with predictions from GR in order to probe whether photons obey GR-like dynamics (Reynolds et al. 1999). We note that recent *XMM-Newton* and Suzaku studies of the relative variability of the broad iron line and X-ray continuum suggest that the X-ray source in some systems may be situated above the disk, close to the spin axis of the black hole. This geometry maximizes the observability of relativistic reverberation effects.

1.1.1.2 Measurement of Black Hole Spin

Con-X will measure mass and spin for a large number of accreting black holes, from stellar mass systems to the 10^9 $M_\odot$ black holes at the centers of giant elliptical galaxies. In addition, Con-X will further our understanding of how matter accretes onto a black-hole – a process providing a significant component of the radiant energy of the observable Universe (the Cosmic X-ray Background).

Black hole spin can be measured by characterizing the low energy tail of the time-averaged broad iron line. Due to the spin dependence of the innermost stable circular orbit, the iron line emitting region of an accretion disk can extend much deeper into the black hole gravitational potential well if the black hole is rapidly rotating, thereby producing a more extensive gravitationally redshifted tail to the iron line. This technique has already been successfully applied to the highest signal-to-noise *XMM-Newton* broad iron line data (Brenneman & Reynolds 2006), but Con-X is required to produce a true survey of black hole spins as more than 100,000 2-10 keV X-ray counts are required for 5-10% constraints on the spin parameter (more details in Question 4). Given the effective area of the Constellation-X mission, this means that sources with 2-10 keV fluxes greater than flux $\sim 10^{-13}$ erg cm^{-2} s^{-1} may be studied with typical exposures 100-300 ks. This target sensitivity is sufficient for studying the evolution of spin over cosmic time as the median redshift of AGN with $10^{-13} < \mathrm{flux}_{2\text{-}10} < 10^{-12}$ is z~0.6 (Barger et al. 2005). It will be critical to have very good constraints on the 10-40 keV continuum, we require that the 10-40 keV band be sufficiently sensitive to allow for deep observations (note that hard X-ray sensitivity depends on both collecting area and telescope angular resolution). There are several thousand AGN in the sky that are sufficiently X-ray bright in the 2 – 10 keV band for these studies (and more than 3600 AGN already identified in the 0.5 – 2keV band from ROSAT). With current wide-field optical spectroscopic follow-up, there should be several hundred X-ray bright spectroscopically-confirmed, higher-redshift AGN for a BH spin survey by 2017.

For supermassive black holes, this spin survey will allow determination of the distribution of black hole spins as a function of host galaxy type and, via comparison with detailed theoretical calculations (e.g., Moderski & Sikora 1996), probe whether supermassive black hole growth has been dominated by accretion or mergers. On both stellar-mass and supermassive scale, correlations between black hole spin and the presence of relativistic jets will provide a clean test of the hypothesis that a rapidly rotating

black hole is the basic power source for these jets. Finally, measurements of the spin of stellar mass BHs and 10^9 $M_\odot$ will test the scale invariance of GR (see also intermediate-mass black holes section in Observatory Science at the end of this response).

1.2 Constellation-X Science Objective #2 – Dark Energy

Improving the constraints on the key Dark Energy (DE) parameters by a factor of ten

Determining the nature of the "Dark Energy" that appears to dominate the energy budget of the Universe and is driving the acceleration of its expansion remains a major goal of both fundamental physics and astrophysics. To constrain Dark Energy we require multiple, independent means of testing its nature so that we may rule out some of the many competing theories. There are important tools available in the X-ray bandpass that provide extremely important tests of dark energy. This is thanks to the nature of the largest gravitationally bound structures in the Universe - galaxy clusters.

X-ray observations of galaxy clusters are crucial since ~85% of the baryons within them are in the hot X-ray emitting gas. Detailed measurements of the temperature and density profiles of this hot gas permit two types of tests of Dark Energy using galaxy clusters, one based upon the observationally-verified baryon mass fraction "standard candle" (a geometric measurement) and the other based on the evolution of the cluster mass function (a 'growth of structure' measurement). Conveniently, the key measurements for both tests can be made using the same set of large, relaxed clusters of galaxies. Constellation-X will observe large samples of clusters of galaxies (> 500 objects) over a wide redshift range ($0<z<2$; median redshift $z\sim1$) with high precision to constrain Dark Energy parameters.

Note that the Con-X DE cluster program is a "Class IV" project (the highest level) according to the classification of the Dark Energy Task Force (DETF). Moreover, the DETF emphasizes how both geometrical measures and those concerning growth of structure should be employed. Con-X will constrain the time evolution of dark energy with a DETF figure of merit $[\sigma(w_a) * \sigma(w_p)]^{-1} \sim 30$. These data will constrain dark energy with comparable accuracy and in a beautifully complementary manner to the best other techniques available circa 2017.

The two separate highly complementary Con-X DE experiments will each, individually, in combination with Planck data, obtain uncertainties on the time-averaged dark energy equation of state w to ±0.05. In combination with other, contemporary constraints (such as those from Planck) Con-X will provide an order of magnitude improvement in our knowledge of the key dark energy parameters.

1.2.1 Measurements for Objective #2 – Dark Energy

To provide precise and accurate measurements suitable for DE studies, Con-X must be able to measure the properties of the X-ray emitting gas on large scales in clusters where gravity dominates (approximately half the virial radius) and the physics is well understood. Neither *Chandra* nor XMM have sufficient collecting area to study sufficient numbers (~500) of distant (z~1) clusters in reasonable exposure times. Con-X must also have sufficient spatial resolution (≤ 15 arcsec) to recognize merging clusters and separate out the complex physics in the centers of clusters.

The strategy for dark energy work with Con-X will involve an initial snapshot program (1ks exposures) to observe the 3000-5000 most X-ray luminous (or highest integrated Sunyaev-Zeldovich flux) clusters known at that time. These snapshots will identify the 500 most relaxed systems, based on their X-ray morphology. These 500 clusters will then be followed up with deeper exposures of, on average, 20ks each, which will be sufficient to measure f_{gas} and predict the Sunyaev-Zeldovich (SZ) flux from the

observed X-ray temperature and gas density profiles to 5% accuracy, corresponding to 3.3% in absolute distance. Similar constraints on dark energy should also be achievable by observing the best 250 clusters for 40ks each, on average. This strategy may be useful if the fraction of relaxed, luminous clusters is found to drop significantly at the highest redshifts.

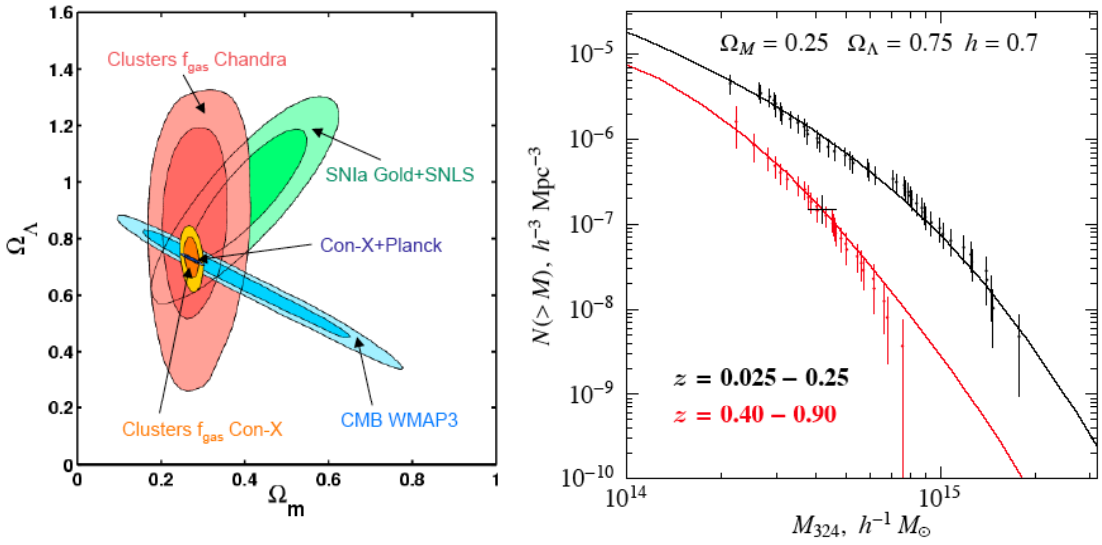

Figure 1-3. Dark Energy Constraints with Galaxy Clusters

Left: The joint 68% and 95% contours on Ω_m and Ω_Λ from the current Chandra $f_{gas}(z)$ data (red/pink). Also shown are the constraints from current SNIa data (green; "gold" sample of Riess et al. 2004 combined with 1-year Supernova Legacy Survey data of Astier et al. 2006) and current CMB studies (light blue; WMAP 3-year; Spergel et al. 2007). The inner contours show the predicted constraints from the Con-X f_{gas} experiment (orange) and f_{gas}+Planck data (dark blue). Right: Current measurements of the evolving cluster mass function based on the Chandra observations of high- and low-z clusters discovered in ROSAT surveys (Vikhlinin et al. 2007). The models are for the "concordance" ΛCDM cosmological model. These data (48 low-z and 40 high-z clusters) provide constraints on the dark energy equation of state parameter, $\Delta w \approx \pm 0.12$, when combined with WMAP.

1.2.1.1 Measurement of Baryon Mass Fractions in Clusters – Geometric Measure

Con-X will directly measure the expansion history of the Universe using absolute distance measurements to galaxy clusters, determined both from measurements of the X-ray gas mass fraction (f_{gas}) in the largest relaxed clusters and using the combination of those measurements with follow-up observations of the SZ effect (for more detail on the SZ work, please see FST presentations at [http://constellation.gsfc.nasa.gov/mission/fst/meetings/index.html].

The matter content of the largest clusters of galaxies is expected to provide a fair sample of the matter content of the Universe. The ratio of baryonic-to-total mass in clusters should therefore closely match the ratio of the cosmological parameters Ω_b/Ω_m (e.g. White et al. 1993). The baryonic mass in clusters is dominated by X-ray emitting gas, the mass of which exceeds the mass in stars by a factor 6, with other sources of baryonic matter being negligible (Fukugita, Hogan & Peebles 1998; Lin & Mohr 2004). The combination of robust measurements of f_{gas} (the ratio of X-ray gas mass to total mass) with determinations of Ω_b and the Hubble constant from cosmic microwave background (CMB) data (or e.g. the abundances of light elements at high redshifts and the local distance ladder) can therefore be used to measure Ω_m. This method provided the first compelling evidence that we live in a low matter density

Universe (White et al. 1993) and currently gives one of our tightest and most robust constraints on Ω_m (e.g. Allen et al. 2004, 2007; LaRoque et al. 2006).

Measurements of the X-ray gas mass fraction, f_{gas} in clusters as a function of redshift can also be used to probe the acceleration of the Universe. This constraint originates from the dependence of f_{gas} measurements (derived from the observed X-ray gas temperature and density profiles, assuming hydrostatic equilibrium) on the assumed distance to the clusters: $f_{gas} \propto d^{1.5}$ (e.g. Sasaki 1996; Pen 1997; Allen et al. 2004). The latest results from this experiment (Allen et al. 2007; see also Ettori et al. 2003, Allen et al. 2004, LaRoque et al. 2006) are based on *Chandra* data for 42 hot (kT > 5 keV), X-ray luminous ($L_X > 10^{45}$ erg s^{-1}), dynamically relaxed systems spanning the redshift range $0 < z < 1$. The restriction to relaxed clusters leads to minimal systematic scatter in the results. In order to determine cosmological constraints, the f_{gas} measurements are fitted with a model that accounts for the expected apparent variation of the observed $f_{gas}(z)$ values as the true, underlying cosmology is varied. The resulting constraints on DE parameters are given in Figure 1-3; the current *Chandra* data give marginalized constraints of $\Omega_m = 0.28 \pm 0.05$ and $\Omega_\Lambda = 0.86 \pm 0.22$ (68% confidence limits). Note that the intrinsic scatter is undetected in current *Chandra* data for 42 clusters, for which the weighted-mean statistical f_{gas} error is only 5% (Allen et al 2007).

1.2.1.2 Constraints on the Growth of Structure, G(z), Using Clusters

Clusters of galaxies are sensitive probes of cosmic structure growth. The perturbation growth factor, G(z), is the second [together with d(z)], crucial dark energy observable. Dark energy constraints from G(z) are highly complementary to those from distance measurements (Linder & Jenkins 2003). Indeed, the combination of these two approaches is uniquely useful to test whether cosmic acceleration is due to the presence of Dark Energy or a modification of the gravitational field equations (Linder 2005).

Future large X-ray and SZ surveys will provide catalogs of ~100,000 clusters spanning the redshift range $0<z<2$. Using "self calibration" methods, where one solves for the cosmology using only the shape of the mass function, clustering information, and priors on key scaling relations (e.g., cluster mass scaling relationships: Majumdar & Mohr 2004; Lima & Hu 2004) such data will constrain dark energy with an accuracy in w of ± 0.08, providing a DETF figure of merit of 5-10. (e.g., Albrecht et al. 2006). The weakness of the self-calibration approach is that it relies on extremely detailed knowledge of all other survey characteristics (e.g., the selection function must be accurate at the sub-percent level).

However, the same or better statistical accuracy on w can be achieved by direct, accurate mass estimates for only the ~1000 highest-mass clusters detected in a survey (Majumdar & Mohr 2003), leading to constraints on w from these objects alone of ±0.06-0.08. X-ray data provide very high-quality M_{tot} proxies, such as the product of ICM mass (derived from X-ray imaging) and average temperature (derived from X-ray spectroscopy) (Kravtsov et al. 2006). The M_{tot} vs. proxy relation can be calibrated using relaxed clusters (the same objects used for the f_{gas} work) for which mass uncertainties at the few percent level from X-ray analyses are already achieved. To achieve the desired percent-level accuracy in M_{tot} determinations across the full redshift range of future surveys will require that second-order effects in the ICM (e.g., turbulence, bulk motions) be under control, utilizing the high spectral resolving power of Con-X. Combining these constraints with the larger, self-calibrated survey data, accuracies in w of ±0.04 or better should be achievable from the growth of structure test (Haiman et al. 2006; Albrecht et al. 2006). The instrument requirements for the G(z) and f_{gas} work are the same.

1.3 Constellation-X Science Objective #3 – Missing Bayons

Unambiguous detection of the hot phase of the Warm-Hot Intergalactic Medium (WHIM) at z>0

For decades, it was thought that the dilute gas prevalent in the early universe eventually formed into the galaxies that we see today. However, when a census was taken of the amount of the normal matter in the galaxies around us, only 10% of the baryons known to exist were found. This began an extensive search for the missing baryons, and studies found that the hot gas in galaxy groups and clusters, combined with the cold gas that produces UV absorption lines could account for up to 40% of the known baryon content. The remaining >60% of the normal matter was still undiscovered. Cosmological simulations are in broad agreement that the majority of the baryons exist in the temperature range $10^5 - 10^{7.5}$ K, with most of the material lying in the lower overdensity filaments that connect clusters and groups.

The high temperature of the Warm-Hot phase of the Intergalactic Medium (WHIM) may only be probed with X-ray spectroscopy due to the ionization states involved. High spectral resolution studies with *Chandra* and XMM have shown the first evidence of detection of the WHIM within the Local Group (see Figure 1-4 for an *XMM-Newton* spectrum) and a suggestion of higher-redshift filaments. Accounting for the remainder of the WHIM remains a major goal of observational astrophysics.

Constellation-X will measure these filaments in absorption along the line-of-sight to background AGN, constraining the hot baryon content of the Universe. With >100 filaments detected at z>0, this will provide the first unambiguous detection of the WHIM.

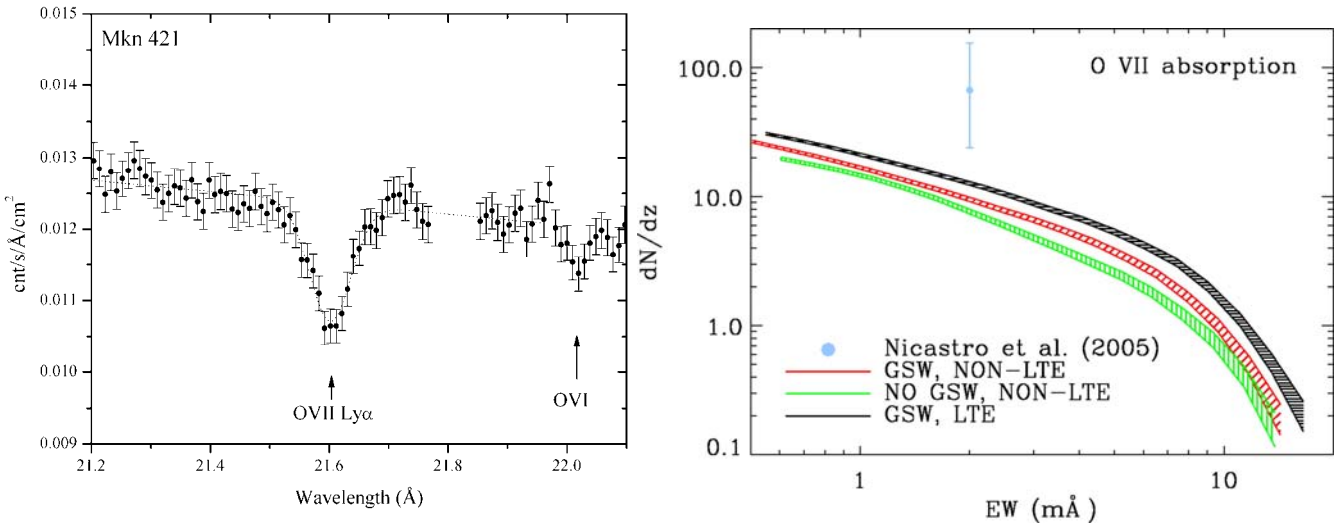

Figure 1-4. Local Group WHIM Detection and Predicted number of WHIM Filaments

Left: The X-ray spectrum of Mkn 421 obtained with the RGS on XMM-Newton, with exposure time 509 ks, such an observation will be obtained with Con-X in <50 ks. The vicinity around the OVII Ly alpha line shows a high-quality detection of this line near zero redshift, so the absorbing material is either in the Galactic halo or the Local Group medium (Bregman and Lloyd-Davies 2007). Right: Predicted number of WHIM filaments as a function of equivalent width from Cen et al. (2006). Abbreviations in the legend include "Local Thermodynamic Equilibrium (LTE), and Galactic Superwinds (GSW)."

1.3.1 Measurements for Objective #3 – Missing Baryons

We feature one major measurement technique (absorption studies with background AGN) for this topic.

1.3.1.1 Measuring Absorption Features on Background Continuum Sources in the WHIM

The most powerful tool for the measurement of the WHIM is through the absorption lines produced upon background continuum sources, such as AGN (see Figure 1-4). Absorption lines created by the WHIM are in the low opacity limit so the equivalent width of the lines translates directly into a column density equal to the average ion density multiplied by the depth of the filament, providing a prime measure for the mass content of the hot gas. Measurement of the redshift of each filament places them in the Cosmic Web connecting all groups and clusters, and determination of the turbulent width of the line measures the gravitational shocks, and galactic superwinds that heat the WHIM.

To *find* the WHIM, we need reasonably bright background AGN (note that there are 50 AGN with $f_X > 10^{-11}$ ergs cm^{-2} s^{-1} in the ROSAT All-Sky Survey and easily hundreds more just slightly fainter than this) and moderately dense filaments. Constellation-X must be able to detect the strongest absorption lines, which are the ground-state resonance lines of hydrogenic and helium-like oxygen, with the possibility of deeper observations that can detect other transitions such as Ne IX and Ne X. The OVII ion is sensitive to gas at $0.5 - 3 \times 10^6$ K and is measured through the 1s-2p transition at 21.60Å (574 eV), while the OVIII ion is common in the $1 - 7 \times 10^6$ K range through its Lyα line at 18.97 Å (654 eV). The ratio of these two lines is a temperature indicator. The other lines will permit more detailed characterization of the ionization state of the gas and will extend the temperature sensitivity to 10^7 K. If high spectral resolving powers are available, the lines will be resolved and effects of turbulent heating or ongoing collapse in the WHIM might be detected.

For good constraints of the WHIM, Constellation-X must detect these absorption features for ~100 filaments (with multiple detections/filaments per observed AGN certainly possible) and should detect these filaments over the redshift interval $0 < z < 0.5$ (with z=1 as a goal). Given that many bright AGN are at modest redshift (z<0.3), the redshift path length for a typical observation will be $\Delta z = 0.3$. If we set a target of observing filaments in the 30 nearest bright AGN, this requires three filaments per target ($dN/dz \sim 10$ for a path length $\Delta z = 0.3$). Figure 1-4 shows the number of anticipated filaments per unit redshift interval as a function of line equivalent width, and this should be a very good prediction because it is normalized by the UV OVI equivalent width distribution (OVI absorbing gas detects about 7% of the baryons). This establishes a target sensitivity of 1 mÅ, which may be achieved for several different combinations of collecting area and spectral resolving power.

1.4 Constellation-X Science Objective #4 – Neutron Star Equation of State

Measuring the mass-radius relation of neutron stars to determine the Equation of State (EOS) of ultra-dense matter

Neutron stars contain the highest density matter known in the Universe and their structure depends on the physics of the interactions between fundamental particles: protons, neutrons and their constituent quarks. The theory of such interactions, Quantum Chromodynamics (QCD), is not yet sufficiently constrained to accurately predict the state of matter at such extremes. The *only* way to constrain the low temperature - high-density regime of QCD is with precise measurements of *both* the masses and radii of neutron stars. Accurate masses for some neutron stars have been obtained from observations of young neutron star pulsars in binary systems, but essentially nothing is known about the radii.

Accreting neutron stars in binary systems provide several unique opportunities to probe the structure of neutron stars: 1) A continuous supply of fresh metals allows higher atmospheric abundances of the line producing elements (such as Fe) to be present than in isolated (non-accreting) neutron stars, increasing the likelihood for the formation of a detectable absorption line spectrum. 2) Accretion also leads to thermonuclear X-ray bursts; brief but bright flashes of thermal X-ray radiation shining through the neutron star atmosphere, during which the spin rate of the neutron star can be observed directly (so called 'burst oscillations"). These old neutron stars have also gained enough mass to probe the mass-radius relation in a different regime than the young pulsars. This leads to the possibility of obtaining mass-versus-radius curves for neutron stars, telling us a great deal about the state of matter at extreme densities (see Figure 1-5; Lattimer & Prakash 2001).

The science requirement for Constellation-X is to determine the radii and mass of several neutron stars to within several percent, providing strong constraints on the Neutron Star Equation of State.

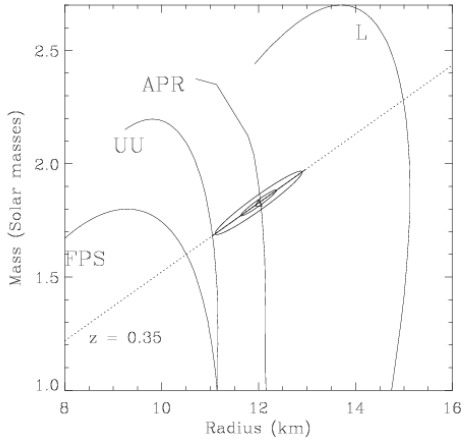

Figure 1-5. Neutron Star Mass-radius Constraints with Constellation-X

The labeled curves show mass – radius (M – R) relations from several different EOS as well as the limits on M and R obtainable with Con-X (based on 4U 1636-53, 582 Hz spin frequency; see also Strohmayer 2004). The elliptical confidence regions are derived from fitting the pulse profiles of burst oscillations. The model for the pulsations is an expanding hot spot on the rotating neutron star surface. The contours denote the statistical quality achievable with one burst (the big ellipse), and six bursts (the small ellipse). The dashed diagonal line (labeled z = 0.35) denotes the constraint from centroiding absorption lines (for EXO 0478-676; see Figure 1-6), and the solid portion of the line gives an estimate of the accuracy in R from measuring the line widths.

1.4.1 Measurements for Science Objective #4 – Neutron Star EOS

Constellation-X will be the first X-ray observatory with the capability of making simultaneous high spectral resolution and fast timing measurements of X-ray bursts. One may then simultaneously use several independent methods to constrain mass and radius, providing important checks on any systematic errors associated with either method.

1.4.1.1 Measuring Absorption Lines in Thermonuclear X-ray Bursts

In order to escape a neutron star's powerful gravitational field, photons will be redshifted and if this can be measured, it will provide a direct measure of the stellar mass to radius ratio, GM/c^2R, also called the compactness. Cottam, Paerels & Mendez (2002) found evidence of narrow, redshifted Fe absorption lines in co-added spectra of 28 X-ray bursts from the LMXB EXO 0748-676 with the *XMM-Newton*

RGS. Their proposed identifications for these lines with the Hα transitions of Fe XXVI and XXV implies a surface redshift of $z = 0.35$ that is consistent with most modern EOS. The line widths are influenced by rotation of the star via the Doppler effect. Since the spin rates of many of these accreting neutron stars are known, the strength of this Doppler effect is directly proportional to the radius of the neutron star through the surface velocity. Accurate measurement of the line profiles can therefore determine the stellar radius. The relatively narrow lines inferred from EXO 0748-676 are consistent with the 45 Hz spin rate found from burst oscillations in this object (Villarreal & Strohmayer 2004), but present data do not have the statistical precision to tightly constrain the radius (Chang et al. 2006). Constellation-X will measure the radius to within a few percent by measuring the widths of absorption lines with much greater precision for this burst source and many others.

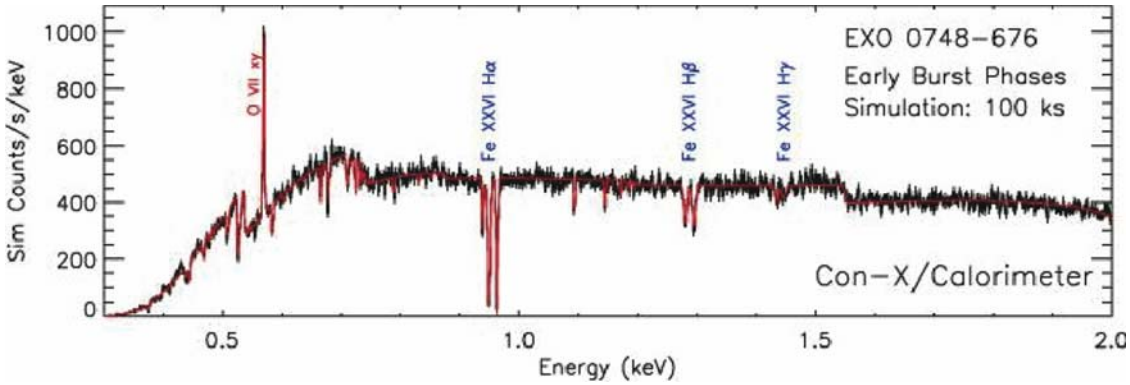

Figure 1-6. Simulated Con-X Spectrum of Neutron Star Thermonuclear X-ray Bursts

The simulated spectrum of the early phases of the X-ray bursts from the accreting neutron star EXO 0748-676 using the Constellation-X (100 ks observation yields 1 ks of burst time). The blue labeled lines are gravitationally redshifted absorption lines from the neutron star atmosphere. The remaining spectral structure originates in the circumstellar material. The model was developed using the XMM-Newton data and theoretical calculations for the absorption line structure.

Moreover, the much larger collecting area of Constellation-X (as compared to the *XMM-Newton* RGS) will enable far more sensitive searches for higher order transitions (for example, the Hβ lines of Fe XXVI ions). If several lines in the series are detected, their relative strengths can be used to provide a measure of the surface density. This quantity is proportional to GM/c^2R^2, which combined with the redshift measurement (GM/c^2R) also leads to a unique determination of both M and R.

Figure 1-6 shows an example of the kind of absorption spectrum that is theoretically achievable with Constellation-X observations of EXO 0748-676. If absorption lines are present at the strength suggested by Cottam et al. (2002), then in about 100 ks of observations it should be possible to detect the Fe XXVI Hα and Hβ absorption lines as well as measure the line widths to better than 10%. Good spectral resolving power near 6.9 keV also may enable study of the Lyα transition, which although lower in equivalent width than the Hα and Hβ lines, provides an important additional constraint on the NS radius.

1.4.1.2 Using Burst Oscillations to Probe Neutron Star Structure

Constellation-X will also be able to probe neutron star structure using the spin modulation of a non-uniform brightness pattern generated on the neutron star surface by thermonuclear burning. Both the amplitude and shape of these pulsations encodes mass and radius information. For example, the modulation amplitude is influenced by gravitational light deflection in the strong gravitational field of the neutron star, which depends directly on the compactness. Fitting of the observed pulses to a physical model of surface emission from a rotating neutron star can provide constraints on the stellar mass and radius (Nath, Strohmayer & Swank 2001; Muno, Ozel & Chakrabarty 2002; Bhattacharyya et al. 2005).

The shapes of surface absorption (or emission) lines from neutron stars may also carry information about fundamental aspects of Einstein's theory of General Relativity. A prediction of Einstein's theory is that a rotating star will drag the local space-time frame of reference with it, a phenomenon known as frame dragging, which affects the motion of objects and photons near the star. It is known from observations of burst oscillations that some of these accreting neutron stars produce an X-ray hot spot during some X-ray bursts. An absorption line observed from such a rotating hot spot will have a double-horned profile (not unlike the relativistic Fe fluorescence line seen from black hole accretion disks). The red-shifted portion is produced as the hot spot recedes, and the blue-shifted component when the spot is approaching. Frame dragging alters the relative strengths of the red- and blue-shifted horns (Bhattacharyya et al. 2006). By observing such line features Constellation-X may be able to measure the amount of frame dragging, and thus test Einstein's theory.

1.5 Non-driving Science Objectives

There are many important astrophysical studies that Constellation-X will carry out as a Guest Observer facility, but it is not feasible to have all of these science topics carried as driving objectives for the mission. The mission performance parameters (listed in Question 4) are driven by the four science objectives. However, there are two very important science topics that we highlight here.

1.5.1 Constraining the Evolution of Supermassive Black Holes

Our understanding of the growth and evolution of massive black holes has undergone a revolution over the last few years as thanks to the *Chandra* Observatory we have finally resolved the Cosmic X-ray Background between 0.3 to 10 keV into individual sources. These X-ray sources are accreting supermassive black holes (AGN) that together are the integrated fossil signature of massive black hole accretion over the history of the universe. The majority of this AGN population is heavily obscured and while our understanding of the X-ray emission from high-redshift AGNs has advanced rapidly since the launches of *Chandra* and *XMM-Newton* (see Brandt et al. 2005 for a review), our current *Chandra* and *XMM-Newton* detections of high-redshift AGNs are just that – detections. Current photon statistics are simply insufficient for detailed investigations of high-redshift AGN continuum and emission-line properties/components. There are a number of important reasons why a better understanding of accreting supermassive black holes is needed, as it now seems likely that the development of supermassive black holes and galaxies are intimately connected (see the next section on Cosmic Feedback). Deep X-ray surveys have indicated that the growth of massive black holes undergoes a curious evolutionary trend whereby the most massive objects are grown first, a process often referred to as cosmic downsizing (e.g., Cowie et al. 2003; Marconi et al. 2004).

Constellation-X will provide direct astrophysical insight into the evolution of the environment around accreting massive black holes by exploring changes in the X- ray spectral shape and components of

luminous AGN out to and beyond z ~ 6. The high-quality data that will be produced by Con-X will reveal a wealth of spectral diagnostic detail, permitting constraints on the continuum shape, absorption, recombination emission, fluorescent iron K line emission, Compton reflection, physical conditions/geometry of emitting plasmas, and the variability of accreting black holes. The energetics and demographics of z>1 obscured/Compton-thick AGNs will be quantified and spectroscopic redshifts of optically invisible obscured AGN will be directly possible from the detection of the iron K emission line. The large-scale AGN outflows (in absorption and emission) that likely regulate star formation in massive galaxies can be studied in the crucial z~1-3 era where black-hole growth and star-formation activity was at its peak, providing estimates of mass and energy outflow rates and chemical enrichment/heating of the IGM.

This science requires that Con-X be able to efficiently characterize sources as faint as $\sim 10^{-15}$ erg cm^{-2} s^{-1} (0.5 - 2 keV), the level at which 80% of the Cosmic X-ray Background is resolved. The median redshift of these sources is z~0.8 (Barger et al. 2005) so soft energy bandpass is also important. With Constellation-X we anticipate gathering ~1000 (0.5-2 keV) counts in 100 ks for a 2×10^{-15} erg cm^{-2} s^{-1} (0.5-2 keV) source. A large enough field of view to observe multiple CXRB sources at once would enable multiple sources to be observed in a single observation. Coincidently, the angular resolution, low background and FOV requirements for Dark Energy measurements with clusters are as stringent as the requirements for CXRB science. Hence, we keep this as a major topic enabled by Con-X but allow DE science to be the driver. Note that the 10-40 keV sensitivity required for the BH spin measurements also enables some hard CXRB studies.

1.5.2 Cosmic Feedback – Measuring the Effects of AGN on the Formation of the Universe

Numerical simulations of the formation of large scale structure and galaxy formation over-produce the most massive galaxies in the Universe. A source of energy that arrests star formation is needed. At present the best explanation for these effects is the 'feedback' between the central black hole and its host galaxy such that they co-evolve (Hopkins et al. 2006). Starburst winds are believed to create similar effects on lower mass galaxies. Many theoretical simulations now use AGN feedback as a knob that is turned to produce the correct number of massive galaxies, but the physics of the mechanism is poorly constrained. Various possibilities include mechanical winds from the central AGN, radiation (Ostriker and Ciotti 2006) and relativistic particles (jets). These same processes may also solve the riddle of cooling flows in galaxies, clusters and groups, and determine why cluster scaling relations differ from those predicted by dark matter only models.

In order to measure what is actually occurring one needs to directly measure the energy injection and this requires X-ray observations that only Constellation-X can provide. With spatially-resolved high spectral resolving power detectors, Con-X will determine the effects of the AGN on surrounding gas (e.g. groups and clusters), as a function of redshift determine the energy input from star formation (e.g. superwinds), and observe the IGM and determine its metallicity as a function of redshift (see Objective #2). Only Con-X of all the missions being presently considered can obtain the needed measurements and provide us with a proper understanding of how structure in the universe forms and evolves.

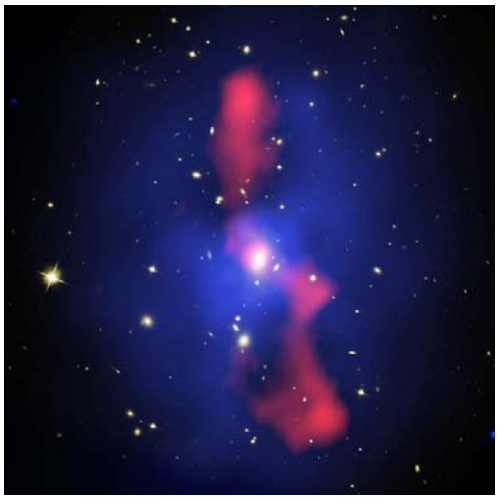

Figure 1-7. Cosmic Feedback in Action: Galaxy Cluster MS0735.6+7421

A composite image (white = optical HST data, blue = Chandra X-ray data, red = radio VLA data) shows the galaxy cluster MS0735.6+7421 (z=0.2). There are enormous cavities in the X-ray gas, each roughly 200 kpc in diameter. The red cavities indicate radio emission (VLA). It is believed this structure is created by jets, but currently the lack of spatially-resolved high spectral resolution detectors prevents detailed charaterization of the kinematics of the hot X-ray gas.

1.6 Observatory Science

Constellation-X is a Guest Observer facility that will serve the whole astronomical community just as the *Chandra* X-ray Observatory before it. Although the four science objectives we have listed are of critical importance and define the basic measurement requirements, the following is a summary of some of the important science that this capability will enable.

1.6.1 Dark Matter

X-ray observations of the hot plasma trapped in the gravitational field of the Dark Matter in clusters of galaxies remain one of the most powerful techniques to map the location of the Dark Matter and constrain its interaction with normal matter. Constellation-X will for the first time bring the spectral resolution and collecting area required to map the velocity field of the plasma on scales of a hundred of km/s, the relevant velocity scale for these systems. By deriving precise mass profiles and directly comparing the baryonic component of clusters Constellation-X will provide a direct measurement of the amount and distribution of dark matter to a unprecedented level or precision and allow accurate comparisons with weak and strong lensing measurements and determinations of the gas content via the Sunyaev-Zeldovich effect. There are no comparable X-ray facilities planned with similar capabilities.

Warm Dark Matter has become a viable “alternate” to the standard cosmological structure formation scenario, as it may resolve many problems in structure formation. Sterile neutrino dark matter, in the standard production scenarios, is detectable or potentially excludable with Constellation-X and by no other means. These particles are expected to decay, but with rather long time scales into two photons. The present best limits on these particles, if they are to represent the bulk of the dark matter, is between 1-20 keV. Constellation-X will be able to improve on the present limits by a factor of over 30, definitely either detecting or ruling out sterile neutrinos as the dark matter.

An additional interesting measurement that will come from these Cluster measurements will be constraints on the mass of the neutrino. The neutrino mass density originates primarily from the fact that the cluster of galaxies X-ray Luminosity Function provides a robust constraint on sigma-8 for a given value of Omega matter, while the CMB data predict sigma-8 as a function of the neutrino mass. So combining the two provides constraints on the neutrino mass (Allen 2003 astro-ph/0306386). Constellation-X data combined with Planck can be expected to place more accurate constraints on the neutrino mass.

1.6.2 Constraints on Binary Black Holes: Precursors to BH mergers

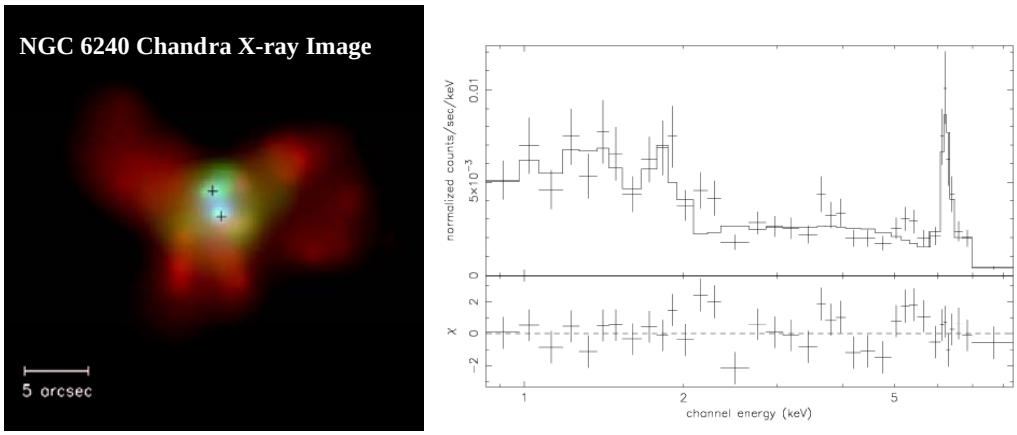

Figure 1-8. Nucleus of NGC 6240

Left: Chandra X-ray image of two SMBH in the nucleus of the galaxy NGC 6240 (Komossa et al. 2003). Right: Chandra X-ray spectrum of the southern nucleus in NGC 6240 (the northern nucleus is very similar)

The formation of SMBH binaries following galaxy merging has been suggested as a natural consequence of galaxy formation for quite some time (Begelman, Blandford & Rees 1980). Among the possible observational indications that coalescence of binary SMBHs has occurred are the peculiar properties of some jets/lobes in radio galaxies (Merritt & Ekers 2002; Liu, Wu & Cao 2003). In a recent review of supermassive black hole (SMBH) studies, Ferrarese & Ford (2005) presented crucial areas of future research. Among these was the determination of the prevalence of SMBH binary systems. X-ray observations of SMBH binaries have already shown great success with in the nearby galaxy NGC 6240 two SMBHs about 1 kpc apart are detected (Komossa et al. 2003; see Figure 1-8).

Constellation-X will search for the dual Fe-K lines which may betray the presence of the binary SMBH (see Figure 1-8). The detection of such features will effectively mimic the resolving power of *Chandra* with high-resolution X-ray spectroscopy by spectrally resolving the narrow part of the iron line into two components in "closer" SMBH binaries. Interestingly, candidate binary black holes are currently being identified with optical spectroscopy in e.g., the DEEP2 survey (Gerke et al. 2007). By 2017, with ground-based observatories such as LSST operating, and a multitude of wider-field optical spectroscopic and X-ray surveys (e.g., XBOOTES; Murray et al. 2006), there should be more candidates for Con-X to follow-up.

For the case of NGC 6240, for instance, the velocity difference between the two cores is approx 20 km/s as the nuclei are separated by ~1 kpc and still very early in the merger process. However, for black

holes farther along in their evolution towards merger (300 km/s will be easily detected), Con-X could well detect the two peaks in the (narrow) iron line.

1.6.3 Intermediate Mass Black Holes

There is a class of luminous, variable, point-like X-ray sources found in many nearby galaxies that may have inferred isotropic luminosities hundreds of times larger than the expected maximum luminosity of a stellar mass black hole. This has led to speculation that some of these ultra-luminous X-ray sources (ULX) may form a new class of black holes with masses in the range from about 100–2000 solar masses, so called intermediate-mass black holes (IMBH). Currently there are 20-30 of these sources known which can be resolved from nearby emission with a 15 arcsec angular resolution.

Constellation-X will spectroscopically confirm the presence of cool accretion disks in IMBH candidates. Currently there are ~6 ULX sources with significant detections of a soft thermal spectral component consistent with an accretion disk with an average inner edge temperature of ~0.15 keV (Miller, Fabian and Miller 2004 astro-ph/0406656). Perhaps more importantly, Con-X will detect relativistic iron K-shell emission lines if they are present. Detection of these lines would confirm the disk origin of the soft X-ray emission, and would strongly rule out beaming arguments for the high inferred luminosities. If Constellation-X confirms the existence of IMBHs, then X-ray probes of General Relativity will be possible across an enormous range of black hole masses.

X-ray timing measurements can identify the characteristic timescales on which the objects are variable. By comparing studies of supermassive black holes with those of stellar mass black holes in our Galaxy, it has been shown that the characteristic variability times scale with black hole mass.

1.6.4 Supernova Remnants

The capabilities of Constellation-X will open a new window into the physics of supernova (SN) explosions through a dramatic improvement in the quality of the observations of young, ejecta-dominated supernova remnants (SNRs). The high angular and spectral resolution of Constellation-X will enable determination of the composition, ionization state and velocity of the material throughout the SNR to build a complete model for the structure of the shocked ejecta and the ambient medium.

Constellation-X observations of core-collapse SNRs, will unveil new information about the core-collapse process by revealing the distribution and dynamics of nucleosynthesis products formed during the explosion, tracking the early evolution of SNRs, unveiling unshocked iron, and measuring the total mass of iron in SN ejecta. A prime target for studies of core-collapse supernovae is the well-studied Cassiopeia A (Cas A), because it is the brightest X-ray remnant with emission dominated by silicon and iron ejecta. The X-ray emission from Cas A is spatially complex, showing structure on scales from the remnant's full ~ 3 arcmin extent to knots and filaments $\leq$ 2 arcsec in size. Constellation-X will enable deeper investigations into the nature of the knots and other complex ejecta structures as its resolution approaches the goal of 5 arcsec.

Constellation-X will also provide the first sensitive measurements of the odd-z trace elements as well as the trans-iron element zinc in supernova remnants. These elements provide insight into the star that originated the explosion, as well as the origin of these elements. The most abundant species from Ne to S all contain an integral number of alpha particles in their nuclei and are believed to come from carbon and oxygen burning in stellar interiors. The less abundant species (Na, Al, P) come from H-burning beyond the CNO cycle (NeNa, MgAl cycles). The Cr, Mn, and Ni species, in particular, are very

important for discriminating among Type Ia SN models. The detection of Zn in a cosmic X-ray source would be a first step towards determining the origin of these elements in a cosmic setting. Again there is no comparable facility that will accomplish these measurements.

1.6.5 Stellar Coronae

Time series analyses of EUV and X-ray observations of active stars have provided evidence that plasma at temperatures $\geq 4 \times 10^6$ K arises purely from flares, analogous to the idea of "nanoflare" theories of solar coronal heating. Constellation-X will provide a sensitive test of flare heating through both Doppler shifts and photon arrival times. A Constellation-X XMS effective area of 6,000 cm^2 at 6 keV and resolving power of $E/\Delta E > 1{,}000$ brings within reach Doppler diagnostics in H-like and He-like S (λ4.73, 5.04), Ar (λ 3.95, 3.73) and Fe (λ1.85).

Another major Constellation-X breakthrough in the study of stellar flares will be the enormous improvement in photometric precision of flare light curves and spectra, allowing direct measurement of coronal loop resonant frequencies themselves. Loop "wobble" velocities on the Sun have reached up to 200 km s^{-1}. Constellation-X detections of loop oscillations, both spectroscopically and photometrically, could provide unique measurements of these quantities in a wide range of stars, from accreting T Tauri stars to evolved giants. Resolving powers of 1000 are needed to make firm detections of line-of-sight velocity components of 100 km s^{-1}.

Detection of hard X-rays in stellar flares would define a major breakthrough for stellar physics. This emission is unequivocally related to impulsively accelerated electrons and ions that do not suffer from magnetic trapping (as radio-emitting electrons do). In the case of the Sun, hard X-rays and gamma rays have been the prime source for the study of energy release physics, particle acceleration in magnetic fields, and coronal heating. The different, and probably more extreme, magnetic configurations in magnetically active stars could lead to quite different acceleration histories and heating efficiencies in large flare events. Detection of hard X-ray components would thus open an entirely new avenue in the study of the energetics of hot, magnetized coronal plasma. For the Constellation-X HXT area of 150 cm^2, bright flares on nearby stars can be detected in only 100 sec.

1.6.6 Solar System – Jovian Planets

X-ray studies of Jupiter's auroral zones near the north and south poles, where the X-ray emission is most intense, offer a probe of Jupiter's magnetosphere (see the review by Bhardwaj and Gladstone 2000). *Chandra* and *XMM-Newton* data show that this auroral emission is due to the precipitation of highly ionized oxygen and either sulfur (favored by *Chandra*) or carbon (favored by *XMM-Newton*) into the polar regions (Horanyi et al. 1988; Cravens et al. 1995, 2003); the ionization states and the line characteristics provide information on the electric fields, thus probing the polar magnetosphere dynamics. Oscillations in the northern auroral flux observed in December 2000 (Gladstone et al. 2002) are likely associated with the energetic particle flux in the outer disk magnetosphere and with quasiperiodic radio bursts from Jupiter (McKibben, Simpson & Zhang 1993; MacDowall et al. 1993; Karanikola et al. 2004). More detailed observations of these oscillations and the conditions under which they appear would further constrain the dynamics of Jupiter's polar magnetosphere.

Chandra observations of Saturn found variations in the averaged X-ray flux of a factor of ~4 over one week (Bhardwaj et al. 2005b) that appeared closely tied to the incident solar X-ray flux. In addition, on timescales of ~0.5 hour, an X-ray "flare" from Saturn was closely linked to the eruption of a solar X-ray flare. The same observations showed emission from the south polar cap and an emission line probably

due to oxygen Kα fluorescence from the rings. These new objects are faint X-ray sources, and detailed investigation of their X-ray properties require the high-throughput and high-energy resolution provided by Constellation-X.

1.6.7 Solar System – Comets

Constellation-X will provide important, unique, and highly diagnostic observations of X-ray emission in comets giving unique insight into cometary origins, spatial and temporal morphology, and simultaneously provide remote observations of the spatial and temporal composition of the solar wind.

X-ray emission from comets was first discovered using the ROSAT X-ray observatory in 1996 (Lisse et al. 1996). This discovery was entirely unexpected as cometary atmospheres are known to be cold with a characteristic temperature between 10 and 1,000 K, much too cold for thermal X-ray production. Observations with *Chandra*, XMM, *Swift*, and *Suzaku* have shown that the X-ray emission is dominated by line emission that is strongly consistent with charge exchange interaction between the highly charged solar wind and neutrals in the cometary halo. The low resolution X-ray spectra obtained by the current generation of X-ray satellites is consistent with both experimental measurements of charge exchange in the laboratory (Beiersdorfer et al. 2003) and with numerical models (Cravens 2002; Lisse et al. 2001; Krasnopolsky & Mumma 2001).

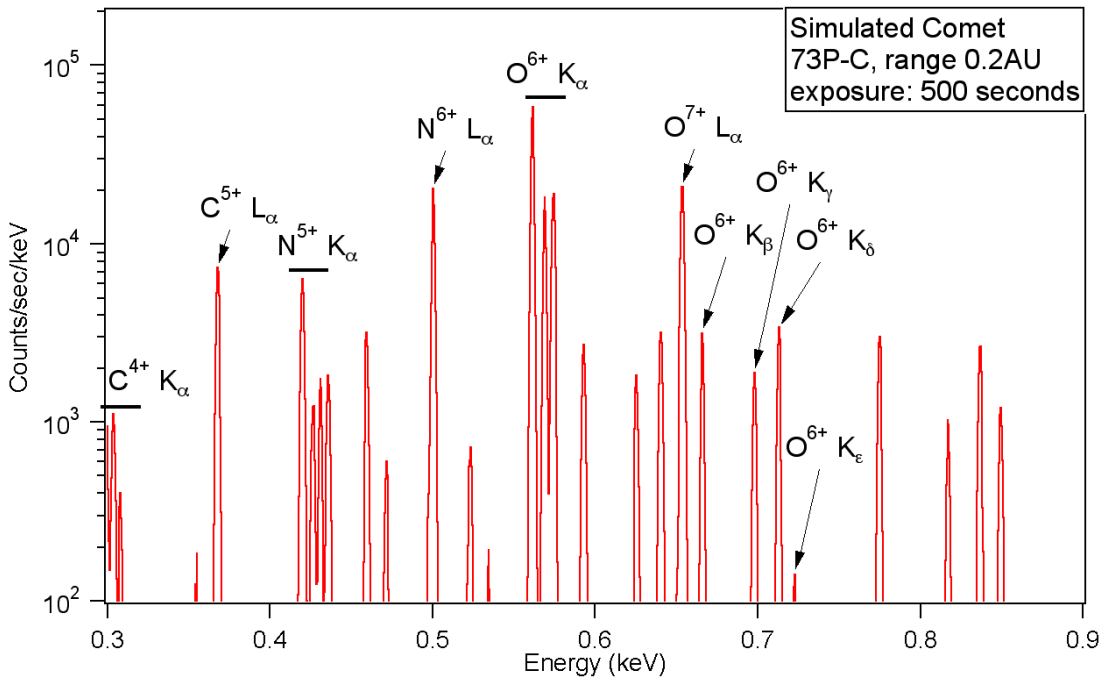

Figure 1-9. Comet Encke

Simulation of a 500 second observation of a comet using the Constellation-X/XMS. The X-ray emission is due to Charge Exchange between the highly charged solar wind and cometary neutrals. The high spectral resolution and large collecting area of Constellation-X make it possible to uniquely determine the species, charge state, and

velocity of the solar wind as well as the spatial and temporal composition, charge state, and density of the cometary coma. This simulation is based on the observed flux and surface brightness of a fairly dim comet, 73P/Schwassmann-Wachmann 3C, at perihelion on June 8, 2006 where it was 0.2 AU from the Earth. Constellation-X will enable routine spatial and temporal observations of the solar wind using short comet observations as well as unparalleled remote diagnostics of the cometary coma. Note that the entire Rydberg series of He-like and H-like C, N, and O transitions are present in the spectrum with the Rydberg series of He-like O6+ labeled as an example.

Unfortunately, current X-ray observatories are limited to a resolving power of ≤15 for diffuse sources in the 0.1-1 keV band where the strongest cometary X-ray emission occurs. With this resolving power, and the limited collecting areas of current satellites, the diagnostic utility of these observations are limited. Currently, we can determine the species and charge state of the most abundant elements in the solar wind and roughly determine the morphology of the X-ray producing region behind the cometary bow shock. However, Beirsdorfer et al. (2003) have shown that the ratio of the higher Rydberg transitions in charge exchange emission are uniquely sensitive to the composition of the neutral material in the cometary coma. This is critically important since this implies that with sufficient collecting area and spectral resolution we can remotely determine the composition, density and ionization state of the cometary coma.

References:

Allen, S. W., Schmidt, R. W., Ebeling, H., Fabian, A. C., and van Speybroeck, L. MNRAS, 353, 457 (2004)

Allen et al. (2007)

Astier, G. J. et al. A&A, 447, 31 (2006)

Barger, et al. AJ, 129, 578 (2005)

Begelman, M. C., Blandford, R. D., and Rees, M. J. Nature, 287, 307 (1980)

Beiersdorfer, P. et al. 2003, Science, 300, 1558.

Bhardwaj, A. and Gladstone, G. R. Rev Geophys, 38, 295 (2000)

Bhardwaj, A., Elsner, R. F., Waite, J. H., Gladstone, G., R., Cravens, T. E., Ford, P. G. ApJ, 624, L121 (2005)

Bhattacharyya, S., Miller, M. C., and Lamb, F. K. ApJ, 644, 1085 (2006)

Brandt, W. N., and Hanisger, G. ARA&A, 43, 827 (2005)

Bregman and Lloyd-Davies (2007)

Brenneman, L. W. and Reynolds, C. S. ApJ, 652, 1028 (2006)

Cen, R. and Fang, T. ApJ, 650, 573 (2006)

Chang, P., Morsink, S., Bildsten, L., and Wasserman, I. ApJ, 636, L117 (2006)

Cottam, J., Paerels, F., and Mendez, M. Nature, 420, 51 (2002)

Cowie, L. L., Barger, A. J., Bautz, M. W., Brandt, W. N., and Garmire, G. P. ApJ, 584, L57 (2003)

Cravens, T. E., Howell, E., Waite, J. H., and Gladstone, G. R. J. Geophys. Res., 100, 17, 153 (1995)

Cravens, T. E. 2002, Science, 296, 1042.

Cravens, T. E., et al. J. Geophys. Res., 108 (2003)

Davis et al. (2007)

Ettori, S., Tozzi, P., and Rosati, P. A&A, 398, 879 (2003)

Ferrarese, L. and Ford, H. Space Science Rev., 116, 523 (2005)

Fukugita, M., Hogan, C. J., and Peebles, P. J. E. ApJ, 503, 518 (1998)

Gerke, B. F., et al. ApJL, accepted (2007); astro-ph/0608380

Gladstone, G. R., et al. Nature, 415, 1000 (2002)

Hopkins, P. F., et al. ApJS, 163, 1 (2006)

Horanyi, M., Cravens, T. E., and Waite, J. H. J. Geophys. Res., 93, 7251 (1988)

Karanikola, I., Athanasiou, M., Anagnostopoulos, G. C., Pavlos, G. P., and Preka-Papadema, P., Planet Space Sci., 52, 543 (2004)

Kaspi, S., et al. ApJ, 574, 643 (2002)

Kharchenko, V. and Dalgarno, A. J. Geophys. Res., 105, 18351 (2000)

Komossa, S., et al. ApJ, 582, 15 (2003)

Krasnopolsky, V. A., and Mumma, M. J. ApJ, 549, 629 (2001)

LaRoque, S. J., et al. ApJ, 652, 917 (2006)

Lattimer, J. M. and Prakash, M. ApJ, 550, 426 (2001)

Lin, Y.-T. and Mohr, J. J. ApJ, 617, 879 (2004)

Linder, E. V. and Jenkins, A. MNRAS, 346, 573 (2003)

Linder, E. V. Phys Rev D, 72, 043529 (2005)

Lisse C. M., et al. Science, 274, 205 (1996)

Lisse C. M., et al. Icarus, 141, 316 (1999)

Lisse, C. M., et al. Science, 292, 1343 (2001)

Liu, F. K., Wu, X,-B., and Cao, S. L. MNRAS, 340, 411 2003

MacDowall, R. J., et al. Planet. Space Sci., 41, 1059 (1993)

Majumdar, S. and Mohr, J. J. ApJ, 585, 603 (2003)

Marconi, A., Risaliti, G., Gilli, R., Hunt, L. K., Maiolino, R., and Salvati, M. MNRAS, 351, 169 (2004)

McKibben, R. B., Simpson, J. A., and Zhang, M. Planet. Space Sci., 41, 1041 (1993)

Merritt, D. and Ekers, R. D. Science, 297, 1310 (2002)

Miller, J. M., Fabian, A. J., and Miller, M. C. ApJ, 614, L117 (2004)

Moderski, R. and Sikora, M. MNRAS, 283, 854 (1996)

Muno, M. P., Ozel, F., and Chakrabarty, D. ApJ, 581, 550 (2002)

Nath, N. R., Strohmayer, T. E., and Swank, J. H. ApJ, 564, 353 (2001)

Netzer, H., et al. ApJ, 629, 739 (2005)

Nicastro, F. et al., Nature, 433, 495 (2005)

Ogle, P. M., Brookings, T., Canizares, C. R., Lee, J. C., and Marshall, H. L. A&A, 402, 849 (2003)

Ostriker and Ciotti (2006)

Pen, U.-L. ApJ 490, 127 (1997)

Reynolds, C. S., Young, A. J., Begelman, M. C., and Fabian, A. C. ApJ, 514, 164 (1999)

Riess, A. G., et al. ApJ, 607, 665 (2004)

Sasaki, S. PASJ, 48, L119 (1996)

Spergel, D. N., et al. ApJ, submitted (2007); astro-ph/0603449

Strohmayer (2004)

Vikhlinin, A., et al. ApJ, 640, 691 (2006)

Vikhlinin, A., Kravtsov, A. V., and Nagai, D. Proceedings of the XLIst Rencontres de Moriond, XXVIth Astrophysics Moriond Meeting: "From dark halos to light", L.Tresse, S. Maurogordato and J. Tran Thanh Van, Eds (2007); astro-ph/0608330

Villarreal, A. R. and Strohmayer, T. E. ApJ, 614, L121 (2004)

Weaver, H. A., et al. ApJ, 576, L95 (2002)

Wegmann, R., Schmidt, H. U., Lisse, C. M., Dennerl, K., and Englhauser, J. Planet. Space Sci., 46, 603 (1998)

White, S. D. M., Navarro, J. F., Evrard, A. E., and Frenk, C. S. Nature, 366, 429 (1993)

2. TECHNICAL IMPLEMENTATION

Question: Describe the technical implementation you have selected, and how it performs the required measurements.

RESPONSE

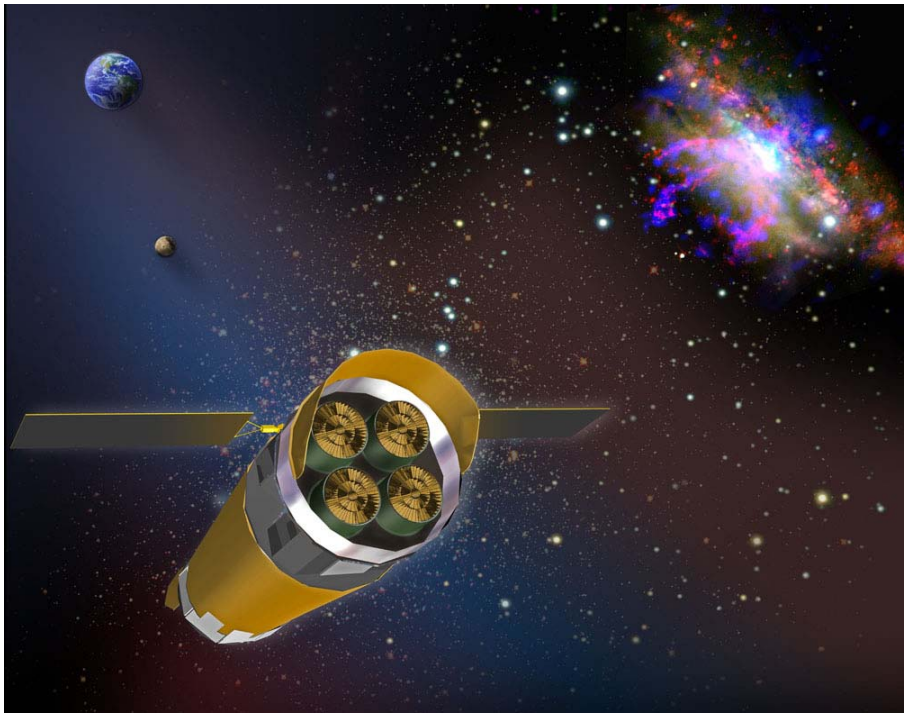

Figure 2-1. The Constellation-X Observatory

Constellation-X (Figure 2-1) is an X-ray observatory dedicated to high resolution X-ray spectroscopy, with 100 times the throughput for high resolution spectroscopy of previous X-ray observatories. The effective area of Constellation-X is compared with the high resolution spectral capabilities of current observatories in Figure 2-2. This throughput is attained using 4 identical, coaligned, high-throughput X-ray telescopes on a single spacecraft. Each telescope has a 10 m focal length and is 1.3 m in diameter. The broad bandpass is attained using three coaligned instruments. An X-ray Microcalorimeter Spectrometer (XMS), located at the focus of each of four mirrors, provides imaging and high-resolution spectroscopy in the 0.6-10.0 keV band. Some of the X-rays are dispersed by a grating spectrometer (the X-ray Grating Spectrometer, XGS), providing high spectral resolution in the 0.3-1.0 keV band. A separate Hard X-ray Telescope (HXT; mirror plus detector) provides imaging and modest resolution spectroscopy in the 6-40 keV band. The rationale for selecting this complement of instruments is found in the response to Question 5; the performance requirements are found in the response to Question 4.

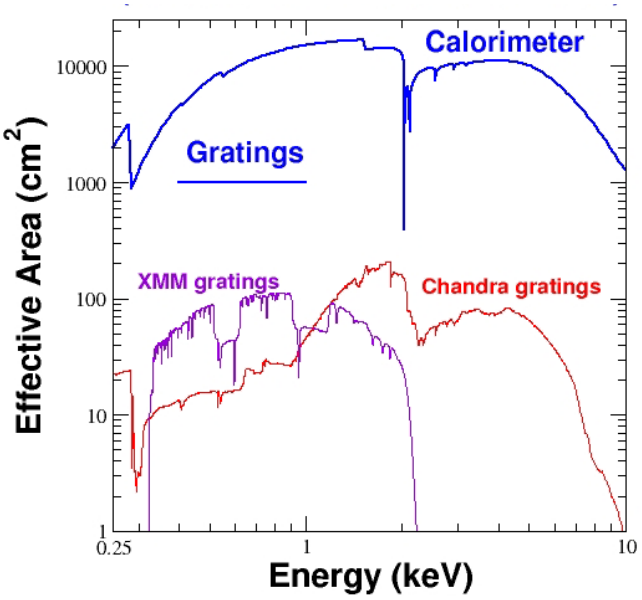

Figure 2-2. Effective Area of Constellation X for High Resolution Spectroscopy

The effective area of Constellation X for high resolution spectroscopy is a factor of 100 times larger than the XMM-Newton gratings (0.6-2.0 keV) or the Chandra gratings (0.25-10 keV).

The observatory is placed into an L2 orbit via an Atlas V 551 launch vehicle. The mission lifetime is 5 years with consumables sized for 10 years. The Atlas V long fairing is large enough (5 m dia x 26.5 m tall) to accommodate the telescopes without the need for an extendable optical bench. The derived performance requirements on spacecraft subsystems (power, attitude control, structure, thermal, communications) are within current capabilities (see response to Question 29). Constellation-X is envisioned as a "sciencecraft" wherein the spacecraft subsystems and instruments are integrated into a single structure in order to make the best use of the fairing volume.

The required measurements are performed to obtain high resolution spectra via pointed observations of selected celestial objects. Observations are anticipated to have durations between ~10^3 s and 10^6 s (see Question 4 for a discussion of sources fluxes and instrument sensitivities). The observatory is designed so that the XMS, XGS, and HXT simultaneously observe each source. Sun angle constraints allow viewing of any location in the sky for approximately 1.5 months per year. Operations are straightforward, and patterned after current and past X-ray observatories. An observing efficiency of 85 percent is expected.

3. REQUIRED MEASUREMENTS

Question: Of the required measurements, which are the most demanding? Why?

RESPONSE

The most demanding measurement is testing General Relativity (GR) in the strong gravity limit with black holes. This measurement sets the requirement for the instantaneous effective area at 6 keV to detect iron line variability on orbital timescales for at least 10 targets (see the response to Questions 4 and 9). This collecting area requirement is driven by the variability timescale at the inner stable orbit surrounding black holes, and the brightness of the inner accretion disk.

For other science objectives, the Constellation-X measurements (see the answer to Question 4) also require a large increase in effective area compared to current missions in order to obtain high quality spectra. These are not time-variable objects, thus, a modest reduction in effective area can be offset through longer exposure times. The consequences of the loss of effective area in this case would be a reduction in the number of targets that can be observed over the 5 year prime mission. This would reduce the "observatory science" that would be accomplished, but would not impact on the Beyond Einstein science.

4. PERFORMANCE REQUIREMENTS

Question: Present the performance requirements (e.g., spatial and spectral resolution, sensitivity, timing accuracy) and their relation to the science measurements.

RESPONSE

The basic Constellation-X performance requirements are listed in Table 4-1 below. A more complete description is documented in the Con-X Top Level Requirements Document (TLRD) which is available on the Con-X web site. The relation of these requirements to the science measurements is summarized in Table 4-2. Key, driving requirements are highlighted in bold face, and are discussed in the text below, as well as in Question 6 (where we address the robustness of the science to the observatory requirements).

Table 4-1. Constellation-X Performance Requirements

Parameter	Value
Overall bandpass	0.3-40 keV
Effective area	1,000 cm^2 over 0.3 keV – 10 keV
	150 cm^2 over 10 – 40 keV
	15,000 cm^2 at 1.25 keV
	6,000 cm^2 at 6 keV
Spectral resolving power (FWHM, $E/\Delta E$)	1250 over 0.3 keV – 1.0 keV
	300 over 1.0 keV – 10.0 keV in central 2.5 arcmin only
	2400 at 6 keV in central 2.5 arcmin only
	10 over 10 – 40 keV
Angular resolution (HPD)	15 arcsec over 0.3 keV – 7 keV
	30 arcsec over 7 keV – 40 keV
Field of view (FOV)	5 arcmin on a side
Bright source capability	Full capability up to 0.25 Crab flux
Temporal accuracy	100 microseconds relative to UTC
Temporal resolution	10 microseconds
Celestial coordinate accuracy	5 arcsec (3 sigma)
Mission lifetime	5 years, consumables for 10 years

Table 4-2. Science Measurements and Derived Performance Requirements

Science Objectives		Performance Requirements					
Objective	**Measurement**	**Bandpass (keV)**	**Area**	**Spectral Resolving Power FWHM @keV**	**Angular Resolution HPD**	**Instantaneous FOV (side of a square)**	**Timing/Other**
Black Holes: Study GR, Measure Spin	Time resolved spectroscopy ($t < t_{orb}$): Measurements of matter and photon orbits using Fe Kα	1.0 – 7.0	**6000cm² @ 6keV**	>1500 @ 6keV	Arcmin sufficient	n/a	Time resolution of seconds is sufficient
	Time averaged spectroscopy ($t > t_{orb}$): Measurements of Black Hole Spin via time averaged Fe Kα line profiles	0.3 – 1.0 **1.0 – 40.0**	15000cm² @ 1.25keV 6000cm² @ 6keV **150cm² @ 40keV**	2400 @ 6keV **10 over 10 – 40 keV**	**30 arcsec >7 keV**	5 arcmin	n/a
Constrain Dark Energy parameters	Imaging spectroscopy: Measurements of baryon mass fractions in clusters of galaxies and SZ effect Imaging spectroscopy: Measurements of the growth of structure G(z) using clusters of galaxies	0.3 – 10.0	**15000cm² @ 1.25keV** 6000cm² @ 6keV	**2400 @ 6keV in central 2.5 arcmin >300 over 1.0 – 10.0 keV band and in central 2.5 arcmin**	**15 arcsec**	**5.0 arcmin**	n/a
Missing Baryons	Time averaged spectroscopy: detection and characterization of WHIM via high resolution spectroscopy of ~100 background AGN	**0.3 – 1.0**	1000cm² over band	**1250 over band**	15 arcsec	5 arcmin	TOOs possible
Neutron Star Equation of State	Time resolved spectroscopy: measurements of gravitationally redshifted absorption lines in thermonuclear X-ray bursts.	0.3 – 7.0	1000cm² @ 0.3 – 1.0keV 6000cm² @ 6keV	>1000 0.3 – 1.0 keV >1000 @ 6 keV	n/a	n/a	TOOs possible 0.1 ms timing **Rates up to 0.25 Crab at full capability**

*Note: Driving requirements are in **bold face, and underlined**. Where the same requirement provides significant enhanced science, we repeat the identical requirement even though it does not drive the mission configuration.*

4.1 Constellation-X Science Objective #1 – Black Holes

Using black holes to test General Relativity (GR) and measuring black hole spin

4.1.1 Measurement of Matter and Photon Orbits Using Fe Kα

Matter in the inner regions of an accretion disk around a super-massive black hole (AGN) can orbit with a period of an hour or less. With sufficient collecting area and spectral resolution we can track the orbits of individual hot spots in the inner edges of these disks. Achieving adequate signal to noise for this observation sets a minimum effective area requirement of 6,000 cm^2 at 6 keV. In order to accurately track the orbital velocities of these hot spots, we require a spectral resolving power of >1500 at Fe Kα. These requirements are reflected in the first line of Table 4-2.

The simulation in Figure 1-2 assumes a black hole mass of 3 x 10^7 $M_\odot$, and a flux of 5 x 10^{-11} ergs/cm^2/s (2 - 10 keV; FOM of 150). A collection of relatively nearby AGN show a range of mass and flux, as indicated in Table 4-3 below. The orbital period of matter near the black hole is directly related to the mass, and is indicated in the fourth column of this table. Our ability to measure the orbits of the bright spots is directly related to the number of photons collected in one orbital timescale. Therefore the

product of the flux and orbital timescale is a 'figure of merit' which we list in the last column. These 25 AGN represent the strawman target list for this science, and we expect that as *Chandra* and *XMM-Newton* observations of these and other AGN continue this target list will grow. Simulations show that a minimum FOM of 50 is required to achieve a measurement with the precision shown in Figure 1-2. A more complete discussion of this target list, its origins, and possible improvements and additions to it can be found in the answer to Question 6.

Most of these targets have longer orbital periods (hence can have longer integrations) than the simulated source, and will therefore yield higher S/N data for the same source flux. This population of AGN will allow us to map the orbits of up to thousands of hot spots during planned Con-X observations. This target list also represents the likely targets for reverberation mapping. The effective area, spectral resolution, and band-pass requirements for reverberation mapping are equivalent to those discussed above. The scientific necessity to observe a statistically significant number of targets translates into a performance requirement for the lifetime of the mission, which when combined with the other science topics discussed below requires a 5 year mission lifetime.

Table 4-3: Target AGN for GR Tests

Target	BH Mass (10^6 $M_\odot$)	2-10 keV flux (10^{-11} erg cm^{-2} s^{-1})	t_{orb} (ks)	FOM (flux*t_{orb})
IC4329A	1	7	1.0	7.0
MGC-6-30-15	2	4	2.0	8.0
NGC 4051	2	2	2.2	4.4
NGC 5506	2	7	2.2	15.5
MKN 766	4	2	4.0	8.0
MKN 335	5	1	5.1	5.1
NGC 7314	5	4	5.1	20.4
NGC 7469	7	3.2	7.7	24.6
NGC 4593	8	4.5	8.1	36.5
NGC 4151	13	10	13.2	132
MCG+8-11-11	15	2.3	15.2	35.0
NGC 3516	23	5	23.3	116
NGC 3783	29	7	29.3	205
NGC 3227	44	2.8	44.5	125
NGC 2922	52	0.4	52.6	21.0
MCG-5-23-16	70	9	70.8	637
MKN 509	72	6.6	72.9	481
F 9	81	2.5	82.0	205
MR 2251-178	98	5	99.2	496
NGC 7213	98	3	99.2	298
MKN 841	100	1	101.2	101
NGC 5548	110	5	111.3	557
ARP 102B	140	1.1	141.7	156
NGC 2110	200	3.5	202.4	708
MCG-2-58-22	350	3.3	354.2	1169

4.1.2 Measurement of Black Hole Spin

The shape of the Fe Kα line provides a direct measure of the black hole spin. Key to measuring this line shape is determining the underlying continuum, which requires measuring the spectrum at energies above and below the line. An area of 150 cm^2, combined with an angular resolution of 30 arcsec to limit background, ensures that sensitivity from 10 keV - 40 keV is sufficient to constrain the high energy portion of the continuum. With this high energy constraint, the number of photons over the 2-10 keV

band required to measure spin to ±5% is ~>100,000. If there is no collecting area above 10 keV, the required number of counts in the 2 keV – 10 keV bandpass increases significantly (by a factor of ~4). This sets our requirements for effective area and spectral resolution from 10 keV – 40 keV (line 2 in Table 4-2).

We will also measure the spin of a large number of black holes in AGN over a range of redshifts out to z > 1. Measuring the shape of the Fe line in these sources is enabled by an effective area of 15,000 cm^2 at 1.25 keV. The Fe lines originating in the reflection component from the accretion disk are often accompanied by complex and narrow absorption features (the so-called "warm absorber"). Current measurements of warm absorbers at soft energies (< 1 keV) show typical velocities of 100 - 200 km/s, thus resolving powers of 1500 - 3000 may be required to resolve these features, and determine the underlying continuum. A resolving power of 2400 further ensures that the various Fe ionization states are deblended, and that most warm absorber components will be resolved. This requirement is carried in line 2 of Table 4-1.

4.2 Constellation-X Science Objective #2 – Dark Energy

Improving constraints on the key Dark Energy (DE) parameters by a factor of ten

To provide precise and accurate measurements suitable for DE studies, Con-X must be able to measure the properties of the X-ray emitting gas on large scales in clusters where gravity dominates (approximately half the virial radius) and the physics is well understood. Given the typical angular size of relaxed clusters, this requires a field of view (FOV) of 5 arcmin on a side. The largest, nearby clusters will overfill this field, and this drives our FOV goal of 10 arcmin.

Neither *Chandra* nor XMM have sufficient collecting area to study sufficient numbers (~500) of distant (z~1) clusters in reasonable exposure times - this large sample of objects can be done if the collecting area is sized to allow fairly fast spectral measurements. Constellation-X must be able to derive accurate temperature profiles (requiring spatially-resolved X-ray spectroscopy) for massive clusters out to z~1 in a reasonable exposure (~25 ks). This exposure time drives our effective area requirement at 1.25 keV to be 15,000 cm^2, and at 6 keV to be 6,000 cm^2. The need to derive accurate temperature profiles over the entire surface of the cluster drives our spectral energy resolution requirement over the full field of view. This is sufficient to resolve the strong transition lines used for temperature diagnostics. These requirements are carried in Table 4-2 line 3.

Con-X must also have sufficient spatial resolution and resolving power to recognize merging clusters and separate out the complex physics in the centers of clusters. This will allow us to measure gas motions in the center of clusters (via the Fe Kα lines) and therefore quantify any non-equilibrium pressure support it may introduce. An angular resolution of 15 arcsec will allow us to remove the complex central regions from our f_{gas} and G(z) analysis when it is necessary (Table 4-2, line 4). A resolving power of 2400 is required only in the center of the FOV, as it is in the center of some clusters where effects of turbulent heating may be detected (velocities are expected to be ~ 100 - 300 km/s so resolving powers of 1000 – 3000 are needed). The f_{gas} measurements can benefit from slightly higher angular resolution, and this drives our 5 arcsec goal for this item (Table 4-2, line 3).

Experience from *Chandra* shows that imaging the low surface brightness of the outer regions of clusters requires that the particle induced detector background be at or below a level of 10^{-2} c/cm^2/s/keV. When combined with the effective area and plate scale effects, the limiting surface brightness for Con-X is predicted to be several times below that of *Chandra*. However, during times of high solar activity

(coronal mass ejections) the *Chandra* background rates are high enough to render the data unusable for low surface brightness studies. This is reflected in our mission design discussed in Question 19.

4.3 Constellation-X Science Objective #3 – Missing Baryons

Unambiguous detection of the hot phase of the Warm-Hot Intergalactic Medium (WHIM) at z>0

Constellation-X will measure these filaments in absorption along the sight to background AGN, constraining the hot baryon content of the Universe. With >100 filaments detected at z>0, this will provide the first unambiguous detection of the hot phase of the IGM.

Most of the baryons in the Universe have yet to be discovered and are expected to reside in a hot (10^5 – $10^{7.5}$ K), diffuse network of filaments distributed throughout the Universe called the Warm-Hot Intergalactic Medium (WHIM). At this time, >60% of this baryonic component is still undiscovered. We can detect these filaments in absorption against bright background objects.

Detectability is a function of both the spectral resolving power and the effective area of the telescope. Note that a given absorption line equivalent width sensitivity may be achieved by various combinations of effective area and spectral resolving power. To detect absorption lines with equivalent widths of 1mÅ (the required sensitivity to detect 100 filaments: see Question 1), we have found that the combination of 1000 cm^2 and 1250 spectral resolving power requirement will meet our needs. Note that meeting the spectral resolving requirement of 1250 at 0. 6 keV (the two strongest features are OVII and OVIII at 574 eV and 654 eV), with a grating spectrometer implies higher resolving power at lower energies, which will ensure that we meet the resolution requirement for higher redshift filaments.

4.4 Constellation-X Science Objective #4 – Neutron Star Equation of State

Measuring the mass-radius relation of neutron stars to determine the Equation of State (EOS) of ultra-dense matter.

By observing spectral lines produced from heavy elements in the atmospheres of accreting neutron stars, Constellation-X can simultaneously determine the masses and radii of such neutron stars. This uniquely determines the neutron star equation of state. There are several unique requirements that neutron star observations set.

Constellation-X will be the first X-ray observatory with the capability of making simultaneous high spectral resolution and fast timing measurements of X-ray bursts. Several independent methods are then accessible to constrain mass and radius, providing important checks on any systematic errors associated with either method. In order to carry out these measurements we require sufficient area at the spectral lines of interest to allow us to observe the atmospheric lines. We expect lines of Fe L-shell ions, and Fe Lyα, and accurate measurement of the line centriod and shapes requires spectral resolution of greater than 1000 at these lines. Pulse shapes of burst oscillations provide a measure of the neutron star radius to a few percent. These oscillation measurements must be made on timescales less than the spin timescale. The spin period of neutron stars can be as short as 1 ms, leading to the requirement of 0.1 ms absolute timing accuracy. High spectral resolution is required during the X-ray bursts, leading to a requirement to maintain full resolving power at fluxes up to 0.25 Crab. These requirements are carried in line 6 of Table 4-2.

5. PROPOSED SCIENCE INSTRUMENTATION

Question: Describe the proposed science instrumentation, and briefly state the rationale for its selection.

RESPONSE

Constellation-X has two distinct telescope systems: the Spectroscopy X-ray Telescope (SXT), covering the 0.3 - 10.0 keV band, and the Hard X-ray Telescope (HXT), covering the 6 - 40 keV band. Constellation-X has four SXT units, each of which consists of a Flight Mirror Assembly (FMA) and an X-ray Microcalorimeter Spectrometer (XMS). One or two SXT units will have an X-ray Grating Spectrometer (XGS). The HXT will consist of one or two mirrors plus detectors, depending on the selected implementation. This overall instrument complement, which all operate simultaneously, has the bandpass, effective, and resolving power needed to achieve the science objectives described in Questions 1 and 4, above. More specific rationales for the individual instrument selections are provided below. A schematic of the Constellation-X instrumentation is shown in Figure 5-1.

The FMA is an element of the observatory, and therefore technically not an instrument. It is treated as one here, however, because it is the subject of mission-enabling technology development.

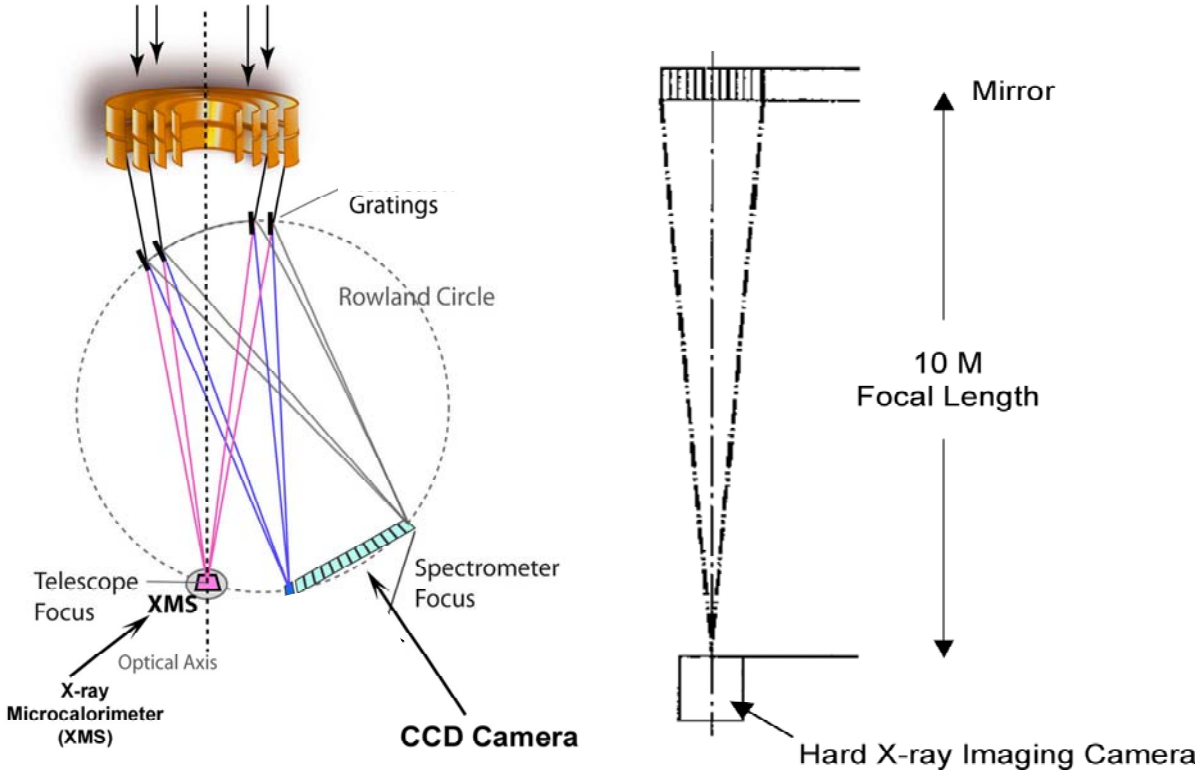

Figure 5-1. Schematic of the Constellation-X Instrumentation

The focal plane of each Spectroscopy X-ray Telescope (SXT) contains one X-ray Microcalorimeter Spectrometer (XMS). One or two SXT units will have an X-ray Grating Spectrometer (XGS), consisting of a grating and a CCD detector. Shown here schematically is an exaggerated view of a transmission grating spectrometer. The Hard X-ray Telescope (HXT) has a separate mirror and detector.

5.1 SXT Flight Mirror Assembly (FMA)

Constellation-X features four identical high-throughput FMAs for illuminating the X-ray microcalorimeters and the grating spectrometer(s). The scientific objectives place performance requirements on the FMA (listed in Table 5-1), the most significant of which is that the mirrors must be large to meet the effective area requirement. Each FMA has an aperture diameter of 1.3 m and a focal length of 10 m. The mirrors utilize a two-reflection Wolter Type I design, in which an image of a distant source is formed on a focal plane via the reflection at near grazing angles off confocal paraboloid (primary) and hyperboloid (secondary) surfaces of revolution. The grazing incidence reflections are necessitated by the physics of X-ray reflection; two reflections are optically required in order to form a true image.

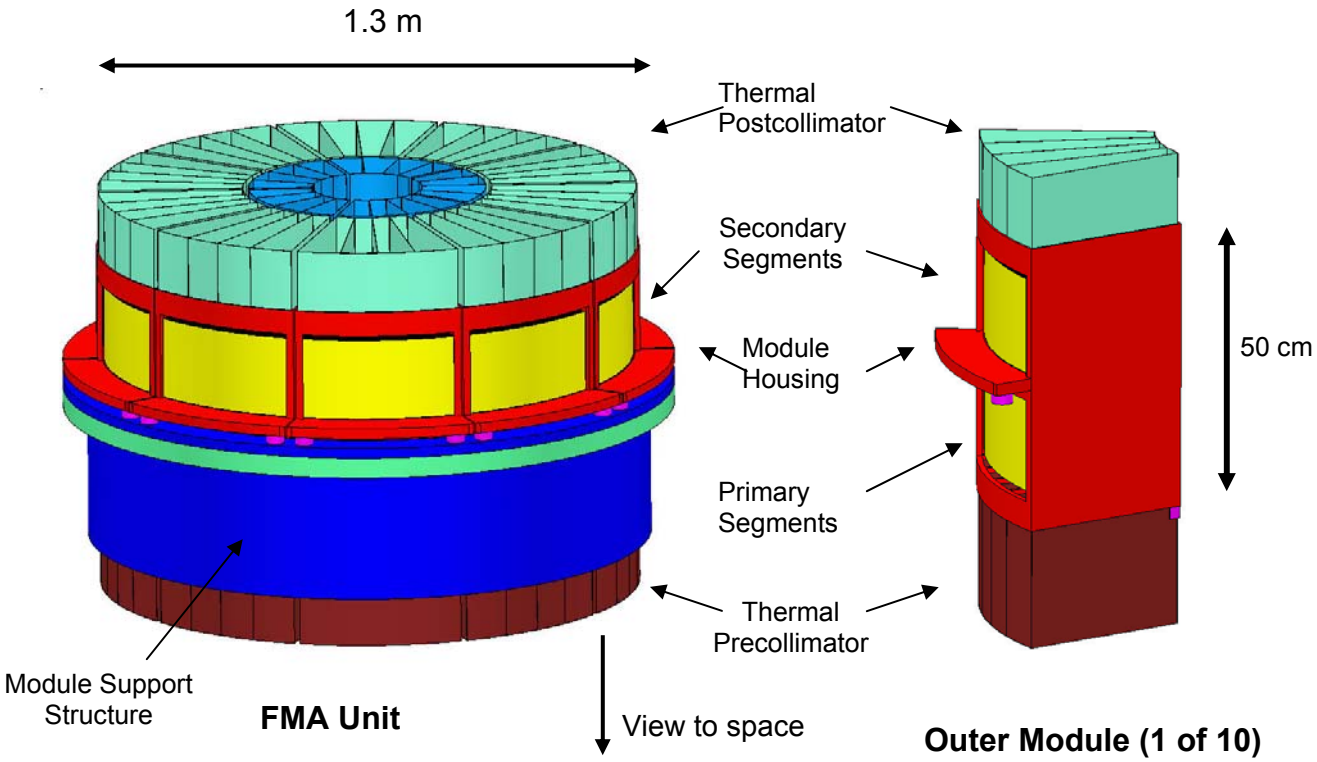

Figure 5-2. Schematic of an FMA

Left: A schematic of a FMA, composed of 5 inner modules and 10 outer modules. It is depicted in its launch orientation. Right: A schematic of an outer FMA module.

The projected reflecting area of a single Wolter I mirror is a small fraction of the surface area. The fact that the Wolter I design incorporates reflections of two inner surfaces allows for the nesting of multiple mirrors. In the SXT design, the aperture is efficiently filled with 163 coaxial mirror "shells," facilitating high throughput of incident radiation. A segmented approach has been adopted, in which each paraboloid and hyperboloid surface of revolution is composed of a number of mirror segments of equal arc length.

The FMA properties are listed in Table 5-2. Each mirror assembly consists of 15 modules; five identical inner modules subtending a 72 degree arc, and 10 identical outer modules subtending a 36 degree arc.

The outer radius of the inner modules was chosen so that the largest inner mirror segments are of comparable size to the largest outer segments. The primary and secondary reflection stages, made of separate mirror segments, are both contained within a module. The five inner modules each contain 66 mirror segment pairs; each of the 10 outer modules contains 97 pairs. A complete FMA thus has 2,600 mirror segments. The mirror segments consist of thermally formed glass substrates coated with an iridium reflecting surface. Module housings will be fabricated from a titanium alloy with a coefficient of thermal expansion (CTE) compatible with that of the mirror segments. A thermal precollimator will be mounted in front of the active reflecting area of each module, and a postcollimator behind. A schematic of an FMA unit is shown in the left panel of Figure 5-2; an outer module is shown in the right panel. As shown in Figure 5-2, the 15 modules will be mounted on a module support structure, fabricated from CTE-matched composite. This complete FMA mounts, along with the other three identical assemblies, to the spacecraft optical bench.

Table 5-1. Flight Mirror Assembly (FMA) Performance Requirements

Parameter	Value
Bandpass	0.3 – 10 keV
Angular resolution (on-orbit)	12.5 arcsec HPD
Effective area at 1.25 keV (on-axis)	4610 cm^2
Effective area at 6 keV (on-axis)	1765 cm^2
Field of View	≥ 7 arcmin diameter

Table 5-2. SXT Mirror Properties

Parameter	Value
Number of SXT Flight Mirror Assemblies (FMA)	4
Optical design	Segmented Wolter I
Focal length	10 m
Diameter (largest/smallest mirror surface)	1.3 m/0.3 m
Mirror segment axial length	20 cm
Mirror segment material	Thermally formed Schott Desag D263 glass
X-ray reflecting surface	Iridium
Number of nested shells	163
Number of mirror segments per FMA	2,600
Number of modules per FMA	10 (outer); 5 (inner)
Number of mirror pairs per module	97 (outer); 66 (inner)
Module housing material	Titanium alloy, CTE-matched to segment glass
Largest mirror segment surface area	0.08 m^2
Mirror segment thickness	0.44 mm
RMS microroughness	0.6 nm

5.1.1 Rationale for Selection

An imaging X-ray mirror is required on Constellation-X to obtain adequate signal-to-noise for high-sensitivity spectroscopy and perform spatially resolved spectroscopy. Multiple mirrors protect against the loss of the mission due to the failure of one instrument. Combined with a 10 m focal length (set by the fairing length) and 1.3m diameter optics, this system meets the effective area performance requirements, without the need for a focal length extension mechanism.The Wolter I mirror design was selected because it affords nesting and therefore the most efficient fulfillment of the effective area requirement (smallest aperture area and fewest focal planes). The modular design was selected for two reasons: segment "wedge" mandrels are more cost effective, more producible and can be readily procured; and the modular design is conducive to mass production. Iridium was selected as the reflecting material because it has the highest X-ray reflectivity at 6 keV of usable materials, and has been flight demonstrated on *Chandra*.

5.2 X-ray Microcalorimeter Spectrometer (XMS)

The XMS uses an X-ray microcalorimeter to sense individual X-ray photons as heat, and determine their energy with high precision. A microcalorimeter is a non-dispersive, photon-counting spectrometer that combines very high spectral resolution with high quantum efficiency over a broad energy band. Thermodynamic limits determine the spectral resolution and drive the need for operation at a temperature below ~0.1 K. Although extraordinarily cold, such temperatures can be readily achieved and maintained using flight-proven techniques.

The operating temperature is a consequence of the instrument requirements – any non-dispersive spectrometer providing 2 eV resolution must operate at such low temperatures. Various schemes for performing efficient, high-resolution, spectroscopic measurements came together to form the field of low-temperature detectors in the last two decades.

Low temperature spectrometers can be classified according to the relative magnitude of the energy of the excitations that form the signal compared with the quanta of energy in the thermal background. In one class are detectors that produce signal excitations much larger than the energy of thermal phonons. Superconducting tunnel-junction devices are in this class. Not all of the energy of the incident X-ray is used to generate these excitations; a large fraction of the photon's energy becomes heat. The fundamental limit on the energy resolution is determined by statistical fluctuations on the division of energy between the system of excitations and thermal energy.

In the other class are detectors that produce signal excitations that are comparable with those in the thermal background. These devices are calorimeters, and all of the energy of the incident photon is converted to heat. To the extent that a calorimeter can be modeled as a closed system, the event-to-event statistical fluctuations that limit the resolution of detectors such as charge-collection devices do not occur. The fundamental limit on the energy resolution of a microcalorimeter is determined by the signal-to-noise of a measurement of a temperature increase on a background of thermal fluctuations.

We selected microcalorimeter technology for Constellation-X instead of superconducting tunnel junctions because, although tunnel-junction devices have achieved exciting results in soft X-ray and UV/optical spectroscopy, they are not competitive with microcalorimeters for high resolution at 6 keV.

The basic microcalorimeter concept can be implemented in many ways. Resistive, capacitive, inductive, paramagnetic, and electron-tunneling thermometers have been used, with varying degrees of success, as

the thermometer in microcalorimeters. We selected a resistive thermometer, the superconducting transition-edge sensor (TES), for the XMS reference design. TES microcalorimeters are operated in the narrow temperature range between the onset of non-zero resistance and the fully normal state. The electrothermal feedback of a voltage bias provides a stable bias point within the sharp transition. Using a superconductor/normal-metal bilayer, the critical temperature (T_c) can be tuned to <0.1 K by choice of the layer thicknesses (the required quantum efficiency is obtained by connecting a separate X-ray absorber to the TES film). The change in resistance is measured by monitoring the current through a voltage-biased TES using a superconducting quantum interference device (SQUID). SQUID ammeters are well matched to these low-resistance devices. The rapid progress in TES technology, the theoretical prediction of 2 eV resolution, and the potential for large scale SQUID multiplexing combined to make TES technology the clear choice for the XMS reference design.

A block diagram of the XMS is shown in Figure 5-3. The reference design consists of 64 x 64 pixels, consisting of a high-performance core array, surrounded by a field-of-view extension. The core array consists of a 32 x 32 array of 250 x 250 micron pixels (5 arcsec x 5 arcsec). Each pixel consists of a TES (which acts as the calorimeter thermometer), an X-ray absorber, and a membrane thermal link to the 50 mK heat sink. The absorber is larger than the TES and its thermal link, making thermal contact to the TES but elsewhere extending cantilevered above the sensor plane by several microns. The gap between adjacent absorbers can thus be on the scale of 5 μm.

For the field of view extension, which has three times the number of spatial elements as the core array, the spectral resolution and speed of the additional elements is relaxed relative to the core array. Thus this extension can be achieved by making design compromises that keep the number of electronics channels from scaling with the increase in pixels. Our basic design for the extension utilizes imaging TES detectors that will have at least eight imaging elements per pair of TES. Position information is obtained by comparing the relative signals on the two TES's while energy is inferred by summing the signals. Both parts of the focal plane will be read using multiplexed SQUID amplifiers. The core array drives the technology development for the SQUID MUX.

In total there will be ~1800 TES microcalorimeters that will be read out using a SQUID multiplexer. First-stage SQUIDs are coupled to each TES, and columns of 32 such input SQUIDs are multiplexed into a second stage using serial addressing (time-division multiplexing). Each second stage comprises a nearby single SQUID and a series array of SQUIDs for amplification and matching to the external electronics. Surrounding five sides of the detector housing will be an active anticoincidence detector, sensitive to ballistic photons produced by charged particles. This will also be read out with SQUID amplifiers to simplify the design of the detector.

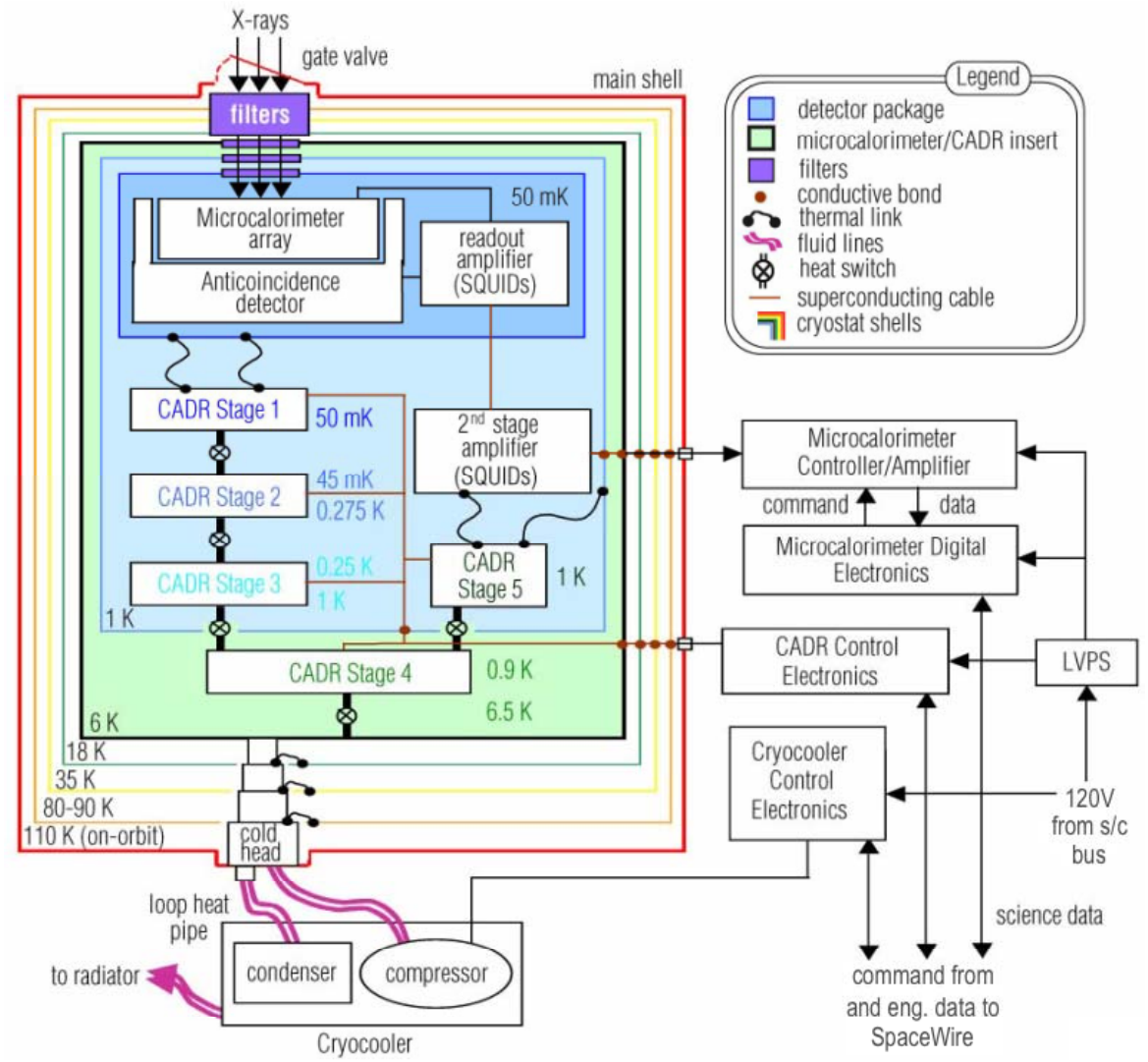

Figure 5-3. Block Diagram of the XMS

The XMS cooling system, consisting of a Continuous Adiabatic Demagnetization Refrigerator (CADR) and cryocooler, has no stored cryogens, thus maximizing the lifetime/mass ratio for the instrument.

Cooling of the detector stage will be achieved using a multistage CADR, which provides the necessary cooling power down to 50 mK. The warmer stages of the CADR are sequentially linked through heat switches and then cycled to transfer heat to the relatively warm cryocooler interface. A mechanical cryocooler will provide the <5 K heat sink for the CADR and will actively cool several thermal shields within the cryostat. It will also thermally anchor internal XMS signal and CADR current leads. The cryostat will provide the necessary structural support and thermal isolation for all microcalorimeter, CADR and cryocooler components contained within the outer shell.

Blocking filters in the aperture of the cryostat prevent heating of the detector stage by non-X-ray radiation. Transmission of these filters determines the low energy limit to the bandpass (~0.25 keV, which is below the required 0.3 keV). The high-energy limit (>10 keV) is determined by the X-ray absorption efficiency of the absorber and the SXT mirror reflectivity. The X-ray photons are amplified,

demultiplexed, triggered, and then analyzed for pulse height, arrival time, and anticoincidence with the analog and digital electronics external to the cryostat. The cryostat will have a one-time-use aperture door that will be opened after launch after outgassing levels are adequately low.

5.2.1 Rationale for Selection

The science requirements on Constellation-X necessitates an imaging X-ray spectrometer with resolving power (>300) and nearly 100% intrinsic quantum efficiency over a ~10 keV energy bandpass, and rapid response time. The field of view and spatial resolution must be sufficiently high to spatially resolve an extended structure larger than the HPD of the SXT mirror without loss of spectral resolution. These requirements can only be achieved with a low temperature spectrometer, and, as detailed above, the leading technology consists of TES microcalorimeters with SQUID multiplexing.

Table 5-3. XMS Performance Requirements

Parameter	Value
Bandpass	0.6-10.0 keV
Core Array Spectral resolving power (E/ΔE)	2400 at 6 keV
Outer Array Spectral resolving power (E/ΔE)	300 (0.6 - 10 keV)
Angular resolution	5 arcsec
Field of view	5 arcmin square field
Temporal resolution	10 microsec

Table 5-4. XMS Properties

Parameter	Value
Number of pixels	64 x 64
Pixel size	250 microns
Energy resolution – core array	4 eV at 6 keV 2 eV at 1 keV
Energy resolution – outer array	8 eV
Intrinsic quantum efficiency	95 percent
Detector speed – core array	<300 microsecond pulse decay time
Operating temperature	0.05 - 0.06 K
Temperature stability	2 microKelvin RMS

5.3 X-ray Grating Spectrometer (XGS)

The X-ray Grating Spectrometer consists of an array of gratings that intercepts the converging X-ray beam exiting the Flight Mirror Assembly and disperses it to a series of CCD detectors, where the energy resolution of the CCD is used to separate the spatially overlapping spectral orders. Two configurations for implementing the XGS are currently under study.

A *transmission grating XGS concept* involves high efficiency transmission grating facets that are arrayed directly behind one of the mirror assemblies in a Rowland Circle geometry that includes the XMS for the zero order focus and a dedicated strip of CCDs to image the dispersed spectra (Figure 5-4, left). Two independent arrays of gratings would be implemented behind one mirror assembly. To maximize the spectral resolution, each of the arrays subapertures the optic with two subarrays of gratings positioned on the outer annuli at opposite sides of the mirror assembly. A strip of 20 CCDs would image the dispersed spectra from each of the two grating arrays. The transmission grating arrays would be spatially fixed for simultaneous spectral coverage with the XMS.

A *reflection grating XGS concept* involves off-plane reflection gratings and an arc of CCD detectors to image the conically dispersed light (Figure 5-4, right). To minimize the mass, the grating array would be implemented close to the focal plane, roughly 3 m above the mirror focus, where fewer grating elements are required to fully sample the converging beam. Off-plane gratings can be moved into the beam of one or two of the SXT units, where they intercept the full beam. The dispersed spectra for each grating array would be imaged by a corresponding array of roughly 7 CCDs.

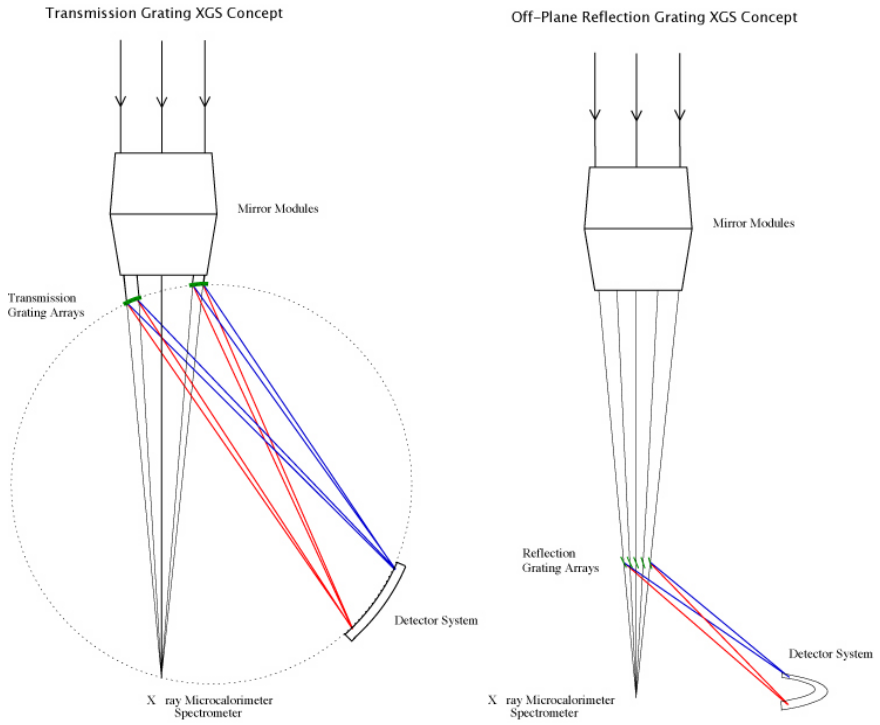

Figure 5-4. Schematics of Two X-ray Grating spectrometer Concepts

Left: Schematic of the transmission grating concept for the XGS. Right: Schematic of the reflection grating concept for the XGS.

Table 5-5. XGS Performance Requirements

Parameter	Value
Bandpass	0.3 -1.0 keV
Effective area	1,000 cm^2 over full band
Spectral Resolving Power (FWHM)	1250 over full band

5.3.1 Rationale for Selection

Only dispersive spectrometers can currently reach the required spectral resolution over the low energy 0.3 - 1.0 keV band. While nondispersive spectrometers have higher quantum efficiency and imaging capabilities, fabrication considerations limit their resolving power at the lowest energies. The spectral properties of grating spectrometers and calorimeters are complementary: the resolving power of the calorimeters increases with increasing photon energy, while the resolving power of the grating spectrometers under consideration is essentially independent of photon energy from 0.3 to 1.0 keV.

5.4 Hard X-ray Telescope (HXT)

The Hard X-ray Telescope (HXT) extends the Constellation-X bandpass to 40 keV. It consists of grazing incidence nested mirrors (conceptually similar to the SXT) that focus X-rays onto an imaging spectrometer located in the focal plane. There are three main differences between the SXT mirrors and the HXT mirrors: (1) the radial dimensions of the HXT mirrors are considerably smaller than those of the SXT mirrors, because higher energy photons require smaller graze angles for efficient reflection; (2) the HXT mirrors must be coated with depth-graded multilayer coatings (rather than the single metallic layer of the SXT mirrors) to extend the bandpass to 40 keV; (3) the HXT mirrors have a less stringent angular resolution requirement. Two implementations are currently under consideration: one using a single HXT mirror and detector, the second using two telescopes and detectors. Tables 5-6 and 5-7 below specify some of the requirements for the HXT mirrors.

Table 5-6. HXT Mirror Performance Requirements

Parameter	Value
Bandpass	6 – 40 keV
Effective area	150 cm^2
Angular resolution	30 arcsec HPD

Table 5-7. HXT Mirror Properties

Parameter	Value	
Mirror module type	Segmented mirrors	Full shell mirrors
Number of HXT units	1	2
Optical design	Segmented Wolter I (5 segments)	full revolution Wolter shells
Focal length	9 m	10 m
Diameter (largest/smallest mirror surface)	70 cm/ 10 cm	36 cm/ 15 cm
Mirror segment axial length	20 cm	60 cm (full shell)
Mirror segment material	Thermally formed Schott Desag D263 glass	Electroformed Ni shells full revolution
X-ray reflecting surface	W/Si depth-graded multilayers	W/Si depth-graded multilayers
Number of nested shells	270	80
Number of mirror segments per FMA	2,700	n/a
Number of mirror pairs per module	540	n/a
Mirror segment thickness	0.200 mm	0.100 mm
RMS microroughness	0.4 nm	0.4 mm

The reference HXT focal plane detector is a cadmium-zinc-telluride (CZT) pixelated solid-state detector. CZT detectors have excellent energy resolution for the energy range of interest (6 - 40 keV), can be made position sensitive, and achieve their limiting spectral resolution even at room temperature (0 degrees C); therefore, they are an excellent choice for hard X-ray imaging astrophysical detectors for space based missions. The performance requirements for the detector are given in Table 5-8. Table 5-9 lists some of the design elements for these detectors.

Table 5-8. HXT Detector Performance Requirements

Parameter	Value
Bandpass	6 – 40 keV
Field of View	5 arcmin
Spectral Resolving Power	>10 (10 – 40 keV)

Table 5-9. CZT Detector Properties

Parameter	Value
Number of pixels	44 x 44
Pixel size	500 microns
Energy range	6 – 100 keV
Energy resolution	< 1 keV FWHM
Intrinsic quantum efficiency	95 percent
Operating temperature	0 degrees C

5.4.1 Rationale for Selection

Hard X-ray focusing telescopes can achieve orders of magnitude improvement in sensitivity compared with the instruments based on coded apertures and collimated detectors that have traditionally been used in this energy band. Coupled with pixellated solid state focal plane detectors, this HXT will provide the Constellation-X Mission with the required sensitivity at high energy to accomplish its science objectives. And, with a lower energy operating range of 6 keV, the HXT provides significant overlap with the SXT, for cross-calibration purposes.

6. PERFORMANCE REQUIREMENT — SENSITIVITY OF SCIENCE GOALS

Question: For each performance requirement, present as quantitatively as possible the sensitivity of your science goals to achieving the requirement. For example, if you fail to meet a key requirement, what will the impact be on achievement of your science objectives?

RESPONSE

We present the major performance requirements (as described in Question 4) for each of our four science objectives, and state the impact of failing to meet those requirements. For Science Objective #1 (Black Holes) there are two classes of measurement that are made. These two cases are treated separately where appropriate. Note that although there are two measurements for Objective #2 (Dark Energy), the sample and performance requirements are the same.

For each of the main performance requirements listed in Question 4, we describe impacts as follows:

Significant Impact: This performance requirement is the most demanding in terms of achieving science objectives. Not meeting this requirement presents a significant loss of science.

Moderate Impact: A measurable performance impact occurs. The impact of not meeting the requirement can be mitigated. For example longer integration times can mitigate a loss of effective area.

Small Impact: The performance requirement impact does not affect primary science.

Little/No Impact: The performance requirement impact does not affect the science.

After the table which steps through overall bandpass, effective area, spectral resolving power, angular resolution and field of view, we list some additional requirements from Question 4. We then expand on impact that reduced area at 6 keV would have on our most demanding measurement: that of testing GR in the strong gravity limit (see Question 3).

Table 6-1. Sensitivity of Science Goals to Performance Requirements

Performance Requirement	Science Objective	Impact Of Not Meeting Requirement
Overall Bandpass **(0.3-1.0 keV, 1.0-40 keV)**	**Black Holes**	
	Sub-Orbital Fe Kα	**Little/No impact** *Continuum knowledge non-critical for this measurement.*
	BH Spin	**Moderate Impact: If 10 - 40 keV bandpass not achieved, reduction in continuum constraint on BH spin measurement** *Without good constraints on the 10 - 40 keV hard X-ray continuum in AGN, constraint of the red wing of the Fe Ka line, the signature of a spinning black hole, will be difficult. Much longer exposure times (4X) will be required.*
	Dark Energy	**Little/No Impact** *Key energies for clusters are 1 - 5 keV for typical cluster temperatures (kT~2 - 10 keV) and redshifts (0.3 < z < 1). Modest bandpass losses at either end may be tolerated.*
	Missing Baryons	**Moderate Impact: Loss of key WHIM transition at high-z** *Loss of soft energy response (~0.3 keV) would seriously limit redshift reach of OVII (0.574 keV) which has E=0.38 keV at z=0.5*
	Neutron Star EOS	**Little/No Impact** *Key Fe transitions are near 0.9 - 1.6 keV; Modest bandpass losses at either end may be tolerated.*

Performance Requirement	Science Objective	Impact Of Not Meeting Requirement
Effective Area **(1000 cm^2 at 0.3 keV, 15000 cm^2 at 1.25 keV, 6000 cm^2 at 6.0 keV, 150 cm^2 at 10-40 keV)**	**Black Holes**	
	Sub-orbital Fe Kα	**Significant Impact: Loss of area at 6** keV **results in fewer observable objects** *Tracking matter on sub-orbital timescales requires a large instantaneous effective area. Modest reductions may cause the loss of a few targets out of the ~10 AGN in Table 4-3.*
	BH spin	**Moderate Impact: Loss of area at 10 - 40 keV results in lower observational efficiency** *Without the 10 - 40 keV collecting area, the BH spin measurements are compromised as measuring the red wing requires good knowledge of the continuum. This is mitigated by 4 times longer exposures needed with 0.3-10 keV coverage alone.*
	Dark Energy	**Moderate Impact: Loss of area from 1.25 to 6 keV results in reduced observing effficiency for large cluster sample** *This is mitigated by increased exposure times for this large (500) target sample.*
	Missing Baryons	**Small Impact: Loss of low energy area results in fewer detectable filaments** *Only the soft energy response is critical for OVII and OVIII transitions out to z=0.5. The detectability of the WHIM scales with both collecting area and spectral resolving power with collecting area being the weaker constraint (longer observation times can compensate).*
	Neutron Star EOS	**Little/No Impact** *Sources may be observed slightly longer to accumulate more burst time.*

Performance Requirement	Science Objective	Impact Of Not Meeting Requirement
Spectral Resolving Power (E/ΔE, FWHM) **(1250 at 0.5 keV, 2400 at 6 keV, 10 at 10-40 keV)**	**Black Holes**	**Moderate Impact: Loss of resolving power at 6 keV compromises line structure determination** *Ambiguous determination of ionization states of Fe if R<2000. If R<1500 then won't resolve turbulent width of warm absorber components near Fe Kα.*
	Dark Energy	**Small Impact: Loss of resolving power** *High spectral resolving power in the 2.5 x 2.5 arcmin FOV is required to obtain the most accurate velocity and temperature measurements, but a resolving power of 1000 (6 keV; see Question 4) achieves science.*
	Missing Baryons	**Moderate Impact: Loss of resolving power at 0.5** keV **reduced the detectability of WHIM** *Detectability scales as resolving power linearly and loss is mitigated by increasing integration times to compensate.* *This is the major driver on spectral resolving power at soft energies.*
	Neutron Star EOS	**Moderate Impact: Loss of resolving power near 1 keV removes one of the independent constraints on EOS** *With R=300 XMM RGS was able to detect gravitational redshifts (minimum requirement) but R=1000 over 0.3-1.0 keV bandpass ensures lines are resolved and provides important independent constrain on neutron star radius.*

Performance Requirement	Science Objective	Impact Of Not Meeting Requirement
Angular Resolution **(15 arcsec requirement < 7 keV, 30 arcsec > 7keV)**	**Black Holes**	**Small Impact** *In order to retain sensitivity and avoid source confusion we require 30 arcsec imaging above 7 keV.*
	Dark Energy	**Moderate Impact: Loss of angular resolution results in poorer resolution of high redshift clusters.** *Angular resolution below 7 keV allows determination of the dynamical state of the cluster, separation of central AGN and resolution of cluster surface brightness profiles. Angular sizes are smaller with increasing redshift to z~1, so the cosmological reach of the experiment is compromised.*
	Missing Baryons	**Moderate Impact: Loss of angular resolution results in fewer detected filaments** *Although good angular resolution is not required for studying absorption features on bright background AGN, the performance of the XGS would be impacted, causing a loss of spectral resolution This secondary impact on spectral resolving power impacts the number of detected absorbing systems.*
	Neutron Star EOS	**Little/No Impact** *Good angular resolution is not needed for these bright, isolated sources.*

Performance Requirement	Science Objective	Impact Of Not Meeting Requirement
Field of View **(5 arcmin x 5 arcmin)**	**Black Holes**	**Little/No Impact** *These AGN are point sources and are isolated. Minimal FOV (75 arcsec on a side) is needed to ensure proper background subtraction.*
	Dark Energy	**Moderate Impact: Loss of field of view results in loss of observing efficiency.** *Science objective is to reach at least r_{2500} for large, dynamically-relaxed clusters. Cluster angular size decreases with redshift from z=0.3 to z=1.0, so main impact is that multiple, tiled observations of z=0.3 - 0.5 clusters might be required for the nearby clusters, costing more observing time.*
	Missing Baryons	**Little/No Impact** *Target background AGN for absorption studies are point sources*
	Neutron Star EOS	**Little/No Impact** *Target neutron stars are bright, isolated point sources.*

Performance Requirement	Science Objective	Impact Of Not Meeting Requirement
Bright Source capability	**Black Holes**	**Little/No Impact** *Sources typically far below 0.25 Crab.*
	Dark Energy	**Little/No Impact** *Sources typically far below 0.25 Crab.*
	Missing Baryons	**Little/No Impact** *Sources typically far below 0.25 Crab.*
	Neutron Star EOS	**Moderate Impact: Loss of spectral resolution** *Some sources at the highest fluxes will have slightly reduced energy resolution at energies >1keV, but no impact below 1 keV. Some of the interesting lines may have reduced energy resolution.*

Performance Requirement	Science Objective	Impact Of Not Meeting Requirement
Temporal accuracy/resolution	**Black Holes**	**Little/No Impact**
	Dark Energy	**Little/No Impact**
	Missing Baryons	**Little/No Impact**
	Neutron Star EOS	**Moderate Impact: loss of temporal resolution will limit studies to NS with longer spin periods.** *This is mitigated by the margin in this capability. Spin periods are typically 10x this requirement. We would have to miss requirement by an order of magnitude to start to have a significant impact.*

6.1 Constellation-X Science Objective #1 – Black Holes

Using black holes to test General Relativity (GR) and measuring black hole spin

6.1.1 Measurement of Matter and Photon Orbits Using Fe Kα

Area at 6keV: Testing of GR in the strong gravity limit necessitates achieving our required area at 6keV as discussed in Questions 3 and 4. In principle, the proposed tests of GR can be accomplished with Constellation-X observations of a single appropriate source. Given the scientific importance of these tests it is apparent that they should be carried out for a reasonable (~10) sample of sources to confirm the validity of the findings. If the required area at 6keV is not achieved, the science impacts are gradual since as discussed below we already have at least 5 sources where the required signal is a factor of 2 or more above the minimum level required to perform the tests with the nominal Constellation-X area plus there are additional viable candidates based on source variability considerations.

The product of the flux (Table 4-3 column 3) and the orbital timescale (Table 4-3 column 4) results in a figure of merit (FOM) that measures our ability to do this science. This figure of merit (FOM) scales linearly with the area at 6 keV. Higher FOM requires lower area to achieve the same signal/noise in one orbital timescale. For 6,000 cm^2, and using the units in Table 4-3, simulations show that a minimum required FOM is 50 (ks x 10^{-11} ergs/cm^2/s 2 - 10 keV). There are 14 AGN in Table 4-3 above this limit, and 11 below it. With the required 6,000 cm^2 these additional 11 targets could be observed when they are in a higher flux state, which would require X-ray monitoring from X-ray All Sky Monitors in order to trigger the observations, or repeated observations to catch the sources in a higher flux state. Flux variations of a factor of two are not uncommon in these sources, and they occasional vary by a factor of 10 or more. We note that the first source above the required value has an FOM of 101, implying that the required effective area would have to be missed by nearly 50% before one source was lost from the target list. The 2 - 10 keV fluxes in this table are from an ASCA survey of bright AGN that was completed several years ago. The ASCA data do not have the fidelity to derive accurate Fe Kα EW measurements, so we have computed these FOMs assuming a Fe line equivalent width (EW) of 200eV.

Given the importance of these GR tests we draw upon work in progress using *XMM-Newton* to measure Fe line EW for a sample of active galactic nuclei. The data show a range of EW with approximately 1/3 of the observed sources having EW > 100 eV. Using the actual EW and 2 – 10 keV fluxes measured by *XMM-Newton* for a subset of the sources shown in Table 4-3 and Figure 6-1, we find that 7 sources indicated by solid diamonds in the figure exceed the required FOM of 50 and have orbital periods <100,000 sec enabling a Constellation-X observing program spanning a number of orbital periods without extending the required measurement time to an unreasonably long duration. We have not changed the locations of the plotted points so the source NGC2922 lies below the threshold in the plot, even though the *XMM-Newton* data show that its flux and Fe line EW now place it above the threshold. These 7 sources form our initial prime sample which will be expanded as additional *XMM-Newton* observations become available.

Using the Fe Kα EW measurements, when available, for the sources in Fig 6-1 and scaling the FOM accordingly (also scaling for the newly measured 2 - 10 keV flux from *XMM-Newton*), we find that there are 8 sources demonstrated to be above our critical threshold for GR testing without having to assume a value for the Fe line EW. One of these, NGC 2110, is so massive that the orbital timescale is 200ks, making it difficult to envision observing the system for more than a few orbits. This system is therefore removed from our consideration, leaving the 7 sources highlighted by filled in diamonds in Fig 6-1. One of these, NGC 2292, was below the critical value based on earlier ASCA flux measurements, but is well above it based on these newer *XMM-Newton* measurements.

Given the available data, we believe that Table 4-3 and this figure are representative of what Con-X can achieve. As measurements improve, the list will certainly change, and likely grow. We note that the mass measurements for many of these systems are uncertain by a factor of a few and in a few cases up to an order of mangnitude, and that the errors in these measurements will also decrease with ongoing ground based (optical reverberation mapping) and space based (X-ray) observations. The measured data for this core sample of AGN suitable for testing GR in the strong gravity limit drives the effective area at 6 keV and makes this the most important requirement for us to achieve.

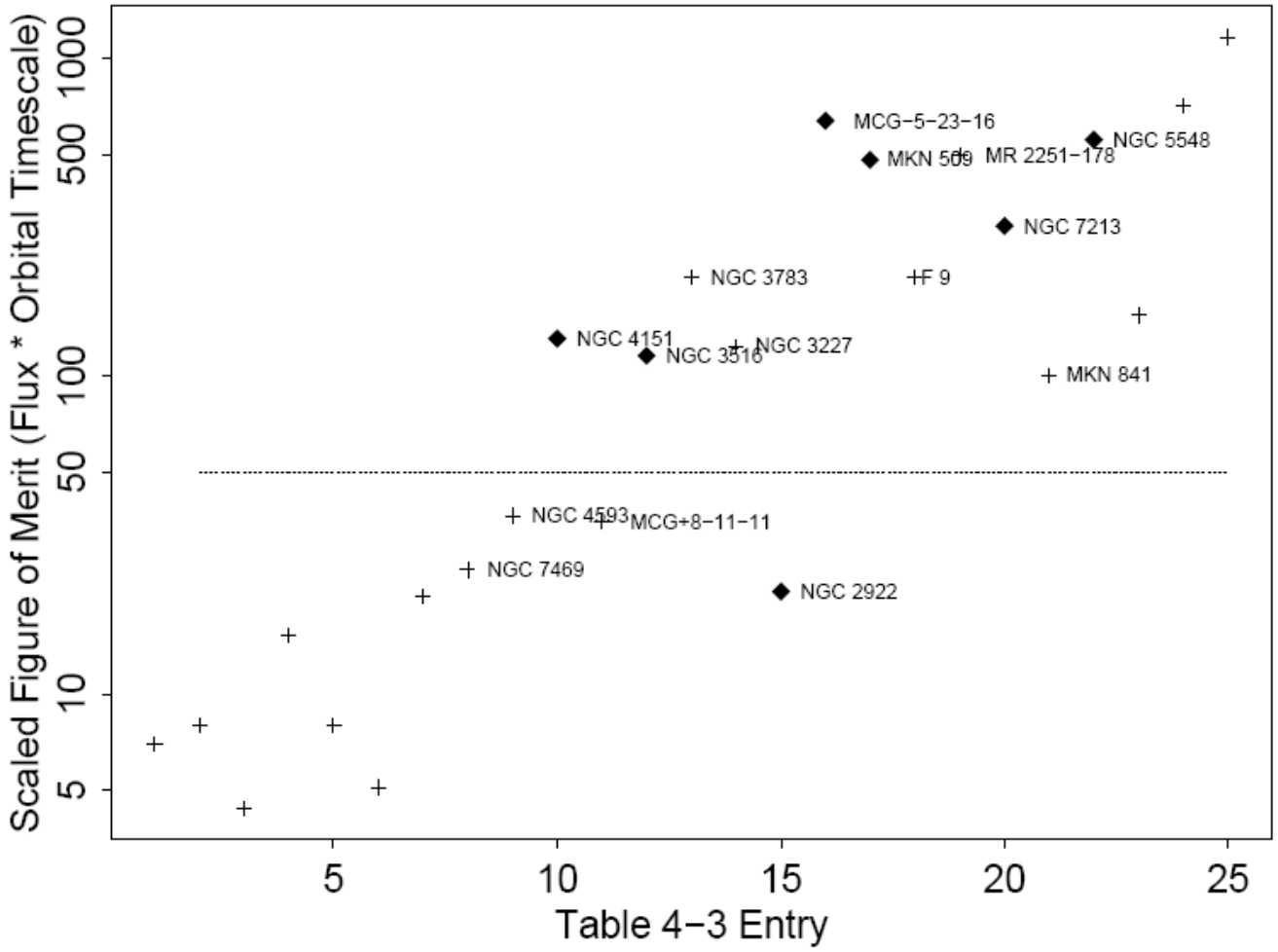

Figure 6-1. Figure of Merit for AGN GR Testing

Each of the AGN listed in Table 4-3 is plotted here, with the x-axis as the entry order in the table and the y-axis as its corresponding Figure of Merit (FOM) for GR testing. An object with a FOM higher than 50 in these units (above the dashed line) will allow single hot spots in the inner disk to be accurately tracked using an effective area of 6000 cm^2 at 6 keV. The AGN which meet both of these criteria form our prime target list and are labeled by name. Four additional AGN which are slightly below the line are also labeled, including NGC 2922. The 7 sources that are labeled with diamonds have more recent measurements of both the flux and the Fe Ka line strength from XMM-Newton that show them to be prime candidates for GR testing because the actual measured EW's of the Fe lines are used when determining that they exceed the required FOM. Note that the y-axis is logarithmic. Should the required 6000 cm^2 of area not be met, the critical FOM would increase by the same percentage that the area decreases. We can further be confident in this approach because NGC 3516 has been shown by Turner et al. (2002) to have transient narrow features seen simultaneously in the Chandra HETGS and XMM-Newton CCDs. This may be the signature of the brightest hot spots.

7. PROPOSED INSTRUMENTATION — TECHNICAL MATURITY

Question: Indicate the technical maturity level of the major elements of the proposed instrumentation, along with the rationale for the assessment (i.e. examples of flight heritage, existence of breadboards, prototypes, etc).

RESPONSE

All of the instrumentation required to fulfill the scientific requirements of Constellation-X have extensive heritage in several flight missions. In Table 7-1 below we summarize the status of the major elements of the Constellation-X instrumentation. This is followed by a detailed discussion of the heritage and maturity level. In all cases, research and development in these areas has progressed significantly toward demonstrating the major components of the technologies that will meet the scientific requirements of the mission. These include an approach for producing X-ray mirrors with very high effective area and excellent angular resolution, large arrays of X-ray microcalorimeters for true imaging X-ray spectroscopy with very high spectral resolution, X-ray gratings that have extremely high resolving power toward lower energies combined with high throughput, and very high-sensitivity X-ray imaging up to 40 keV.

The technology maturity of the Con-X instrumentation was assessed by an independent team as part of a review commissioned by the Director of the Goddard Space Flight Center in late 2005. The technology readiness levels assessed by that panel are summarized in Table 7-1.

7.1 SXT Flight Mirror Assembly (FMA)

7.1.1 SXT FMA Heritage

Con-X employs 4 identical Flight Mirror Assemblies (FMA), each comprising a pre-collimator module, a post-collimator module, and fifteen mirror modules. Of the 15 mirror modules, 5 are identical inner ones and 10 identical outer ones.

The Con-X FMA has its heritage in several X-ray astronomical missions. Its optical design is Wolter-I, the same as those of *Einstein*, ROSAT, *Chandra*, and *XMM-Newton*. Its modular approach has heritage in the Japan-U.S. missions ASCA and *Suzaku*, requiring similar numbers of mirror segments: 10,400 for Con-X vs. 6,800 for *Suzaku*. Its mirror segment fabrication technology, i.e., the thermal forming of glass sheets, has its heritage in the recently flown High-Energy Focusing Telescope (HEFT) — a collaborative effort between Caltech, Columbia University, and Lawrence Livermore National Laboratory. Its alignment and integration method has heritage in the extremely precise and successful *Chandra* mirror assembly. Also important, the development methodology of using normal incidence visible light metrology to accurately predict grazing incidence X-ray performance has been repeatedly demonstrated on all the aforementioned successful flight programs.

Table 7-1. Constellation-X Major Technologies and Status

Con-X Element	Heritage		Con-X	TRL
	Mission	Similarities to Con-X	Changes from proven heritage	
SXT FMA	Einstein ROSAT ASCA Chandra XMM-Newton HEFT Suzaku	Wolter Type I – type optics (all), thin mirror segments (ASCA, Suzaku), mass production (ASCA, Suzaku), mandral fab (XMM-Newton), hundreds of co-aligned mirror segments (ASCA, Suzaku), Angular resolution (XMM-Newton), Areal density (Suzaku and HEFT)	Combine: ▪ Angular resolution demonstrated by XMM-Newton. With: ▪ Number of mirror segments and areal density demonstrated on Suzaku and Heft	4
XMS – Microcalorimeter	XQC suborbital payload Suzaku/XRS	Microcalorimeter technology, wafer processing, operating temperature, ADR technology, data processing	Increased pixel count, multiplexed readout, cryogen-free operation	4
XMS – ADR	XQC suborbital payload Suzaku/XRS	Same basic technology as XRS ADR	Multistage ADR, passive heat switches, somewhat more complex control algorithm	4-5
XMS – Cryocooler	Under development for JWST	Low vibration, minimum power, cooling power	possibly use ^{3}He instead of ^{4}He to achieve lower operating temperature	5
XGS – Gratings	Sounding rockets Einstein Exosat Chandra XMM-Newton	Basic fab techniques, alignment tolerances, number of grating elements, data analysis	Increased line density, blazed transmission gratings or radially-grooved high line-density off-plane gratings	4
XGS – CCD's	ASCA Chandra XMM-Newton Suzaku	Number and size of pixels, basic fab processes, backside thinning, data processing and analysis	Higher efficiency backside processing, faster readout scheme	4
HXT – Optics	Swift InFocus HEFT HERO	Highly nested, graded multilayer coated mirrors for 10 – 40 keV (InFOCuS, HEFT). Electroformed thin Ni shells (HERO, Swift) Thermally formed segmented glass mirrors (HEFT)	Improved angular resolution for glass mirror or thinner electroformed shells for nickel mirror	5
HXT – Detector	Swift InFocus HEFT HERO	Number and size of pixels, basic fab processes, data processing and analysis	Improved shielding design and fabrication	5.5

Every aspect of the Con-X FMA technology has been achieved in past missions. Technology development for the Con-X FMA is to achieve the required and unique combination of good angular resolution, low mass, and high throughput. While its required angular resolution is comparable to that of *XMM-Newton*, the Con-X FMA must achieve this angular resolution with an areal mass density that is six times smaller. The required FMA areal mass density is comparable to those of *Suzaku* and HEFT, but the Con-X FMA must achieve this with an order of magnitude better angular resolution.

Figure 7-1. Mirror Segment Fabrication

Left: An illustration of the glass thermal forming process. The oven temperature is gradually increased from left to right. Right: A finished mirror segment

Our technology development has focused on constructing a mirror module, the basic building block for large mirror assemblies. Each mirror module consists of a number of mirror segments precisely aligned and bonded to a housing. Our technology development has two components: (1) fabrication of mirror segments and (2) alignment and bonding of those segments into a housing. The approach we have adopted meets requirements on mass, throughput, production schedule and cost. Hence, the focus of the technology development is to satisfy the angular resolution requirement.

7.1.2 Mirror Segment Fabrication

The fabrication of a mirror segment starts with a commercially available (Schott D263) borosilicate glass sheet, 0.44 mm thick. We place the sheet inside an electric oven atop a figured and polished fused quartz mandrel (Figure 7-1 left). As the oven temperature gradually ramps up to about 600°C, the glass sheet plastically deforms under gravity and wraps itself around the mandrel. After a period of time at 600°C to achieve thermal equilibrium, the oven temperature ramps down slowly to properly anneal the formed glass mirror. Once it cools to room temperature, we trim the formed mirror to its required dimensions. A layer of iridium is then sputtered onto the inner (concave) surface of the mirror to enhance its X-ray reflectivity (Figure 7-1 right).

Over the past five years, we have studied all aspects of this glass thermal forming process. We have shown that the thermal forming process is deterministic and is capable of producing mirrors meeting Con-X requirements. We are now consistently making mirrors which metrology shows to perform at 13 arcsec Half Power Diameter (HPD), to be compared with a 10 arc-sec HPD requirement at the mirror component level. The current performance of 13 arcsec is dominated by distortions near the mirror edges which may be caused by inadequate annealing, gravity, coating, etc. In the next year we will understand and mitigate those distortions to make mirror segments consistently meeting requirements over the full aperture.

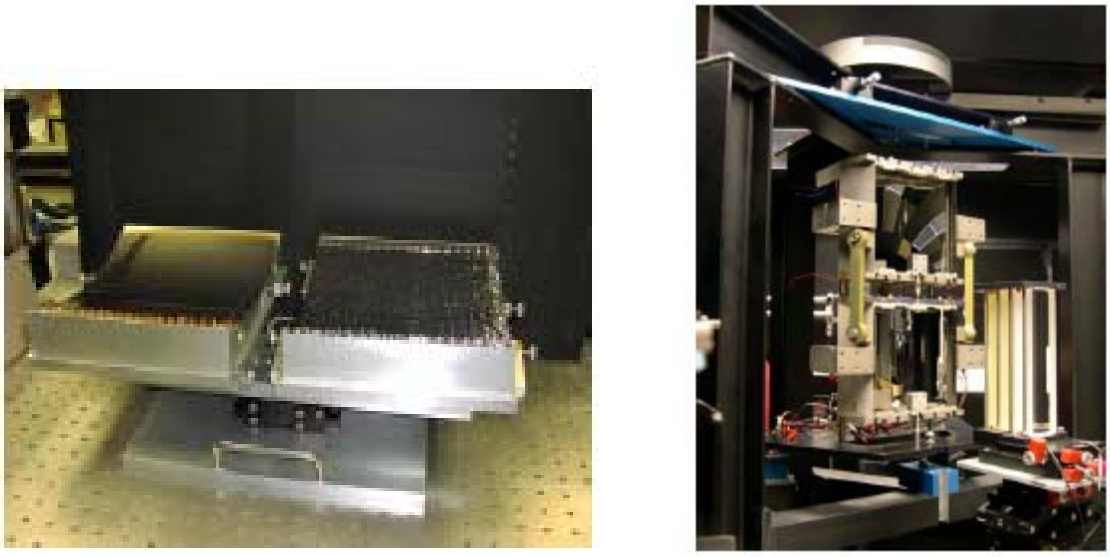

Figure 7-2. Mirror Mounting Methods

Two methods for mounting a mirror for metrology, alignment, and bonding into a module housing. Left: Method 1 or "passive" approach, horizontally oriented. Right: Method 2 or "active" approach, vertically oriented.

7.1.3 Mirror Segment Mounting and Alignment

We are developing two mounting methods in parallel. In each, we first mount the mirror segment to a rigid structure for alignment and bonding. In the first method (Figure 7-2, left), also known as the "passive" approach, the mirror lies on its back (reflective surface up), supported by an array of very soft springs and temporarily bonded to a rigid frame. Next we place the supported mirror on a 6 degree-of-freedom (DOF) stage for integration into the module. We then align the mirror using the Hartmann test with a collimated beam of visible light and bond the mirror in place (Figure 7-3). In this "passive" approach, we hold each mirror in its natural shape. The Hartmann test alignment metrology is identical to that used for *Chandra*, which had substantially tighter alignment requirements. After completing these steps for a mirror, we repeat them for the subsequent mirrors. The alignment sequence – the order of aligning the various primary and secondary mirrors to achieve confocality of the many mirror shells – also was developed and employed on the *Chandra* Observatory. In the second method (Figure 7-2 right), also known as the "active" approach, we utilize 10 radial actuators (5 each at the forward and aft ends of the mirror segment) to tip, tilt, and radially translate the mirror. We also can use the actuators to improve the mirror's low order figure, should it be necessary. Otherwise, the second method proceeds the same way as the first method (Figure 7-3), except that we maintain a vertical orientation during alignment and bonding to minimize gravity distortion.

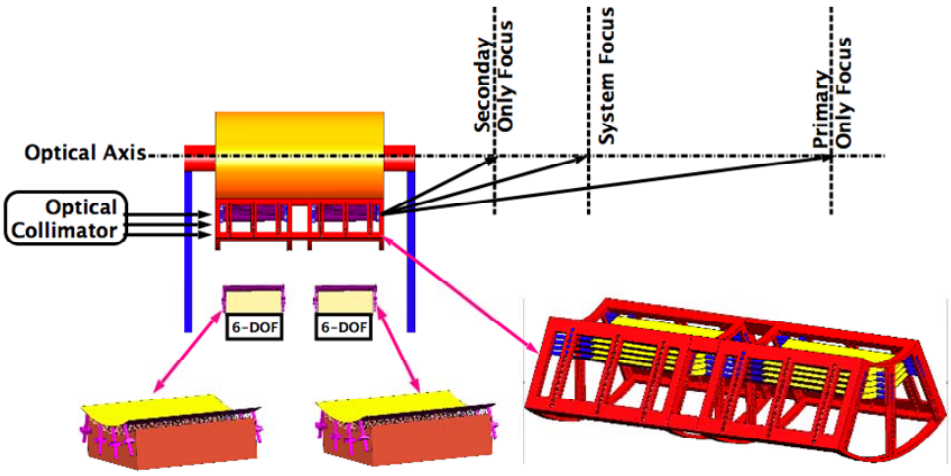

Figure 7-3. Mirror Alignment and Bonding

An illustration of the mirror alignment and bonding process using Method 1 ("passive" approach). Procedures for alignment and attachment to the module housing ensure both optical precision and mechanical robustness. The apparatus for Method 2 ("active" approach) is similar, but vertically oriented.

Thus far, we have learned how to hold and mount individual mirrors. We are investigating specific procedures to bond the mounted mirrors to a rigid structure simulating a module housing. Meanwhile, we are beginning to design a module housing that is capable of accommodating multiple pairs of mirrors, in order to demonstrate alignment of many mirrors simultaneously.

7.2 X-Ray Microcalorimeter Spectrometer (XMS)

7.2.1 Microcalorimeter Heritage

The XMS instrument is based on X-ray microcalorimeters for high resolution, high throughput X-ray spectroscopy that have been developed over the last 20 years for astrophysics and laboratory spectroscopy. The first implementation of a microcalorimeter for astrophysics was on a suborbital payload for measuring the spectrum of the diffuse X-ray background (McCammon et al. 2002). This research program continues today and a flight with an improved array is being prepared for launch in later 2007. A major benchmark for the XMS technology readiness is the XRS instrument on the *Suzaku* Observatory. This instrument featured a 32-channel microcalorimeter array (Figures 7-4 and 7-5) operating at 60 mK, a single-stage ADR, and digital processing electronics capable of on-board optimal pulse height analysis. These implementations have used ion-implanted Si for the thermometer with separately attached X-ray absorbers.

Given the flight heritage of this technology, TES microcalorimeters were identified at the beginning of the Con-X development program in 1998 as the best approach for producing significantly larger arrays of faster, higher- resolution pixels (see response to Question 5 for a more comprehensive discussion). The rapid progress in TES technology, the theoretical prediction of 2 eV resolution, and the potential for large scale multiplexing with superconducting read-out combined to recommend TES development for the XMS baseline. Since the mid-1990's, an extensive and comprehensive research and development program in TES technology, including their superconducting readout electronics, has been carried out by

several groups around the world. In parallel with this, the field of sub-kelvin cooling technologies has advanced to the point where one can plan for a long-life, cryogen-free instrument. Significant milestones in this development program are itemized in the response to Question 16.

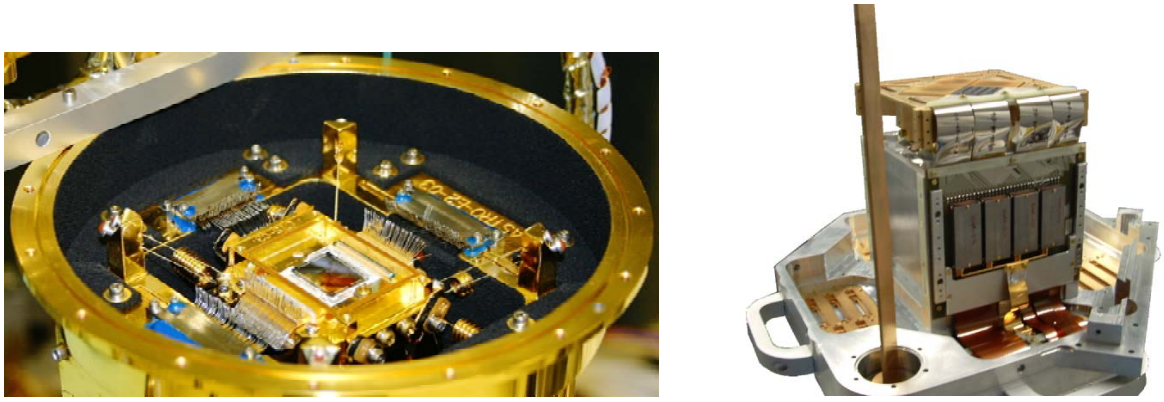

Figure 7-4. Suzaku and SCUBA Detectors

Left: The Suzaku/XRS focal plane assembly. The 32-channel microcalorimeter microcalorimeter array is at the center. There are two JFET amplifier assemblies on either side. The detector box is suspended on tensioned Kevlar stings for high strength, a high mechanical resonant frequency for isolation from launch vibrations, and yet very low mass and very high thermal isolation. Right: The SCUBA-2 850-μm camera, with one of four 1,280-pixel sub-arrays installed, represents the state of the art in a very large focal plane assembly for thermal detectors (in this case bolometers, but essentially the same as microcalorimeters.) These two assemblies encompass the range of technologies needed to produce the Con-X XMS focal plane assembly.

The time-division SQUID multiplexers to be used for the TES readout are now in use in a large number of instruments for a wide range of applications, including astronomy (millimeter-wave and submillimeter), nuclear and particle physics, and materials analysis. In particular, a large number of astronomical instruments are incorporating NIST SQUID time-division multiplexers (TDM) to read out their transition-edge sensors. Cosmic Microwave Background instruments using NIST TDM include the Atacama Cosmology Telescope (PI institute: Princeton), CLOVER (United Kingdom), SPIDER (Caltech), PAPPA (Goddard Space Flight Center), MUSTANG (NRAO / University of Pennsylvania), and BICEP-2 (Caltech). Submillimeter instruments incorporating NIST TDM include SCUBA-2 (United Kingdom), ZEUS (Cornell), GISMO (Goddard Space Flight Center), and FIBRE (Goddard Space Flight Center).

The largest of these is the SCUBA-2 instrument, a submillimeter camera that will have more than 10,000 superconducting transition-edge sensors operating at 450 μm and 850 μm (Figure 7-4). The SCUBA-2 instrument is divided into 8 sub-arrays, each incorporating 1,280 pixels of TES submillimeter bolometers and SQUID multiplexers.

SCUBA-2 will be a facility instrument on the James Clerk Maxwell Telescope on Mauna Kea in Hawaii later this year. While the technical requirements of the SCUBA-2 instrument are different from Constellation-X's (particularly in the bandwidth requirements), this instrument has driven the development of mature infrastructure for reading out many thousands of pixels of multiplexed transition-edge sensors.

Other significant non-astronomical applications incorporating time-division SQUID multiplexers include particle physics, soft X-ray spectroscopy for materials analysis for the semiconductor industry,

and hard X-ray and gamma-ray spectroscopy for nuclear materials analysis for the National Nuclear Security Administration (NNSA). A collaboration of NIST and Los Alamos National Laboratory (LANL) has developed arrays of multiplexed TES gamma ray spectrometers for this application.

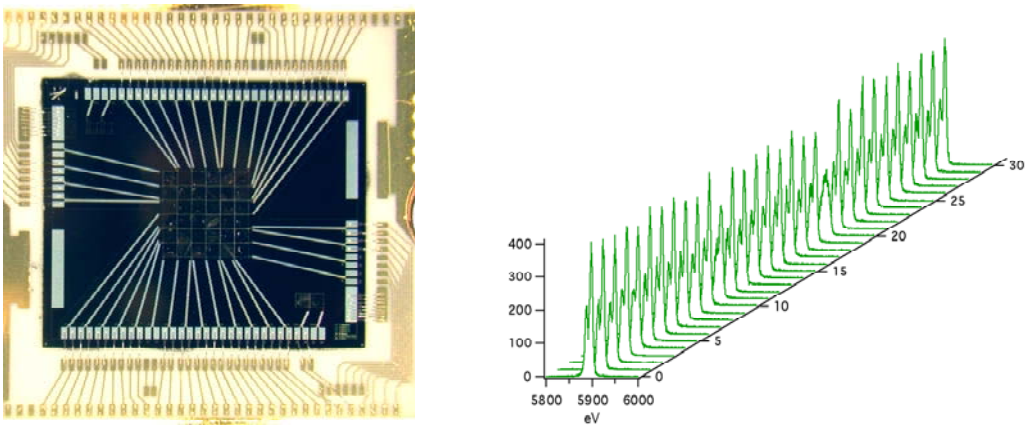

Figure 7-5. Suzaku XRS Array and Spectral Performance

Left: The Suzaku/XRS microcalorimeter array. The pixels are each 625 μm and based on ion-implanted Si with HgTe absorbers. Right: The XRS achieved 7 eV in orbit and demonstrated a very high degree of uniformity. The ADR system required to cool the array to 60 mK also worked flawlessly.

7.2.2 Microcalorimeter Array

Members of the Con-X team are among the leading groups advancing the technologies of TES calorimeters. We routinely fabricate close-packed 8x8 arrays and have recently demonstrated a design using Au absorbers that achieves a spectral resolution of 2.5 eV (FWHM) at 6 keV (Figure 7-6). This resolution meets the Con-X requirement and the results are in preparation now for publication. This result was obtained in a laboratory system that incorporates many of the components required for a flight detector system, including associated superconducting electronics (single channel only, non-multiplexed), a single-stage ADR, temperature regulation, and appropriate magnetic shielding.

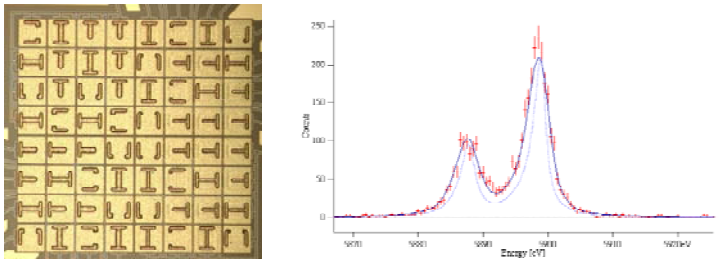

Figure 7-6. TES Development Array

Left: An 8x8 development TES array for Con-X with 250 μm pixels. Each pixel has a 4-μm-thick Au absorber and meets the Con-X requirement for fill-factor and quantum efficiency. Right: Pulse height spectrum obtained using 55Fe source. The energy resolution is 2.5 eV (FWHM) and meets the Con-X requirement for spectral resolution at 6 keV.

7.2.3 Particle Veto Detector

The XRS instrument on *Suzaku* utilized a charge-sensitive anticoincidence detector behind the calorimeter array operated at the same temperature as the array (60 mK). We will employ a similar approach for the XMS, but will modify the sensor to be compatible with the SQUID readout technology that will be used for the TES's. Minimum ionizing particles, which are expected to be the main source of in-band background events, deposit around 4 MeV/cm in Si. A particle traversing a 400 μm Si wafer will therefore deposit at least 160 keV. Instrumented with TES sensors, such a wafer placed in close proximity to the microcalorimeter array would serve as a highly efficient anti-coincidence detector. The rise and fall times of the pulses are on the order of a few μs and 100-μs, respectively, which are very similar to the X-ray signal pulses. This permits 100% efficiency in correlating the anti-coincidence and microcalorimeter events. Particle detectors based on this principle have been used in dark matter searches for several years. The Cold Dark Matter Search (CDMS) Project has been able to achieve an energy resolution of 300 eV FWHM with detectors that are 7.5 cm in diameter and 1 cm thick.

7.2.4 Focal Plane Assembly Technology

The focal plane assembly includes the microcalorimeter array, SQUID electronics, particle veto detector, thermometry, thermal isolation suspension systems, heat sinking, wiring interconnects, and high-density wiring feedthroughs. The assembly must maintain the following at an acceptable level: 1) thermal stability, thermal gradient across array, and thermal crosstalk, 2) electrical crosstalk, microphonics, magnetic shielding, and susceptibility to interference, and 3) conducted and radiative heat loads on all the temperatures stages. The design of this assembly will be guided by the flight experience with *Suzaku*/XRS, the X-ray Quantum Calorimeter sounding rocket program, and our laboratory test platforms, including numerous systems in use at NIST, Goddard, and LLNL.

7.2.5 Array Readout

The resistance change in each TES is sensed by measuring the change in current in its bias circuit with a SQUID. To meet the bandwidth requirements, series-array SQUIDs must be used as one stage of the current amplification. Although a 32 x 32 TES microcalorimeter array, for example, can be read out using 1024 independent channels of electronics, reducing the number of channels through use of a SQUID multiplexer significantly reduces the heat load on the ADR, and the complexity of the front-end assembly. A time-division multiplexing scheme in which each 32-pixel column is read by one series-array SQUID is in development. Each TES pixel is sampled by its own input SQUID, which is switched on and off by the MUX controller.

While multiplexed readout of large arrays of submillimeter-wave transition-edge sensors (TES's) has been successfully demonstrated, the development of multiplexed arrays of TES X-ray microcalorimeters is more challenging. Fast X-ray pulse response times place stringent demands on the multiplexer dynamic range and bandwidth. In the current state of the art for X-ray TES read-out, a resolution of 3.74 ± 0.12 eV (FWHM) measured at 6 keV from a sub-150 μs TES in an 8-channel MUX has been achieved. In addition, we have calculated the number of detectors that can be multiplexed as a function of open-loop system bandwidth, amplifier noise, and detector time constant. The open-loop bandwidth and SQUID noise required for a 32-channel MUX for the XMS are 12 MHz and 0.25 $\mu\phi_0/\sqrt{\text{Hz}}$, respectively.

7.2.6 ADR Technology

7.2.6.1 ADR Heritage

ADRs are solid-state coolers with the capability of reaching temperatures well below those required for Constellation-X, with the advantages of very high efficiency and no reliance on gravity for operation. They have significant flight heritage, having been used successfully on the XRS instrument on *Suzaku*, and on three suborbital rocket flights. All of these were single-stage ADRs operated with a superfluid helium bath (at 1.3-1.5 K) in a single-shot manner. Constellation-X, however, requires a significantly larger operating range, since the ADR must reject heat to a < 6 K cryocooler, and it requires significantly higher cooling power to support the larger detector arrays. It will therefore use a Continuous ADR (CADR) that is uniquely capable of meeting these requirements within allowable mass constraints.

7.2.6.2 ADR Status

The CADR contains multiple stages connected in series through heat switches. Each of these stages is configured and operated in the same manner as a single-stage ADR. The basic elements are a magnetic refrigerant suspended in the bore of a superconducting magnet, and a heat switch to connect it to a heat sink. Magnetizing the refrigerant aligns the magnetic spins and suppresses their entropy, resulting in the generation of heat; conversely, demagnetizing allows the spin system to absorb heat and to cool down. The typical cycle is a discrete sequence of steps where 1) the refrigerant is magnetized to warm it above the heat sink, 2) the heat switch is closed so heat is transferred to the sink as magnetization continues, 3) the heat switch is opened once full field is reached, and 4) the refrigerant is demagnetized to cool down to, and maintain, the operating temperature.

Using multiple stages in series allows detectors to be cooled continuously, with several very important benefits that include much higher cooling power, lower temperature capability, higher heat sink temperatures and lower overall mass. One stage is used to maintain constant detector temperature, and a number of upper stages are used to periodically transfer heat from that stage in cascade to the heat sink. The number of upper stages depends on the temperature span and heat switch characteristics, and for Constellation-X is three, requiring a total of four stages. But because the cycle period can be short – as little as 15 minutes – the mass of each of these stages is considerably less than for single-shot systems. Thus, the prototype CADR for Constellation-X (Figure 7-7) achieves more than 10 times the cooling power of the XRS ADR, with about half the mass. Additionally, operating temperatures as low as 35 mK have been demonstrated, as well as the ability to reject heat at temperatures as high as 5 K.

The CADR uses the same basic design and configuration for salt pills, magnets and heat switches as the XRS ADR, and the assembly and manufacturing processes for nearly all components are extensions of those developed during its flight build. The main differences are the use of passive, rather than active, gas-gap heat switches for the upper stages, the use of a superconducting heat switch for the first (or continuous) stage, and the much smaller refrigerant capsules (called “salt pills”) and magnets. All of these have been extensively tested over several years of developing the prototype 4-stage CADR, and wherever specific concerns existed for the XRS ADR, new designs and manufacturing techniques were employed to eliminate them. For example the gas-gap heat switch used on XRS was part of the structural load path for the salt pill, and it used epoxy and solder seals that had to be leak tight after repeated thermal cycling. The new heat switch design has far fewer joints and seals, uses only braze or indium seals, and removes the switch from any salt pill load path. Therefore, at the component level, the XRS heritage conveys a high level of maturity to present designs.

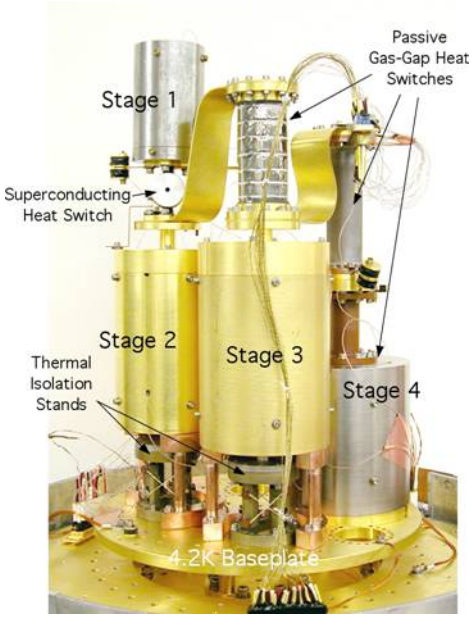

Figure 7-7. Photo of Technology Demonstration Continuous ADR

7.2.7 XMS Cryocooler

7.2.7.1 XMS Cryocooler Technology Heritage

Cryocoolers with all Constellation-X essential technology have flown in space since the early 1990's with near-perfect performance. Half of the coolers have been operating for 5-10 years, some having outlived their instrument or mission. All of these applications required cooling between 50 K and 80 K. Coolers operating around 35 K have also been developed, but Constellation-X requires even lower temperature cooling.

To address cryocooler development for a new generation of space observatories, requiring cooling at 6-18 K, NASA initiated the Advanced Cryocooler Technology Development Program (ACTDP) in 2001. The James Webb Space Telescope (JWST), the Terrestrial Planet Finder (TPF), and the Constellation-X programs provided detailed requirements for prototype ACTDP refrigerators. Three alternate concepts were developed during the program: two hybrid systems using Stirling/Joule-Thomson and pulse tube/Joule-Thomson combinations, and the other a four-stage pulse tube.

Ball Aerospace's ACTDP cryocooler concept utilizes a multistage Stirling refrigerator to precool a Joule-Thomson (JT) loop powered by an Oxford-style compressor with reed valves. The JT loop provides remote cooling of both 6 K and 18 K loads to as much as 25 meters. The Northrop-Grumman ACTDP cryocooler concept is similar in operation to Ball's, but the Northrop version utilizes a three-stage pulse tube cryocooler to precool the JT loop instead of a Stirling cooler. Lockheed-Martin's ACTDP cryocooler concept utilizes a 4-stage pulse tube refrigerator to directly cool 6 K and 18 K loads.

Though the Ball and Northrop coolers targeted JWST requirements and the Lockheed cooler targeted Constellation-X requirements, all three technologies remain candidates for the XMS cooler.

7.2.7.2 Cryocooler Technical Maturity Level

At the completion of the Advanced Cryocooler Technology Development Program (ACTDP) in January 2006, 6-Kelvin cryocooler technology was considered at TRL-5. The Northrop-Grumman cooler was selected for use on the James Webb Space Telescope which, through further development, will reach TRL-6 by the end of January, 2007. Lockheed-Martin has since pushed their ACTDP technology to develop a 4.5 K cryocooler for a ground-based DOD application. This advance addresses the ADR-cooler interface temperature risk identified by the 2006 NASA technology assessment.

7.2.8 XMS Blocking Filters

The XMS requires a series of blocking filters to minimize the thermal load on the coldest stages of the dewar system and detector array, yet provide the highest possible X-ray transmission. This is typically done with very thin aluminized polymer films. The *Suzaku* XRS instrument had five such filters that were about 150 nm thick each. The outermost of the five, mounted to the dewar mainshell, also had a nickel mesh for additional structure support. The filters were manufactured by the Luxel Corporation, which has produced the blocking filters for all X-ray observatories over the last 25 years. For the XMS, the blocking filters will be about a factor of two thinner to enable throughput down to 0.3 keV (and below in transition bands just below the carbon K-edge and aluminum L-edge). Luxel has maintained a continuous research and development program in this field to produce polyimide films optimized for strength at very low temperatures. This work has been funded to a large extent by the NASA Small Business Initiative Program (SBIR). Their track record in this field has been excellent and it is highly likely that they could produce the blocking filters required for the XMS.

Although Luxel is certainly a frontrunner in the field of thin-film blocking filters for use in low temperature systems, there are other labs that could produce such filters. The Lebow Company is another viable commercial supplier of X-ray filters. Another possibility is the X-ray group at the University of Wisconsin (D. McCammon). They have extensive experience producing very thin parylene filters for low-energy diffuse X-ray background work, including the XQC calorimeter sounding rocket payload. They have also embarked on a research program to make very fine Si support meshes for blocking filters that, in additional to providing additional structural support, can be patterned with resistive heaters and used to defrost filters with very low power (much like automobile rear window defrosters).

7.3 X-ray Grating Spectrometer (XGS)

7.3.1 Flight Heritage

The Con-X XGS will consist of an array of dispersive grating elements implemented along the optical path of the SXT, and CCD detectors to image the spectra. Two different XGS concepts are currently under study, one that utilizes transmission gratings and one that utilizes reflection gratings. Each of these concepts builds on a strong heritage of successful flight operations. Transmission gratings have been flown on the Objective Grating Spectrometer (OGS) on *Einstein*, and the Transmission Grating Spectrometer (TGS) on *EXOSAT*, among other X-ray missions. Transmission gratings are currently in use on the High- and Low-Energy Transmission Grating Spectrometers (HETGS and LETGS) onboard the *Chandra* X-ray Observatory. Reflection Gratings are used in two different configurations, “in-plane” where the incident light is perpendicular to the grooves, and “off-plane” where the incident light is parallel. In-plane reflection gratings are currently in use on the Reflection Grating Spectrometer

(RGS) on *XMM-Newton*. Off-plane reflection gratings have been flown on numerous UV and X-ray sounding rocket missions, including the recent flight of the University of Colorado's 'Cygnus X-ray Emission Spectroscopic Survey' (CyXESS). X-ray CCD detectors have a rich history and heritage. They are currently in use on the Advanced Camera for Imaging Spectroscopy (ACIS) on *Chandra*, the European Photon Imaging Camera (EPIC) on *XMM-Newton*, the X-ray Imaging Spectrometer (XIS) on *Suzaku*, and have been used by many other satellites and balloon missions.

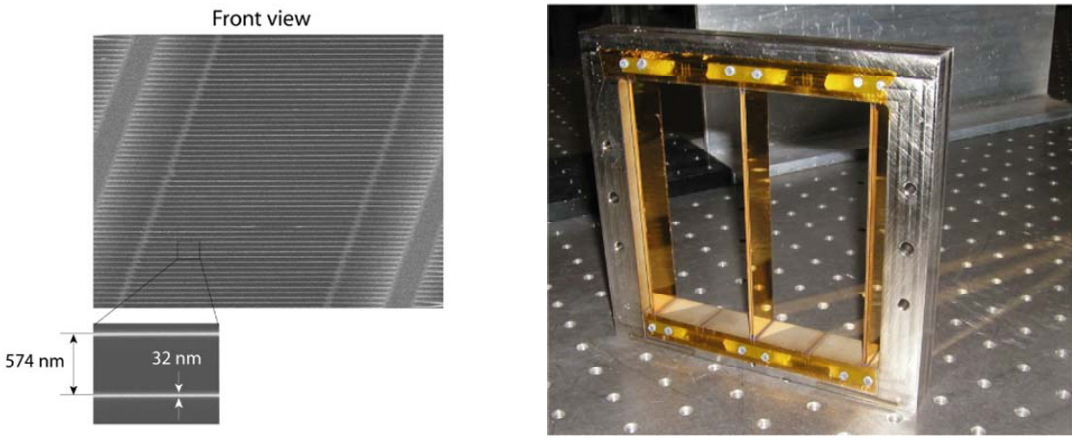

Figure 7-8. Images of Transmission Gratings and Off-plane Reflection Gratings

Left: Electron micrograph of the blazed transmission grating fabricated at the Space Nanofabrication Laboratory at MIT. Right: Three mounted off-plane gratings used in University of Colorado sounding rocket.

7.3.2 Transmission Grating Fabrication

The transmission gratings proposed for the Con-X XGS involve a few key technology advances compared to the transmission gratings previously flown. To achieve the high spectral resolution, the gratings require a factor of two increased line density and a factor of 10 increased facet size compared to the *Chandra* HETGS gratings. To achieve the high efficiency, the gratings are blazed such that all of the dispersed efficiency lies asymmetrically in the positive spectral orders. This requires fabricating extremely smooth, thin, high aspect ratio bars that are inclined at angles less than the critical angle of total internal reflection. Each of these fabrication elements has already been demonstrated as part of the Con-X grating technology development program. Gratings have been fabricated with the necessary line density of 10,000 lines/mm. Gratings have been fabricated with a diameter of 300 mm, which are much larger than the proposed 15mm by 15 mm facets. Super-smooth reflection gratings, fabricated by anisotropic etching of crystalline silicon, have been fabricated and have shown record high spectral efficiency. The same etching technology is used to produce the blazed transmission gratings. A blazed transmission grating has been fabricated that meets the required smoothness, aspect ratio, and angle (Figure 7-8 left). A flight prototype grating is scheduled for completion and testing by the Spring 2008.

7.3.3 Reflection Grating Fabrication

The reflection gratings proposed for the Con-X XGS also involve technology advances relative to the reflection gratings previously flown. To achieve high spectral resolution, the gratings require line densities in excess of 5,000 lines/mm with grooves that are radially oriented rather than parallel in order to match the convergence of the X-ray beam. These XGS gratings would also need to be thinner and flatter than those used in sounding rocket experiments. Each of these key properties has been

demonstrated on previous missions or as part of the Con-X grating development program. In the configuration currently under study, the reflection gratings substrates flown on the *XMM-Newton* RGS are sufficiently thin and sufficiently flat for the XGS. Radially-grooved off-plane reflection gratings have been flown on X-ray sounding rockets, but with lower line densities. The gratings flown on the recent CyXESS sounding rocket had line densities of 5670 lines/mm, although they were not radially-grooved (see Figure 7-8 right). The commercial vendor Horiba Jobin Yvon (France), in collaboration with the University of Colorado is in the process of manufacturing a holographically-ruled radially-grooved reflection grating with a line density in excess of 5000 lines/mm. The completed grating will be delivered in the summer of 2007.

7.3.4 CCD Detectors

The basic technology used to fabricate the *Chandra* and *Suzaku* CCDs can be used to fabricate the devices for Con-X. Special backside processing is required to achieve the required low energy quantum efficiency. The Molecular Beam Epitaxy (MBE) process, which has recently been developed at MIT/Lincoln Laboratory, will be used for the XGS devices. X-ray tests of MBE processed devices show spectral resolutions of ~50 eV at the low energy end of the Con-X grating band. X-ray quantum efficiency tests have not yet been performed: however, modeling the charge collection properties from the resolution measurements suggests these devices have the necessary QE. Optical blocking filters are required to minimize the electronic noise on the detectors. The CCD devices planned for the XGS will utilize on-board pixel summation, or "superpixels," to achieve frame readout rates of 13.8 ms. At these rates, 100 Å of aluminum directly deposited on the surface of the CCD, is sufficient to limit the light leakage. Direct deposition of aluminum has been demonstrated on the *XMM-Newton* RGS CCDs.

7.4 Hard X-ray Telescope

Figure 7-9. Images of HXT Mirror Technology

Left: HEFT nested glass mirrors. Right: Two nickel mirror shells installed in structure prior to testing at the Panter X-ray Facility.

7.4.1 Flight Heritage

The two fabrication concepts under consideration for the Hard X-ray telescope mirrors, thermally formed segmented glass and electroformed nickel shells of full revolution, have considerable flight heritage (Figure 7-9). The overall design for the mirrors are similar in both cases, the major difference being the technology used to produce the mirror shell. The nickel shells are manufactured using a replication process in which thin nickel shells are electroformed on super-polished electroless-nickel-plated aluminum mandrels from which they are later released by differential thermal expansion. The glass shells are fabricated by placing thin sheets of glass onto forming mandrels and applying heat to thermally slump the glass to the mandrel. The thermally formed segments are then assembled into a complete shell.

Thermally formed segmented glass technology with multilayer coatings has been flown on the HEFT instrument (Figure 7-9, left). This mirror module is similar to the design concept for the Constellation-X HXT, but with a less stringent angular resolution requirement. The thermally formed segmented glass, which is under development now at GSFC for the SXT mirror, will more than meet the 30 arcsec requirement.

The electroformed-nickel-replication process has been used very successfully on previous missions to fabricate the telescopes for *Swift* and *XMM-Newton*.

Both of these telescopes have angular resolution of less than 20 arcsec, which more than meets the 30 arcsec requirement of Constellation-X, however these shells are thicker than those necessary to meet the mass constraints for Constellation-X. Since the Technology Assessment Panel in 2005, several milestones for nickel replication have been met: shells of the appropriate thickness of 100 microns have been fabricated, multilayer coated, assembled (Figure 7-9, right) and tested in full beam illumination and have been shown to have angular resolution of better than 30 arcsec.

The cadmium-zinc-tellurium (CZT) detectors being considered for the HXT focal plane are well developed and also have considerable flight heritage. CZT focal plane arrays have flown on satellite missions such as *Swift* and also on HEFT and InFOCuS balloon flights. Considerable work has also been accomplished on the design of the particle shielding, a concern listed in the Technology Assessment.

8. OVERALL COMPLEXITY LEVEL OF INSTRUMENT OPERATIONS

Question: Briefly describe the overall complexity level of instrument operations, and the data type (e.g., bits, images) and estimate of the total volume returned.

RESPONSE

8.1 Overall Operational Complexity

On-board operational complexity is low for the Con-X instrument suite. All of the instruments view the same target, and operate simultaneously. Observing plans are uplinked to the spacecraft on a regular basis (approximately twice per week), and normal operations of the instruments do not require real-time contacts. There are no event-driven changes to instrument operations except for safehold.

There is one science mode for the XMS and HXT and a handful of science modes for the XGS (see Question 13 for a description of the instrument operational modes). Each instrument also has a calibration mode that may involve turning on (or bringing into the field of view) a calibration source. Such a mode still produces the standard data output.

Each instrument also has a limited number of engineering modes, such as initialization, diagnostic, bakeout, etc (see Question 13 for a more information on engineering modes). Execution of these modes are typically determined on the ground, and the commands to execute a mode are uplinked as part of the regular ground contact. With the exception of safehold, these modes are not autonomously implemented.

8.2 Data Type and Volume

The data produced by each instrument is a time-tagged photon event list with energy and positional information, from which images and spectra can be constructed on the ground. This event list is a de facto standard for X-ray astronomy satellites.The total volume of data will depend directly on the number of sources observed with a specified flux. We have developed a very conservative (i.e., brighter than we expect) “average” source and a “bright” source, which allow us to estimate the count rates and data volumes for planning purposes (sizing of the onboard communications system hardware and protocol, Ka band data link, on-board storage, and ground data system capabilities, etc). This “average” source is 5 mCrab, with a power law index of 1.8, while the “bright” source is 0.25 Crab. Using these sources, we reiterate in Table 8-1 the information contained in Question 34, except that we do not include the spacecraft and instrument house-keeping rates, which are comparatively small.

To estimate the total data volume, we followed the protocol of using the average data rate for 97% of the mission life, and the peak data rate for 3% of the mission. Note that for sizing purposes, we assume that the instruments operate 100% of the time.

Table 8-1. Instrument Data Types and Volumes

Instrument	Nominal Data Generation Rate (kbps)	Peak Data Generation Rate (kbps)	Data Type	Total Volume Returned (5 year life) (Terabytes)
XMS	38	300	time tagged photon event lists	7.4
XGS	87	867	time tagged photon event lists	17.8
HXT	17	150	time tagged photon event lists	3.4
TOTAL				**28.6**

9. DESCOPE OPTIONS

Question: If you have identified any descope options that could provide significant cost savings, describe them, and at what level they put performance requirements and associated science objectives at risk.

RESPONSE

Our general approach to the Constellation-X mission has been to establish requirements absolutely needed to achieve the science objectives. In a few areas we have established performance goals - angular resolution and spectral resolution for example - where achievement of the goals (or even nearing them) would produce a very substantial increase in science performance. We are optimistic that these goals can be achieved (or least significant steps towards them are possible). Performance levels associated with goals have not yet been demonstrated, so setting them as goals limits potential cost and schedule impacts while we endeavor to achieve them and realize the substantial gains they provide.

In direct response to the question posed here, we have identified three descope options. If mass margins are substantially eroded or costs increase substantially, we would consider them in the order presented here (see also Question 22)

9.1 Reduce the Outer Diameter or Number of Nested Shells in the 4 SXT Configuration

A range of mass and cost savings can be achieved under this option depending on how many and which shells are deleted, so it could be tailored to deal with the actual scale of a problem. For example, deleting the outermost 16 shells (~10%) from the four mirror assemblies would reduce the area at 1.25 keV by ~25% while reducing the area at 6 keV by only ~2%. Mass savings in the optics and the associated structures would be of order 320 kg for this descope option, or about 5% of the mission mass.

Cost savings would depend on the timing of such a descope, particularly since mirror mandrels are purchased early in the program, design work for the Flight Mirror Assembly (FMA) is scheduled upfront, and plans and construction of facilities for FMA production are also long-lead items.

In terms of science impact, the General Relativity (GR) tests using iron lines would see minimal impact from such a descope, while we would compensate for photons lost at lower energies by increasing exposure times as described further under option 2.

9.2 Reduce from 4 to 3 SXTs

Under this descope, the area at all energies would be reduced to 75% of the predicted level. For many observations longer exposure times could compensate for reduced throughput, although fewer observations could be accomplished over a fixed mission lifetime. The most significant impact of this potential descope would be for observations requiring detection of substantial numbers of photons on short time-scales. For example, to carry out X-ray tests of strong field GR using matter orbits or photon orbits to probe the spacetime metric with a reduced area, we would either have to select from a smaller set of the brightest sources and/or select sources with larger black hole mass and therefore proportionally longer time-scales of interest.

The mass savings from deleting one SXT would be very substantial, ~741 kg for the FMA and XMS alone, with additional reductions likely occurring elsewhere in the structure and spacecraft. For this

descope, the cost savings would be ~$50M which represents the incremental production costs of the 4th FMA and the 4th XMS. There would be further modest savings associated with spacecraft bus subsystems such as power and mechanical as well as reduction in time needed for payload integration and test and overall shortening of the mission development schedule by 3 - 4 months.

9.3 Delete All or Part of the HXT

This descope could provide a mass reduction up to 100kg with modest cost savings in the range $20 - 30M. Impacts on GR tests via rapid iron line variability would be minimal. However, there would be science impacts on studies of active galactic nuclei - especially the obscured sources which may dominate the 20 - 40 keV all-sky X-ray signal - and the precise measurements of black hole spins. This would also impact our ability to constrain relativistic particles or magnetic fields in clusters.

An option to mitigate deletion of the HXT would be to add multi-layers to the SXT mirror assembly to extend performance to higher energies while also extending the upper energy range of the XMS detectors. Risks associated with such an option include lessened angular resolution for the SXT contrary to our goals of achieving of 5 arcsec angular resolution (vs. a requirement of 15 arcsec). A descope which includes this mitigation option is unlikely to result in a net savings in cost, but would provide an option for dealing with mass growth.

Given the modest cost and mass savings associated with this descope option, it is unlikely that we would recommend its implementation.

10. SCIENCE AND INSTRUMENTATION — THREE PRIMARY TECHNICAL ISSUES/RISKS

Question: In the area of science and instrumentation, what are the three primary technical issues or risks?

RESPONSE

The foundation for the scientific success of Constellation-X has been established by the many thousands of sources already observed by *Chandra* and *XMM-Newton*. Source positions, fluxes, and many low-resolution spectra are already available, enabling Constellation-X users to plan their observing programs with high precision. For the brightest sources, *Chandra* and XMM grating observations show emission and absorption features which assure us that the detailed spectroscopy planned for Constellation-X will be incredibly rich, providing anticipated results for specific experiments along with a bounty of surprises opening new discovery space. Because of the wealth of existing knowledge about the X-ray cosmos, we have the assurance Constellation-X will achieve its scientific potential, provided the instrumentation performs as expected.

The three top science and instrumentation risks are listed below. The conventions used for risk ratings is provided in Appendix C.

1. **Mirror Angular Resolution**
2. **XMS Field of View**
3. **XGS/HXT Accommodation**

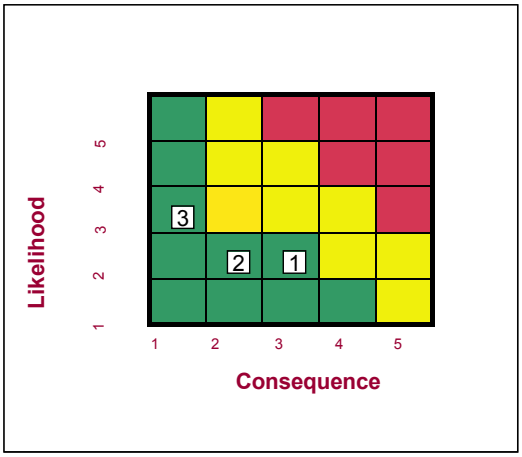

Figure 10-1. Science/Instrumentation 5x5 Risk Matrix

10.1 Risk #1 (Instrumentation) – Mirror Angular Resolution

Risk Statement: If no further improvements are made in the mirror technology development, then the mission may not meet its full angular resolution requirement.

Impact:

Only one of the four primary science objectives, constraining dark energy parameters, drives the Constellation-X angular resolution requirement. For some clusters of galaxies, resolution slightly worse than 15 arc seconds will make separating out the complex central phenomena more challenging and reduce the redshift reach of the study.

Likelihood – Low:
If no further improvements are made in the mirror resolution despite the ongoing technology development program, and assuming that system level error budget terms are exceeded by 10 percent, then the SXT would achieve an angular resolution of 17 arc seconds HPD.

Consequence – Moderate:
There is a small impact on the Dark Energy science: the sample would be restricted to lower redshifts (see Question 4). This will not compromise any of the primary science objectives.

Mitigation:
The ongoing technology development program will lead to angular resolution improvement. The program includes:

- Development of mirror segment fabrication process improvements leading to higher quality mirror segments.
- Pursuit of parallel paths on mirror segment mounting techniques: active and passive approaches as discussed in responses to Questions 7 and 16.
- Series of prototypes and an engineering unit will facilitate improvements in the mirror mounting structure.

10.2 Risk #2 (Instrumentation) – XMS Field-of-View (FOV)

Risk Statement:
If unexpected difficulties are encountered in the development of position-sensitive microcalorimeters (used in the outer array of the XMS) or their integration with the central 2.5 x 2.5 arcmin core array, then the XMS field of view requirement may not be met.

Impact:
The field of view may be limited to 2.5 x 2.5 arcmin. Observations requiring large fields of view must then be accomplished utilizing raster scans, which will take approximately four times longer. The only primary science objective requiring the 5 x 5 arcmin field of view is constraining dark energy parameters.

Likelihood – Low:
Position sensitive microcalorimeters were first conceived as a way of increasing the number of imaging pixels per instrumented sensor. Theoretical optimizations resulting in minimal impact to the spectral resolution relative to an independent, single-pixel sensor were performed. The Con-X requirements for the spectral resolution of the outer pixels is about a factor of 4 lower than for the central core, thus they make relatively modest demands relative to their design goal. Although investment in this technology has been modest, promising results have already been achieved. The Position Sensitive TES (PoST) is a device with a continuous or segmented absorber strip between two TES's. In geometries that have not been close-packed, we have already achieved 8 – 12 eV resolution at 6 keV across 9 spatial elements read by 2 TES's. Design improvements that have been made to the independent-pixel design, such has TES-noise-mitigation features, have not yet been applied to the PoST design, thus there is margin for improvement.

An alternative for increasing the field of view is using a 64 x 64 array of identical pixels. Due to the lower resolution requirements on the outer array, engineering compromises likely can be made to reduce the number of electronics channels needed. The challenges of dissipating the associated higher total bias power and the increased wiring density in the focal plane could be met by allowing larger gaps between the array pixels.

Consequence – Low:
The multiple pointings required to observe extended sources will consume additional observing time and result in sacrificing some of the Constellation-X science program. It is expected that observations addressing observatory science will be affected, not those supporting primary science objectives.

Mitigation:
Early demonstration of detectors with at least four spatial resolution elements per TES sensor and a resolution on each of better than 8 eV, in a design that is readily arrayed in a close-packed configuration, is an important component of mitigating this risk. The result of this near-term effort will dictate how best to allocate further development resources.

10.3 Risk #3 (Instrumentation) – XGS and HXT Accommodation

Risk Statement:
If there are unforeseen difficulties accommodating the XGS and HXT instruments, then it may take more mass to fully implement the selected concept than currently allocated.

Impact:
The mass margin could decrease. The accommodation details are specific to the implementation selected – light paths, baffling, relative placement and stability requirements, thermal requirements, etc.

Likelihood – Moderate:
The XGS and HXT concepts submitted in response to the SEP RFI present a wide range of viable implementations. Enveloping the variations of these instruments included in the submitted concepts is not practical. Moreover, since the XGS and HXT instruments will by selected via a NASA Announcement of Opportunity, instruments that have not been studied by the Constellation-X project could be selected.

Consequence – Very Low:
There is sufficient mass reserve to accommodate a modest amount of mass growth by the XGS and the HXT. Early selection of the instruments allows incorporation of any new, implementation-specific requirements on the overall telescope system design (SXT plus HXT). There is sufficient volume within the spacecraft envelope to accommodate the XGS and HXT.

Mitigation:
- Select the XGS and HXT instruments early (FY09 – Phase A) so that specific designs can be incorporated into mission studies.
- Until selection, envelope accommodation requirements as fully as possible.

11. INSTRUMENT TABLE

Question: Fill in entries in the Instrument Table to the extent possible. If you have allocated contingency please include as indicated, if not, provide just the current best estimate (CBE).

RESPONSE

11.1 Instrument Tables

Tables 11-1, 11-2, and 11-3 are provided for the three instrument types, as well as for the Flight Mirror Assembly (FMA) shown in Table 11-4.

Con-X includes four identical X-ray Microcalorimeter Spectrometers (XMS), each at the focus of a Flight Mirror Assembly. Con-X also includes allocations for an X-ray Grating Spectrometer (XGS) and a Hard X-ray Telescope (HXT). Since the selections will result from a future competed process, the allocations provided bracket the various concepts that have been suggested. Where the concepts cannot be bracketed by a single allocation, both options are presented.

While the Flight Mirror Assembly is not an instrument, it is included here for completeness.

Table 11-1. X-ray Microcalorimeter Spectrometer (XMS)

X-ray Microcalorimeter Spectrometer (XMS)		
Item	**Value/Description**	**Units**
Number and type of instruments	4	Number
Number of Channels (# pixels provided)	4096	# Pixels per XMS
Size/dimensions (for each instrument)	0.75 x 1.0	Dia x length, m, per XMS
Payload mass with contingency	230 (w/30%)	Kg, %, per XMS
Average payload power with contingency	525 (w/30%)	W, %, per XMS
Average science data rate with contingency	9.4 (w/30%)	Kbps, %, per XMS
Instrument Fields of View (if appropriate)	5 x 5	Arcmin, square field
Pointing requirements		
Knowledge (Y, P, R)	5, 5, 20	Arcsec (3-sigma)
Control (Y, P, R)	10, 10, 30	Arcsec (3-sigma)
Stability (all axes)	1	Arcsec/100 microsec

Table 11-2. X-ray Grating Spectrometer (XGS)

X-ray Grating Spectrometer (XGS)		
Item	**Value/Description**	**Units**
Number and type of instruments	2	Number
Number of channels (number of pixels per CCD provided)	1600 x 512 (15 microns)	# of pixels (and size)
Size/dimensions		
Reflection Grating Concept		
Gratings (coverage)	360 deg, 0.33, 0.1	Ang. extent x ODia. x Depth, m
Number of Grating arrays	1 or 2	Number
Number of CCDs	~ 7	Number per array
CCD Detector System	0.2, 0.1, 0.1	Length, Width, Depth, m
Transmission Grating Concept		
Gratings (coverage)	144 deg, (0.324, 0.659), 0.004	Ang. Extent, Dia. (ID, OD), Depth, m
Number of Grating arrays	2	Number
Number of CCDs	20	Number per array
CCD Detector System	0.5, 0.05, 0.03	Length x Width x Depth, m
Payload mass with contingency	130 (w/30%)	Kg, % contingency
Average payload power with contingency	53 (w/30%)	W, % contingency
Average science data rate with contingency	87 (w/30%)	Kbps, % contingency
Instrument Fields of View (if appropriate)	n/a	Arcsec
Pointing Requirements		
Knowledge (Y, P, R)	5, 5, 20	Arcsec (3 sigma)
Control (Y, P, R)	10, 10, 30	Arcsec (3 sigma)
Stability (all axes)	2	Arcsec / 13.8 millisec

Table 11-3. Hard X-ray Telescope (HXT)

Hard X-ray Telescope (HXT)		
Item	**Value/Description**	**Units**
Number and type of instruments	1 or 2	Number
Number of channels	44 x 48 (500 microns)	# of pixels (and size)
Size/dimensions (for each instrument) Nickel Mirror Glass Mirror Detector housing	 0.40 x 0.66 0.75 x 0.45 0.164 x 0.6	 Dia x length, m Dia x length, m
Payload mass with contingency	130 (w/30%)	Kg, % contingency
Average payload power with contingency	32 (w/30%)	W, % contingency
Average science data rate with contingency	17 (w/30%)	Kbps, % contingency
Instrument Fields of View (if appropriate)	5	Arcmin, square field
Pointing requirements (knowledge, control, stability) Knowledge (Y, P, R) Control (Y, P, R) Stability (each axis)	n/a 10, 10, 40 20, 20, 40 2	Deg, deg/s Arcsec (3 sigma) Arcsec (3 sigma) Arcsec / 100microsec

Table 11-4. Flight Mirror Assembly (FMA)

Flight Mirror Assembly (FMA)		
Item	**Value/Description**	**Units**
Number and type	4	Number
Number of channels	n/a	
Size/dimensions (for each)	1.36 x 1.0	Dia. x length, m
Payload mass with contingency	511 (w/30%) each	Kg, %
Average payload power with contingency	285 (w/30%) each	W, %
Average science data rate with contingency	n/a	
Instrument Fields of View (if appropriate)	>10	Arcmin, dia.
Pointing requirements (knowledge, control, stability)	n/a	Deg, deg/s

12. SCIENCE INSTRUMENTATION – CONCEPT, FEASIBILITY, OR DEFINITION STUDIES

Question: For the science instrumentation, describe any concept, feasibility, or definition studies already performed (to respond you may provide copies of concept study reports, technology implementation plans, etc).

RESPONSE

12.1 Introduction

Escalating launch costs and real-year cost increases due to funding limitations and associated launch delays have led us to consider several alternative implementation approaches to reduce costs while maintaining performance capability. They are summarized here to demonstrate that the Constellation-X team takes both cost limits and performance requirements very seriously, as well as to demonstrate the mission's flexibility for implementation. We discussion mission level feasibility studies here because many of the feasibility issues surrounding instrument implementation are dealt with in these studies.

At the time of the Technology Readiness and Implementation Plan (TRIP) Review in early 2003, the Constellation-X reference configuration consisted of 4 separate observatories launched 2 at a time on Atlas V 551's. The instrumentation on each observatory consisted of a Spectroscopy X-ray Telescope (SXT) with a 1.6m diameter mirror assembly, an X-ray Microcalorimeter Spectrometer (XMS) and a Reflection Grating Spectrometer (RGS) comprised of reflection gratings and CCD readouts. Each of the 4 observatories also contained 3 Hard X-ray Telescope optics and detectors (HXT).

During 2005, we thoroughly evaluated a single Delta IV Heavy launch approach with the same complement of optics and instruments on a single satellite. Cost savings were quite substantial and the mission appeared quite feasible, but a subsequent large increase in Delta IV costs motivated us to consider an approach based on a single Atlas V launch.

This configuration has been developed and shaped by a series of trade studies by the Con-X mission study team with the support of a session with the GSFC Integrated Mission Design Center (IMDC) in December 2006. The single Atlas V configuration was also presented to NASA HQ on two occasions and was reviewed and strongly endorsed at the December 2006 meeting of the Constellation-X Facility Science Team. This implementation approach is the basis for the information presented during this BEPAC review, and it is described in responses to Questions 2 and 5 in this package. Substantial mass reductions were achieved between the 2003 TRIP configuration and the present single Atlas V configuration via reduction in the SXT mirror assembly outer diameter, smaller or fewer grating elements, fewer HXT units, and a single spacecraft rather than 4. If we compare the cost of the single Atlas V configuration to the TRIP implementation in real year dollars, a cost reduction of approximately $500M has been achieved.

Because of the large number of studies and the extent of some of the documentation, the actual study products (reports, memoranda, presentations, etc.) are available upon request.

12.1.1 General Studies

Several concept, definition, and feasibility studies have been performed as part of the Constellation-X program at the mission level. These studies are pertinent because of the attention paid to the instrument systems. For each study we describe the purpose, methodology employed, and results.

Technology Readiness and Implementation Plan (TRIP) Report – January 2003

> This report, written in response to a request from NASA Headquarters, is the most comprehensive study to date of the Constellation-X mission. It describes concisely all aspects of the mission: Scientific objectives, mirror architecture, status and technology development plans for mirrors and instruments, spacecraft description, operations plans, assessment of most significant risks, and end-to-end mission schedule and costing.

Integrated Mission and Design Center (IMDC) – December 2006

> As part of the ongoing effort to ensure mission feasibility, the Con-X team participated in its latest run at the IMDC in December 2006. The IMDC product is a Mission Configuration and Observatory design that meets Con-X requirements, and allows for an independent assessment of costs, feasibility, and risks. This current study covered all major mission systems and subsystems: launch vehicle, flight dynamics, GN&C, mechanisms, propulsion, thermal, power, RF comm.,C&DH, flight software, I&T, mission operations, radiation environment, and reliability.

12.2 SXT FMA Studies

Numerous analytic and feasibility studies have been undertaken to support the FMA development. Significant ones are listed below. Studies not specifically described here include thermal modeling of the forming ovens and forming mandrels, mirror system environment/thermal requirements, and thermal pre-collimator design (including the feasibility of using capillary heat pumps). Numerous finite element analyses for structural modeling have been performed, including the mirror elements and the FMA, metrology mounts (for fabrication metrology), and support of the slumping mandrels during forming.

12.2.1 Mirror Design Study for Delta IV H Launch October 2005

As part of mission planning for a Delta IV H single launch, telescope configurations were studied, ranging from 4 mirrors with 1.6 m diameter to a single 4 m diameter system. A range of focal lengths was considered, from 8.5 m to 35 m, where focal lengths of 15 to 35 m were implemented using extendable optical benches. Notably, the different SXT configurations all achieved comparable effective area performance, demonstrating the robustness of the mission concept.

12.2.2 Mirror Design for 3 and 4 SXT Single Spacecraft Single Atlas V Launch September 2006

A comparison was carried out of mirror designs that can be accommodated on a single spacecraft launched on an Atlas V. The goal of the study was to maximize the effective area of the mirror system while keeping its mass within its allocation. Secondary considerations included complexity; i.e., the number of nested shells per mirror. Three and four mirror systems were considered. A design for each was found that meets the mission requirements at 1.25 and 6 keV with an iridium coating. The four-mirror system was selected, primarily because of its effective area at 6 keV, where it exceeds the three-mirror design by 20 percent. The four-mirror design has the additional advantages of requiring fewer mandrels and mirror surfaces than the three-mirror design, and also provides more off-axis effective area.

12.2.3 Mirror Fabrication Study – March 2003

This study was undertaken for the Con-X program by Swales Aerospace to support the TRIP report. Working to the baseline program (4 x 1.6 m diameter SXT mirrors on 4 separate spacecraft and 2 Atlas V launches), they defined a fabrication process flow and then proceeded to estimate number of stations, floor space, and time required for the complete operation. While using what is today a number of out-of-date processes and instrument parameters, they demonstrated that the telescopes could be built in the required time interval, based on the mission level schedule. They also provided scaling relationships that make possible the sizing of a facility and effort for different delivery assumptions.

The Constellation-X mirror team is currently updating this analysis, using this report and current assumptions about processes, mirror size, and number of segments and modules.

12.2.4 Off-axis Mirror Performance of SXT Mirror – August 2006

The degradation of the angular resolution as a function of off-axis angle was studied for the baseline optical design. Wolter I optics (the Con-X optical design) produce a perfect on-axis image, but off-axis they introduce coma and field curvature. It was found that the cumulative effect of these aberrations on the anticipated imaging performance is small. The degradation was found to be insignificant even for a mirror meeting the 5 arcsec performance goal, at an off axis angle corresponding to twice the size of the field of view.

This work was documented in a Con-X memorandum.

12.2.5 Alternative Mirror Prescriptions – 2003

A study was carried out to determine whether a simpler surface prescription than a Wolter-I suffices for the Con-X telescopes. In this alternative design, both primary and secondary mirrors of any particular shell have the same axial curvature. The potential advantage of such a design is that it may simplify the specification of thermal forming mandrels. A final review and decision on the surface prescription will be carried out in Phase A.

This work was documented in a paper published in Applied Optics: T. T. Saha & W. W. Zhang, "Equal-Curvature Grazing-Incidence X-ray Telescopes," Applied Optics, 42, 4599 (2003).

12.2.6 Impact of Mirror Focus Correction Upon Imaging Performance – 2003

Finite element modeling was undertaken of the limits of allowable focus correction that can be achieved by warping the thin mirrors so as to change their cone angles. As expected, warping the mirror in this manner produced both the desired effect of changing the cone angle, and the undesired effect of introducing local figure error (distortions). The impact of the distortions on imaging was estimated by calculating the resulting surface slope errors. Limiting the magnitude of the slope errors to an imaging error budget term defined for this contribution then also serves to limit the allowable amount of cone angle change. This sets the amount of focus error correction that is consistent with the error budgeting and this methodology. Alternatively, it also set fabrication tolerances on the mirror cone angle error and average radius error (a measure of the mirror size).

This study was documented in a Con-X memorandum.

12.3 X-ray Grating Spectrometer Studies

Extensive analytic and technical studies of the various aspects of grating spectrometers have been performed over the past 12 years. Originally, the "Reflection Grating Spectrometer" utilized in-plane reflection gratings. As part of the technology development program, test gratings were fabricated and X-ray tested. Full grating efficiency models were generated and fit to the measured data. Raytraces of the instrument performance were generated and used to optimize the design parameters. In 2003 the project began studying off-plane reflection gratings as an alternative to in-plane gratings. Extensive raytrace studies were completed to determine the feasibility and design of an off-plane grating spectrometer. Test off-plane gratings were fabricated and X-ray tested. Full grating efficiency models were generated for the off-plane gratings, fit to the measured data, and used for parameter optimization. Analytic and technical studies of off-plane reflection gratings are documented in internal memos and in more than 12 SPIE publications over the past three years. Following these studies, the choice was made to move to off-plane reflection gratings because of their potential for improved performance relative to the in-plane gratings.

In October 2006, after the Con-X project moved to the current Atlas V single launch configuration, an RFI was issued for instrument concepts that would provide high spectral resolution at low energies or high throughput at high energies. Eight white papers were received. Each described a specific instrument configuration, the predicted performance, the technical feasibility and maturity, and the impact of integrating the instrument on the payload. Four white papers described instrument concepts that would enhance the low energy performance, and two specifically described alternate grating spectrometers.

A select list of publications related to the gratings:

Grating arrays for high-throughput soft X-ray spectrometers A.P. Rasmussen et al. 2004, Proc. SPIE 5168, 248.

Efficiency of a grazing-incidence off-plane grating in the soft-X-ray **region** J.F. Seely et al., 2006, Applied Optics, 45, 1680

The Constellation-X RGS options: raytrace modeling of the off-plane gratings K.A. Flanagan et al. 2004, Proc. SPIE 5488, 515.

Off-plane grating mount tolerances for Constellation-X W.C. Cash & A.F. Shipley 2004, Proc. SPIE 5488, 335.

12.4 Hard X-ray Telescope Studies

Much work has been carried out on the development of focusing hard X-ray telescopes which have response well above the 40 keV required by Constellation-X. In particular, the feasibility of an imaging hard X-ray system has been demonstrated by several balloon flights: InFOCuS, HERO and HEFT. The Technical Readiness Implementation Plan (TRIP) of 2003 included a report on the development of the HXT for Constellation-X. After the move to the Atlas V single launch, the requirements for the HXT were revised and, as stated above, an RFI was issued in October of 2006 for instrument concepts which included the extension of the high energy response. Three of the eight white papers received describe concepts that would extend the high energy response of Constellation-X; two of these papers describe concepts for a Hard X-ray Telescope.

Over the past several years, numerous SPIE publications have documented the progress of both mirror technology and detector technology as applied to grazing incidence focusing hard X-ray telescopes. A selection of these publications:

Hard X-ray optics: from HEFT to NuSTAR, Jason E. Koglin et al. Proc. SPIE Vol. 5488, p. 856-867, Oct. 2004.

Characterization of a large-format, fine-pitch CdZnTe pixel detector for the

HEFT balloon-Borne experiment, C. M. H. Chen et al, IEEE Transactions on Nuclear Science, Volume 51. No 5. Part 1. 10/2004. pp 2472-2477.

Technology Development for High-Energy X-Ray Optics, M. Gubarev, B. Ramsey, D. Engelhaupt, T. Kester, C. Speegle, Proc. SPIE Vol. 6266, p. 62661I1-8, May 2006.

Development of a Prototype Nickel Optic for the Constellation-X Hard X-Ray Telescope: IV, S. Romaine et al. Proc. SPIE Vol 6266, p. 62661C1-6 May 2006.

12.5 XMS Studies

An enormous amount of work has been carried out on the development of X-ray microcalorimeter spectrometers for both space and ground-based instruments. This includes both the first generation of ion-implanted Si devices as well the transition edge sensor microcalorimeters being developed for Con-X. Members of this team are authors on more than 300 papers on microcalorimeters, their readouts, and their applications. For an introduction to this technology, we recommend the following two articles. In addition there are Con-X specific references listed below.

Quantum Calorimetry, Novel detectors that operate at 60 millikelvin to study cosmic gas at millions of Kelvin, *Caroline Kilbourne Stahle, Dan McCammon, and Kent D. Irwin, Physics Today, August 1999.*

Seeing with Superconductors, Kent Irwin, *Scientific American*, November 2006.

The *Suzaku* High Resolution X-Ray Spectrometer, R.L. Kelley et al. PASJ, 2007, in press. This is a comprehensive paper on the design, implementation and in-flight performance of the XRS.

Internal TRL-6 roadmaps:

Detector system technology roadmaps: 2001, 2005, 2007 (see response to Question 16 for latest assessment). Various analyses of wire-count, heat loads, mass, power, and data rates performed for mission configurations under study.

Strawman multiplexer design for Constellation-X, Memorandum, W.B. Doriese, Nov., 2005. Goes through a full feasibility study for MUXing a kilopixel array with Con-X-like pixels. Assumes a multiplexer with 12 MHz open-loop bandwidth and 0.25 $\mu\phi_0/\sqrt{\text{Hz}}$ non-MUX'ed SQUID noise.

Significant Publications:

The *Suzaku* High Resolution X-Ray Spectrometer, R.L. Kelley et al. PASJ, 2007, in press. This is a comprehensive paper on the design, implementation and in-flight performance of the XRS.

Design and fabrication of superconducting transition edge X-ray calorimeters, Tralshawala N, Aslam S, Brekosky RP, Chen TC, Figueroa Feliciano E, Finkbeiner FM, Li MJ, Mott DB, Stahle CK, Stahle CM, 2000, NIM A, 444, 188. This paper contains the first description of the fabrication of our high-fill-factor absorbers.

Arraying compact pixels of transition-edge microcalorimeters for imaging X-ray spectroscopy, Stahle CK, Lindeman MA, Figueroa-Feliciano E, Li MJ, Tralshawala N, Finkbeiner FM, Brekosky RP, and Chervenak JA, 2002, Proceedings of the 9th International Workshop on Low Temperature Detectors – 2001, ed. Porter FS, McCammon D, Galeazzi M, and Stahle CK, AIP Conference Proceedings, 605, 223. This paper shows that compact pixel-structures, with narrow silicon-nitride perimeters around the TES, can be made with the thermal conductance needed for the Constellation-X array.

Effect of high-flux astronomical sources on the Constellation-X X-ray microcalorimeter spectrometer, Figueroa-Feliciano E, Bandler, S Boyce K, Chervenak J, Finkbeiner F, Hammock C, Kelley R, Lindeman M, Porter, FS and Stahle CK, 2004, NIM A, 520, 303. This paper models the response of a Constellation-X TES pixel to the flux of the Crab nebula, showing that even at very high fluxes, the device with not latch up.

The science and technology of microcalorimeter arrays, Kilbourne CA, 2004, NIM A, 520, 402. This overview of array microcalorimeters enumerates important design issues for large arrays.

Position-sensitive transition-edge sensors, Iyomoto N, Bandler SR, Brekosky RP, Chervenak JA, Figueroa-Feliciano E, Finkbeiner,FM, Kelley RL, Kilbourne CA, Lindeman MA, Murphy K, Porter FS, Saab T, Sadleir JE,. and Talley DJ, 2006, NIM A, 559, 491. 8-eV resolution obtained in imaging TES device with 7 imaging elements between two TES's. This is the state-of-the-art in position-sensitive TES's.

High-density arrays of X-ray microcalorimeters for Constellation-X, Kilbourne CA, Bandler SR, Brown AD, Chervenak JA, Figueroa-Feliciano E, Finkbeiner FM, Iyomoto N, Kelley RL, Porter FS, Saab R, Sadleir J, and White J, 2006, Proc. SPIE, 6266, 626621. Describes vacuum-gap absorber geometry that led, ultimately, to a breakthrough in resolution in close-packed TES arrays. Results shown are for Au/Bi absorbers; development of electroplated Au is described, but breakthrough results had not yet been obtained.

Progress toward kilopixel arrays: 3.8 eV microcalorimeter resolution in 8-channel SQUID multiplexer, NIMPRA: LTD-11 conference proceedings, R. Doriese, et al, 2006. Presents results of 8- and 16-channel MUX demos of fast, high-resolution TESs. This is still the state of the art in X-ray TES multiplexing.

A 14-pixel, multiplexed array of gamma-ray microcalorimeters with 47 eV energy resolution at 103 keV, In preparation for Applied Physics Letters, Doriese, et al, 2007. A 2-column x 8-row MUXed array of high-res gamma-ray detectors. Detectors are slow (2 msec). Focus of article is on detector-array issues, not necessarily MUX, since the MUX was so easy.

This paper is not yet finished – there are a few details left out in the crosstalk section, for instance, and has not been reviewed, so please don't circulate.

Prototype system for superconducting quantum interference device multiplexing of large-format transition-edge sensor arrays, Review of Scientific Instruments, Reintsema, et al, 2003. The details of the NIST time-division multiplexer architecture.

Time-division superconducting quantum interference device multiplexer for transition-edge sensors, Review of Scientific Instruments, De Korte, et al, 2003. Testing and details of the 1x32 MUX chip and TDM architecture.

Superconducting multiplexer for arrays of transition edge sensors, Applied Physics Letters. Chervenak, et al, 1999. The concept of the time-division SQUID multiplexer.

An application of electrothermal feedback for high resolution cryogenic particle detection, Applied Physics Letters, Irwin, 1995. The paper that launched the field. Introduced the voltage-biased TES.

Characterization and reduction of unexplained noise in superconducting transition-edge sensors, Applied Physics Letters Ullom, et al, 2004. Introduction of normal-metal bars and B-field sensitivity of TESs, and how they affect alpha and unexplained noise.

Array-compatible transition-edge sensor microcalorimeter gamma-ray detector with 42 eV energy resolution at 103 keV, Applied Physics Letters Zink, et al, 2006. Describes a high-resolution gamma-ray TES.

Optimized transition-edge X-ray microcalorimeter with 2.4 eV energy resolution at 5.9 keV, Applied Physics Letters, Ullom, et al, 2005. A study of how to design a TES to optimize for energy resolution, given constraints on dynamic range, etc. The state of the art in X-ray TES microcalorimeters.

Cryocooler Technology:

A session was held at the 2005 Cryogenic Engineering Conference for presentations on the outcome of the Advanced Cryocooler Technology Development Program (ACTDP). The Con-X requirements were included in the ACTDP. A summary of the program was presented along with reports on the three individual cryocooler technologies. Accompanying papers were published in Volume 51 of *Advances in Cryogenic Engineering*. The project reference XMS concept, incorporating the Lockheed-Martin ACTDP cryocooler, was presented at the 2003 Space Cryogenics Workshop and published as part of the workshop proceedings in Cryogenics (Volume 44, pp. 543-549, 2004). Additionally, Ball Aerospace completed a conceptual study, "Ball Aerospace, Con-X Cryo-Thermal System Study" of 3 June 2003, assessing several XMS cryostat options incorporating their ACTDP cryocooler.

CADR Technology:

The Continuous Adiabatic Demagnetization Refrigerator (CADR) technology has been developed from concept to working prototype using the detector cooling requirements for Constellation-X as a baseline. This addresses system level feasibility issues by ensuring that the CADR architecture and performance were consistent with all candidate XMS detector technologies, and ACTDP cryocooler technologies. The CADR has been included in the Reference Design for Constellation-X that was described in detail

in the Technology Readiness and Implementation Plan report. CADR performance and candidate layouts for the XMS instrument have also been detailed in *Cryogenics* (Volume 44, pp. 581-588, 2004). A study is presently underway with Lockheed-Martin to develop mechanical and thermal models the CADR/cryocooler interface (assuming use of the Lockheed-Martin ACTDP cryocooler) to verify end-to-end performance of the combined subsystems.

13. INSTRUMENT OPERATIONS

Question: For instrument operations, provide a functional description of operational modes, and ground and on-orbit calibration schemes.

RESPONSE

For each instrument, there are a limited number of operational modes. These fall into 2 main categories: Science Modes and Engineering Modes. The text below outlines specific modes for each instrument. Since each detector is pixel based, there is a conceptual similarity in the detector's operational modes. It is noteworthy that all three instruments operate simultaneously, and view the same target at all times.

13.1 Operations Modes

13.1.1 XMS Operations Modes

The XMS instrument is very simple to operate and all of the essential features of the XMS instrument have been demonstrated in space on the *Suzaku* observatory. Basically, there are two general hardware modes of operation: cycling the ADR to reach the operating temperature of 50 mK and then maintaining that temperature in closed-loop control for the science mode operations.

XMS ADR Operations

Operating the ADR, whether a single-stage version or once with a series of salt pills and heat switches to enable continuous operation, is carried out autonomously using a simple software algorithm. As an example, we outline the procedure for the XRS instrument:

- Cycling the ADR is accomplished by 1) ramping up the magnetic field, causing the salt pill to warm as work is done on the spin system, 2) closing the heat switch and continuing the ramp to full field, 3) waiting until the salt pill cools back down as the heat of magnetization is conducted to the heat sink and then opening the heat switch, and 4) ramping the magnetic field down to cool the detectors to 50mK.
- The operation of a continuous ADR is based on this simple algorithm by sequentially cycling the ADR salt pills so that all but the “coldest” salt pill (which cools the array) provides the heat sink for another, and the total heat of magnetization is ultimately shunted to the cryocooler stage.

XMS Science Mode

- There is only one science mode, which is an imaging where events in the detector are processed and transmitted to the spacecraft for telemetry to the ground.
- XMS Engineering Modes:
- Memory Upload/Dump – in this mode, new flight code can be uploaded. Likewise, the memory (or sections of it) can be dumped.
- Diagnostic Mode – A diagnostic mode is available for monitoring instrument performance or collecting more detailed information than normally available. For example, in this mode, no data compression is performed.
- Filter Decontamination Mode – Heaters mounted near the aperture filters are enabled to remove contaminants from the filters.

13.1.2 XGS Operations Modes

The CCD readout for the grating spectrometer will build on the *Chandra* Advanced CCD Imaging Spectrometer (ACIS) heritage. It will encompass – and go beyond – all of the ACIS operational flexibility. In operation, the CCD chips are read out and processed for events. Event-recognition algorithms are used to identify true X-ray events, reducing the data volume that is transmitted to the ground. Only a few modes of operation are expected in normal operation. Many of these modes are common to those of *Chandra* ACIS operation. However, one additional feature of the Constellation-X CCD readout is its ability to use on-chip pixel summation. For example, in nominal operation, a 2 column by 8 row summed "superpixel" is defined. The two parallel imaging sections, each 1600 columns by 512 rows, can be read out in 13.8 ms (frame rate 72 Hz). The superpixel size can be selected to optimize the science observation, according to the needed sampling size and frame rate. Other modes common to ACIS are described at [http://acis.mit.edu/acis/sreqj/]. A summary of expected operational modes for the CCD readout is given below, divided into 2 main categories: Science Modes and Engineering Modes.

XGS Science Modes:

- Timed Exposure (TE) – Photons are collected in a frame for a selectable exposure time before being read out.
- Continuous clocking (CC) – The CCD is read out continuously; each output pixel represents the integrated flux received as the charge crosses the array. The main advantage of CC mode is that it can reduce pile-up and makes it possible to look at bright sources.
- Submodes can be represented by selectable parameters – superpixel configuration, number and location of chips read out, collection time (in timed exposure mode), window (restricted region to be read-out), subarray (restricted rows to be read-out in TE mode), energy filter, and science mode event telemetry, including:
  - Faint mode event telemetry– a 3x3 pixel island of pixels is telemetered
  - Graded mode event telemetry – the center pixel and the grade are telemetered
  - Very Faint mode event telemetry– a 5x5 island of pixels is telemetered

XGS Engineering Modes:

Diagnostic Modes:

- Raw mode – the raw, unprocessed pixel data are telemetered, bypassing the event detection algorithms so that all of the pixel information can be seen. This diagnostic mode produces large amounts of telemetry.
- Reverse Clocking or "Squeegy" Mode – the CCD's serial output shift registers are clocked in the reverse direction. This diagnostic mode allows the decay rate of charge traps to be measured.
- Histogram Mode – in TE mode, pulse-height histograms for those pixels above threshold are provided from the respective output nodes. This diagnostic mode provides a picture of output node performance without resorting to raw modes which require large amounts of telemetry.

Calibration Modes:

- Over time, CCD properties are changed by radiation damage. Calibration modes provide a way of monitoring these changes. An existing science mode (described above) is used, and the standard science data are telemetered to the ground to determine the desired calibration information. These include:
- Charge Transfer Inefficiency (CTI) – The CCDs are exposed to an onboard calibration source and collected in TE mode with Faint event format.
- CCD dark current – TE data is compared with different exposure times
- Other – An observation is performed as with CTI above, but different analysis on the ground is employed to examine Spectral Resolution, Energy to Pulse Height Gain, CCD Quantum Efficiency, and Background Event Rate

Other Engineering Modes:

- Read memory – data are downloaded
- Write memory – commands are uplinked
- Patch – Software modifications are uplinked
- Bake-out – Software serial commands are sent to heaters to raise the CCD temperature for contamination bake-out.

13.1.3 HXT Operations Modes

The operation of the HXT solid state detector is relatively simple, and conceptually comparable to the XMS detector.

HXT Science Modes:

- Imaging – there is only one major science mode, which is an imaging mode where events in the detector are processed and transmitted to the spacecraft for telemetry to the ground.
- Calibration mode – run initially before any data is collected and will be run periodically thereafter to check the gain of the system. For this gain calibration an X-ray calibration source will be used and will be turned off or rotated out of the field of view after calibration.

HXT Engineering Modes:

- Initialization Mode – a pulse is injected to each channel to verify the integrity of the electronics
- Memory Upload/Dump – in this mode, new flight code can be uploaded. Likewise, the memory (or sections of it) can be dumped.
- Diagnostic Mode – A diagnostic mode is available for monitoring instrument performance or collecting more detailed information than normally available. For example, in this mode, no data compression is performed.

13.2 Calibration Schemes

Constellation-X has developed a draft calibration plan, which is available upon request.

The Constellation-X calibration philosophy is to calibrate those systems and sub-systems which require ground calibration, at the lowest possible level, and to utilize those calibrations as baselines in next-higher-assembly calibrations. Note that calibrations can be accomplished on the ground and with existing facilities – this is particularly important for the optics, which can be calibrated using MSFC's X-ray Calibration Facility (XRCF). This piece-wise calibration is robust, and allows for calibrations to occur in parallel for different subsystems. Underlying this guiding philosophy is the concept to employ system and sub-system calibration data to constrain theoretical and semi-empirical models for the performance of the individual sub-systems and systems. In principle, the enormous ensemble of calibration data over-determines model parameters and thus tightly constrains these models; thus – "The model is the calibration." By virtue of this approach, not only does one require calibration of the system hardware, but also verification and validation of the associated predictive software.

The instrument calibration is thus based on a physical model of the various instrument components. For example, the SXT/grating includes the mirror response, the grating response in the case of the RGS (including reflectivity, shape errors, alignment and vignetting) and the detector response (QE, observed energy distribution for a given monochromatic input energy, transmission through various layers, CTI corrections and gain and cross talk in the electronics). During ground calibration various components will be calibrated and the physical model for each component refined. These will be verified in-flight. For those calibration elements that can be adequately calibrated in flight, minimal ground calibrations will be performed; enough only to ensure that in-flight performance will meet the mission goals. A subset of the calibration elements will be monitored on an ongoing basis (such as contamination of the optics and detectors, changes in gain and CTI due to radiation damage, bright and dark pixels, etc).

A diagram of showing the approach to final the effective area calibration – using both ground-based calibration data and models, and observations of cosmic sources, is shown below.

The calibration of Constellation-X proceeds in three primary, time-ordered stages, with Phases 1 and 2 taking place on the ground.

- Phase 1 – Pre-delivery calibrations of individual detectors and optics
  - A key aspect of the Con-X calibration scheme is that calibration data will be obtained on all optical and detector systems using existing facilities prior to their delivery for integration and testing. In particular, the Con-X optics and detectors can be tested using the X-ray Calibration Facility (XRCF) that was developed at MSFC for calibrating the *Chandra* systems.

- Phase 2 – System Level calibrations:
  - System level calibrations take place following delivery of optics and detectors to the prime contractor. At the system level, optics and detectors are calibrated together. Calibration of telescope systems that require the delivered components (i.e., such as alignment and focus mechanisms) take place at this time.)
- Phase 3 – On-orbit calibration activities:
  - Phase 3a: Early Operations Verification Activities and Calibrations
  - Phase 3b: Normal Operations Calibrations (including cross calibrations between instruments and with other missions).

In Phase 1, detector and optics calibrations are performed and include:

- Quantum efficiency as a function of position, energy, read-out mode, position, and temperature.
- Spatial resolution as a function of energy, read-out mode, position, and temperature.
- Spatial linearity as a function of energy, position, and incident angle.
- Dark current and system noise as a function of position and temperature.
- Energy resolution as a function of energy, read-out mode and position.
- Charge-transfer and charge-collection efficiency, as functions of position, energy, and temperature (for CCDs).
- Gain as a function of energy, position, and temperature.
- Energy scale as a function of energy and operating conditions.
- UV and optical response as a function of energy and position.

In Phase 2, activities will focus on calibration items that cannot adequately be evaluated by the individual optic and detector groups. Flight detectors may be calibrated using GSE optics and vice-versa. The system level calibrations have unique features which complement sub-assembly laboratory calibrations and in-flight calibration. Observatory level model calibration priorities have been identified, and include, but are not limited to:

- Alignment related:
  - Measure co-alignments of the SXT and HXT optics
  - Measure co-alignments of detectors.
- Effective area related:
  - Scans over known edges/features
  - Search for unexpected edges/features
  - Verify/measure detector effects on effective area (e.g., mode, gain, rate, rate linearity)
  - Molecular contamination
  - Backgrounds

- Focus & PSF/LRF:
  - Measure PSF/LRF near core for a few energies
  - Measure cross-dispersion response at core
  - Search PSF/LRF for unexpected wing features
  - Ghost image searches

In Phase 3, the in-flight calibrations fall into two classes: instrument hardware-based (i.e., radioactive sources (Cd-109, Ca-41, Fe-55) as well as electron-impact sources) and cosmic sources. For example, the XMS implements an electron-impact/fluorescent target X-ray calibration source for calibrating the energy scale in flight, with calibration data being obtained for a short period before and after each observation. Calibration activities begin during the post-launch spacecraft and instrument checkout and continue throughout the mission.

- Normal Calibrations:
  - Normal calibration monitoring will be conducted on a per-AO cycle. These calibrations consist of routine & periodic calibrations to check stability of boresight, plate scales, effective areas, gains (as a function of temperature), wavelength scale, CTI, astrometry, contamination, etc.
  - Cross-calibrations with other missions: target lists exist for key calibration targets for *Chandra*, *XMM-Newton* and *Suzaku* that will be utilized to develop a comprehensive cross-calibration.

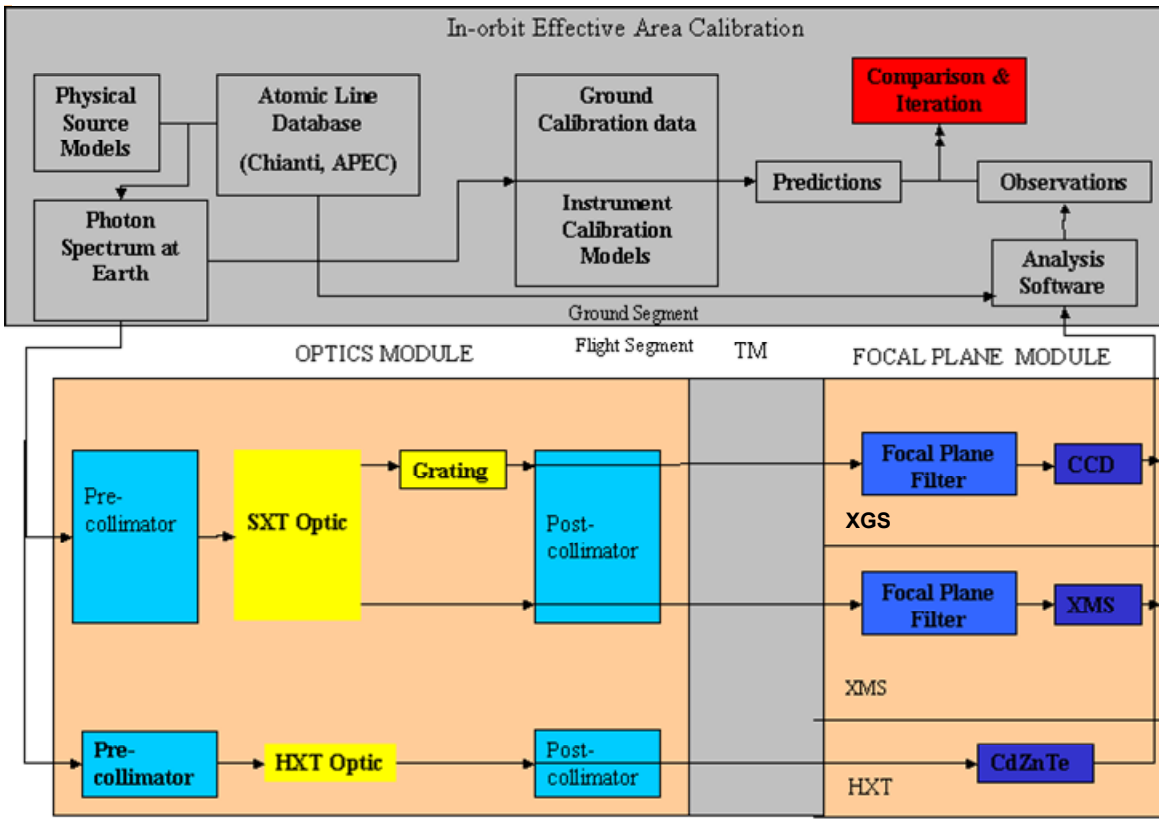

Figure 13-1: Effective Area Calibration Flow Diagram

14. ANALYZING DATA TO ACHIEVE SCIENTIFIC OBJECTIVES

Question: Describe the level of complexity associated with analyzing the data to achieve the scientific objectives of the investigation.

RESPONSE

The scientific data from the Constellation-X (Con-X) mission will be of a type and format that we are experienced with from prior missions, most recently *Chandra*, *XMM* and *Suzaku*. As a result, many of the complexities associated with analyzing the data have been addressed, algorithms have been developed, software tools exist and the observer community is familiar with their use. Given the commonality with data types from prior missions, existing software and community experience, we consider the level of complexity to be moderate to low, posing no risk to the program.

In the discussion below, we provide a brief summary of (a) the instruments planned for Con-X, the form of the data and commonality with data from current and prior missions (Section 14.1), (b) the steps required to process the data (Section 14.2) and (c) the analysis approach and tools needed by observers to derive scientific results from the data (Section 14.3).

14.1 The Con-X Instruments and Data

As discussed in Question 5, Con-X has two distinct telescope systems: the Spectroscopy X-ray Telescope (SXT), covering the 0.3-10.0 keV band, and the Hard X-ray Telescope, (HXT) covering the 6-40 keV band. The SXT consists of the SXT flight mirror assembly (FMA), and the X-ray microcalorimeter spectrometer (XMS). X-ray Grating Spectrometer (XGSs) are included on 1 or 2 SXTs. All the instruments provide a time-tagged photon event list from which spectra, images and timing data can be constructed, requiring spectral, spatial, and timing analysis tools.

Table 14-1 summarizes the data and specific analysis types for the Con-X instruments, and shows the commonality with instruments from current and prior missions.

Table 14-1. Summary of Con-X Instrument Data and Mission Commonality

Con-X Instrument	Detector Data Type (Level 0)	Analysis Required	Prior Instrument Experience
XMS	Pixelated high spectral resolution, moderate spatial resolution	Spectral, timing, spatial	Suzaku XMS, Chandra ACIS (spectral), RXTE, Chandra (timing), Chandra ACIS/HRC (spatial)
XGS	Dispersed high-resolution spectra	Dispersed spectral, timing	Chandra HETG, LETG, XMM-Newton RGS
HXT	Pixilated, moderate spectral and spatial resolution	Spectral, timing, spatial	Suzaku HXD, InFOCμS, HEFT, HERO (spectral), RXTE, Chandra (timing), Chandra ACIS/HRC (spatial)

14.2 Standard Processing of Con-X Data

The Con-X science data are well suited to the 'Standard Processing' paradigm used for *Chandra* and other missions. Data are received in raw telemetry format from the Deep Space Network and processed by the Con-X Science and Operations Center (CXSOC) Science Data System through a series of three levels: Level 0, 1 and 2. In Level 0 processing, the raw spacecraft telemetry is split into standard FITS format files and the telemetry is divided along observation boundaries. In Level 1, instrument-dependent corrections are applied including scaling, application of the aspect solution, application of

statistical filters and count-rate dependent corrections. We note that the aspect solution uses optical star tracker data to determine the proper location on the sky for each detected X-ray. In Level 2 processing, standard corrections and filters are applied at the source level to generate the spectra, images and light curves required for final analysis by the observer. Figure 14-1 shows a representative dispersed spectrum observed with the *Chandra* High Energy Grating Spectrometer together with the processed spectrum for the star Algol. The processing and analysis software used for these data will be directly applicable to the XGS data for Con-X.

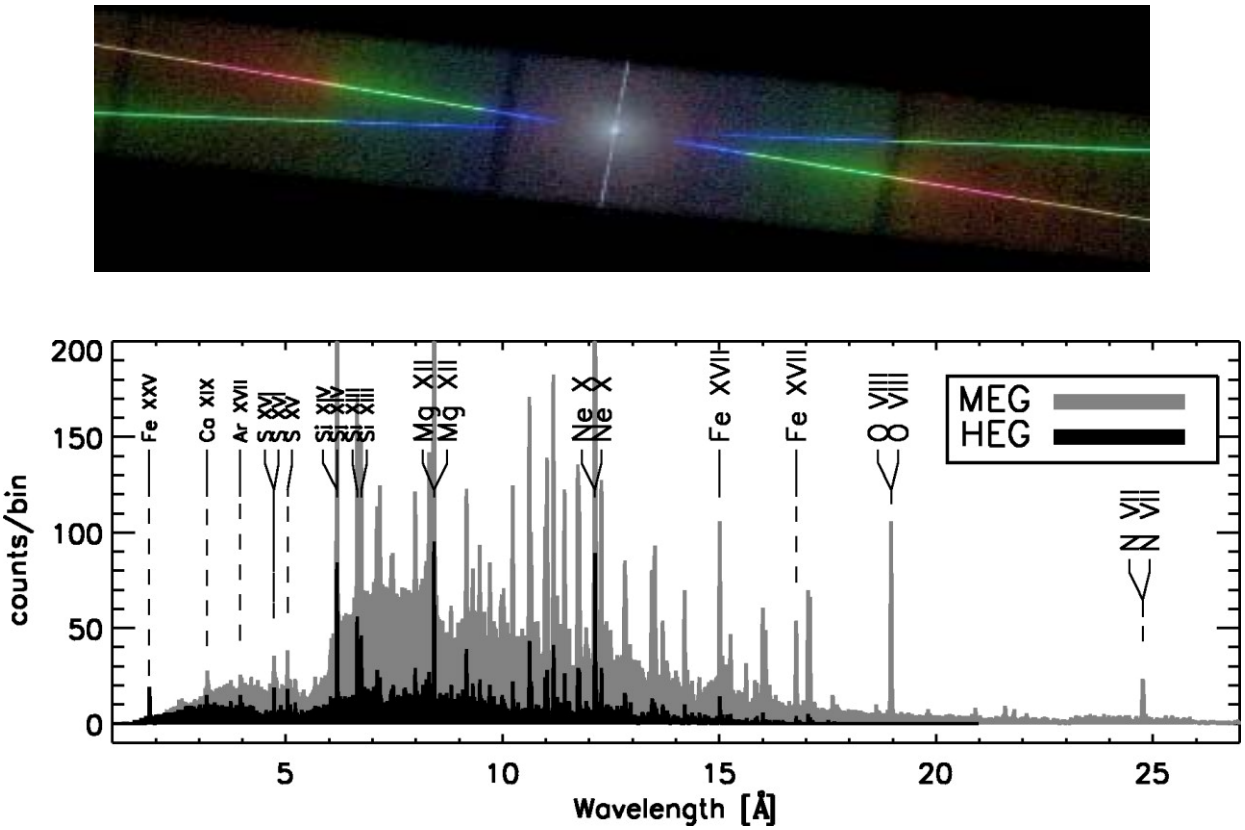

Figure 14-1. Chandra Grating Data from Algol

A representative CCD image of Chandra grating spectra (upper). The processed spectrum with line identifications for the star Algol (lower)

The Level 0 - 2 processing will be automated and will re-use the existing *Chandra* pipeline processing system infrastructure with tools reused from *Chandra* and *Suzaku* and updated to reflect the specific Con-X instrument calibrations. The existing system can also deal with data for specialized observations such from a tracked moving target or a raster scan on the sky.

Note that key ground calibration data, instrumental characteristics and instrument and mirror simulations (e.g., ray traces) will be produced during the Con-X development phase and captured by the CXSOC. The products and initial versions of pipeline and user analysis software will be validated as part of the extensive ground calibration of the instruments and mirror modules. This strategy ensures that the data

products and software are available for use post-launch, ensures experience by the science center team, and reduces risk for observer science return.

14.3 Con-X Analysis Tools

The analysis tools developed for *Chandra*, *XMM-Newton, Suzaku*, the *Rossi X-ray Timing Explorer* (*RXTE*) and other X-ray missions are well suited to analyze Con-X data and form a sound basis for the required tool set for observers. Existing analysis packages that provide tools for non-dispersive and dispersive spectral data, as well as for spatial and timing analysis include CIAO Sherpa, HEAsoft xspec (spectral fitting), CIAO spatial, HEAsoft ximage (spatial), CIAO Timing and HEAsoft xronos (timing). In addition, data visualization and processing tools exist (e.g., SAOImage-ds9). The *RXTE* mission has also developed extensive software and methodology for timing analysis of X-ray data. These tools also allow observers to export data in standard formats to use their own tools, or other existing or future tools. Modifications and extensions to the tools will be made during the development phase of the mission and will be verified using ground calibration data. The tools will also serve to analyze the ground calibration data and provide the initial set of products in a standard format (CalDB) for use by the pipleline and analysis tools at the start of the science mission.

While many of the tools needed for Con-X data analysis are in place, there will undoubtedly be a need to update existing plasma models and atomic physics data to refine the scientific interpretation. In the case of *Chandra*, similar revisions were driven by what was seen in the data from the dispersive gratings (HETG and LETG) once the mission launched. We expect this to be addressed both as part of the scientific preparation for Con-X, and then through active work by the science community during the mission.

We note that as a Science Center for a Great Observatory, the *Chandra* X-ray Center carried the mandate to develop software analysis tools and provide data in a standard format so that experts and non-experts alike could be scientifically productive with *Chandra* data. Given this, many of the complexities associated with deconvolving the instrumental response, dealing with subtle instrumental effects such as CTI and non-uniform and time-dependent gain, have been understood and software developed to address them. This provides confidence that the tools together with other prior mission tools such as the HEAsoft suite, form a solid basis for use with Con-X. The *Chandra* pipeline and analysis tools also benefited from being developed under a co-located science and operations center environment where instrument development and operational issues could be seamlessly incorporated into the tools. Based on this lesson, we plan the same approach for Con-X.

14.4 Analysis Software

14.4.1 X-ray Spectral Data Analysis

The most common method of analyzing astronomical X-ray spectra is the “forward-fitting method.” The following provides detail of the analysis steps required to analyze Con-X spectral data. As discussed above, software is largely in place to support the analysis.

- Calculate a model spectrum
- Multiply the result by the instrumental response matrix (convolve with telescope and detector response)
- Compare the result with the actual observed data

- Modify the model-spectrum and repeat until the best value of the comparison statistic is obtained.

The model spectrum is (usually) expressed in terms of a small number of parameters (e.g., power-law index and normalization for a simple power law) and the "best-fit" values of these parameters and their confidence regions are obtained.

Models are available for the basic emission mechanisms: blackbody, thermal bremsstrahlung, power-law, collisional plasma and line emission. Specialized models for accretion disks, comptonized plasmas, non-ionization equilibrium plasmas and multi-temperature collisional plasmas also exist or have been developed by the community. Special and General Relativity effects on line formation have been included. There is also support in existing packages for including user-supplied models.

14.4.2 Timing Analysis

Timing measurements probe fundamental physical timescales of systems including orbital, spin, dynamical, and pulsational timescales. These yield significant physical insights into X-ray binaries, X-ray bursts, pulsars, accretion physics and quasi-periodic oscillations (QPO). The techniques include: time series analysis, Fourier techniques, FFT period searches, power spectra characterization, epoch folding, Z^2 methods and Bayesian Blocks. Such methods have been extensively used by the *RXTE* mission, and have been developed for application to the imaging data of the *Chandra* HRC and ACIS data.

14.4.3 Spatial Analysis

Steps used for spatial analysis of point and point-like sources include modeling the point response function of the telescope and detector, background subtraction, correction for spatial variations in the instrument response (application of the exposure map), source detection, and determination of source properties: intensity, spatial extent, spectral hardness, and variability. For extended sources a more sophisticated approach is taken to modeling the background and background maps are employed. This is needed to account for the more complex variations in the background and the expected low surface brightness of the sources. Such methods have been developed and refined for analysis of data from many X-ray imaging telescopes with angular resolution comparable with Con-X (e.g., *Einstein* and *XMM-Newton*) and extended to those with much higher resolution (*Chandra*).

14.4.4 Other Techniques

Techniques have also been developed for joint spatial-spectral and spectral-timing analysis and are available for use with Con-X.

15. INSTRUMENT DEVELOPMENT SCHEDULE

Question: Provide an instrument development schedule if available.

RESPONSE

Development schedules are provided for the instruments and the Flight Mirror Assembly (FMA) in Figures 15-1 through 15.-4. The FMA is on the mission critical path. The top level mission schedule is provided and discussed in the response to Question 33. The schedules coordinate with the technology development schedules given in the response to Question 16, as appropriate.

15.1 Instrument Schedules

Schedules for the X-ray Mircrocalorimeter (XMS), X-ray Grating Spectrometer (XGS) and Hard X-ray Telescope (HXT) instruments are provided in Figures 15-1, 15-2 and 15-3 respectively. The instrument developers will be selected by competitive Announcement of Opportunity (AO) released by NASA Headquarter. Each instrument development schedule begins at AO award and progresses through design, fabrication, assembly and test, calibration and delivery. For each instrument we include the design and build of an engineering model. Funded schedule reserve is held prior to each instrument delivery.

15.2 Flight Mirror Assembly (FMA) Schedule

The Flight Mirror Assembly (FMA) program (schedule shown in Figure 15-4) begins with a six month study conducted by two or more potential industry partners in Phase A. The flight development contractor is selected by a Request for Proposal (RFP). The FMA contractor is responsible for design, fabrication, engineering unit build and test, flight system fabrication, assembly and test. Funded schedule reserve, of 3 months is held prior to delivery of the FMA #1; and 1 month prior to delivery of FMA #4.

Since the FMA development activity lies on the Constellation-X program critical path the schedule has been developed in considerable detail, with a roll-up provided in Figure 15-4. Particular attention has been paid to mandrel fabrication, segment forming and processing and the assembly and alignment of segments into the mirror module housings. This analysis determined the schedule durations as well as the equipment and facilities needed to support the FMA development program.

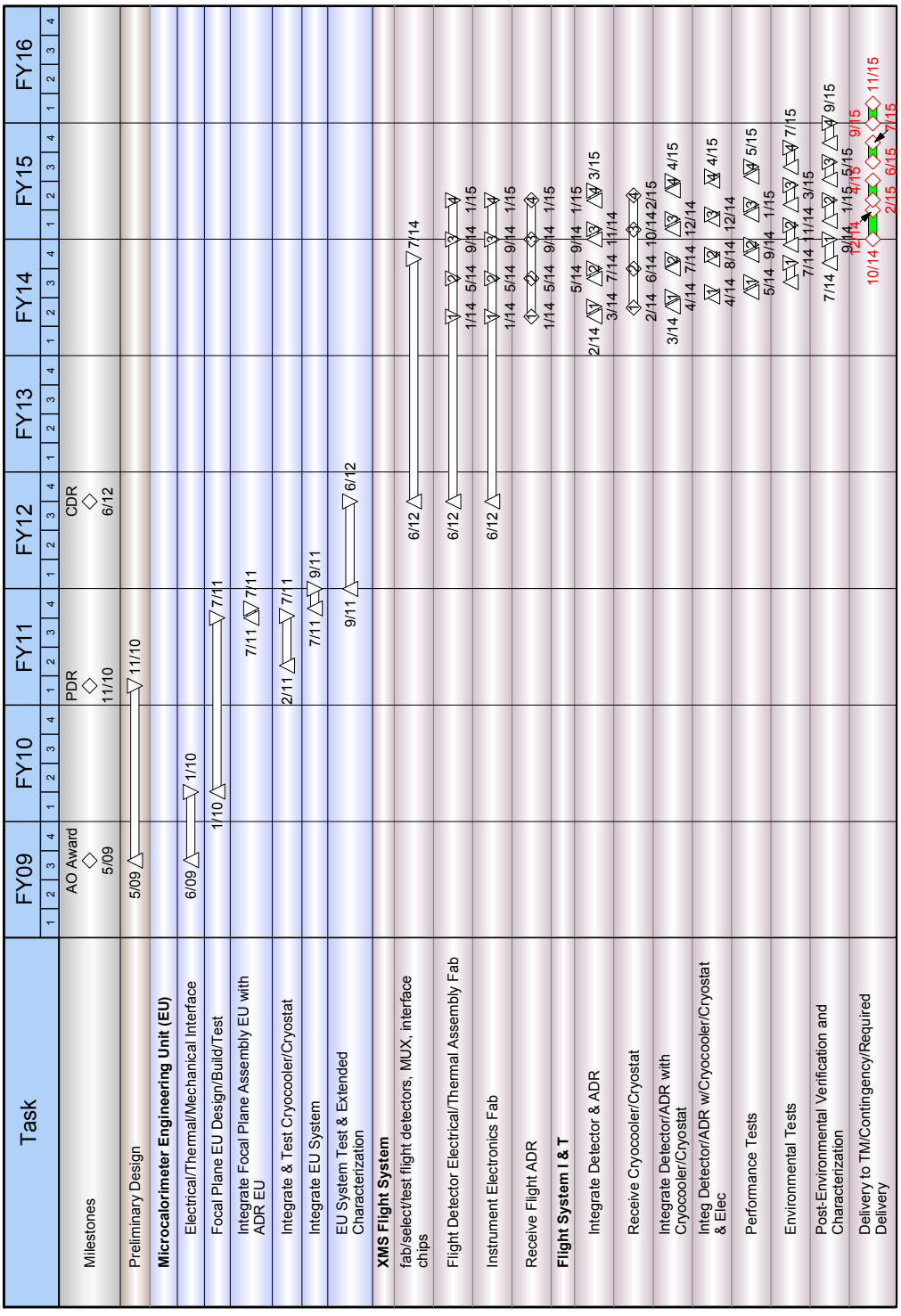

Figure 15-1. XMS Development Schedule

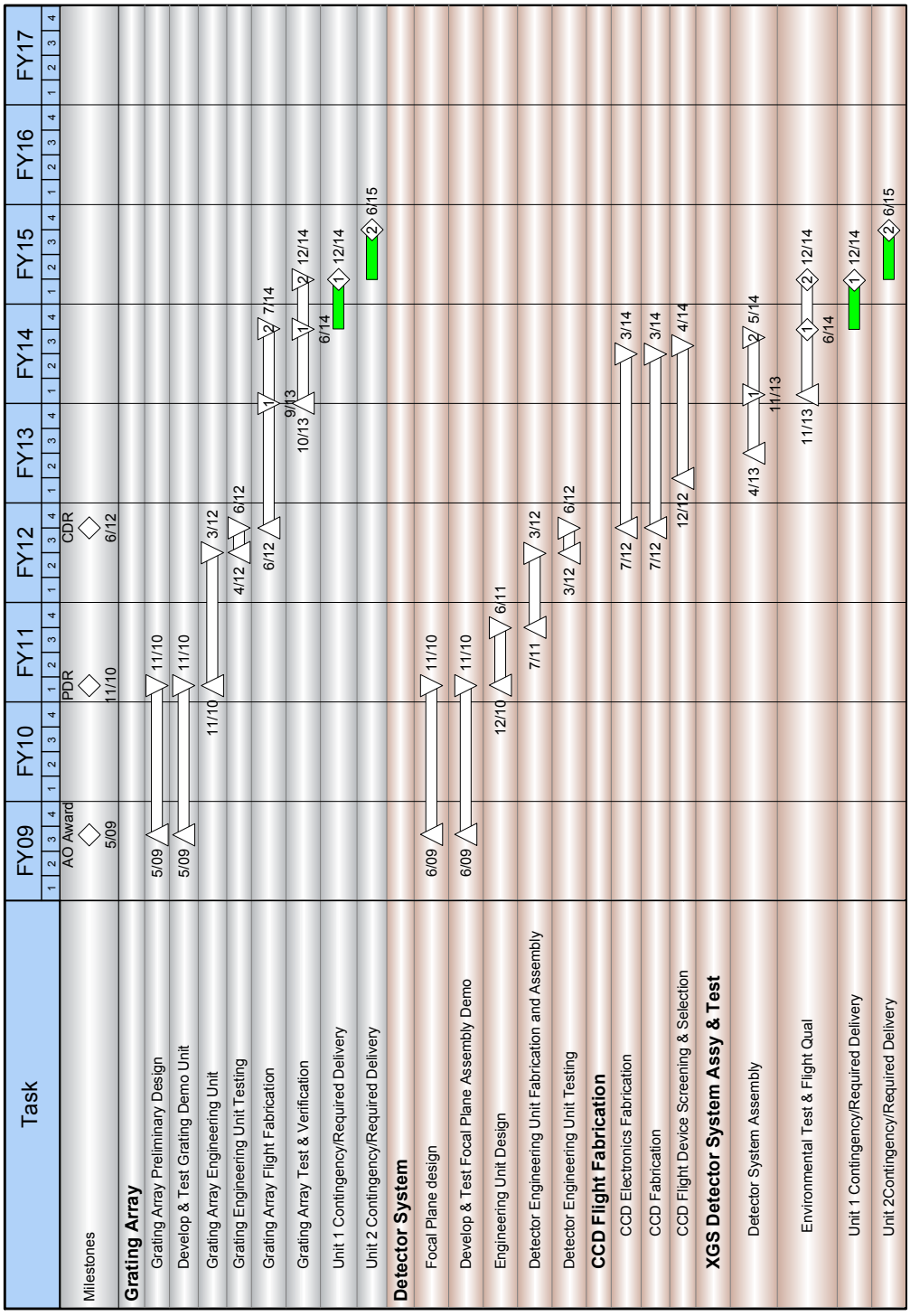

Figure 15-2. XGS Development Schedule

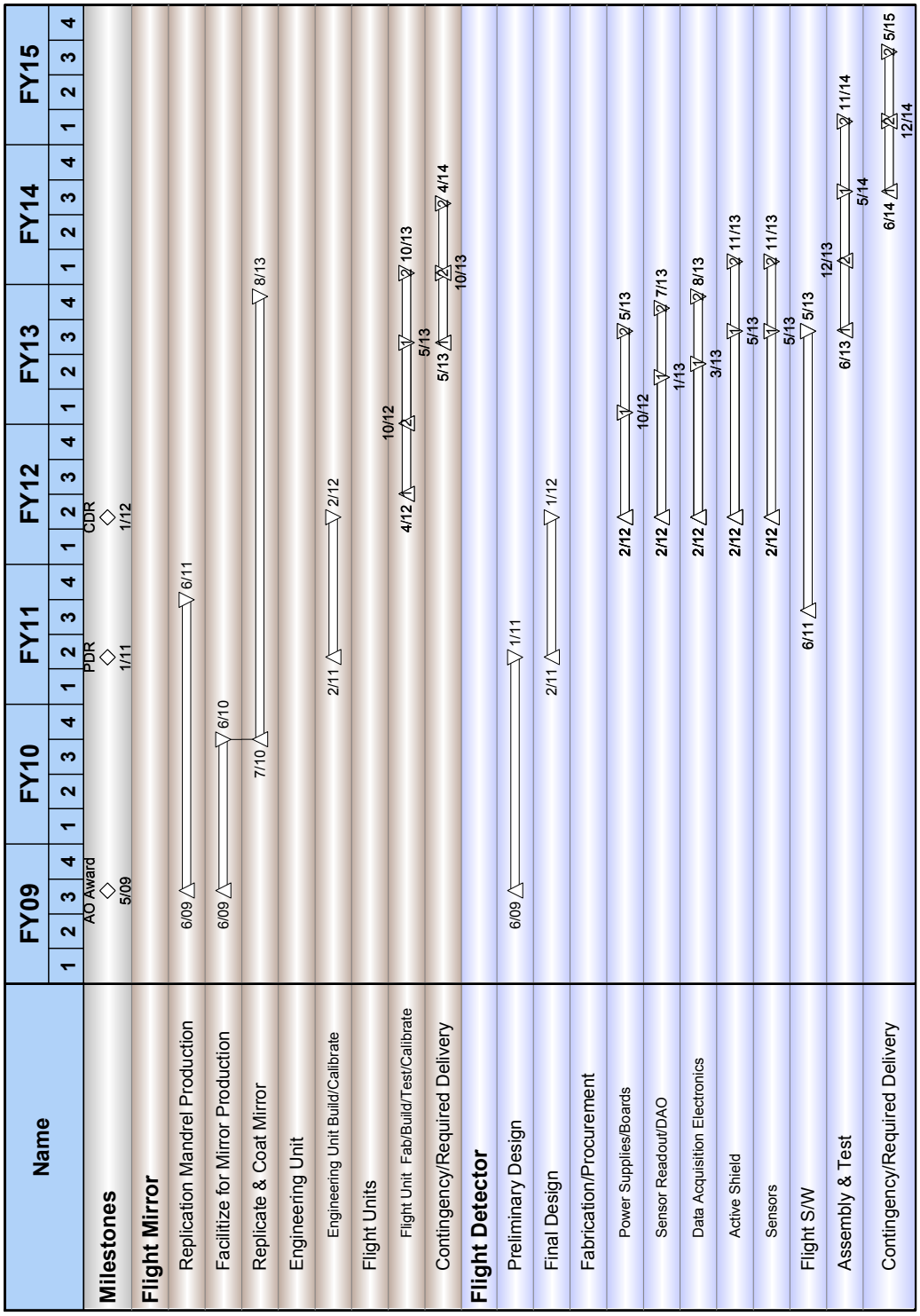

Figure 15-3. HXT Development Schedule

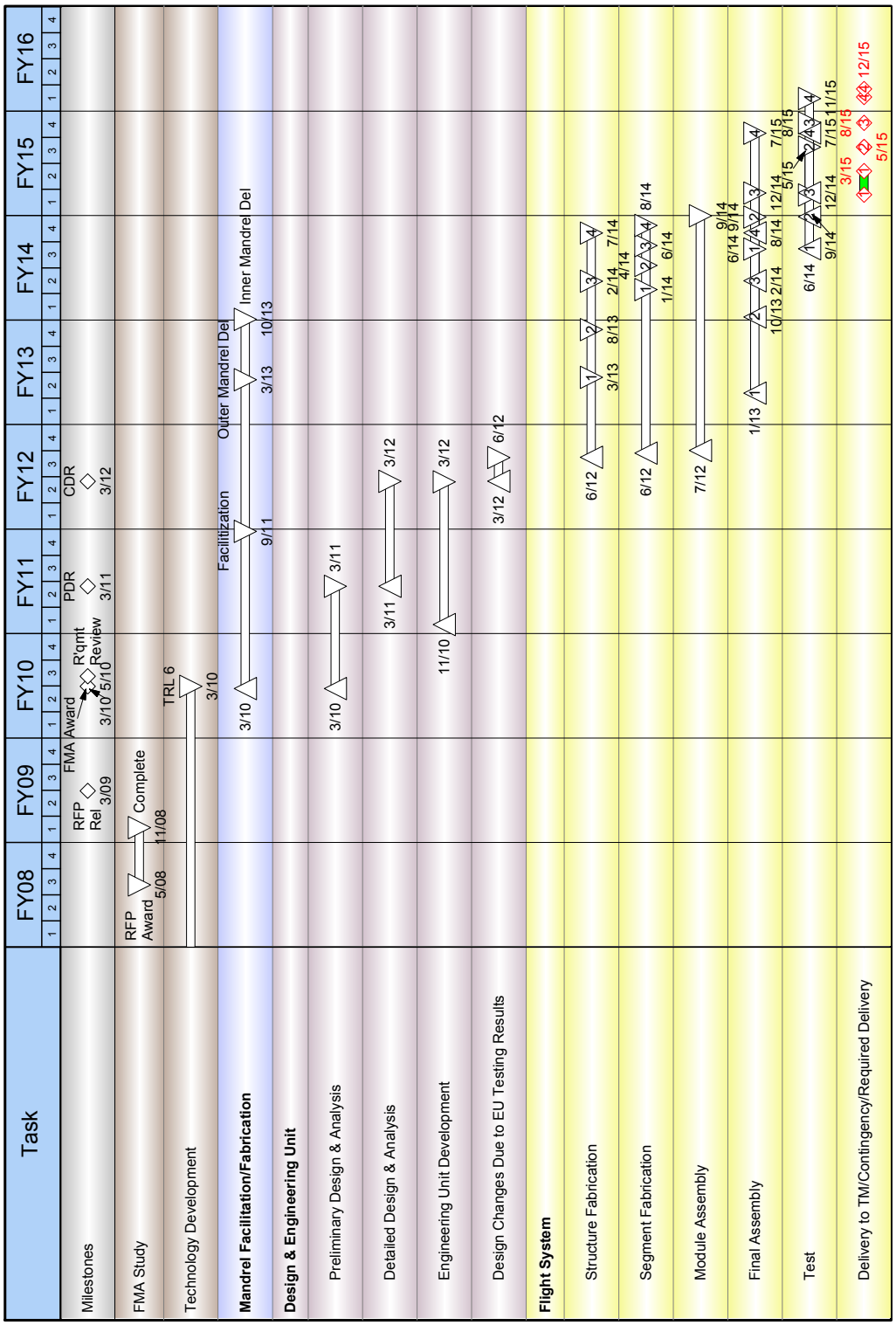

Figure 15-4. Flight Mirror Assembly (FMA) Schedule

16. SCHEDULE AND PLANS FOR TECHNOLOGY DEVELOPMENTS

Question: Provide a schedule and plans for addressing any required technology developments, and the associated risks.

RESPONSE

A targeted technology development program has been implemented and continuously assessed over the last 9 years to ensure that the critical technical issues are being addressed so that a transition to flight development can proceed with low programmatic and post-launch risk. Technology roadmaps were developed early on and refined for the NASA Technology Readiness Implementation Plan (TRIP) in 2003. The basic elements of the roadmap have not changed: the central issues are developing very high throughput optics, large arrays of high spectral resolution microcalorimeters, very high resolving power gratings, and very high sensitivity X-ray imaging up to 40 keV. The technology roadmaps have been developed with extensive insight and wisdom from the collective experience in developing earlier versions of the science instruments for previous missions. In all cases, and unlike any previous observatory designed for X-ray astrophysics, there is extremely relevant flight experience that has gone into the design of the Con-X technology development plan. The schedule for FMA and all instrument developments are summarized in Figure 16-1. We note that FMA technology is fully funded by Con-X, while the XMS technology funding comes from multiple sources that include Con-X. The XGS and HXT developments, however, are funded by independent sources prior to the AO. Thus, only the detailed schedules of the FMA and XGS technologies are provided. In the sections that follow, we itemize the critical technical issues that are central to ultimately achieving the mission requirements of Con-X.

16.1 Spectroscopy X-ray Telescope (SXT) Flight Mirror Assembly (FMA)

Technology development for the SXT Flight Mirror Assembly (FMA) focuses on two key areas, as described in our response to Question 7: mirror fabrication, and mirror alignment and mounting (which includes bonding). Thus, the goals of our technology plan are: (1) to establish a robust process for fabricating mirror segments that meet Constellation-X requirements, and (2) to demonstrate alignment and mounting of multiple mirrors into a module at the required accuracy. FMA technology development will culminate in a prototype inner module which will be X-ray and vibration and acoustic tested to achieve an overall TRL-6. Figure 16-2 summarizes the technology schedule, with the following milestones:

- Fabricate mirrors to required precision:
  - Fabricate mirror segments with 50 cm diameter (FY08)
  - Fabricate mirror segments with 1.3 m diameter (FY09)
- Align and mount mirrors to required accuracy:
  - Align and mount one mirror pair with the passive approach (FY08)
  - Align and mount one mirror pair with the active approach (FY08)
  - Align, mount, X-ray and environmental test multiple mirror pairs with passive and active approaches (TRL 5, FY09)
  - Down select alignment approach (FY09)

- Build and X-ray and environmental test a prototype inner module (TRL 6, FY10)
- Build and X-ray test a wedge demonstration unit (inner and outer module) (FY11)

16.1.1 Mirror Segment Fabrication Technology

Over the past few years, we have improved the thermal forming process and are now fabricating mirror segments with figure errors that are close to meeting requirements, as discussed in the response to Question 7. We will focus on the following key areas in achieving the mirror segment performance:

- Refine metrology methodology - We will implement modifications to the metrology setup to reduce its error contribution to mirror figure near the edges.
- Produce a mirror segment with 50 cm diameter - We will minimize mirror figure errors by optimizing the forming temperature cycle, smoothing further the mandrel release layer which is the interface layer between the mirror segment and the forming mandrel, and reducing the segment coating thickness. In addition, we will also refine the process to improve the mirror fabrication yield.
- Produce a mirror segment with 1.3 m diameter – After establishing the mirror fabrication process with the 50 cm diameter segment, we will proceed to producing the 1.3 m diameter segment which is the largest mirror size for Constellation-X.

16.1.2 Alignment and Mounting Technology

As the mirror fabrication process has progressed, we have focused more on the alignment and mounting technology. To mitigate risk, we are pursuing two approaches, "passive" and "active" alignment, as described in our response to Question 7. Our plan to develop this technology is as follows:

- Mount, align, and test one mirror segment pair in the housing – For the active approach, we will improve the stability of the alignment station to facilitate easier alignment and bonding. For the passive approach, we will develop procedures for transferring the mirror from the metrology mount to the housing and for bonding. In parallel, we will perform vibration and acoustic tests, using mirror segments, to guide the detailed design of the housing structure.
- Mount, align, and environmental test three segment pairs in the housing to achieve TRL 5 – We will improve the repeatability of each technique and demonstrate mass alignment with multiple pairs. We will perform X-ray tests and vibration and acoustic tests, and then down select the alignment approach for prototype development.
- Develop and test a prototype inner module to achieve TRL 6 – We will build an inner module that will have aligned mirror pairs and non-optical segments to simulate the remaining mirrors. We will perform X-ray test, and vibration and acoustic tests. We will thus achieve all of the required technology developments with this milestone.

We will, as part of the technology development, refine our optical model and finite element analysis, and correlate the models with the performance test results at key steps identified above. The processes and methodologies that we develop will be extendable to meeting the mission goal of 5 arcsec angular resolution. Subsequent to the development of the prototype inner module, we will also build and test a wedge, which consists of one inner module and two outer modules. The wedge development effort will allow us to be a "smart buyer" as we transition to the flight implementation phase.

16.2 X-Ray Microcalorimeter Spectrometer (XMS)

The XMS detector system technology development roadmap consists of major milestones tied to significant demonstrations of the integrated detectors and read-outs, each fed by supporting demonstrations in the detector and superconducting electronics subsystems separately (see schedule in Figure 16-3). In addition to these major and supporting milestones, there are two concept demonstrations scheduled to vet lower-priority components that have not received investment comparable to close-packed arrays of independent superconducting transition-edge sensor (TES) microcalorimeters and SQUID multiplexer technology.

The XMS focal plane requirements stipulate a 5 arcmin x 5 arcmin field of view sampled at 5 arcsec. The highest spectral resolution, 2.5 eV is required of the central quarter of the array, or 2.5 arcmin x 2.5 arcmin. The required spectral resolution of the rest of the array is 8 eV at 6 keV and below.

Our plan to meet these requirements is to fill the focal plane with a combination of a high-performance core array and a field-of-view extension. The core array is a 32 x 32 array of 5 arcsec independent microcalorimeters. Each pixel consists of a TES (which acts as the calorimeter thermometer), an X-ray absorber, and a membrane thermal link to the 50 mK heat sink. The absorber is larger than the TES and its thermal link, making thermal contact to the TES but elsewhere extending cantilevered above the sensor plane by several microns. The gap between adjacent absorbers thus can be on the scale of 5 microns. For the field of view extension, which has three times the number of spatial elements as the core array, the spectral resolution and speed of the additional elements is relaxed relative to the core array. Thus this extension can be achieved by making design compromises that keep the number of electronics channels from scaling with the increase in pixels. Our basic design for the extension utilizes imaging TES detectors that will have at least four imaging elements per TES. Both parts of the focal plane will be read using multiplexed SQUID amplifiers. The core array drives the technology development for the SQUID MUX.

16.2.1 Core Array Pre-demonstration

Multiplexed (2x8) read-out of 16 different flight like pixels in an 8x8 array with better than 4-eV resolution at 6 keV and pulse fall time < 1 ms. [July 2007]

Supporting milestones:

- 8 channel SQUID MUX switching and speed demonstration. [DONE June 2006]
- Verification of 8x8 close-packed (flight-like) array, with at least 16 pixels showing better than 4 eV resolution at 6 keV and pulse fall time < 1 ms when tested individually. [May 2007]

Discussion:

The recent success of the vacuum-gap absorber-contact geometry (see Kilbourne et al 2006 in response to Question 12), which permits the use of high-quality electroplated gold for the X-ray absorbers of TES devices, makes these near term milestones feasible. Gold reliably and reproducibly thermalizes the energy of the incident X-rays. Four individual pixels, three on the same array, have demonstrated energy resolution in the range 2.2 – 3.3 eV at 6 keV. While experiments to optimize the contact geometry of the absorber will still be carried out, revisions to the photolithographic mask set are being made that will include several arrays with identical pixels in one of the geometries that has already shown promise. It is with these arrays that we anticipate achieving this near-term milestone.

16.2.2 Extended Field-of-View Concept Demonstration

Demonstrate feasibility of extending the field of view to a total coverage that is a factor of 4 times the 32x32 array of 5" pixels that constitute the core array. As the requirements for the spectral resolution and speed of the additional elements is relaxed relative to the core array, this extension can be achieved by making design compromises that keep the number of electronics channels from scaling with the increase in pixels. This milestone will be met by demonstrating detectors with at least 4 spatial resolution elements per TES sensor and a resolution on each of better than 8 eV, in a design that is readily arrayed in a close-packed configuration. [December 2007]

Discussion:

The Position Sensitive TES (PoST) is a device with a continuous or segmented absorber strip between two TES's. In geometries that have not been close-packed, we have already achieved 8 – 12 eV resolution at 6 keV across 9 spatial elements read by 2 TES's. Design improvements to the independent-pixel design have not yet been applied to the PoST design. We predict that 8-eV resolution is attainable in a close-packed design using a segmented absorber design based on the successful electroplated gold absorbers used in the independent pixels, and that better resolution may be possible by combining electroplated bismuth with electroplated gold. The feasibility of scaling up the core array to 64x64 will also be investigated.

16.2.3 Particle Veto Concept Demonstration

Demonstrate proof-of-principle one-sided anti-coincidence detector for particle veto and design a feasible scheme for its integration behind the microcalorimeter array. [January 2009]

Discussion:

An anticoincidence detector has been presumed for XMS. The *Suzaku*/XRS had an antcoincidence detector based on charge collection in Si. The detector was situated just behind the calorimeter array and was operated at the same temperature (60 mK), and it was read out using a similar JFET amplifier scheme to the pixels of the array. In the case of Constellation-X, we are considering a similar design scheme that uses the same readout as the detector array, in this case SQUID technology. We presume a design in which TES's are placed on the surface of a silicon crystal; this is an approach that is already in use in terrestrial dark matter searches and that would be readily adaptable for the XMS anticoincidence detector. At the time of designing the engineering unit, schemes for 5-sided anti-coincidence that incorporate the veto detector into the detector housing will be investigated, but demonstration of a 1-sided veto is adequate for technology verification.

16.2.4 Core Array Demonstration Unit

Multiplexed (3x32) read-out of 96 different flight like pixels in a 32x32 array with better than 3 eV resolution at 6 keV and below, and pulse fall time < 0.5 ms. [August 2008]

Supporting milestones:

- 32-channel MUX switching and speed demonstration [June 2008]
- Verification of 32x32 close-packed (flight-like) array, with at least 96 pixels meeting XMS requirements for the core array when tested individually [June 2008]

Discussion:

This demonstration requires the SQUID MUX to operate at the ultimate design speed (12 MHz open loop bandwidth), which will be realized with straightforward design changes from the prior demonstration. The development required in scaling the core array from 8x8 to 32x32 lies mainly in routing of the signal leads (fine-line micro-striplines are now required) and in heat sinking the array structure to handle the bias power of 1024 pixels and minimize thermal crosstalk. The micro-stripline technology is already in hand. Proper heat sinking without mechanically over-constraining the device is a development hurdle that must be surmounted before the more complex integration of the TRL6 demonstration is attempted. The concepts are straightforward, however, thus the associated risk is small.

16.2.5 Focal Plane Assembly Prototype (TRL6)

Multiplexed (4x32) read-out of portion of full focal plane array – 96 different pixels in a 32x32 core array with better than 2.5-eV resolution at 6 keV and below, and pulse fall time < 0.5 ms and 32 PoST channels (at least 128 pixels with better than 8-eV resolution at 6 keV) . A particle-veto has been integrated into the test set-up. Component-level environmental tests have been passed. Electrical and thermal interconnects and staging are approaching a flight-worthy design, but a flight design is not fully realized. [December 2009]

Supporting milestones:

- Array vibration tests [March 2008]
- SQUID and detector radiation tests [September 2008]
- Verification of expanded focal plane array comprising 32x32 core array and PoST array extension, either in a monolithic array or a composite structure. [May 2009]
- Electrical/thermal/mechanical assembly designed and fabricated [May 2009]

Discussion:

The difference between this demonstration and the Engineering Unit is that only the focal plane array will be of a flight-like design. The detector assembly will not be designed to accommodate every electronics channel, nor will it be engineered to vibration or mass specifications. The purpose of this demonstration is to bring the various components of the focal plane assembly together to develop the technologies needed for their thermal and electrical integration into the focal plane assembly. The design of this assembly includes mechanical suspension systems, wiring interconnects, high-density wiring feedthroughs, thermal sinks, and kinematic mounts. The assembly must maintain the following at an acceptable level: 1) thermal stability, thermal gradient across array, and thermal crosstalk, 2) electrical crosstalk, microphonics, magnetic shielding, and susceptibility to interference, and 3) conducted and radiative heat loads on all the temperatures stages. The design of this assembly will be guided by experience with *Suzaku*/XRS, the X-ray Quantum Calorimeter sounding rocket program, and our test platforms. The design will require systematic quantification of materials parameters and a careful balancing of the competing needs of the electrical, thermal, and mechanical elements of the integration. The risks associated with this development can be minimized by allocation of adequate resources.

16.2.6 Continuous Adiabatic Demagnetization Refrigerator (CADR) Development

CADR development efforts over the past 6 years have resulted in a prototype that meets the operating temperature (50 mK) and cooling power (>5 microwatts) requirements for the XMS detectors, while

operating with a heat sink as warm as 5 K. Additional development is needed to meet the temperature stability requirement of 2 microKelvin rms, and possibly the need to operate from a 6 K heat sink.

Obtaining a high degree of temperature stability is more difficult with the CADR because of periodic reversals of heat flow in the low temperature stages that must occur during each cycle. The changing heat flow and associated temperature gradients can cause momentary disturbances in the base temperature of 100 microKelvin or more. The magnitude depends on many factors, including how fast the reversals occur and the bandwidth of the temperature controller. They can be completely eliminated if the CADR cycle is slowed sufficiently, but this reduces the system's cooling power. Until the instrument design is more mature and the cooling power requirements are better known, the approach will be to modify the CADR and its control system, including the implementation of feed-forward techniques, to minimize the disturbances without reducing cooling power. A major milestone in this effort was the delivery of custom control electronics made by LakeShore Cryotronics, a company that specializes in instrumentation for cryogenic applications. Its integral magnet power supplies and temperature controllers achieve much higher control bandwidth, and therefore can assert more aggressive control to overcome disturbances. The high rate also improves the ability of the controller to anticipate heat flow changes and exert preemptive control. This technique has shown promise in the past, but was severely limited by the slow control rate. Together with changes in the cold hardware to increase thermal time constants, it is expected that temperature stability at the required level can be obtained throughout the CADR cycle. The risk if this effort is not completely successful is that it could be necessary to discard data collected when the temperature is not stable, which presently is less than 5% of the total cycle time.

Concerning the heat sink temperature, it is important to note that 6 K is not an absolute requirement since some Advanced Cryocooler Technology Development Program (ACTDP) cryocoolers have demonstrated the ability to operate at less than 5 K, within the range of the prototype. However, meeting the requirement will provide additional flexibility in system design and optimization, with potential benefits to the power subsystem. To do so requires advances in superconducting wire with higher critical temperatures to produce superconducting magnets capable of operating at 6 K or higher. Much progress has been made in this area in the past 2-3 years with Nb_3Sn wire, to the point that under a Small Business Innovative Research grant, we have received and tested a magnet capable of producing 4 Tesla at 10 K with only 8 amps of current. The current focus is to decrease both the size and current needed, and conduct a demonstration of 6K heat rejection with the CADR prototype by the time of instrument selection (see schedule in Figure 16-4).

16.2.7 Cryocooler Technology Development

Cryocooler technology development that meets current requirements and associated risk has been completed. Though one of the ACTDP vendors targeted XMS cooling requirements during the program, no development model cooler was made that addressed all system requirements. It is expected that this will be accomplished with the design and fabrication of a necessary ETU cooler, to integrate as part of an ETU XMS, following instrument selection.

16.3 X-ray Grating Spectrometer (XGS)

Technology development for the XGS involves the parallel development of the grating elements and the CCD devices. The major milestones to achieve TRL 6 are the same for the transmission grating and reflection grating spectrometer concepts. These include the fabrication of a prototype grating array and

demonstration of the X-ray performance, fabrication and testing of the CCD devices, and the development of engineering units. Within the Con-X budget there are currently not sufficient funds to support the XGS technology development. All technology development prior to the instrument AO is now funded by independent sources. The selection of a specific XGS configuration will occur as part of the instrument AO process.

16.3.1 Grating Array

Key milestones in the technology development of the grating array include:

- Fabrication and X-ray testing of flight prototype grating: All of the critical fabrication elements have been demonstrated for both the transmission and reflection gratings, but individual grating elements with all of the necessary properties have not yet been fabricated. A flight prototype transmission grating will be fabricated and X-ray tested by the spring of 2008. A prototype reflection grating is scheduled for delivery in the summer of 2007. X-ray efficiency tests can be completed by the spring of 2008. X-ray resolution tests of the off-plane gratings that had been arranged before the Con-X budget cuts, now await alternate sources of funding.
- Demonstration of flight prototype array: The development and demonstration of a prototype array involves mounting and aligning the grating elements within the support structure, environmental tests of the integrated array, and X-ray efficiency and resolution performance tests. This is scheduled for completion by the instrument Preliminary Design Review (PDR).
- Grating Array Engineering Unit: The development and testing of a grating array engineering unit is scheduled for completion by the instrument Critical Design Review (CDR).

16.3.2 CCD Detector System

Key milestones in the technology development of the CCD detector system include:

- Fabrication and X-ray testing of flight prototype CCD chip. This includes development of improved high-speed, low-power readout circuitry for the devices, fabrication of the prototype devices, deposition of the aluminum blocking filter, and X-ray tests. A flight prototype CCD will be completed and tested by the instrument PDR.
- Detector System Engineering Unit: The development and testing of the detector system engineering unit is scheduled for completion by the instrument CDR.

16.4 Hard X-ray Telescope (HXT)

Technology development for the HXT involves development of mirrors and detectors.

Both technologies are fairly well advanced and have only a few milestones to complete before achieving TRL 6. However, no funding exists in the present Constellation-X budget to advance these technologies. Any technology development prior to the instrument AO, which is expected in May 2009, must be funded by sources other than Constellation-X.

16.4.1 Mirror Modules

Two technologies are being developed in parallel to reduce risk and provide competition: 1) thin glass segments assembled into a segmented nested mirror and 2) electroformed nickel shells of full revolution assembled into a nested mirror. Both technologies include W/Si depth graded multilayer coatings to

provide the required response at high energies, and both mirror technologies focus onto a CZT solid state detector. Key milestones required for each mirror technology to reach TRL 6 are :

- Glass segments: X-ray test of prototype mirror to show 30 arcsec requirement.
- Electroformed shells: Vibration testing of prototype mirror in prototype mount.

16.4.2 Solid State Detector

Key milestones required to reach TRL 6:

- Detectors flown on the HEFT balloon flight are similar to those required for the HXT. Active shield must be modelled, optimized and tested for Constellation-X orbit.

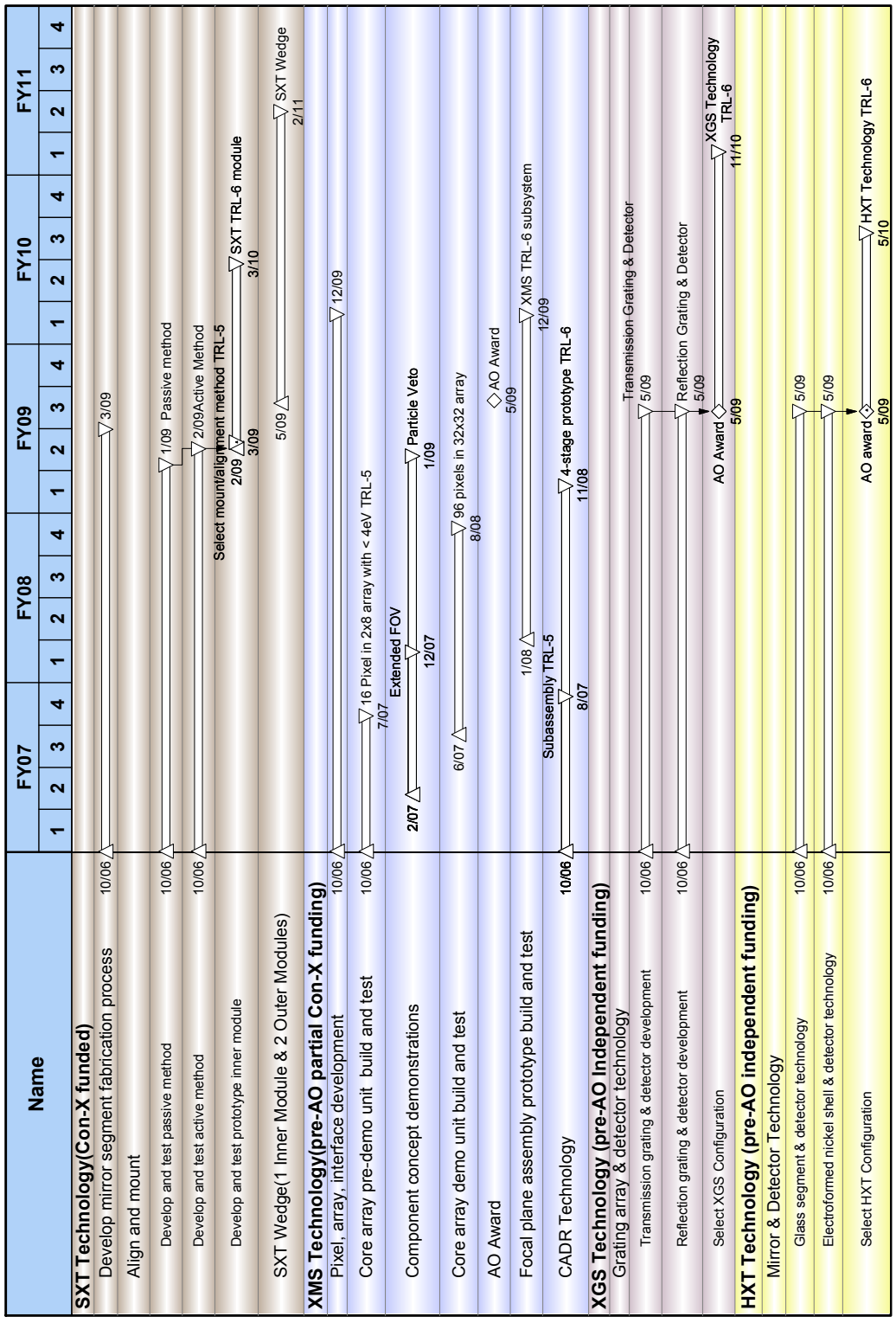

Figure 16-1. Con-X Technology Development Schedule

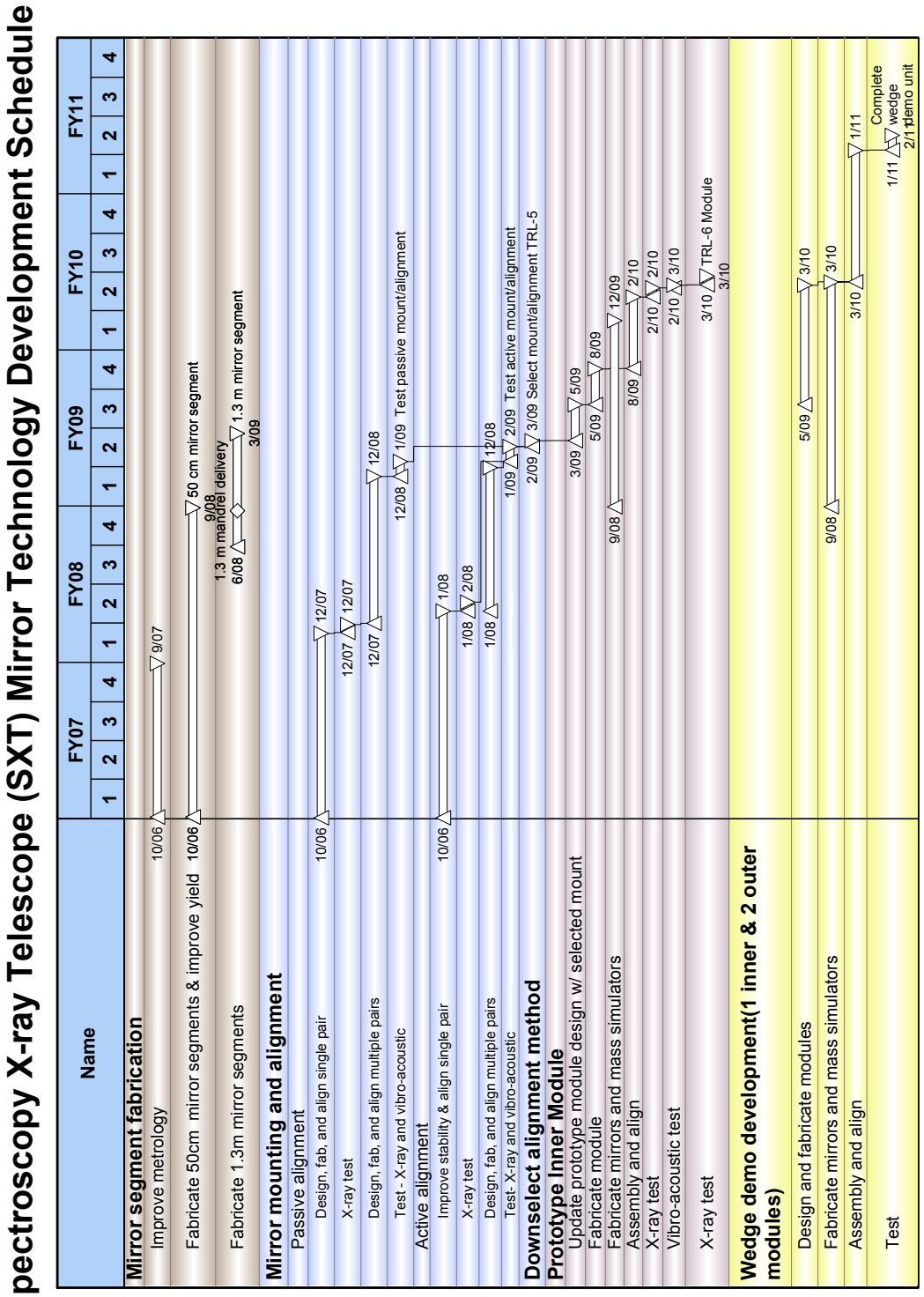

Figure 16-2. SXT Mirror Technology Development Schedule

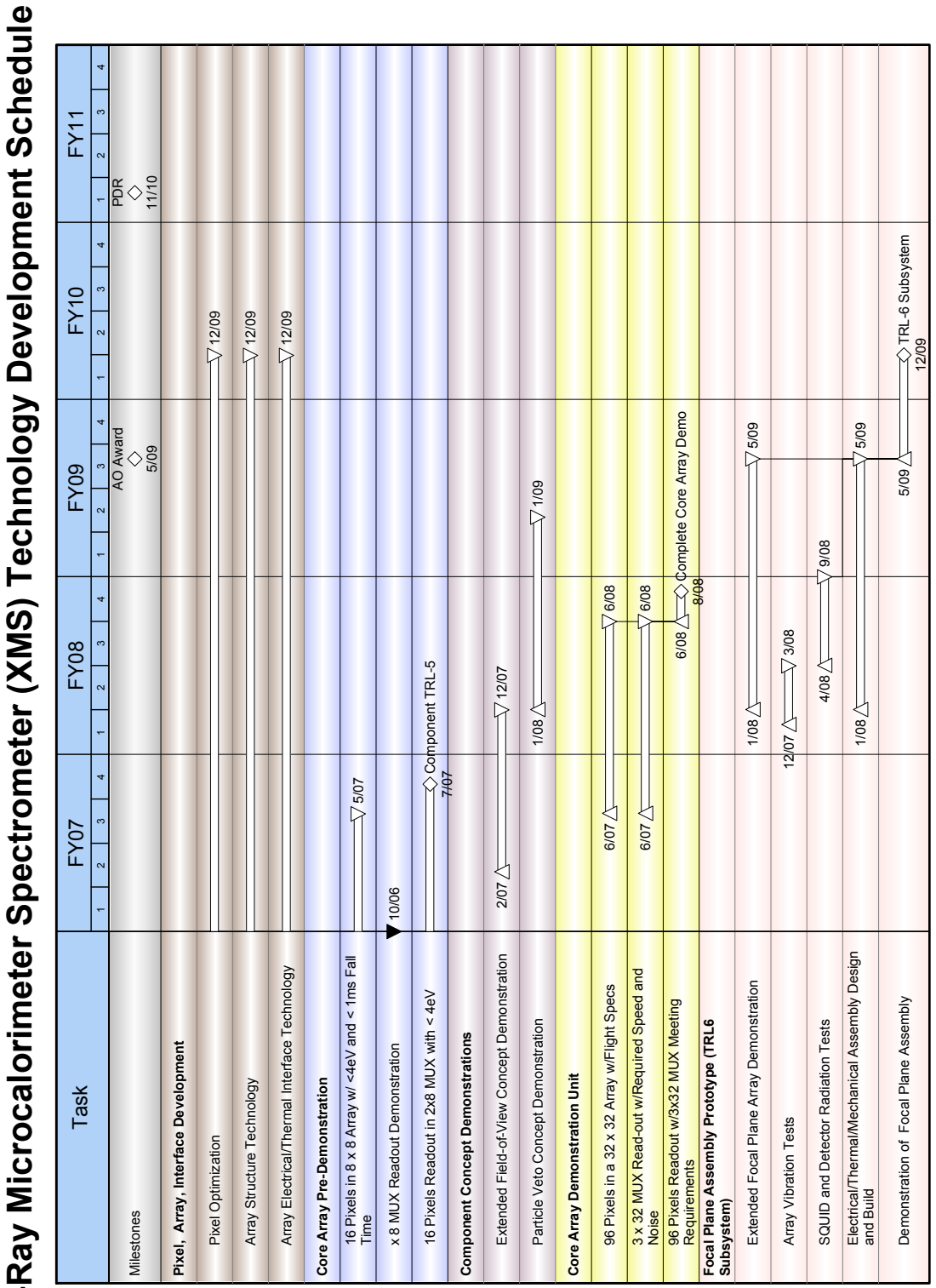

Figure 16-3. XMS Technology Development Schedule

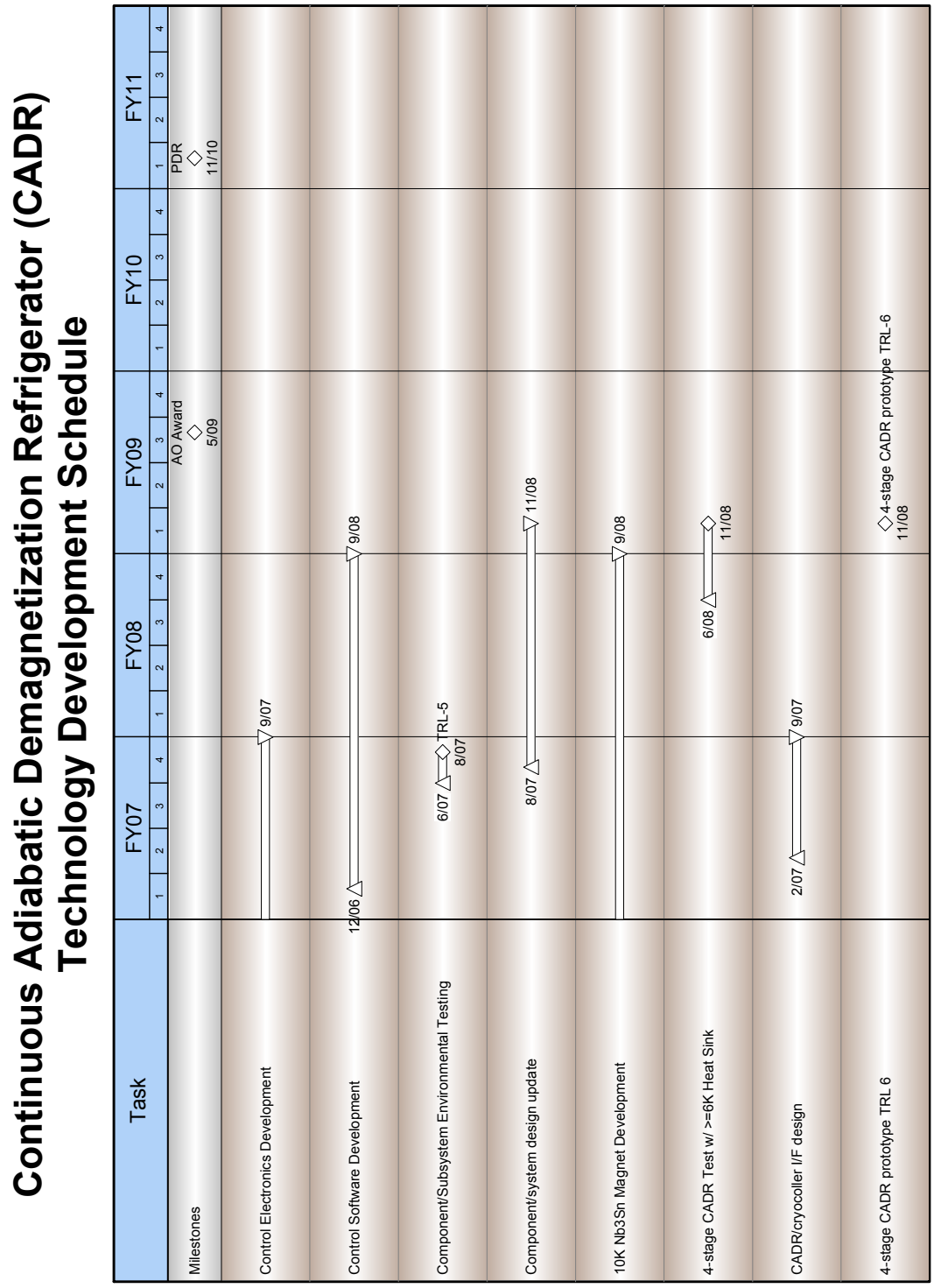

Figure 16-4. CADR Technology Development Schedule

17. INSTRUMENT FLIGHT SOFTWARE

Question: Describe the complexity of the instrument flight software, including estimate of the number of lines of code.

RESPONSE

The software for each instrument will perform the following major functions:

- Monitoring of the instrument (voltages, currents, temperatures) for health and safety, providing this information to the spacecraft, and maintaining statistics.
- Allow for maintenance of the software, including memory uploads and dumps, and diagnostic capabilities.
- Performs the science operations (data acquisition, event processing, data compression, diagnostic operations).
- Interfaces to the spacecraft and sends the data to the s/c for telemetry to the ground, and responds to spacecraft commands (such as commands to safe the instrument).

Software complexity depends on factors such as the code modularity, number of mechanisms to be controlled, the number of external interfaces, etc. At this point in time, we cannot provide a detailed assessment of the software complexity based on traditional metrics such as logical (cyclomatic) complexity (i.e., the number of linearly independent test paths, data complexity (types and parameter passing), calling complexity, GOTO usage, or nesting levels. However, a general assessment would be that flight software for each of these instruments will be moderately complex, based on our experience *with the comparable Chandra and Suzaku instruments.*

When possible, the software code size has been estimated from current flight missions (the XMS code estimate is based on the *Suzaku* XRS instrument, the XGS is based on the *Chandra* ACIS estimate), or on recent balloon flights (InFOCuS and HERO for the HXT). The details for each instrument are provided below. We expect a substantial re-use of the conceptual design and algorithms from these flight instruments, and a significant portion of direct re-use of the code. Portions of the codes that are related to mechanism control and spacecraft interfaces will be new. Similarly, the verification and validation of flight software will be based on the *Chandra* and *Suzaku* software V&V approaches, which will provide a high fidelity starting point.

Table 17-1. Summary of Lines of Code Estimate

Instrument	LOC (estimate)	Heritage For Estimate
XMS	15,000	Suzaku XRS
XGS	130,000	Chandra ACIS
HXT	25,000 - 50,000	HERO, InFOCuS, NuSTAR

17.1 XMS

The main instrument–specific functions of the XMS flight software will be to operate the CADR and regulate temperature, drive the multiplexing of the detector channel readouts, and process the calorimeter pulses. The array multiplex control will be implemented in hardware. In the current plan, the triggering will also be performed in hardware, so, conceptually, the software will be simpler than on the *Suzaku* XRS.

The *Suzaku* XRS digital processor had about 20,000 lines of assembly language. We will probably have somewhat more complexity in the Fast Fourier Transform (FFT), and implementing a higher degree of data compression. With margin, we estimate that the data processing code will be on the order of 10,000 lines of high level (C-type) code.

The CADR controller will be even simpler. The XRS ADR controller had about 7,000 lines of assembly code. The XMS will have multiple CADR magnets to control for XMS, increasing the line count. With margin, we estimate approximately 5,000 lines of high level (C-type) code.

The cryocooler software resides in the cooler control electronics and is designed so that the revisions can be installed and verified on orbit. A copy of the baseline cryocooler software routines required to prove normal cryocooler operation (such as initialization, temperature control and monitoring) are carried onboard. Upon power-up this copy is utilized as the default.

In total, we estimate that the XMS instrument will have on the order of 15,000 lines of high level flight software that will need to be verified. The *Suzaku* XRS software verification plan will serve as a high-fidelity reference for this.

17.2 XGS Software

The onboard software for the X-ray Grating Spectrometer CCDs will be patterned on the software used for the *Chandra* Advanced Camera for Imaging Spectroscopy (ACIS) CCDs. The ACIS flight software was roughly 130,000 lines of code in high level languages such as C and C++. Since the XGS CCDs will be conventional in design, the core algorithms will be essentially the same as those used for ACIS. The use of more modern processors, with longer word lengths and larger caches should slightly reduce the number of lines of code.

17.3 HXT

The main function of the HXT detector software will be pulse processing. The operation of the solid state detectors is relatively simple, and there is only one science operation mode – the high voltage is turned on and data are collected. There is an initialization which is carried out to test the integrity of the electronics for each channel, before turning on the high voltage for the first time. There is also a calibration mode which will be run initially before any data is collected and will be run on a regular interval to check the gain of the system.

The software estimate for the HXT is based on two separate balloon programs, and on the basis of the Phase A study for the NuSTAR satellite.

- InFOCuS: 8,000 lines of C code
- HERO: 10,000 lines of C code
- NuSTAR 4,700 lines of code

We estimate that the additional requirements for an Observatory level flight program will increase these numbers by a factor of approximately 5, resulting in an estimate of 25,000 - 50,000 LOC.

18. SCIENTIFIC REACH COMPARED WITH OTHER PLANNED MISSIONS

Question: Compare the scientific reach of your mission with that of other planned space and ground-based missions.

RESPONSE

18.1 The Big Picture

The James Webb Space Telescope (JWST), the Atacama Large Millimeter Array (ALMA), and the Giant Segmented Mirror Telescope (GSMT) will be operating at the same time as the first Beyond *Einstein* mission. These telescopes are well matched to the capabilities of Constellation-X. The two order of magnitude increase in effective area of Constellation-X (relative to the *Chandra* and *XMM-Newton* gratings) means it will be the X-ray counterpart to these new large facilities. This will finally bring X-ray astronomy on a par with the spectroscopic capabilities that are routine in other wavebands. As such, Constellation-X will be a great observatory comparable in scope to HST, *Chandra* and Spitzer. Together Constellation-X, JWST, ALMA, and GSMT will be similar to the current situation with the Great Observatories where *Chandra*, Spitzer and HST are well matched in capabilities to study many different classes of sources and together provide a unique science-enabling role.

Constellation-X together with the IR capabilities of JWST will provide a powerful combination. The Universe is transparent to both IR and X-ray photons, so many targets - ranging from AGN buried in star burst galaxies, to nearby star formation regions - will be accessible to both missions. For example the *Chandra* X-ray Observatory has detected many sources which cannot be studied spectroscopically from the ground: these include ultra-luminous X-ray (ULX) sources in nearby galaxies, X-ray bright AGN with "optically dull" galaxy counterparts, distant clusters of galaxies and all but the very near-by isolated neutron sources. These will be prime targets for both Constellation-X and JWST. Constellation-X will provide detailed plasma diagnostics and direct redshift measurements (Figure 18-1). JWST will provide very sensitive NIR spectroscopy and imaging that will resolve the nature of the optical counterpart. The optical counterparts of most of the *Chandra* and XMM deep survey sources are rather faint with M(I) > 25 which have proven to be impossible to obtain spectra for from the ground even in very deep Keck and VLT exposures. The near IR capability of JWST allows high signal to noise spectra of such objects in exposures of only 3,000 secs. The combination of JWST and Con-X spectra for these objects will allow the study of the bulk of the AGN population out to $z > 6$. A recent discovery with Spitzer data shows that ULXs have high ionization near IR lines, but the spectral resolution was inadequate for detailed study. The combination of JWST and Con-X will allow the same quality of data for ULX in many nearby galaxies that one now obtains for X-ray binaries in the milkyway with respect to spectroscopic and timing studies. There are many other areas of overlap, but the basic point is that JWST and Con-X are well matched in spectroscopic capabilities for the bulk of sources discovered by *Chandra* and XMM.

ALMA will be the premier ground based telescope for millimeter astronomy with unprecedented angular resolution, sensitivity and spectral resolution. Again there is a very large range of synergy between ALMA and Constellation-X in the study of: star forming regions in nearby galaxies, highly absorbed active galaxies, the Sunyaev-Zeldovich effect, and non-thermal behavior in young stars and accretion powered sources. For example, deep *Chandra* surveys have shown that at least 40%, and possibly all, of the bright (850μm > 4mJy) sub-millimeter galaxy population host heavily obscured AGN (e.g., Alexander et al. 2005 Nature, 434, 738). The energetics of the AGN activity is too low to explain

the large bolometric output of the submillimeter galaxies and they are almost certainly dominated by star formation. But the large AGN fraction implies that the super-massive black holes (SMBH) are growing almost continuously throughout these periods of vigorous star formation. The superior angular resolution of ALMA will permit detailed studies of the dynamics of gas within the environment of the SMBH. At the same time Con-X will be able to constrain the contribution of accretion onto the SMBH (Figure 18-1). For SCUBA (850μm) sources with no *Chandra* X-ray counterpart, Con-X spectrophotometry will answer the question as to whether they are merely X-ray faint or perhaps harboring Compton-thick AGN. In either case, the true role of AGN in these vigorously star forming galaxies will be resolved.

The GMST, a 30m class ground based optical telescope, is another major capability that is expected to be operational in the latter part of the next decade. Again there is strong synergy with Constellation-X. The GSMT will be able to derive the velocity dispersions and optical properties of the z ~ 1 clusters being studied by Con-X. Also GSMT studies of starburst galaxies will be able to measure the outflows on a galaxy by galaxy basis (this can now only be done in a statistical sense) for a direct comparison of the winds in starbursts being studied with Con-X.

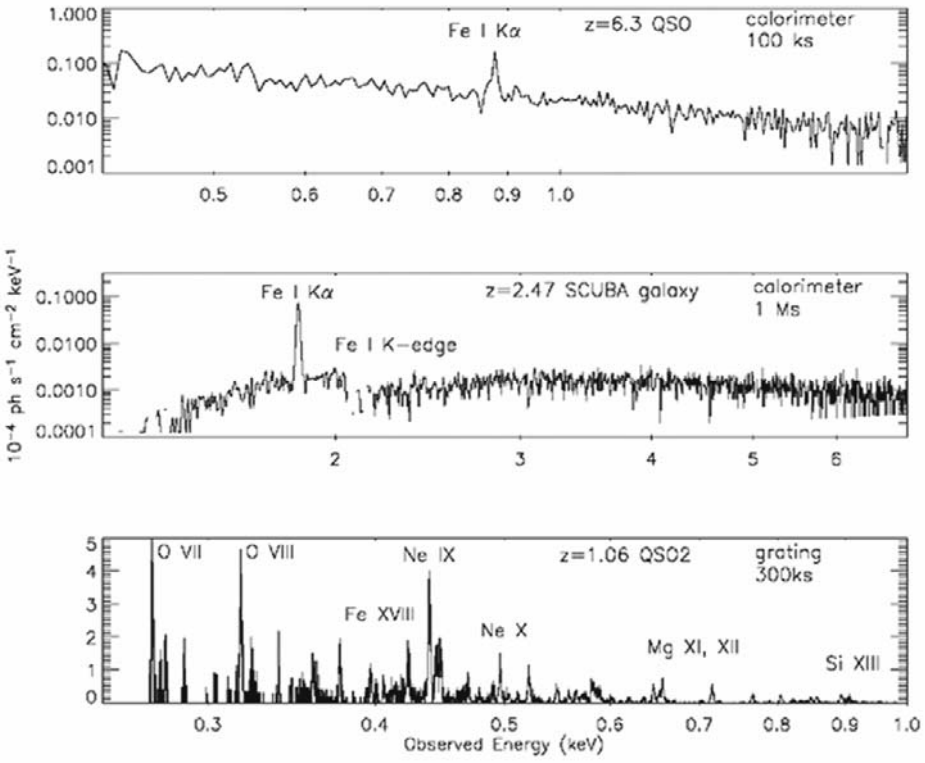

Figure 18-1. Simulated Spectra of 3 High Red Shift AGN

Simulated spectra demonstrating the capabilities of Constellation-X for three source classes relevant to ALMA and JWST: (1) a z = 6.3 quasar, (2) a z = 2.47 Compton-thick AGN in a sub-millimeter-bright star-forming galaxy, and (3) a z = 1.06 obscured quasar. Interesting spectral features are highlighted that provide redshift, abundances, density and velocity diagnostics.

Constellation-X will provide constraints on Dark Energy with a precision comparable to that of the Large Survey Telescope (LST). The use of the X-ray emission from clusters as precision Cosmological probes can only be done from space because X-rays cannot penetrate the Earth's atmosphere. The three different approaches that Con-X will bring to the Dark Energy measurements (two measuring the expansion of the Universe and one using growth of structure) will provide independent measures of both the Dark Energy equation of state and its evolution with cosmic time. These can be combined with the planned ground based experiments, and with those from Planck. Even if, in the time frame of Constellation-X, the issue of Dark Energy is settled by the ongoing ground based experiments or a theoretical breakthrough, the cluster observations necessary for the Dark Energy experiment will still return timely and high quality scientific results on the physics of clusters, which remain of great cosmological interest in their own right.

We note that the clusters to be used by Constellation-X for the Dark Energy measurements will come from currently planned surveys with sub-mm telescopes (the South Pole Telescope, ALMA, Planck), and analysis of archival X-ray data. This is a beautiful synergy between these planned ground and space based measurements and the future X-ray great observatory Constellation-X. The sensitivity of Con-X is such that the majority of the Planck and SPT clusters are accessible for detailed spectroscopic study.

18.2 Previous Academy Studies

The science reach of Constellation-X relative to other space and ground-based missions was assessed and prioritized in 2000 by the Astronomy and Astrophysics in the New Millennium Survey (AANM). In this survey Constellation-X was ranked as the second priority large space based facility (after JWST). The *Connecting Quarks to the Cosmos* study in 2003 also assessed the capabilities of Constellation-X and calls out the unique ability of Constellation-X to address science at the intersection of astronomy and physics. The strategy laid out in both reports was reaffirmed by the mid-term review undertaken by the CAA (reported in a letter to NASA HQ on 2005, Feb 11). These two reports and the mid-term review all highlighted the unique ability of Constellation-X to address pressing and timely science questions, and its importance as part of a balanced space and ground based astrophysics program.

18.3 Science Per Dollar

We have evaluated the science reach of Constellation-X in terms of a science per dollar metric, which can be assessed against that of other planned space and ground based missions. The simplest approach is taking the total mission cost and dividing by the total amount of time dedicated to each topic. These times were estimated from the science white papers generated by the Facility Science Team over the past two years, taking into account the time estimated as required to accomplish the identified key objectives, and allocating the remainder for observatory science over a 5 year mission life. Of course, we anticipate that the actual science selection and peer review process will somewhat modify these percentages. This gives the break down shown in Table 18-1. Given the breadth of the Constellation-X science and the relative cost for each topic, the mission provides high science value for money both in terms of each science topic and overall.

This is consistent with the well-proven paradigm of a NASA Great Observatory where a mission driven by a few key science goals at the same time realizes a major increase in capability applicable across many science areas. This is in contrast to the more focused science goals of the more modest PI-led missions (such as Explorer and Discovery).

Table 18-1: Science Cost by Topic for Constellation-X

Topic	Percent Time	Cost
Black Holes	30%	$649M
Dark Energy	18%	$389M
Neutron Star Equation of State	14%	$303M
Missing Baryons	11%	$238M
Observatory Science	27%	$584M
Total Mission Cost		$2.162B

18.4 International Plans for X-ray Observatories

We provide a summary of international plans for future X-ray missions, which might overlap with the goals for Constellation-X. At present, there are no approved missions capable of achieving the Constellation-X science objectives.

The SIMBOL-X mission is under Phase A Study by France and Italy. It is a focusing hard X-ray (10 - 60 keV) telescope with capabilities similar to the Constellation-X Hard X-ray Telescope. SIMBOL-X does not have high throughput at lower energies, nor does it have the high spectral resolution of Constellation-X below 10 keV. At present the launch date is ~2013, and there are no plans for US involvement in the mission.

Japan's NeXT mission is primarily a hard X-ray telescope (10 - 60 keV), again similar to the Constellation-X HXT. NeXT will probably also have an X-ray calorimeter with a telescope operating below 10 keV, but would have an effective area 10 - 50 times less than Constellation-X with poorer 1 arcmin spatial resolution and smaller field of view, limiting it to study of the brightest sources. The mission may begin Phase A studies in April 2008 with a possible launch in ~2013. US participation in this mission is possible, but has yet to be proposed or approved.

An X-ray survey mission covering the energy band up to ~10 keV is under study by Germany and Russia. The prime goal is to conduct an all-sky survey ~10 times deeper than ROSAT, while extending to somewhat higher energies as well. This mission could provide an invaluable catalog of sources for Constellation-X including ~10,000 clusters for Dark Energy and Dark Matter studies. Launch might be in the 2011 - 2012 time-frame, and there are no plans at present for US participation.

ESA is contemplating a call for new mission concepts, possibly as early as this year. The call will be for both medium missions capped at €300M and large missions capped at €650M. With the ESA science program currently fully subscribed to 2015 and beyond, ESA has instituted a cost saving review for all of its science programs. It appears highly unlikely that any new large ESA astrophysics mission could launch until well after 2020. A large X-ray mission called the X-ray Evolving Universe Spectroscopy (XEUS) mission has been under study in Europe (with contributions from Japan) and will be proposed in response to this call. The driving science goal for XEUS is the detection and study of the first black holes at redshift ~10. The mission requirements for effective area and angular resolution are substantially more demanding than Constellation-X, and the current mission concept involving

formation flying telescope and detector spacecraft is also very challenging. These factors raise some questions as to the viability of this mission concept under the stated cost caps, and therefore some question as to if or when it might actually launch. There are at present, no plans for US participation in this mission.

19. BRIEF DESCRIPTIVE OVERVIEW OF THE MISSION DESIGN

Question: Provide a brief descriptive overview of the mission design (launch, orbit, pointing strategy) and how it achieves the science requirements (e.g. if you need to cover the entire sky, how is it achieved?

RESPONSE

Launch Vehicle:

- Atlas V 551 with the Long Fairing (5 m dia x 26.5 m tall)
- Throw Mass to nominal orbit: 6305 kg with a C3 of -0.5 kg^2/s^2
- Launch from Kennedy Space Center (KSC) mid-2017

Transfer Orbit:

- Constellation-X is launched from KSC directly to an L2 halo orbit following a direct insertion path, as shown schematically in Figure 19-1. No Lunar gravity assist or phasing loops will be used.
- The cruise duration to L2 is approximately 100 days. Mirror covers will remain closed during the cruise phase.

Nominal L2 Orbit:

- The Constellation-X orbits around the Sun-Earth L2 Libration Point with a Y amplitude of 700,000 km (coordinate axes defined in Figure 19-2).
  - This orbit ensures that Constellation-X remains mostly within the Earth's Magnetosheath with its beneficial radiation shielding effects rather than in the free solar wind (greatly improving observing efficiency and mission success).
- Direct "zero delta-v" insertion into an L2 halo orbit with 800,000 km Y amplitude.
- Perform a maneuver to lower the Y amplitude of the orbit to 700,000 km, requiring a delta-v of 25 m/s.

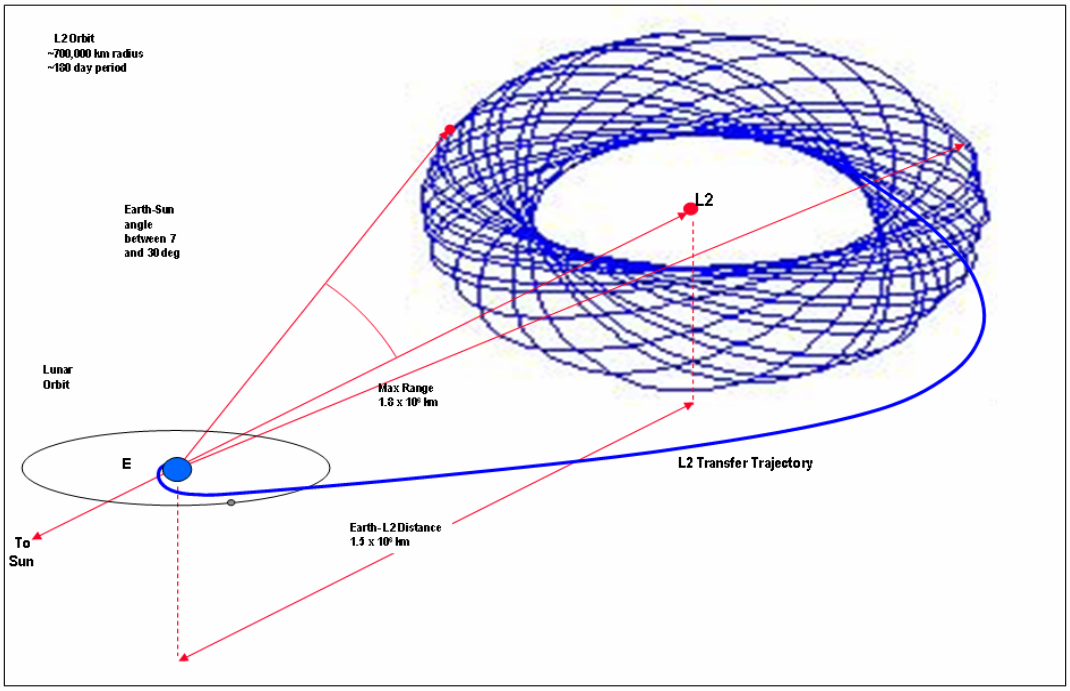

Figure 19-1. Isometric View of the Constellation-X Transfer and L2 Orbit (Courtesy: Mike Menzel & Mark Beckman, JWST)

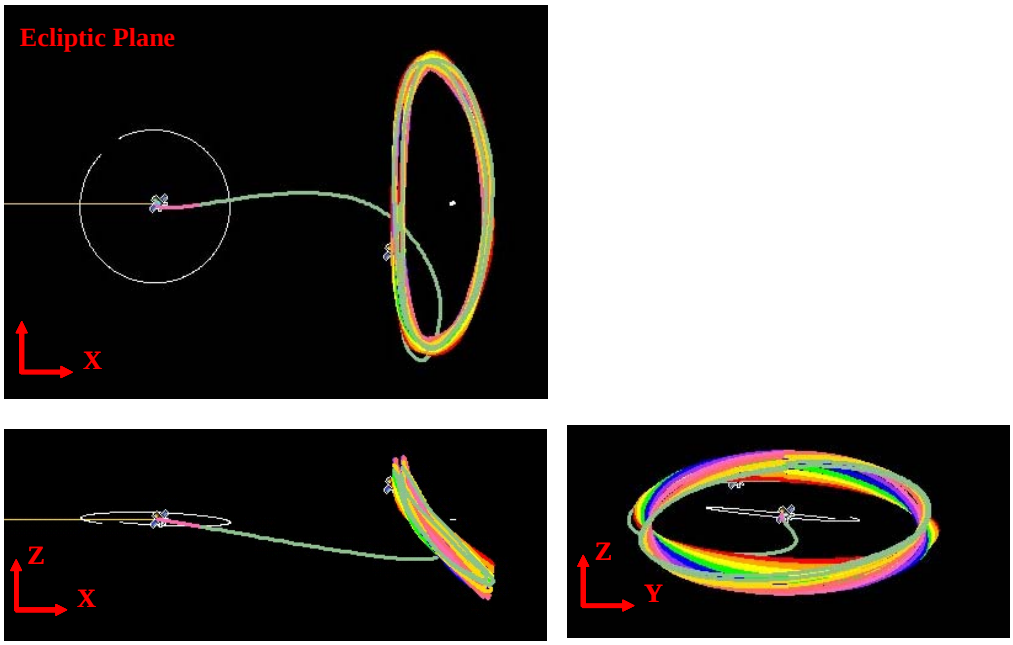

Figure 19-2. Constellation-X Orbit Plots in Sun-Earth Coordinate System Referenced to the Ecliptic Plane (X-Y plane)

Observatory Attitude during Transfer Orbit:

- In its nominal cruise attitude, the Observatory's solar panels are oriented to within 5 degrees of the Sun.
- Deviations are allowed only for brief periods not to exceed 15 minutes:
  - Initial attitude acquisition after Launch Vehicle separation.
  - Major propulsion burns for: Launch Vehicle Dispersion Correction, Mid-Course Corrections, and L2 Orbit Insertion.
  - During these burns, the attitude is defined for optimum thruster alignment.

Observatory Attitude during Nominal L2 Orbit:

- After telescope cover deployment and cryogenics cool-down, the Observatory will keep the solar arrays pointed to within 20 degrees of the Sun.
- 360 degrees of rotation about the spacecraft-Sun line and ±20 degree pitch allowance permits observation within a 360 degree x 40 degree annulus.

Science Operations Field of Regard (portion of the sky accessible for observations)

- Pitch: ±20° off Sunline
- Yaw: ±180°
- Roll: ±20° off Sunline
- Every location on the celestial sphere must be accessible for observations for at least one month per year.

Pointing Control (3σ)

- Pitch: 10 arcsec
- Yaw: 10 arcsec
- Roll: 30 arcsec

Pointing Knowledge (3σ):

- Pitch: 5 arcsec
- Yaw: 5 arcsec
- Roll: 20 arcsec

Observation Duration:

- Average 10 hours
- Maximum 48 hours

Slew:

- The average maneuver is 60 degrees and must be completed in 1 hour, including settling time.
- An average of 2.5 slews per day is required over the duration of the mission.

Observing Efficiency:

- The required observing efficiency is 85% when averaged over the mission life.

Mission Life:

- The required mission is 5 years duration. 10 years duration is required for consumables.

20. MISSION DESIGN TABLE

Question: Provide entries in the mission design table to the extent possible. Those entries in italics are optional. For mass and power, provide contingency if it has been allocated, if not – provide just your current best estimate (CBE). To calculate margin, take the difference between the maximum possible value (e.g. launch vehicle capability) and the maximum expected value (CBE plus contingency).

RESPONSE

Table 20-1. Mission Design Table

Parameter	Value				Units
Orbit Parameters (apogee, perigee, inclination, etc.)	700,000 km elliptical L2 Halo orbit				km
Maximum Eclipse Period	The baselined orbit results in: ▪ There are no eclipses that interfere with science observations. ▪ Partial (less than 15% obscuration) Lunar eclipses of the Sun lasting less than 5 hrs, occur up to twice per year ▪ There are no Earth eclipses of the Sun				hrs
Mission Lifetime	5 years required, 10 years for consumables				years
Spacecraft Dry Bus Mass and contingency	▪ Spacecraft Bus mass, including the metering structure: ▪ CBE: 1,845 kg ▪ Allocation: 2,398 kg, including 30% contingency				kg, %
Spacecraft Propellant Mass and contingency	▪ CBE: 257 kg, sized for 10 years, including ~15% contingency on delta-v's ▪ Allocation: 335 kg, including 30% contingency				kg, %
Launch Vehicle	Atlas V. 551 with the Long Fairing and the 173 inch Payload Attach Fitting				
Launch Vehicle Mass Margin	88 kg				kg
Spacecraft Bus Power and contingency by Subsystem		**CBE**	**Cont**	**Allocated**	
	Mechanical	17	30%	22	
	ACS	75	30%	98	
	Thermal	100	30%	130	
	Propulsion	29	30%	38.0	
	C&DH	119	30%	155	
	RF Comm	110	30%	143	
	PSE	192	30%	250	
	Harness Loss	8	30%	10	
	Bus Total	**650**	**30%**	**845**	
Mass weighted reuse percentage of payload and spacecraft subsystem components	Apart from the mission specific items (such as the structure or SXT covers), virtually all spacecraft bus subsystem components are commercially available "off-the-shelf", with extensive space flight heritage.				
Mass weighted redundancy of payload and spacecraft subsystem components	All spacecraft subsystems are either fully redundant, have functional redundancy capability with no mission degradation (i.e. multiple thermistors near each other), or have graceful degradation redundancy with sufficient margin to ensure no mission degradation after a single failure (i.e. extra switched battery cells). The payload consists of multiple identical instruments with selective internal redundancies providing for graceful degradation.				

21. DIAGRAMS OR DRAWINGS OF THE OBSERVATORY

Question: Provide diagrams or drawings (if you have them) showing the observatory (payload and s/c) with the components labeled and a descriptive caption. If you have a diagram of the observatory in the launch vehicle fairing indicating clearance, please provide it.

RESPONSE

The following diagrams are provided:

- Figure 21-1 – Exterior view
- Figure 21-2 – Constellation-X in the Atlas V 551 long fairing
- Figure 21-3 – Constellation-X main elements
- Figure 21-4 – Constellation-X observatory structure
- Figure 21-5 – Constellation-X aft end
- Figure 21-6 – Payload electronics bay
- Figure 21-7 – Metering structure
- Figure 21-8 – Spacecraft bus module and mirror bench
- Figure 21-9 – View of the flight mirror assemblies

21.1 Exterior View

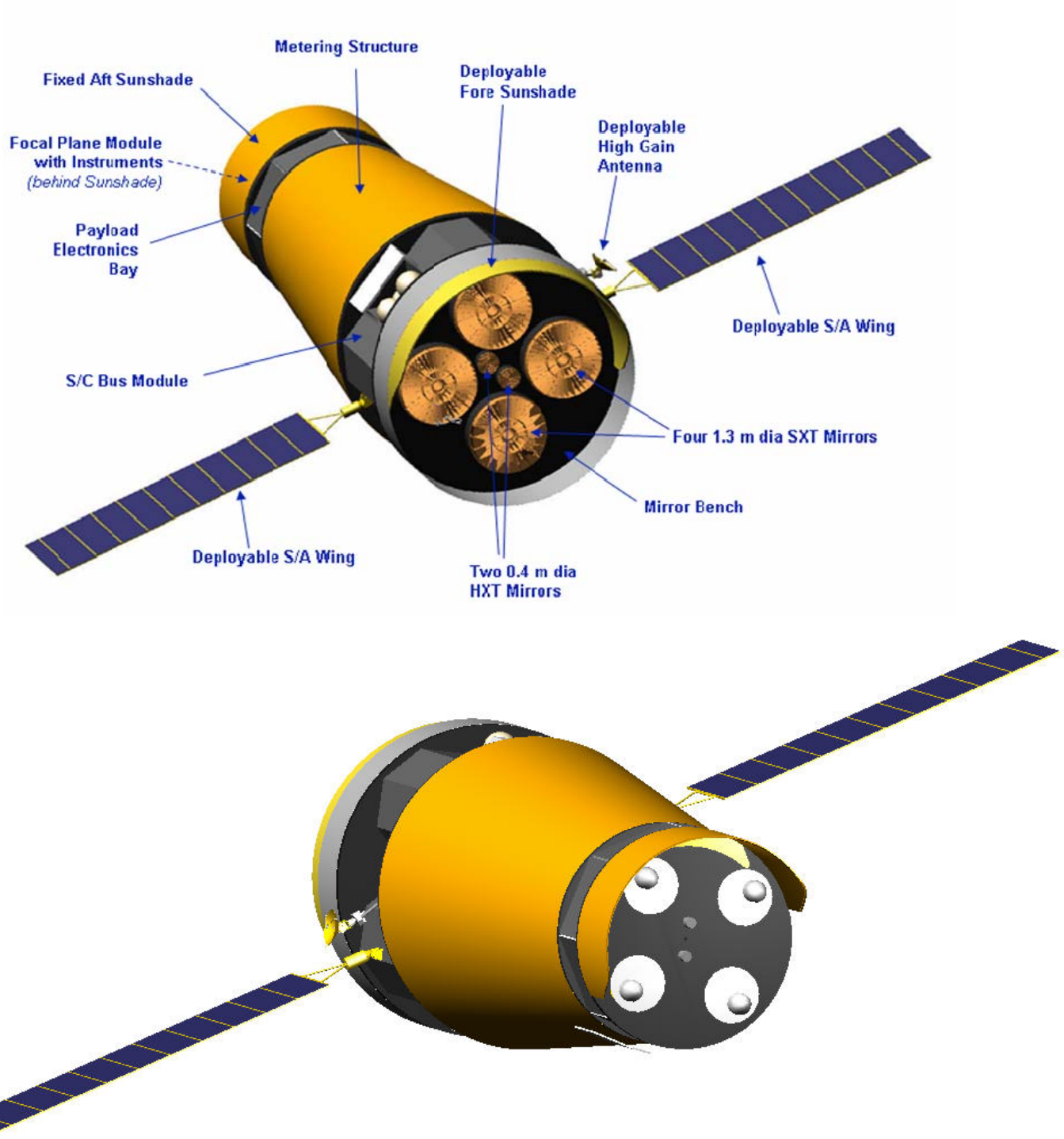

Figure 21-1. Constellation-X in the Science Observing Configuration Fore and Aft Views

21.2 Constellation-X in the Atlas V 551 Long Fairing

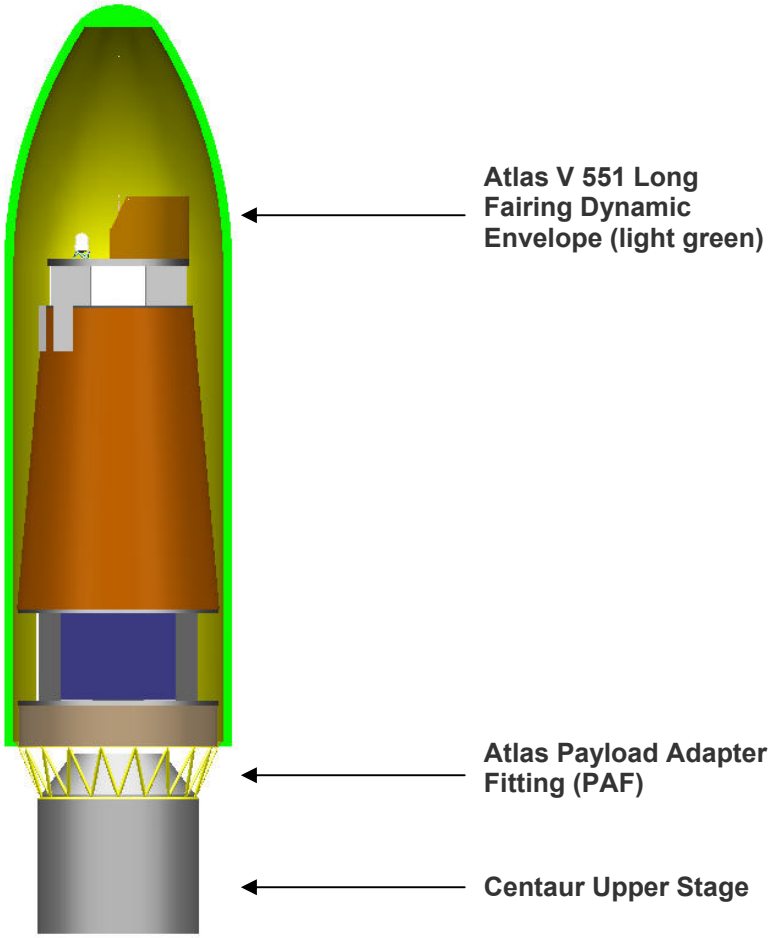

Figure 21-2. Constellation-X in its Launch Configuration

The observatory is shown within the dynamic envelope of the Atlas V long fairing. The observatory was designed to fit with adequate clearance to the dynamic envelope of the Atlas V fairing (> 89 mm clearance near the launch vehicle interface and > 605 mm at the opposite end).

21.3 Constellation-X Main Elements

The Con-X primary structure is composed of three main elements:

- Focal Plane Module with the Payload Electronics Bay
- Metering Structure
- Bus Module with the Mirror Bench

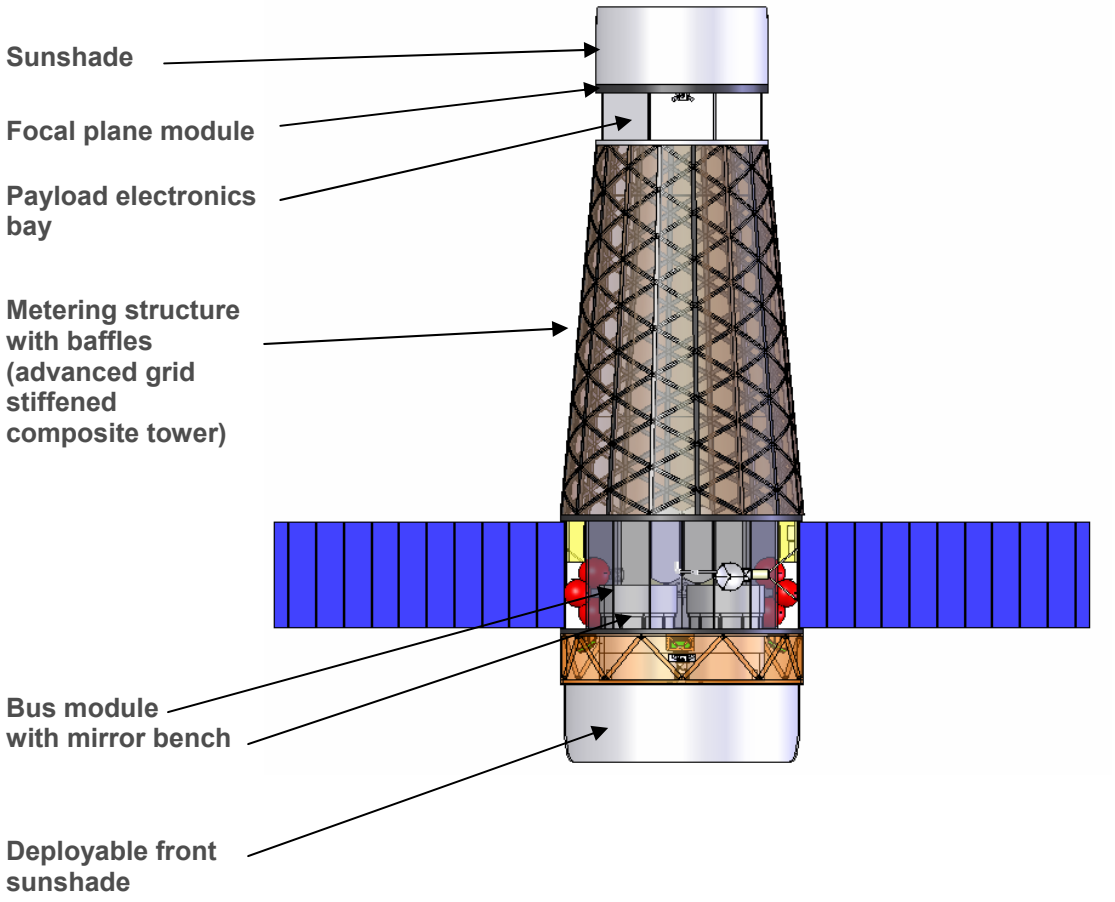

Figure 21-3. Constellation-X Main Elements

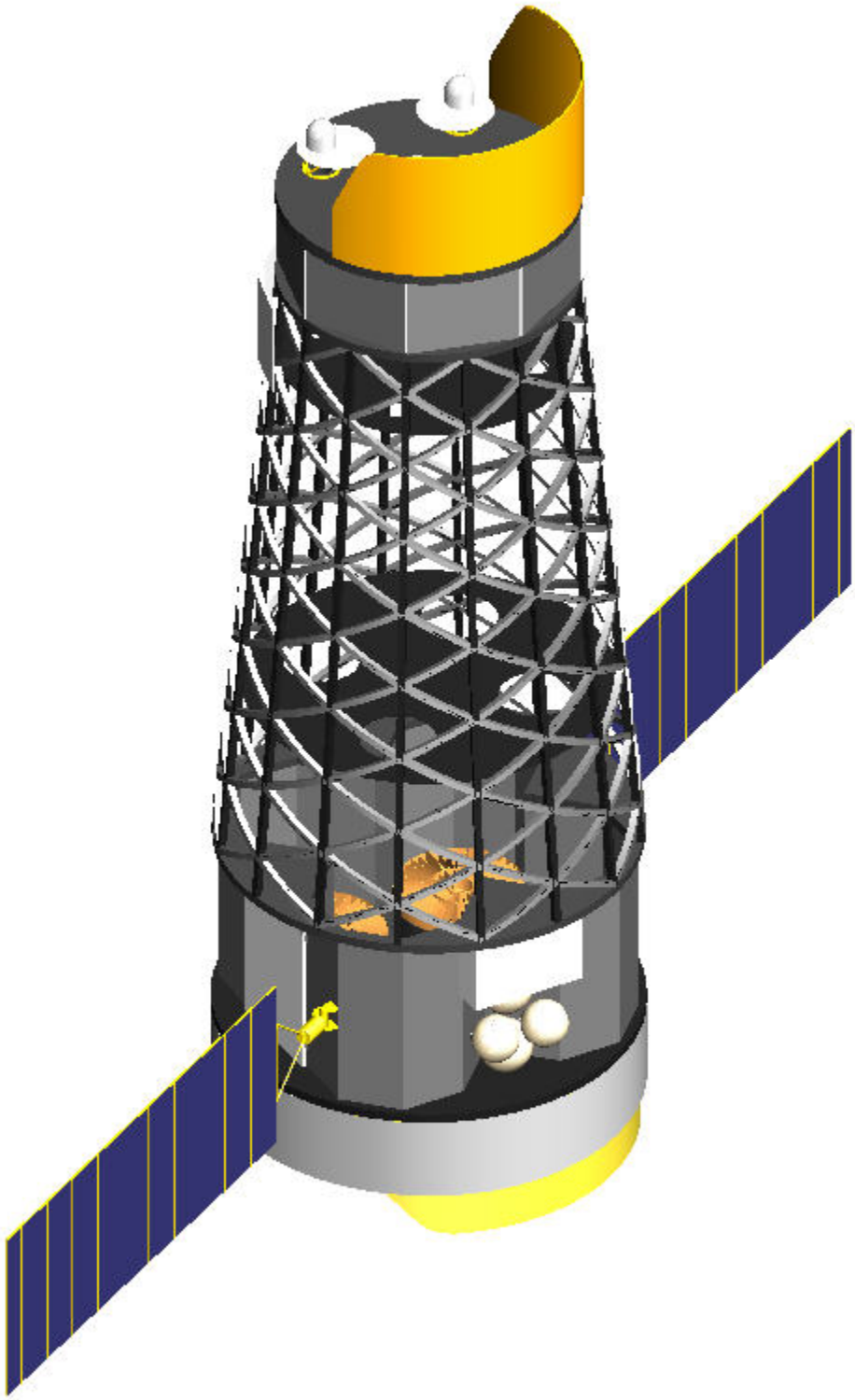

Figure 21-4. Constellation-X Showing the Metering Structure and Aperture Baffles

21.4 Constellation-X Aft End

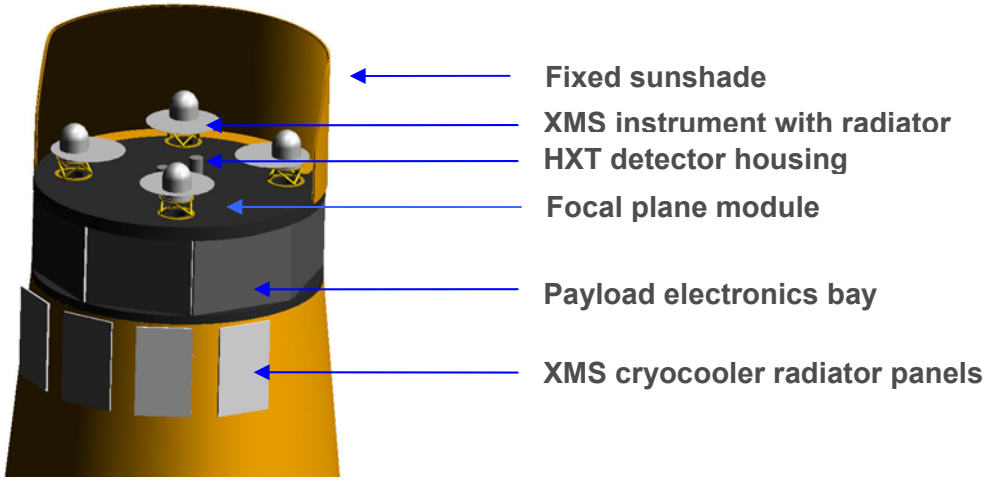

Figure 21-5. Close-up of the Observatory Aft End

The Focal Plane Module (FPM) includes:

- A fixed (nondeployable) aft sunshield to keep the FPM and XMS cryostats in shadow
- Four XMS instruments, and the HXT and XGS detectors (not shown)
- Instrument preamp electronics

The payload electronics bay, located under the Focal Plane Module, contains most of the payload electronics boxes as well as some S/C Bus electronics (such as the aft C&DH routers), all mounted to the interior of the closeout radiator panels.

21.5 Metering Structure

The metering structure is an approximately 6.7 meter tall advanced grid stiffened or “isogrid” structure made from near-zero thermal expansion graphite-epoxy composites.

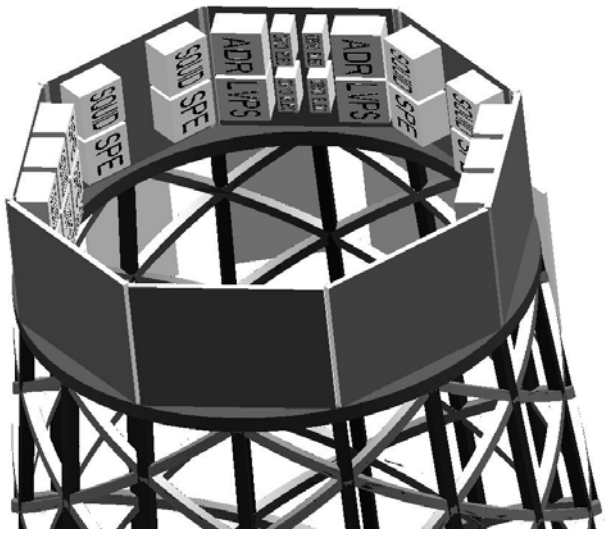

Figure 21-6. Metering Structure Showing the Interior of Payload Electronics Bay

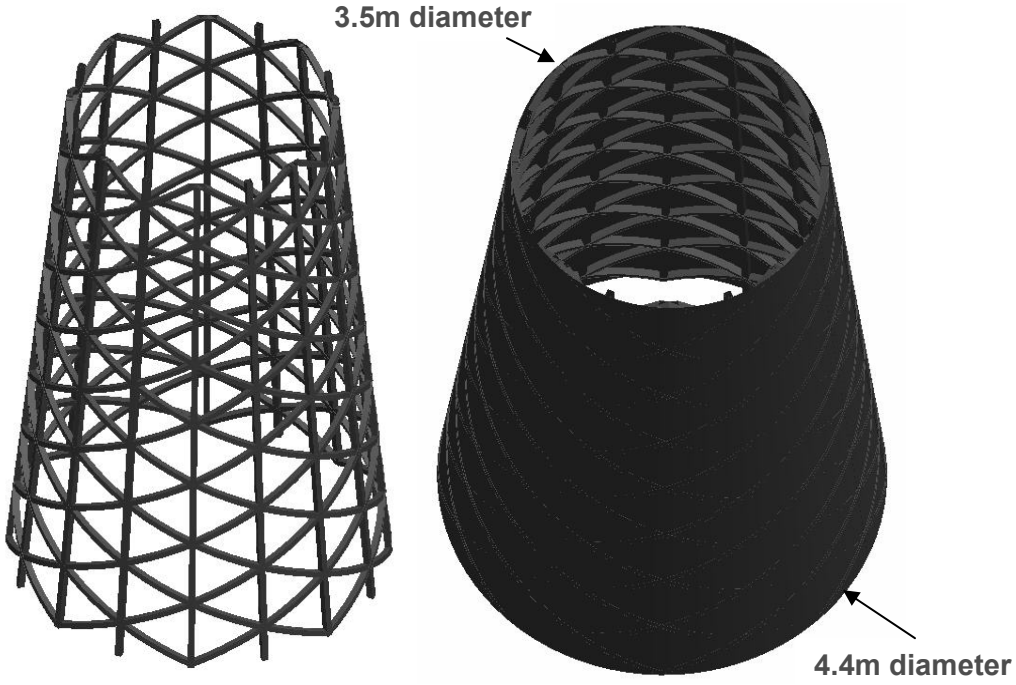

Figure 21-7. Metering Structure Ribs and Longerons with and without Outer Skin

21.6 Bus Module and Mirror Bench

The Constellation-X Bus module is 4.2 meters in diameter and 2.1 meters tall. It consists of a top deck, walls in a "rosette" pattern that fits around the Flight Mirror Assemblies (FMA), and at the bottom a mirror bench which supports the following:

- The Flight Mirror Assemblies with covers
- The deployable sunshade
- The Hard X-ray Telescope mirror(s)

The rosette pattern of honeycomb panels form volumes for spacecraft bus components. The majority of electronics boxes are fastened to equipment panels which are hinged for easy access. Other components such as the tanks are fastened to the internal walls.

The spacecraft and instruments are modular, allowing easy access for I&T and sub-system testing.

The top deck mates to the equipment panels below and the metering structure above.

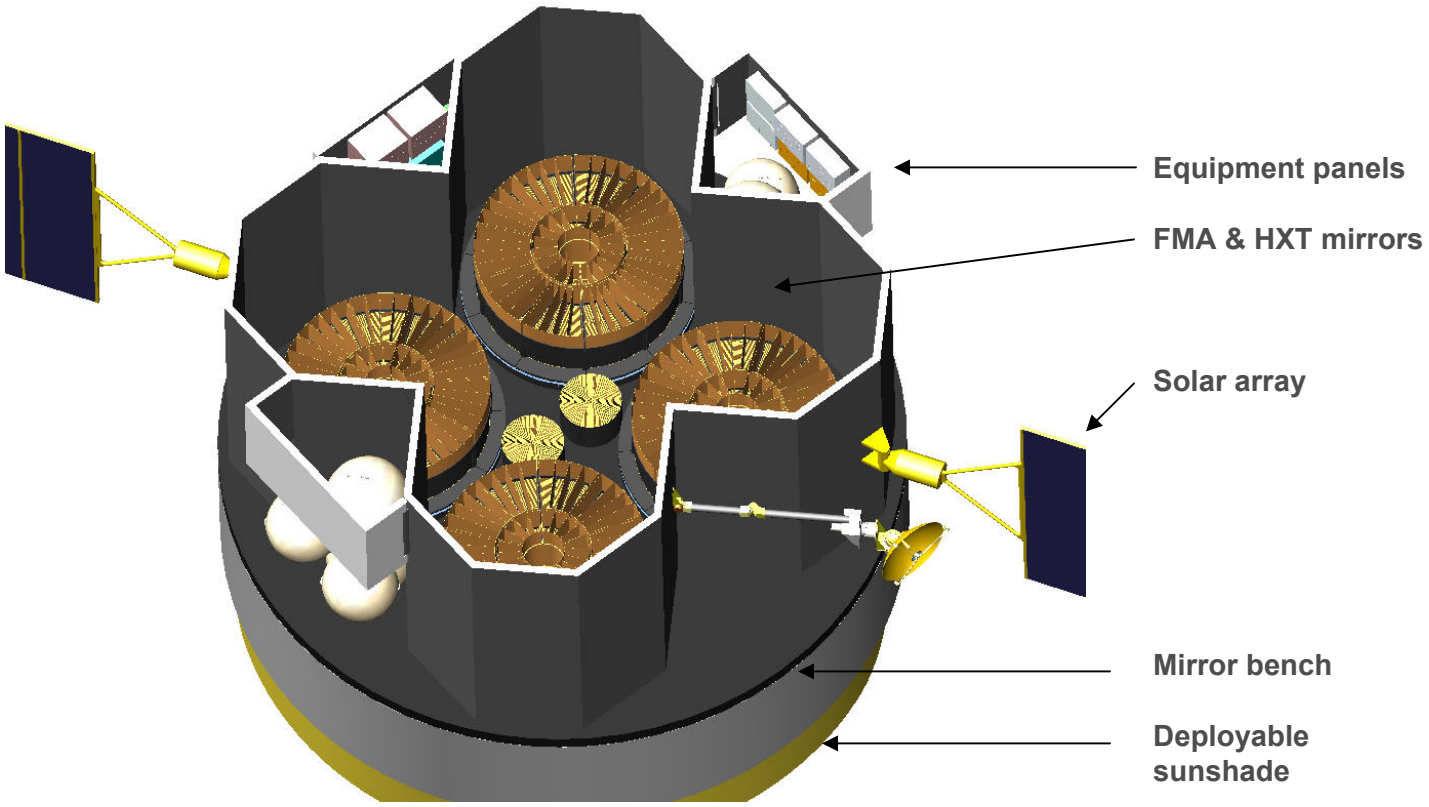

Figure 21-8. Spacecraft Bus Module and Mirror Bench, as seen from the Aft Side

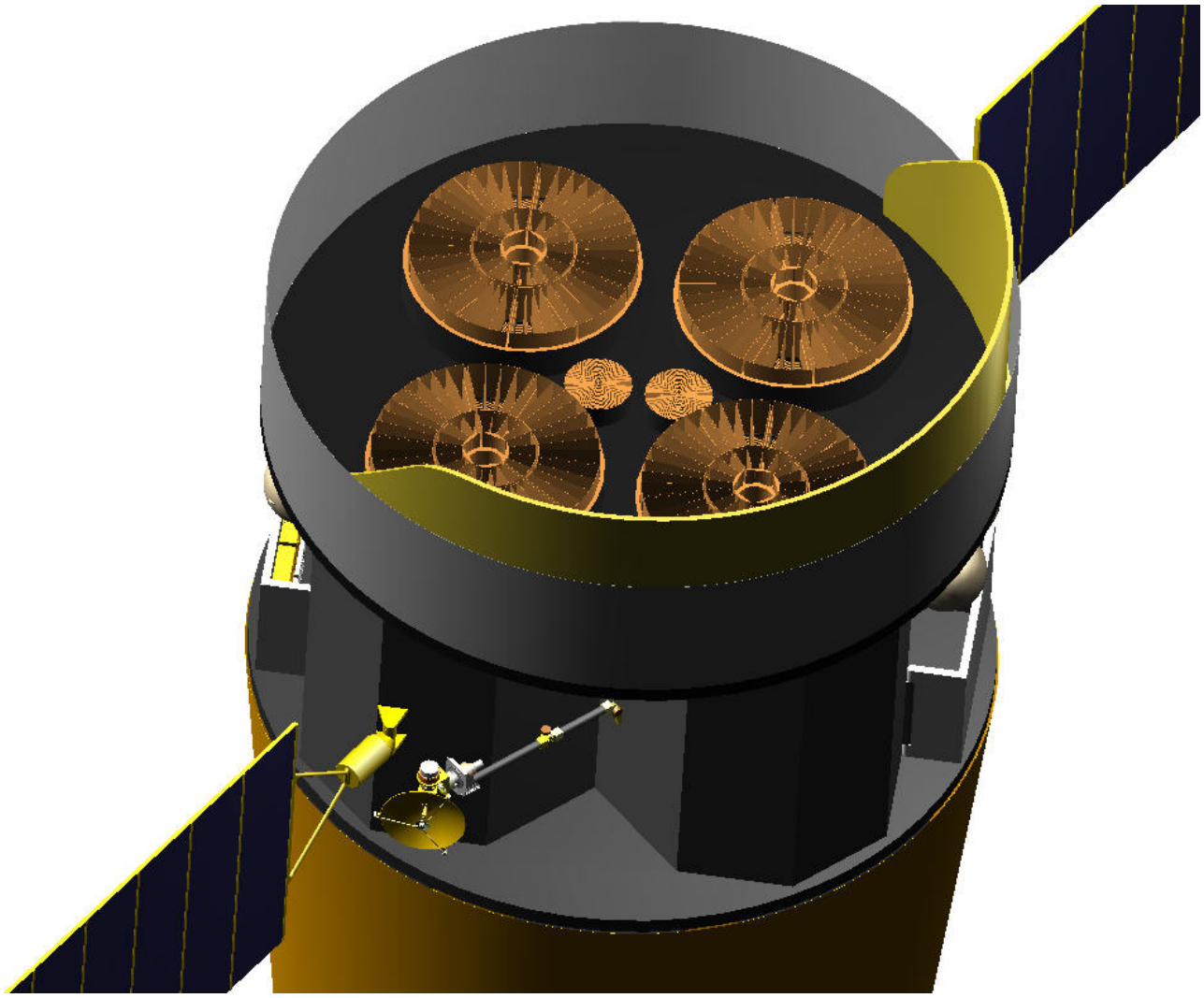

Figure 21-9. View of Flight Mirror Assemblies (SXT & HXT)

22. Overall Science, Mission, Instrument and S/C Three Primary Risks

Question: Overall (including science, mission, instrument and S/C), what are the three primary risks?

Response

Three primary overall risks are shown on the risk matrix in Figure 22-1. The convention used for the risk assessment ratings is provided in Appendix C.

1. **Technology development funding (Schedule)**
2. **Flight Mirror Assembly Schedule**
3. **Mass Growth (Technical)**

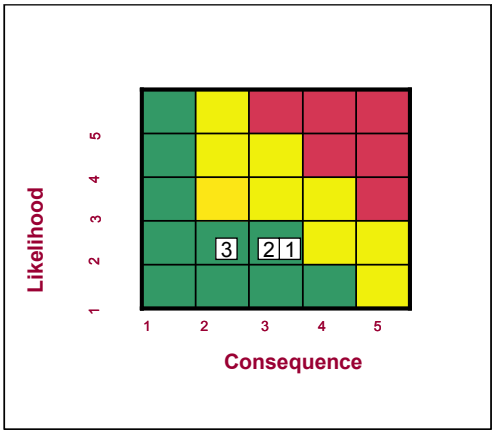

Figure 22-1. Overall 5 x 5 Risk Matrix

22.1 Risk #1 (Overall) – Technology development funding

Risk Statement:

If sufficient funding for the technology development is not available the technology development milestones will not be met.

Impact:

If the technology development milestones are not met, then the project schedule will slip accordingly. The cost of the project will increase with inflation.

Likelihood – Low:

The Constellation-X plan is based on the assumption that Constellation-X is selected as the first Beyond *Einstein* mission.

Consequence – Moderate:

Small schedule slips can be tolerated within the technology development schedule slack. Beyond that, the project will slip until the technology development milestones are met.

Mitigation:

- Schedule slack is built into the technology development plans
- Leverage funding from other sources such as IR&D and DDF

22.2 Risk #2 (Overall) – FMA Manufacture Schedule

Risk Statement:
If the FMA takes longer to build than planned, the FMA delivery will be late.

Impact:
Once the FMA production schedule slack has been consumed the project critical path will be impacted.

Likelihood – Low:
The schedule for the FMA is based on detailed analysis of the processes (e.g., oven utilization and alignment station (CDA) utilization) and the mandrel delivery schedules based on vendor inputs. Process flow and times are based on existing procedures in use at GSFC. Since 80 days of contingency are built into the FMA schedule and the bulk of the schedule is based on a 5-day/week, single shift work schedule, the likelihood that the critical path will be impacted is low.

Consequence – Moderate:
At most, a small impact to the critical path can realistically be envisioned.

Mitigation:
- 80 working days of contingency are built into the FMA schedule
- Ability to use multiple vendors (e.g., mandrel production)
- Continuously update planning as inputs are received from technology development teams or vendors

22.3 Risk #3 (Overall) – Mass Growth

Risk Statement:
If the mission mass grows beyond the allowed contingency, then solutions that impact science performance may be required.

Impact – Low:
Science performance may be affected (e.g., effective area may be reduced or the instrument complement may be reduced)

Likelihood – Low:
The current overall mission mass contingency of 30% (with an additional 88 kg of margin), is in the acceptable range, however, the margin is low. The Constellation-X mission implementation concept and mass has been assessed based on conservative estimates. Many trade studies have already been performed (see response to Questions 12 and 24, and several options for mass reduction are discussed in the response to Question 9). There are several potential avenues identified for increasing mass margin that will not impact mission performance; these include design optimization as well as some of the trade studies discussed in the response to Question 24. Therefore we assign the mass growth risk as a low likelihood of occurrence.

Consequence – Low:
Mass reduction solutions gradually impact the ability to fully meet science requirements. Reductions in the number of flight mirror shells populated into the assembly, or number of Hard X-ray Telescopes

may be required. As discussed in the response to Question 9, an eventual descope could be implemented to save mass (and cost), and while it affects mission performance, the minimum mission performance can still be met. Since minimum mission requirements can still be met under this condition, we assign a "Low" rating in terms of consequence to this risk.

Mitigation:

- Design optimization studies will result in more accurate mass estimates.
- Optimize design, especially for heavier elements (e.g., perform good fidelity FEM and shave off mass where possible).
- Embrace lightweight design solutions in detailed design. Audit / rethink design for possible mass savings. Trade for mass
- Use tight resource management practices.

23. LAUNCH OPTIONS

Question: If you have investigated a range of possible launch options, describe them, as well as the range of acceptable orbit parameters.

RESPONSE

23.1 Launch Vehicle Options

The Atlas V 551 with the Long Fairing (5 m dia x 26.5 m tall) provides a throw mass of 6305 kg (C3 of -0.5 kg^2/s^2) and meets the launch requirements of Constellation-X.

Table 23-1. Launch Vehicle Options

Launch Vehicle Options	Throw Mass
Delta IV Heavy (4050H-14)	9380 kg
Atlas V 551 (Baselined)	6305 kg
Atlas V 541	5790 kg
Atlas V 531	5175 kg
Delta 4450-14 (largest of the non-Heavy Delta Ivs)	4545 kg

Please refer to the response to Question 12 for discussion of launch options studied for previous Con-X configurations.

23.2 Orbit Insertion

Constellation-X is launched to a L2 halo orbit following a direct insertion trajectory. No lunar gravity assist or phasing loops are required.

Insertion using lunar gravity assist was considered, and would yield a mass advantage of about 200 kg; however, Constellation-X opted for direct insertion after evaluating the radiation environment experienced by WMAP. JWST has selected a similar direct insertion trajectory.

23.3 Orbit Parameters

For an L2 halo orbit, the delta-v required to insert into that orbit is a function of the Y-amplitude (roughly the radius) of the orbit. As the Y-amplitude increases less delta-v is required to insert a satellite into that orbit. When the orbit amplitude gets sufficiently large, the insertion delta-v reaches zero. The smallest such orbit has a Y-amplitude of ~800,000 km.

The Constellation-X halo orbit (Figure 23-1) radius was selected based on a 2005 Constellation-X study on radiation effects, which recommended an orbit mostly within the Earth's magnetosheath (700,000 km or less) to shield the observatory from solar protons.

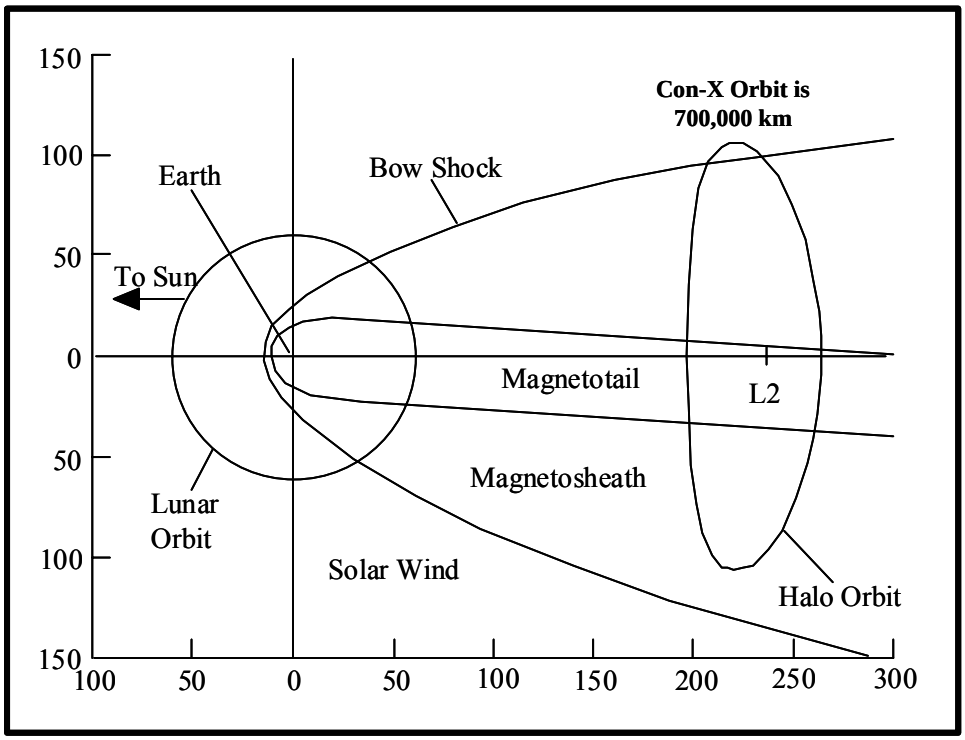

Figure 23-1. Schematic Illustration of the Constellation-X orbit Relative to the Earth's Magnetosheath

24. KEY MISSION TRADEOFFS AND OPTIONS TO BE INVESTIGATED

Question: If you have identified key mission tradeoffs and options to be investigated describe them.

RESPONSE

Optimization of the mission reference architecture is an ongoing process and includes trades that have been identified to reduce cost, as well as to improve performance. The Table below lists a set of the key current mission trades (including some recently closed ones) and their current status. These trades also address the top level risks where appropriate. A number of older, previously closed trades have not been listed.

Table 24-1. Summary of the Constellation-X trade studies

Trade	Options	Key Drivers	Status/Selection
Orbit	LEO/L2/HEA/Drift	Thermal environment; Viewing efficiency, mass	Closed. L2 selected.
L2 orbit insertion	Direct insertion to L2 vs. lunar swing-by	Mass, time to L2, radiation	Closed. Direct insertion selected.
Launch vehicle	Atlas V, Delta IVH	Cost, Performance	Closed Atlas V selected.
Optical BenchType	Fixed bench vs. precision formation flying	Effective area, resolving power, complexity, cost	Closed. Fixed bench
	Fixed bench or extendable bench options	Effective area, complexity, Reliability	Closed. Fixed bench.
	25m, 15m, 10m	Effective area, mass, Packaging	Closed. 10m selected.
Number of SXTs	3 or 4 SXT systems	Effective area, packaging, cost, mass	Closed. 4 selected.
RF Comm	Ka/X vs. Ka/S	Implementation complexity	Closed. Ka/S selected.
Fiducial Light System	Other	Angular resolution Optical bench stability	Closed. None for current requirement. Revisit if angular resolution goal is approached.
Front Door	One large vs. one per telescope	Mass, reliability, Complexity	Closed. One per telescope. Revisit in Phase A.
Ground station	DSN, dedicated, commercial	Cost; timing capabilities	Closed. DSN. Re-visit in Phase B.
XMS Field of View	2.5x2.5 arcmin vs. 5x5 arcmin FOV	Implementation complexity, Science performance	Closed. 5 X 5 arcmin selected. Revisit in Phase A.
Front aperture cover	One-shot vs. re-closable	Protection of instrumentation, mass, reliability	Closed. One-shot (jettisoned) selected, revisit in Phase A
Grating design	In-plane reflection, Off-plane reflection,	Effective area, resolving power,	Ongoing

Trade	Options	Key Drivers	Status/Selection
	Transmission	mass, complexity	
XGS/HXT Accommodation	Single or multiple XGS and HXT instruments	Mass, accommodation, redundancy	Ongoing
Detector background	Shield mass vs. propellant mass to lower orbit below magnetosheath	Mass, observing efficiency, Sensitivity	Ongoing
SXT thermal control	Post collimator; thermal control of bench	Angular resolution, mass	Ongoing
Focus Mechanism	Focus mechanism or not	Optical bench fabrication, alignment & performance characteristics vs. mass, complexity	Ongoing
	Common mechanism or one per detector	Mass, complexity, imaging performance	Ongoing
	1- or 3-axis	Mass, complexity, imaging performance	Ongoing
SXT stray light baffling	Internal aperture stops, precollimator	FMA optical design details	Ongoing
On-board calibration source location	Above mirror vs. integrated into instrument	Calibration maintenance; complexity, cost	Future/Phase A
Orbit Solution	Batch Least Squares vs. Kalman filter	Absolute timing accuracy, propellant usage, stationkeeping	Future/Phase A
FMA ground calibration	Full aperture testing ; Sub-aperture testing	Calibration accuracy, Schedule	Future/Phase A
Focal plane electron suppression	None, Magnetic broom, bulk shielding	Detector background Mass	Future/Phase A
Solar array	Articulated vs. increased size of deployed/fixed for cosine effect, and addition of body mounted panel	Mass, power, reliability	Future/Phase A

25. SPACECRAFT CHARACTERISTICS AND REQUIREMENTS

Question: Describe the spacecraft characteristics and requirements. Include, if available, a preliminary description of the spacecraft design and a summary of the estimated performance of the spacecraft.

RESPONSE

25.1 Spacecraft Requirements

The top level spacecraft requirements are as follows:

Lifetime:

- 5 years, in an L2 halo orbit with radius ≤700,000 km
- Expendables shall be sized for twice the mission lifetime (10 years)

Pointing:

- 3-axis stabilized pointing required
- Every location on the celestial sphere must be accessible for observations for at least one month per year.
- Autonomous pointing operations with buffer capacity for at least one week of attitude commands
  - Attitude control and reconstruction:
    - Pointing Control (3 sigma):
      --Pitch: 10 arcsec
      --Yaw: 10 arcsec
      --Roll: 30 arcsec
    - Pointing Knowledge (3 sigma):
      --Pitch: 5 arcsec
      --Yaw: 5 arcsec
      --Roll: 20 arcsec
    - Pointing Jitter: <2 arcsec/13.8 milliseconds

Maneuvers:

- Maximum observation duration is 48 hours
- Complete one 60 degree slew and settle in a one hour or less
- Compatible with 30 maneuvers per day

Operating Modes:

- Provide adequate power (Table 25-2) and attitude control resources to support five operating modes
  - Launch mode
  - Cruise mode
  - Science mode
  - Thruster mode
  - Safehold mode

Instrument Accommodation:

- Alignment
  - XMS to FMA focus within +/- 1 mm
  - XMS center to FMA axis within +/- 0.25 mm
  - FMA axis co-alignment to within 10 arcsec
  - HXT mirror to detector focus within +/- 2 mm
  - HXT detector center to HXT mirror axis +/- 1 mm
  - HXT mirror axis to FMA axis within 1 arcmin
  - The two different XGS concepts have significantly different alignment and stability requirements, and these are currently being assessed. The worst case alignment tolerance of the gratings to the FMA are on the order of a few arcsec, and the worst case stability knowledge (of the CCDs relative to the telescope optical axis) is on the order of 50 microns/13.8millisec.
- Thermal environment (operations and survival) see section 29
- Power – 3351 W peak for all instruments
- Light tightness – there must be no direct light path to the detectors from outside the spacecraft
- Science Data rate – 1317 kbps peak; 142 kbps average
- Data storage capacity – 2 days of data, assuming 25% peak data rate, and 75% average

Communications:

- Approximately 2 uplinks per week for commanding
- One's day's science data can be downlinked in a single pass less than one hour
- Real time communications capability during downlink

Reliability:

- Constellation-X is a Class B mission. Parts reliability and spacecraft subsystem redundancy philosophy is defined accordingly.
- No single point failure should result in the loss of more than one SXT.

Characteristics:

The Constellation-X observatory has an integrated design (as a "sciencecraft") so that it may be accommodated within the Atlas V long fairing. Schematic figures of the observatory can be found in Section 21. The ~12m x ~4.5m canonical primary spacecraft structure has a custom design using flight proven materials. The spacecraft outer skin is micrometeoroid resistant and wrapped with multi-layer blankets for stray-light protection.

Deployables include the launch vehicle separation system, solar array panels, high gain antenna, fore sunshield, and internal Flight Mirror Assembly (FMA) covers. External FMA covers are jettisoned. The only articulated mechanism is the high gain antenna.

Spacecraft subsystem requirements and characteristics are described in the responses to Questions 29 and 34. All spacecraft subsystems either have flight heritage or will be flown on a pending mission (see Question 30).

The instrument accommodations satisfying the requirements listed above are described in Section 31.

The tables below contain a breakdown of the observatory mass and power. The telemetry data volume is discussed in Question 35.

The baseline spacecraft bus design meets or exceeds all of the spacecraft bus requirements.

25.2 Observatory Mass Breakdown

Table 25-1. Observatory Mass Budget

Payload			
	Estimate (kg)	**Contingency**	**Allocation (kg)**
FMA	1572.0 kg	30%	2043.6
XMS	708.0 kg	30%	920.4
XGS	100.0	30%	130.0
HXT	100.0	30%	130.0
Misc Payload Items	35.6	30%	46.3
Payload Total	**2515.6 kg**	**30%**	**3270.3 kg**

Bus			
	Estimate (kg)	**Contingency**	**Allocation (kg)**
C&DH	92.4	30%	120.1
Attitude Control	68.0	30%	88.4
Communications	30.0	30%	39.0
Mechanisms	146.6	30%	190.6
Structure	981.2	30%	1275.6
Power	104.0	30%	135.2
Propulsion	48.0	30%	62.4
Thermal	186.3	30%	242.1
Harness	188.0	30%	244.4
Bus Total	**1844.5 kg**	**30%**	**2397.8 kg**

Observatory			
	Estimate (kg)	**Contingency**	**Allocation (kg)**
Science Payload Total	2515.6	30%	3270.3
Bus Total	1844.5	30%	2397.8
Separation System	164.8	30%	214.3
Vehicle Dry Mass	**4524.9 kg**	**30%**	**5882.3 kg**
Propellant Mass	257.4	30%	334.6
Observatory Wet Mass	**4782.3 kg**	**30%**	**6217.0 kg**
Throw Mass: 6305 kg		**Project Margin**	**88.0 kg**

25.3 Observatory Power Loads

The spacecraft is required to provide power to the Instruments as listed in Table 25-2. The table also shows power budgets for each of the five Operating Modes of the Observatory. The Science Mode is the design case.

Table 25-2. Observatory Power Loads

Payload															
	Science Mode w Comm [W]			Stationkeeping manuevering [W]			Launch [W]			Cruise [W]			Safehold [W]		
	Estimate	Cont.	Allocated	Estimate	Cont.	Allocated	Estimate	Cont.	Allocated	Estimate	Cont.	Allocated	Estimate	Cont.	Allocated
XMS	1616.0	30%	2100.8	1280.4	30%	1664.5	0.0	30%	0.0	1616.0	30%	2100.8	1280.4	30%	1664.5
FMA Thermal	877.0	30%	1140.1	877.0	30%	1140.1	0.0	30%	0.0	877.0	30%	1140.1	877.0	30%	1140.1
XGS, HXT	85.0	30%	110.5	0.0	30%	0.0	0.0	30%	0.0	85.0	30%	110.5	46.0	30%	59.8
Payload Total	**2578.0**	**30%**	**3351.4**	**2157.4**	**30%**	**2804.6**	**0.0**	30%	**0.0**	**2493.0**	**34%**	**3351.4**	**2157.4**	**33%**	**2864.4**

Bus															
	Estimate	Cont.	Allocated	Estimate	Cont.	Allocated	Estimate	Cont.	Allocated	Estimate	Cont.	Allocated	Estimate	Cont.	Allocated
Mechanical	17.0	30%	22.1	17.0	30%	22.1	5.0	30%	6.5	17.0	30%	22.1	5.0	30%	6.5
ACS	75.0	30%	97.5	469.0	30%	609.7	0.0	30%	0.0	66.0	30%	85.8	57.0	30%	74.1
Thermal	100.0	30%	130.0	100.0	30%	130.0	0.0	30%	0.0	100.0	30%	130.0	232.0	30%	301.6
Propulsion	29.2	30%	38.0	5.0	30%	6.5	5.0	30%	6.5	5.0	30%	6.5	5.0	30%	6.5
C&DH	119.0	30%	154.7	119.0	30%	154.7	22.0	30%	28.6	66.0	30%	85.8	74.0	30%	96.2
RF Comm	110.0	30%	143.0	44.0	30%	57.2	0.0	30%	0.0	44.0	30%	57.2	44.0	30%	57.2
PSE	192.0	30%	249.6	184.6	30%	240.0	1.8	30%	2.3	182.4	30%	237.1	165.9	30%	215.7
Harness Loss	7.5	30%	9.8	7.3	30%	9.5	0.1	30%	0.1	7.2	30%	9.4	6.6	30%	8.6
Bus Total	**649.7**	**30%**	**844.6**	**945.9**	**30%**	**1229.7**	**33.9**	**30%**	**44.1**	**487.6**	**30%**	**633.9**	**589.5**	**30%**	**766.4**

Observatory															
	Estimate	Cont.	Allocated	Estimate	Cont.	Allocated	Estimate	Cont.	Allocated	Estimate	Cont.	Allocated	Estimate	Cont.	Allocated
Obs. Total (W)	**3227.7**	**30%**	**4196.0**	**3103.3**	**30%**	**4034.3**	**33.9**	**30%**	**44.1**	**2980.6**	**34%**	**3985.3**	**2746.9**	**32%**	**3630.8**

25.4 Observatory Telemetry Data Volume

The Observatory Telemetry Data Volume is discussed in the response to Questions 8 and 35.

26. Overall Assessment of the Technical Maturity of the Spacecraft Subsystems and Critical Components

Question: Provide an overall assessment of the technical maturity of the subsystems and critical components. In particular, identify any required new technologies or developments or open implementation issues.

Response

All technologies used in the Constellation-X spacecraft bus are mature. The requirements for the spacecraft subsystems can be met without any new technologies. With the exception of custom items such as the structure, harnesses, and propulsion plumbing, commercial "off the shelf" components meet the requirements for spacecraft bus subsystems. See the response to Question 32 for a breakdown of technical readiness by subsystem.

27. THE THREE GREATEST RISKS WITH THE S/C

Question: What are the three greatest risks with the S/C?

RESPONSE

The overall spacecraft design for Constellation-X is straightforward and low risk. Most spacecraft components can be off-the-shelf. The spacecraft system and subsystems implementation are conventional. A summary of the risk assessment is provided in the 5 x 5 risk matrix in Figure 27-1, and each of the risks are further discussed below. The conventions used for the risk ratings are provided in Appendix C.

1. **Solar Array Deployment Failure**
2. **High Gain Antenna Deployment Failure**
3. **Contamination**

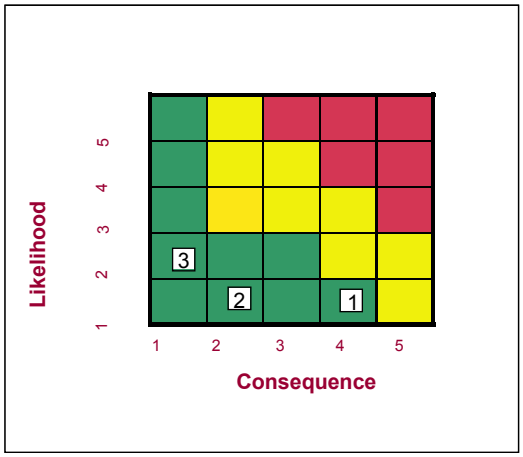

Figure 27-1. Spacecraft 5 x 5 Risk Matrix

27.1 Risk #1 (S/C) – Solar Array Deployment Failure

Risk Statement:

If one Solar Array wing fails to deploy, then the observatory would have reduced power generation and would use propellant at greater rate (to offset the increased disturbance torques due to the observatory asymmetry).

Impact:

- If one of the solar array wings fails to deploy, the resulting power budget would be only sufficient to operate the spacecraft and less than half of the payload complement .
- The additional propellant usage would reduce the 10 year lifetime by a small fraction (<< 50%).

Likelihood – Very Low:

Many examples of solar array deployment/release mechanisms with substantial flight heritage exist. The selected mechanisms will be fully redundant, and deployment will be tested under simulated flight conditions.

Consequence – High:
Reduced power output could translate to loss of science capability, due to inability to operate entire instrument complement.

Mitigation:

- Full redundancy required for release/deployment mechanisms
- Simulated flight environment deployment tests
- A future trade study will consider a combination of fixed and deployed arrays (articulated vs non-articulated). Moving some of the solar array to the spacecraft body directly mitigates the impact of this risk and assures minimum mission requirements can be met.

27.2 Risk #2 (S/C) – High Gain Antenna Deployment Failure

Risk Statement:
If the High Gain Antenna does not deploy or if the gimbal fails, then the observatory will have to be re-pointed to close the Ka-band communications links.

Impact:
Mission operational efficiency will be reduced by the time taken to re-point to the communications attitude (< 45 min), the time for the communications (~30 min), and the time to re-acquire the science attitude (< 45 min). Conservatively, this results in 2 hrs/day, or < 10% loss in mission efficiency.

Likelihood – Very Low:
Many examples of high gain antenna deployment/release and articulation mechanisms with substantial flight heritage exist. The mechanisms will be fully redundant, and deployment and gimbal motion will be tested under simulated flight conditions.

Consequence – Low:
Observing efficiency will be reduced by less than 10 percent. Mission planning can take into account the need to orient the spacecraft for downlinks and restore a substantial fraction of the reduced efficiency.

Mitigation:

- Redundancy required for release/deployment mechanisms
- Simulated flight environment deployment tests

27.3 Risk #3 (S/C) – Contamination

Risk Statement:
If the cleanliness of the metering structure (a large hollow structure with limited access) is not maintained prior to launch, contamination on the mirrors and/or detectors could result.

Impact:

- Decrease in mission effective area

Likelihood – Very Low:
The mission contamination limits control plan will be structured to ensure that contamination remains within acceptable levels. The contamination limits and control plan will be modeled after previous missions with similar contamination sensitive surfaces, primarily *Chandra*.

Consequence – Low:
The XMS outer blocking filter is the most likely surface in the optical path to have a layer of contaminating material deposited on it, because it is the coldest such surface. A contaminant layer will reduce the transmission of the lowest energy X-rays (less than 0.5 keV). However, at these energies it is the XGS that provides the higher spectral resolution. For the FMA surfaces, a thin contaminant layer actually enhances the effective area at some energies. The primary consequence for the FMA is reduction of the validity of ground calibration data.

Mitigation:
- Cleaning requirements taken into account when structure is designed
- Rigorous and regular cleaning and bake-out planned
- Maintain a robust in-flight calibration program.

The main shell temperature of the XMS dewars will be extremely cold (< 150K), and thus the mainshell filter has the potential for adsorbing outgassing products from the spacecraft. We expect to implement several components for preventing the buildup of contamination on the blocking filter, including cold baffles near the aperture and a mainshell filter heater system (which was implemented on the *Suzaku*/XRS system) that can be operated continuously if required.

The FMA contaminants effects on throughput will be monitored as part of the in-flight calibration program.

28. S/C TECHNOLOGIES, DEVELOPMENTS OR OPEN ISSUES

Question: If you have required new S/C technologies, developments or open issues and you have identified plans to address them, please describe (to answer you may provide technology implementation plan reports or concept study reports).

RESPONSE

The Constellation-X spacecraft bus employs no new technologies, or developments, and has no open issues.

29. SUBSYSTEM CHARACTERISTICS AND REQUIREMENTS

Question: Describe subsystem characteristics and requirements to the extent possible. Such characteristics include: mass, volume, and power; pointing knowledge and accuracy; data rates; and a summary of margins.

RESPONSE

The characteristics of each spacecraft subsystem are described below. Each subsystem description includes: a list of requirements, a list of implementation details, and mass and power tables. Block diagrams are included for some subsystems.

29.1 Thermal Subsystem

Requirements:

- The thermal control system shall maintain all operating components within their operational limits.
- The thermal control system shall maintain all non-operating components within their survival limits.
- Size spacecraft heaters for 120 VDC bus

Table 29-1. Component Temperature Requirements

FMA Temperatures	**Operating**	**Survival**
Flight Mirror Assembly	+20°C	+10°C to +30°C
Gradients: max gradient = 1°C		
Stability: ±- 0.5°C (across a single flight mirror assembly)		
XMS Temperatures	**Operating**	**Survival**
Cryostat Shell (operating point expected in this range)	80 K° to 100°K	< 30°C
SQUID MUX Control and Readout Electronics	-20°C to +50°C	-30°C to +70°C
Signal Processing Electronics	-20°C to +50°C	-30°C to +70°C
Low Voltage Power Supply	+10°C to +40°C	-30°C to +70°C
ADR Control/Housekeeping Electronics	+10°C to +40°C	-30°C to +70°C
Cryocooler Radiator	-10°C to +40°C	-20°C to +50°C
XGS Temperatures	**Operating**	**Survival**
Grating Array:	+20°C ±- 0.5°C	+10 to +30°C
Detector Housing:	-80°C to -60°C	-100 to +30°C
Electronics	-5°C to +25°C	-65 to +40°C
HXT Temperatures	**Operating**	**Survival**
Optics	+20°C ± 1°C	+10 to +30°C
Detector	-80°C to -60°C	-100 to +30°C
Electronics	-5°C to +25°C	-65 to +40°C
Spacecraft Temperatures	**Operating**	**Survival**
All Electronic Components	-10°C to +40°C	-20°C to +50°C
Li-Ion Battery for Spacecraft	0°C to +30°C	-10°C to 40°C
Solar Array	-120°C to +100°C	-130°C to +110°C
Propulsion		
Fuel lines	+10°C to +40°C	0°C to +50°C
Thruster valves	+10°C to +40°C	0°C to +50°C
Hydrazine Tank	+10°C to +40°C	0°C to +50°C
Fill & Drain	+10°C to +40°C	0°C to +50°C
NTO Tank	-10°C to +40°C	-20°C to +50°C
Pressurant Tank	-10°C to +40°C	-20°C to +50°C
High Gain Antenna		
Gimbal Motors	+10°C to +40°C	0°C to +50°C
Damper	-15°C to +35°C	-40°C to +60°C
Potentiometer	-55°C to +110°C	-65°C to +120°C
Release Mech. and Actuator	-20°C to +50°C	-65°C to +60°C

Implementation:

- Simple thermal control design system for the spacecraft bus
- Operating and survival mode heater power is sized for worst cold case
- Spacecraft radiators are sized for worst hot operating case
- Spacecraft radiator area required is ~3.8 m^2 to dissipate ~800 Watts of spacecraft component power
- Spacecraft radiators coating (e.g., NS43G white paint for spacecraft component radiators)

- Back side of solar array panel coating (e.g., NS43G white paint)
- External Multi-Layer Insulation (MLI) for the spacecraft bus; the outer layer is Germanium Black Kapton MLI, conductive; the blanket is comprised of 15 layers of MLI
- Internal surface coatings of spacecraft bus are high emittance surfaces (e.g., Aeroglaze Z306 Black Paint)
- Prime and redundant external and internal thermistors for each critical component at its mounting interface (e.g., Type YSI 44910 thermistors)
- Solar array panel thermistors are Platinum Resistance Thermometers (PRTs) (e.g., Goodrich 0118MF2000A)
- Kapton film heaters mounted to box / panel interfaces (e.g., Tayco); all heater circuits are redundant
- Heater circuits are thermostatically controlled with redundant thermostats (e.g., Honeywell 701 series)
- Thermally and electrically conductive interface material (e.g., ChoSeal) at box to panel interfaces

Table 29-2. Thermal Components Mass and Power

Mass (CBEs)	
Spacecraft Bus Heaters (184)	9.2 kg
Thermal Blanket (MLI)	54 kg
Thermistors (210)	5.3 kg
Thermal Blanket Vents	20 kg
Collimator Heater System (4)	57.6
Loop Heat Pipes	18 kg
Embedded Heat Pipe Radiator Panel	13.6
TOTAL	**186 kg**
Survival Heater Powers	
XMS Cold Head Radiators (4)	556 W
XMS Electronics (4)	846 W
Flight Mirror Assemblies (4)	1140 W
Propulsion System	147 W
Spacecraft Bus	85 W

29.2 Propulsion Subsystem

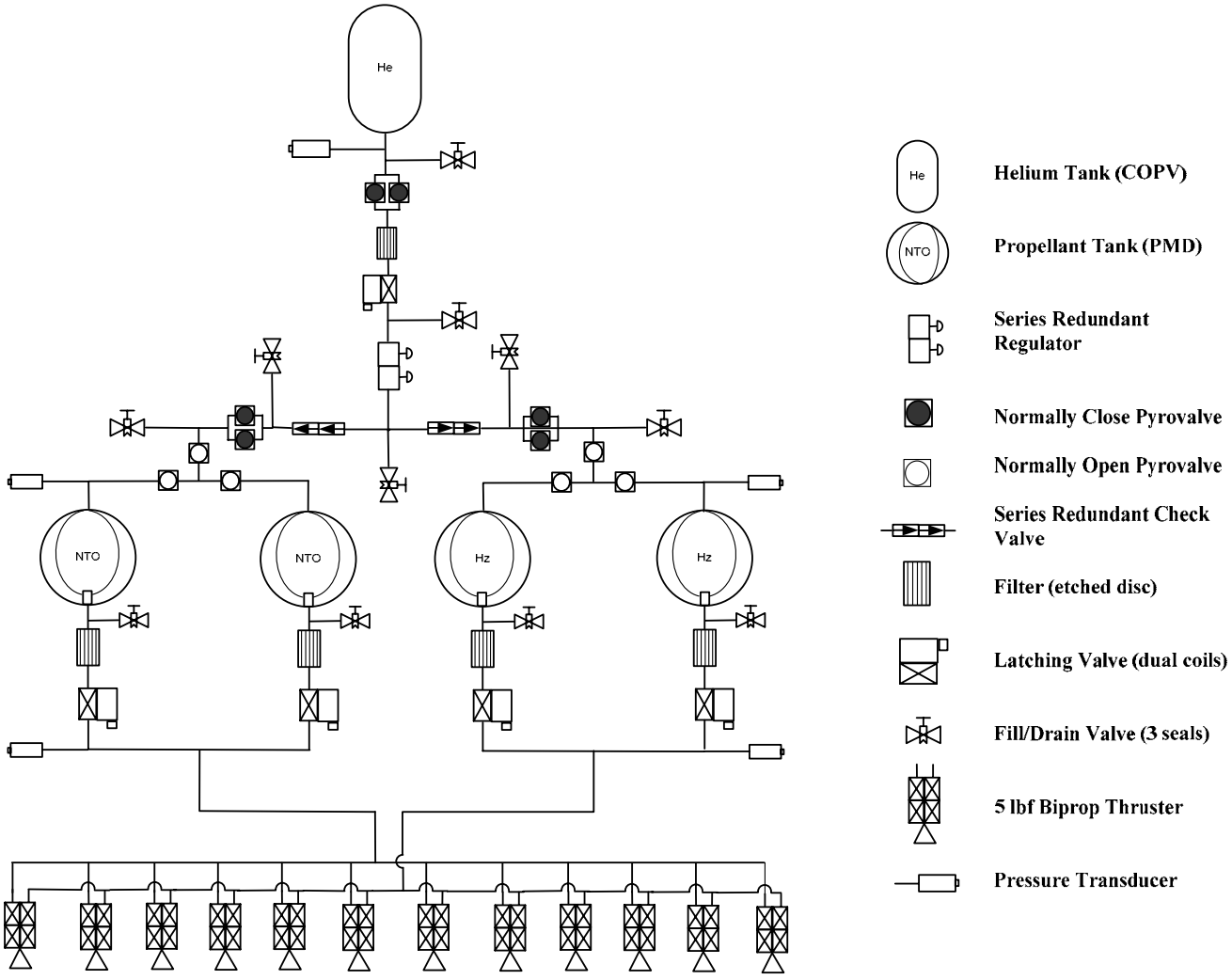

Figure 29-1. Propulsion Subsystem Block Diagram

Requirements:

- Load propellant for maximum lift-off mass = 6305 Kg
- Provide a thruster suite for six-degrees of freedom
- Design for a 5 year mission life with 10 years propellant
- Design with flight heritage components
- Single fault tolerance (selective redundancy); no credible single point failures (GSFC-STD-1000, Rule 1.05); dual fault tolerant where required by range safety
- Minimize contamination to optically sensitive surfaces

- Locate thrusters to minimize spacecraft plume impingement and avoid direct line of sight between thruster nozzles and optical surfaces
- Thruster performance matched to < 5% thrust

Implementation:

- Pressure regulated, Hydrazine/NTO, biprop propulsion subsystem
- 12 single-string 22N Biprop thrusters for all burns: orbit maneuvers, momentum unloading, and station keeping; performance matched to < 5%
- Specific impulse: 285 sec steady state, 150 sec short burns
- Pressurant: He gas
- Pressurant control: He gas regulator (series redundant) with high pressure isolation latch valve for long life operation
- Pressurant tank: 1 composite overlay pressure vessel; Ti tank, volume = 50,013 cm^3
- NTO and Hydrazine tanks: monolithic Ti, 2 each
  - Hydrazine tank volume = 91,440 cm^3 (INMARSAT Tank)
  - NTO tank volume = 58,584 cm^3 (Mars Observer Tank)
  - Mean Effective Operating Pressure = 400 psia
  - Surface tension propellant management device
  - Propellant manifolds and components are all Titanium
  - Titanium/stainless steel bimetallic joints used to transition from the Titanium manifold to the stainless steel thruster propellant control valves

Table 29-3. Propulsion Mass and Power

Mass and Power (CBEs)	
Subsystem Dry Mass	48.0 kg
NTO	119 kg
Hydrazine	138 kg
Total Propellant Mass Load	257 kg
Power For Pressure Transducers is 5 watts **Thruster power is booked in the Avionics subsystem, Thermal control of tanks, lines, thrusters is booked in the Thermal subsystem*	

29.3 Attitude Control

Requirements:

- Pointing control: 10 arcsec pitch/yaw, 30 arcsec roll, (3-sigma)
- Pointing knowledge: 5 arcsec pitch/yaw, 20 arcsec roll, (3-sigma)
- Jitter: < ~2 arcsec/13.8 milliseconds
- Momentum storage and slew: >2 days between momentum unloads
- Momentum unloading shall perturb the orbit by less than 0.5mm/s per day

- Perform a 60 degree slew and settle within 60 minutes
- Provide for a power positive attitude at all times

Implementation:

- Three-axis stabilized, inertial pointing
  - X axis is normal to the solar array (positive in the direction of the Sun)
  - Z axis is the telescope boresight axis (positive in the direction of the target)
- Power positive attitude is maintained in all modes: Science, slew, maneuver, safehold, and cruise
- Three star trackers and one Inertial Measurement Unit (IMU) are mounted on mirror bench
  - The three star trackers are offset from one another, with overlapping fields of view
  - Two trackers are active; one is reserved as a cold spare
- Four reaction wheels arranged in [4:4:1] pyramid to provide enhanced momentum storage in the Y axis
- Momentum unloading carried out using thrusters on intervals of 3 days or longer
  - Thrusters are placed to maximize torque, while not violating contamination constraints
    - Minimizes residual delta-v
    - Maximizes fuel efficiency
- Six coarse sun sensors provide 4π steradian coverage during safe mode
- Fine sun sensors provide accurate solar position determination
- Control modes and hardware used in each mode:
  - Cruise Mode: star trackers, sun sensors, IMU, reaction wheels
  - Thruster Mode (orbit maneuvers and momentum unloading): star trackers, IMU, thrusters provide coarse 6 degree of freedom actuation
  - Science Mode: star trackers, IMU, reaction wheels
  - Slew Mode: star trackers, IMU, reaction wheels
  - Safehold Mode: sun sensors, reaction wheels, thrusters

Table 29-4. Attitude Control Mass and Power

Mass and Power (CBEs)					
	Vendor	**Model**	**Qty**	**Mass Subtotal [kg]**	**Total Pwr, Avg [W]**
Reaction Wheels	Honeywell	HR14 (75)	4	42.4	32
IMU	Litton	SIRU	1	5.44	22
Coarse Sun Sensors	Adcole	Coarse Sun Sr	6	0.96	0.1
Fine Sun Sensors	Adcole	Model 20910	2	2.722	2.8
Star Trackers	Ball Aerospace	CT-602	3	16.227	18

29.4 Command & Data Handling

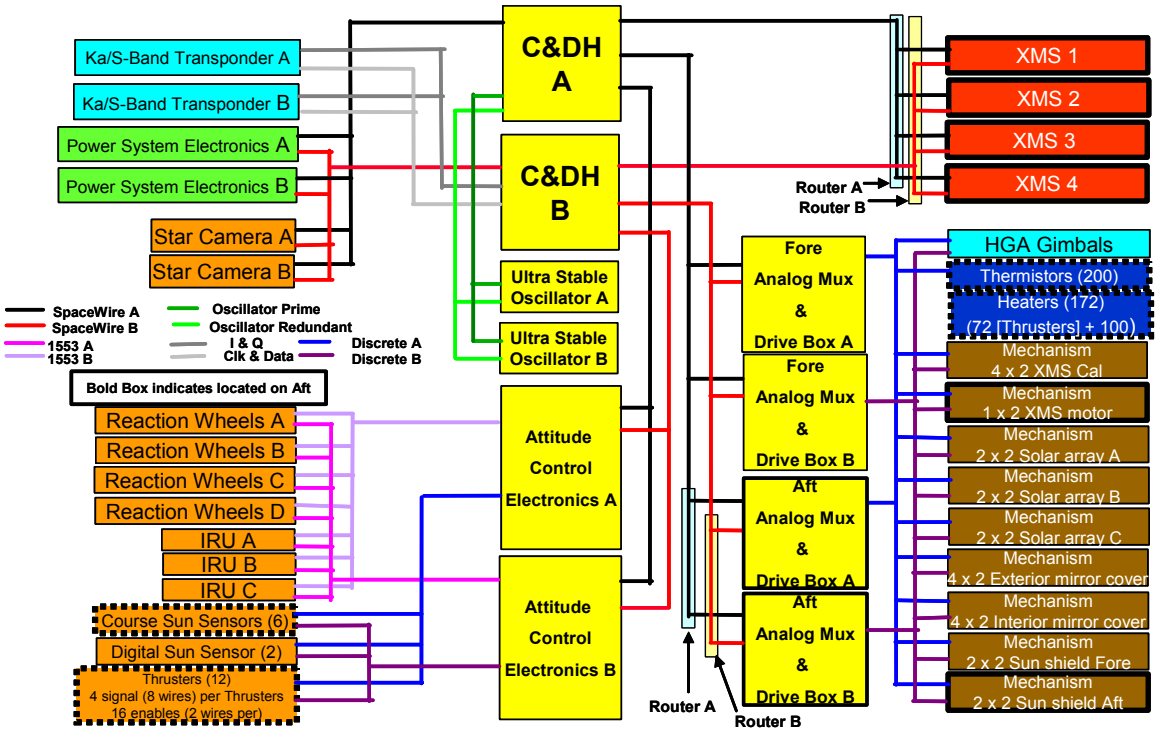

Figure 29-2. C&DH Block Diagram

Requirements:

- Collect, store, packetize, and downlink science and housekeeping telemetry data
- Receive uplinked commands, process them and distribute them appropriately
- Control observatory operation, provide safehold and safing functions
- Data storage capacity: >115 Gbits (worst case: 150 kbps * 3600 sec/hr * 18 hrs * 2 days + 1325 kbps * 3600 sec/hr * 6 hrs * 2 days) * 1.3 (contingency) * 1.15 (CCSDS overheads).
- Science timing accuracy within 100 microseconds UTC

Implementation:

The avionics system consists of:

- 2 redundant spacecraft computers
- 2 redundant attitude control electronics units
- 2 redundant aft analog mux & drive box
- 2 redundant fore analog mux & driver box
- 2 redundant routers
- 2 redundant ultra stable oscillators

Redundancy: hot/cold avionics boxes:

- All interfaces are cross-connected to redundant boxes
- Instrument interfaces are redundant to each spacecraft element
- SpaceWire based point-to-point architecture (1553 interface ports also available)
- S-Band communication card is always powered in each C&DH box
- 144 Gbits (18 Gbytes) SDRAM board, includes Reed Solomon protection on SDRAM (not included in downlink stream)
- SDRAM bulk storage board in each C&DH, each board stores 18 Gbytes
- Processing: ~80 MIPS, 4 MB NVRAM, 16 MB SRAM

Table 29-5. C&DH Mass and Power

Mass and Power (CBEs)							
	Mass [kg]			Power by Mode [W]			
	Qty	Ea	Total	Launch	Cruise	Safehold	Science
Spacecraft Computers	2	14	28	26	26	4	67
Attitude Control Electronics	2	12	24	0	22	22	22
Fore Analog Mux & Driver Box	2	9	18	0	4	0	8
Aft Analog Mux & Driver Box	2	9	18	0	4	0	8
Router	2	1.8	3.6	0	6	0	6
Ultra Stable Oscillator	2	0.4	0.8	4	4	4	4
TOTAL			**92.4**	**30**	**66**	**30**	**115**

29.5 Power Subsystem

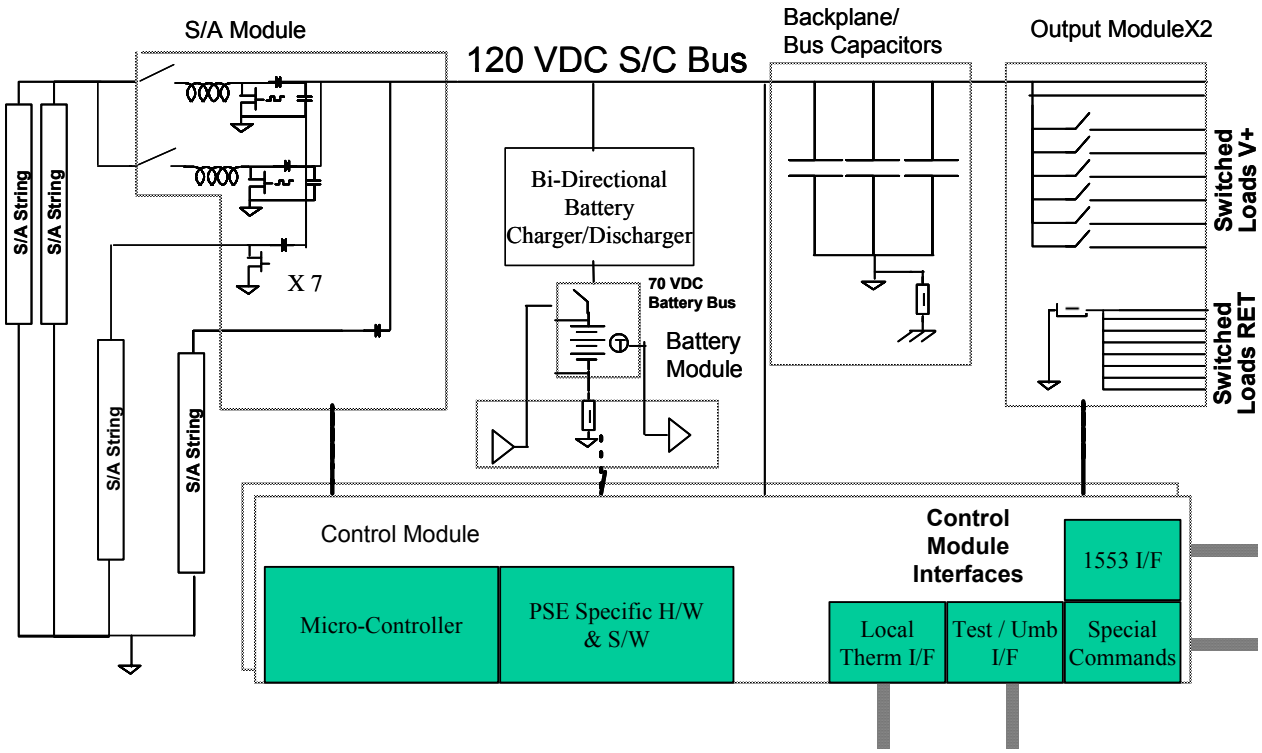

Figure 29-3. Power Subsystem Block Diagram

Requirements:

- Provide 4200W over the entire mission lifetime to the Constellation-X bus
- Provide battery power for the post-launch period prior from launch vehicle separation until sun acquisition
- Distribute power to instruments and spacecraft systems at 120V

Implementation:

- Solar Array area of 21.8 m^2, sized for 10 years, 28.4 deg cosine angle, and 85 deg C temperature
- Battery: 20 Ah Li-ion battery with cell by-pass switches 18 cells for a 70 VDC battery bus. 50% maximum depth of discharge after launch
- PSE: EOS Terra type 120 VDC PSE with a battery bus of 70 VDC. This single bus will provide redundancy with string redundancy and dual isolation and circuit protection for limited area single point bus. Use of voltage regulated bus is EOS Terra and ISS heritage 120VDC

Table 29-6. Power Subsystem Mass

Mass (CBEs)	
Solar Cells	39.6 kg
Battery	13.9 kg
Power Supply Electronics	50.5 kg
TOTAL MASS	**104.0 kg *(excl. Harness that is carried under Systems)***

Note: Harness mass is carried separately solar array substrates and hinges are carried in the mechanical subsystem

29.6 RF Communications Subsystem

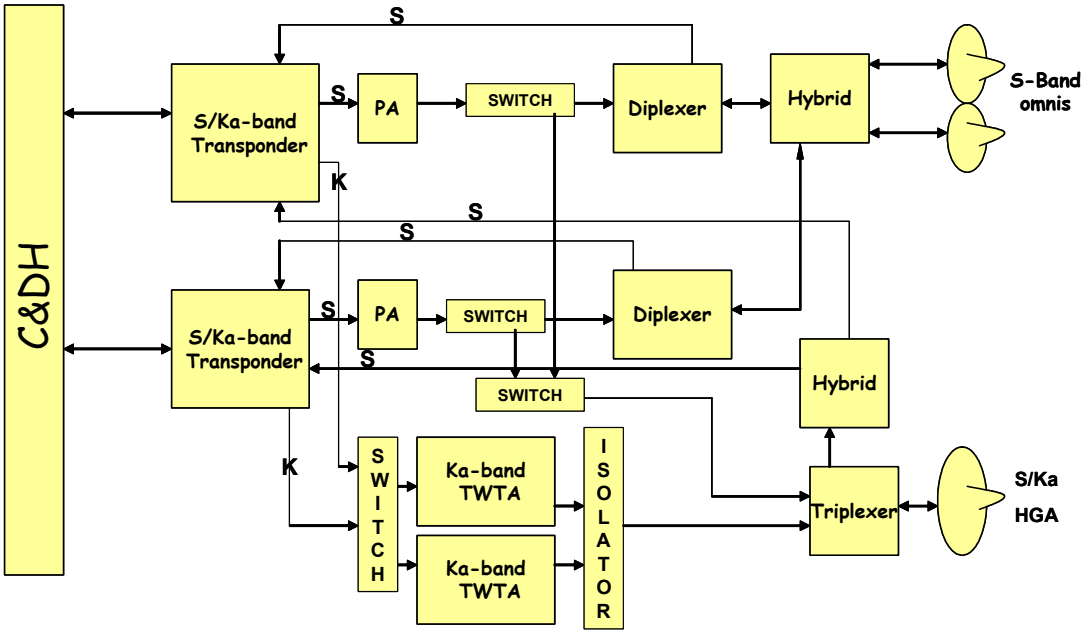

Figure 29-4. RF Communications Block Diagram

Requirements:

- Instrument data rate: 142 kbps average, 1.3 Mbps peak
- Instrument housekeeping: 4 kbps
- Spacecraft housekeeping: 4 kbps
- Nominal transmission rate: 206.5 kbps
  - Instruments: 142 kbps
  - Contingency data: 30%
  - Housekeeping: 8 kbps
  - CCSDS overhead: 15%
  - Transmitted nominal daily volume: 19 Gbits

- Data downlink rate: 14 Mbps
- Additional peak data volume each month: 38 Gbits
  - 1.175 Mbps for 6 hours
  - Contingency data: 30%
  - CCSDS overhead: 15%

Implementation:

- Ka-band for science and data dumps via DSN 34 meter
  - Data dumps at 14 Mbps
  - One 30 minute contact required per day
- S-band Telemetry Tracking & Communications (TT&C) via High Gain Antenna (HGA) to Deep Space Network (DSN) 34 meter
  - 2 kbps command
  - 8 kbps telemetry
- S-band TT&C via omni antennas to DSN 34 meter
  - 1 kbps command
  - 2 kbps telemetry
- S-band thru TDRSS for launch and early orbit critical events
  - 1 kbps command
  - 1 kbps telemetry
- Telemetry bit error rate: 10^{-6}
- Ranging for orbit determination
- Latency: 72 hours

Table 29-7. RF Communications Mass and Power

Mass and Power (CBEs)		
	Total Mass [kg]	Power Peak/Avg [W]
S/Ka Transponder (2)	6.1	30/26
S/Ka Antenna (0.5m) (Antenna only)	3	30/2
10 watt Ka TWTA (2)	12	30/22
5 watt S-band PA (2)	1	20/2
S-band omni (2)	2	
Diplexer (2)	0.5	
Triplexer	1	
Hybrids (2)	0.4	
Switches (4)	1	
Isolator and cabling, misc.	3	
TOTALS	**30.0**	**110/52**

29.7 Mechanical Subsystem

Requirements:

- Support all instruments and spacecraft components for launch loads
- Maintain optical alignments of the optics to the detectors and each other
- Design compatible with the launch vehicle fairing and payload adapter dynamic envelope
- Design for the center of pressure and center of mass to be within 1m in the science configuration
- Maintain optical alignments of the optics to the detectors
- Allow access to optics and detectors during ground servicing
- Allow access for cleaning during ground servicing
- Design of the metering structure shall be light tight
- All mechanisms shall be implemented in a manner such that there are no single point failures.

Implementation:

The Constellation-X primary structure is divided into three main parts: the focal plane module/detector bench, the metering structure, and the bus module/mirror bench. Images and a brief description of each are shown in the response to Question 21.

Launch Vehicle Payload Adapter:

The observatory mounts to the launch vehicle via a payload adapter. A 4.2 meter diameter truss adapter was selected to provide clearance around the X-ray mirrors. This truss attaches to the Centaur upper stage.

Mechanisms and Deployables:

Constellation-X uses the following mechanisms and deployable devices:

- Two deployable non-articulated solar arrays
- One deployable high gain antenna with azimuth and elevation articulation for Earth pointing
- One deployable fore sunshade to shadow the flight mirror assemblies
- Four flight mirror assembly covers that are jettisoned prior to science operations
- Four flight mirror assembly covers located near the postcollimators that are opened prior to science operations

Table 29-8. Mechanical Mass

Mechanical Subsystem Mass (CBE)	Kg
Metering Structure	
Longerons	84.5
Right Hand ribs	72.2
Left Hand ribs	72.2
Skin	106.5
TOTAL	**333.5**
Focal Plane Module	
Detector Deck	70.5
Bottom Deck ring	6.7
Equipment Panels (8)	38.4
Longerons (8)	4.6
TOTAL	**120.2**
Bus Module	
Top Deck	37.9
Optical Bench (bottom deck)	61.9
Bus Interior Panels (rosette)	126.9
Equipment panel (door)	10.4
Half doors	11.4
PAF spacer ring truss	120.0
TOTAL	**368.5**
Secondary Structures	**157.0**
Mechanisms	**146.6**
TOTAL	**1127.8**

30. FLIGHT HERITAGE OF THE SPACECRAFT AND ITS SUBSYSTEMS

Question: Describe the flight heritage of the spacecraft and its subsystems. Indicate items that are to be developed, as well as any existing instrumentation or design/flight heritage. Discuss the steps needed for space qualification.

RESPONSE

The baseline Constellation-X spacecraft and subsystems have substantial flight heritage.. As the Constellation-X spacecraft bus will be procured competitively from Industry, the heritage base presented here is for reference purposes only.

The majority of the components baselined for the Constellation-X spacecraft bus have flight heritage. Those without flight heritage are flight qualified and will be flown well in advance of Constellation-X on missions currently under development. The flight heritage of the Constellation-X payload has been discussed in the Response to Question 7. The flight heritage of the Constellation-X spacecraft bus subsystems and components is discussed below.

Additionally, orbit and mission aspects of the Constellation-X mission leverage the WMAP and JWST missions. The scientific, technical, and mission operations design leverages from *Chandra*, *XMM-Newton*, and *Suzaku*.

30.1 Thermal Subsystem

The thermal subsystem is a conventional design. Comparable designs have been successfully used in space for at least 20 years. Recent component heritage is listed below.

- **Flight mirror assembly precollimator heater control** *Chandra*, other X-ray missions, and HEAO-B/*Einstein* (launched in 1978)
- **Heat pipes** (CCHPS, and VCHPS by SAI) have flown on TRMM, ICESat/GLASS
- **Loop heat pipes** have flown on ICESat/GLASS (launched in January 2003), and were used in the repair of HST NICMOS
- **Heaters** (Tayco or Minco) flew on COBE, TRMM, Cassini, WMAP, and many others
- **Thermostats** (Elmwood) flew on COBE, TRMM, WMAP, and many others
- **Interface material** (NUSIL or GELVET) flew on numerous GSFC missions
- **Paint**, Z93 white (AZ Tech), Z306 (Lord Corp), NS43G (GSFC) flew on numerous GSFC missions

30.2 Propulsion Subsystem

The propulsion subsystem design has extensive flight heritage. Hydrazine/NTO and MMH/NTO biprop propulsion systems have considerable flight heritage (e.g., Lockheed-Martin Series 5000/7000 and A2100 spacecraft, Boeing 601 and 702).

The subsystem also leverages recent design heritage. SDO will be put into a geostationary orbit by an MMH/NTO biprop propulsion subsystem that utilizes AMPAC 22N MMH/NTO. The Constellation-X thrusters are identical to SDO's except for injector modifications due to the different fuel. A Hydrazine/NTO blowdown propulsion subsystem is baselined for JWST.

Component heritage is listed below.

- **Thrusters**: The AMPAC Hydrazine/NTO thruster, baselined for Constellation-X, was successfully flown on an Orbital Sciences Corporation classified spacecraft. The AMPAC 22N MMH/NTO thruster has flight heritage on an NRL spacecraft, and will fly on SDO. The AMPAC 22N Hz/NTO thruster has been subjected to extensive qualification testing that has demonstrated performance robustness over a wide range of feed pressures (4:1 blowdown) and mixture ratios (0.65 to 1.2).
- **Tanks**: The baseline Hydrazine and NTO tanks for Constellation-X were successfully flown on GE Astrospace INMARSAT III and V, and the Mars Observer spacecraft, respectively. Both tanks were developed and qualified by ATK/PSI, Inc.

  The helium pressurant tank baselined for Constellation-X has flight heritage from the ATK-PSI composite overlay pressure vessel, ETS8 xeon pressurant tank. Other similar ATK-PSI composite overlay pressure vessel tanks of various sizes have considerable flight heritage on Boeing, Loreal and Lockheed-Martin spacecraft.

Other components (valves, filters, regulators, etc.) have extensive flight heritage with hundreds, and in some cases thousands, successfully flown in space.

30.3 Attitude Control Subsystem

The attitude control subsystem design (three-axis inertial stabilization, star tracker-IRU attitude determination, reaction-wheel actuation) has extensive flight heritage. Component heritage is listed below.

Components baselined for Constellation-X are commercial off-the-shelf components with extensive flight heritage, with the exception of the Honeywell HR14(75) reaction wheels, that are TRL = 8 (having been qualified for space, but without space flight heritage).

Component heritage:

- Star tracker (Ball CT602): EOS Aqua
- IRU (Litton SIRU): EOS Aura, EOS Aqua, GLAST
- Course sun sensors (Adcole): TOPEX, SMEX, P91-1, XTE, TRMM, GFO,WIRE, TRACE, MAP, QUICKSAT, EO-1, MIGHTYSAT, PROTEUS, HESSI, Swift, CORIOLIS, CLOUDSAT.
- Two axis fine digital sun sensor (Adcole): SESAT, EOS-AM, XTE, RADARSAT, ISO, TOPEX, EUVE, SPARTAN, GRO, OLYMPUS, ERBS, EXOS-C, DYNAMIC EXPLORER, ESD, MMS, IRAS, IUE, MAGSAT.

30.4 Command & Data Handling Subsystem

No new items need to be developed or space qualified.

The **data bus interface** baselined for Constellation-X, SpaceWire, was used on *Swift* (launched Nov. 2005).

The following missions (all in advanced stages of implementation) will also use **SpaceWire**:

- LRO and LCROSS (both launch in 2008)
- JWST (~ 2013 launch)

- GOES-R (~2012 launch)
- MMS (~2013 launch)

30.5 Electrical Power Subsystem

Fully mature technologies are used in the design of the Electrical Power Subystem.
Component heritage is listed below:

- **Li-Ion batteries** like the one baselined for Constellation-X have been used in space for years.
  - In Use: Calipso 78 Ah battery made from Saft 26 Ah cells; ST-5; MER (JPL mission), Mars Rovers
  - Future Use: SDO, LRO and Themis with the 18650 types LiIon cells; IBEX to use 12 Ah Yardney cells; MMS to use Li-Ion cells
- **Solar arrays** with triple junction GaAs cells like those baselined for Constellation-X have been used in space for at least 5 years.
  - In use on Messenger, GALEX, HESSI, several Boeing Comm. Satellites, ST-5
  - Future Use: LRO, GLAST, SDO, JWST, GPM, Themis, IBEX, MMS
- **Power system electronics (PSE)** similar to the one baselined for Constellation-X has been flown on EOS Terra (120 VDC PSE with a battery bus of 70 VDC). Use of voltage regulated bus is EOS Terra and ISS heritage 120VDC.

30.6 RF Communications Subsystem

- **S-band** RF communication hardware comparable to the hardware baselined for Constellation-X (**transponder, power amplifier, hybrids, omnidirectional antennas**) is standard COTS space flight hardware flown on hundreds of missions: e.g., WMAP, WIRE, AMPEX, COBE, all SMEX Missions
- **Ka-band transmitter** operating at 26 GHz has no flight heritage, but is being implemented on SDO (2008 launch) and LRO (2008 launch). A custom designed Ka-band Transmitter operating at 32 GHz flew on DS-1.
- **Ka-band switch/waveguide**: only "future use" on SDO (2008 launch). X-band switches flew on WMAP, *RXTE*, TRMM
- Ka-band travelling wave tube amplifiers (TWTA): only "future use" on LRO (2008 launch)
- **0.5m diameter high gain dish antenna (HGA)**: 0.75m S/Ka-band HGA "future use" on LRO (2008 launch), 0.75m Ka-band HGA "future use" on SDO (2008 launch), 0.6m Ka-band HGA "future use" on JWST (2013 launch)

Note: Constellation-X has baselined a combined S-band transponder/Ka-band transmitter, as opposed to a separate S-band transponder and Ka-band transmitter configuration that will be flown on SDO and LRO. To forego development, separate units similar to SDO and LRO can be used with a ~7 kg mass penalty.

30.7 Mechanical Subsystem

Only fully mature technologies are used in the design of the structures and mechanisms.

- **Bus module/mirror bench and focal plane module structures** (honeycomb panels using composite facesheets and aluminum core; fittings and inserts made from titanium, aluminum, and invar): Well understood flight heritage, flown on most space telescopes in last 15 years including HST, TRMM, WMAP, *Chandra*, XMM, and *Swift*.
- **Brackets & mounts for the FMAs** (titanium flexures and mounts): flight heritage includes *Swift's* X-ray telescope which used titanium flexures to mount to a composite optical bench.
- **Metering structure** (Advanced Grid Stiffened (AGS) composite structure (isogrid)): The Constellation-X composite isogrid metering structure baselined has heritage from the Minotaur AGS rocket fairing (December 2006) and the Boeing 787 Dreamliner main fuselage sections. Aluminum isogrids have been used in aerospace since the 1960s. The composite material will be determined after future trade-studies. Constellation-X baseline material for the isogrid structure is M54J/954-3. This material has extensive flight heritage at GSFC.

31. ACCOMMODATION OF THE SCIENCE INSTRUMENTS BY THE SPACECRAFT

Question: Address to the extent possible the accommodation of the science instruments by the spacecraft. In particular, identify any challenging or non-standard requirements (i.e. Jitter/momentum considerations, thermal environment/temperature limits etc.).

RESPONSE

All of the Constellation-X science instrument accommodation requirements can be met using standard spacecraft technologies.

31.1 Mechanical Accommodations

- The Spectroscopy X-ray Telescope (SXT) and Hard X-ray Telescope (HXT) mirrors are located at the forward end of the telescope structure, and the detectors are located at the aft end. Aperture plates with optical baffles will be mounted to the telescope structure approximately 1/3 and 2/3 of the focal distance.
- Structure:
  - Sized to accommodate Atlas V551 launch loads.
  - Designed to minimize and allow prediction of gravity release and other deformations.
- Alignment:
  - SXT focus: XMS to FMA focal distance shall be 10m ±1 mm
  - XMS to FMA alignment shall be within ±0.25 mm
  - SXT to SXT coalignment shall be within 10 arcsec
  - HXT detector shall be located within 2 mm of the nominal focal length (9 m or 10 m)
  - HXT detector center to HXT mirror axis +/- 1 mm
  - HXT to SXT coalignment shall be within 1 arc minute
  - The two different XGS concepts have significantly different alignment and stability requirements, and these are currently being assessed. The worst case alignment tolerance of the gratings to the FMA are on the order of a few arcsec, and the worst case stability knowledge (of the CCDs relative to the telescope optical axis) is on the order of 50 microns/13.8millisec.

31.2 Thermal Accommodations

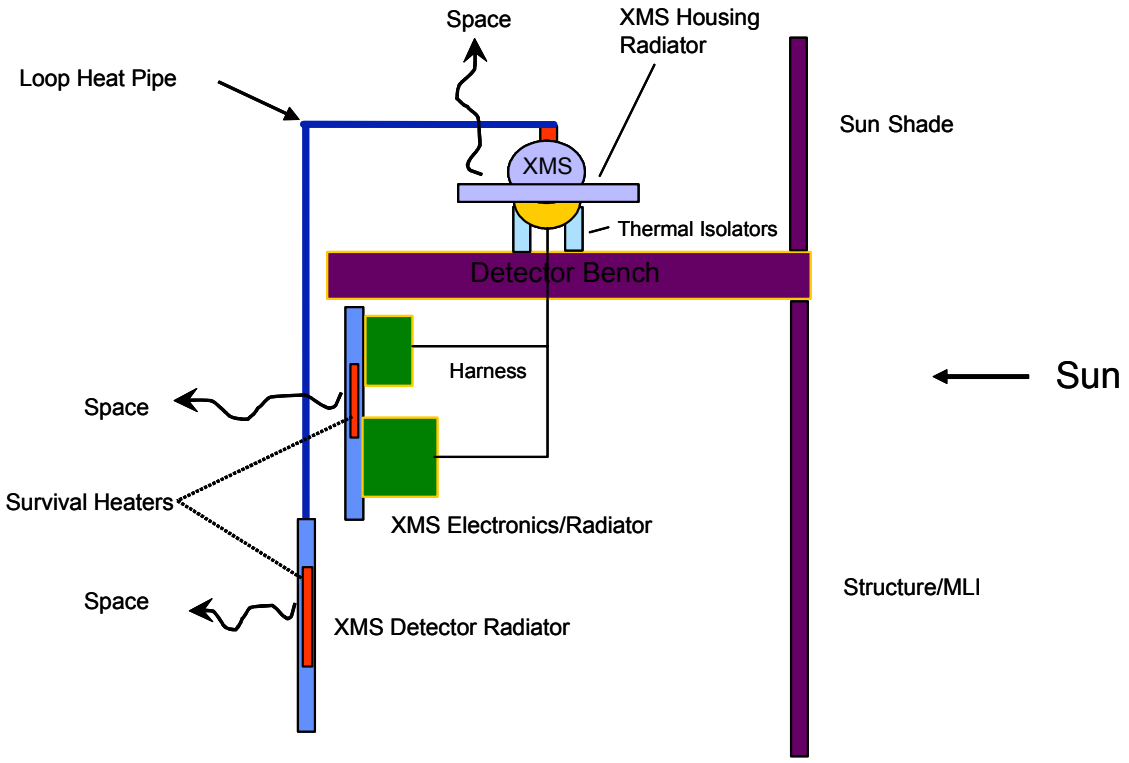

Figure 31-1. Thermal Accommodation of XMS Instrument

- Mirror bench: Passive thermal control via deployable Sunshade
- Flight mirror assembly:
  - Operating temperature is 20±0.5°C. The temperature of each mirror is maintained by thermostatically controlled heaters located on the Pre- and Post-Collimators. The mirror assembly is thermally isolated from spacecraft equipment bays.
  - Survival temperature is +10 to +30 deg C
  - Maximum allowable temperature gradient is 1 deg C
  - HXT mirror operating temperature is 20±1°C
- Detector bench / focal plane: Passive thermal control via fixed sun shade
- X-ray Microcalorimeter Spectrometer (XMS):
  - Cryostat outer shell operating point will be in the range between 80 - 110K. The temperature is controlled passively via an integrated radiator and a fixed sun shade.
  - Cryostat outer shell temperature stability is 5 K/day
  - Waste heat from cryocoolers is removed by loop heat pipes to dedicated radiators
  - The XMS is thermally decoupled from the detector bench by means of multi-layer insulation and isolators.
- X-ray Grating Spectrometer and Hard X-ray Telescope detectors:

  - Cooling to detectors is provided by a heat pipe to an external radiator. (Precision thermal control is maintained by detector system.)
  - Each detector has thermostatically controlled survival heaters
- Instrument electronics
  - The instrument electronics are mounted in the payload electronics bay on aluminum honeycomb radiator panels with a full view to space.
  - Each electronics box has thermostatically controlled survival heaters.

31.3 Guidance, Navigation & Control Accommodations

Field of Regard (instantaneous portion of the sky accessible for observations):

- Pitch: ±20° (deviation from Sunline with respect to the solar array normal)
- Yaw: ±180°
- Roll: ±20° (deviation from Sunline with respect to the solar array normal)
- Over six months the 0.98 deg/day rotation of the 20° x 180° band about the ecliptic normal allows access to any location in the celestial sphere for a minimum of 1.5 months.

Pointing Control (3σ):

- Pitch: 10 arcsec
- Yaw: 10 arcsec
- Roll: 30 arcsec

Pointing Knowledge (3σ):

- Pitch: 5 arcsec
- Yaw: 5 arcsec
- Roll: 20 arcsec
- Jitter: < ~2 arcsec/13.8 milliseconds

31.4 Power Accommodations

- All instruments receive 120VDC off the main power bus, and down-convert and regulate internally.

31.5 Command & Data Handling (C&DH) Accommodations

- All instruments are connected to the C&DH via routers that packetize the data and transmit them to the C&DH unit. SpaceWire point-to-point wiring is used between the instruments, routers, and the C&DH unit.
- Accommodated data volumes and data rates are specified in the responses to Question 34 and Question 11.

31.6 Contamination Control

- Both particulate and molecular contamination potentially impact the performance of X-ray optics and instrumentation, especially at low energies. While we have not yet established contamination-control requirements for the X-ray optics, we expect that they will be somewhat

looser than those specified and achieved for the *Chandra* optics — namely, $< 0.5 \times 10^{-4}$ fractional areal coverage by particulates and < 0.5 microgram/cm^3 thickness of molecular contaminant.

The corresponding requirements on the focal-plane instrument will be about two orders of magnitude looser than those on the optics, primarily due to near-normal (versus grazing) incidence upon the instrument's entrance-aperture filter. The mainshell temperature of the XMS dewars will be extremely cold (< 150K), and thus the main shell filter has the potential for adsorbing outgassing products from the spacecraft. We thus expect to implement several components for preventing the buildup of contamination on the blocking filter, including cold baffles near the aperture and a mainshell filter heater system (which was implemented on the *Suzaku*/XRS system) that can be operated continuously if required.

32. TECHNOLOGY READINESS LEVEL OF CRITICAL S/C ITEMS

Question: Define the technology readiness level of critical S/C items along with a rationale for the assigned rating.

RESPONSE

Every spacecraft component baselined for Constellation-X has a technology readiness level (TRL) of 6 or higher. The TRL ratings below reflect the high degree of flight heritage for the components selected.

Constellation-X is built on a conventional spacecraft bus:

- The spacecraft bus and all of its subsystem requirements are well understood.
- All key requirements of the spacecraft bus are enveloped by requirements flown on previous missions.
- Most spacecraft bus component requirements can be met with commercial "off the shelf" equipment.

32.1 Structure

The primary structure of Constellation-X is at TRL 6 as it needs to be customized and qualified for this mission.

32.2 Mechanisms

The requirements for Constellation-X mechanisms are readily achieved with minor modifications to existing flight mechanisms, therefore the mechanisms are at a TRL of 6.

32.3 Thermal Control Subsystem

The thermal control subsystem components have a TRL of 8 or higher.

32.4 Propulsion Subsystem Subsystem

The Hydrazine/NTO biprop propulsion subsystem components have a TRL of 8 or higher.

32.5 Attitude Control Subsystem

The attitude control subsystem components are at a TRL of 8 or higher (all components are commercial "off-the-shelf").

32.6 Command & Data Handling Subsystem

The command & data handling subsystem components are at a TRL of 8 or higher.

32.7 Power Subsystem Subsystem

The electrical power subsystem components are at a TRL of 8 or higher.

32.8 RF Communications Subsystem

The RF communication subsystem components are at a TRL of 8 or higher, with the exception of the 26 GHz S/Ka-band Transponder which is at a TRL of 6.

Note: Constellation-X has baselined a combined S/Ka-band transponder, as opposed to separate Ka-band transmitter / S-band transponder configuration like that planned for SDO and LRO. A 26 GHz combined S/Ka-band transponder does not presently exist as a single unit, but could easily be developed from the existing 32 GHz X/Ka-band small deep space transponder. The 32 GHz frequency is assigned to deep space missions, which Constellation-X is not. To forego development, separate S-band transponders and Ka-band transmitters (similar to SDO and LRO) can be used with a ~7 kg mass penalty.

33. PRELIMINARY SCHEDULE FOR THE SPACECRAFT DEVELOPMENT

Question: Provide a preliminary schedule for the spacecraft development.

RESPONSE

A master schedule for the Constellation-X Mission, supporting a launch date of June 2017, is shown in Figure 33-1. This schedule assumes that Constellation-X is selected as the first Beyond Einstein mission, and begins Phase A in FY2008. Phase B begins in early FY2010, and Phase C/D begins in early FY2012. Five years of mission operations are planned.

The Observatory development program includes industry concept studies, by two or more potential industry partners in Phase A. The studies are followed by a competitive procurement to select a prime contractor for the development of the spacecraft bus, (including the observatory optical bench structure), integration and test of the observatory, and launch support.

The spacecraft bus schedule is given on a single line in Figure 33-1. Spacecraft development begins with observatory prime award. Long lead procurement items are initiated soon after Preliminary Design Review. Note that the spacecraft bus major reviews are scheduled with the mission reviews. Spacecraft subsystems are environmentally tested before delivery to spacecraft bus module integration and functional test. There is an eight-month overlap between the beginning of mission system Integration and Test (I&T) and the end of spacecraft I &T. This overlap allows for early integration of instrument focal plane assemblies and electronics into the focal plane module and payload electronics bay.

The mission critical path, indicated by a red line above the respective activity lines, goes through the Flight Mirror Assembly (FMA) build, through Mission System Integration and Test, to Launch Site Activities. There is a total of 9 months slack on the critical path; 1 month in the FMA development, 2 months in the Mission System Integration and Test, and 6 months held just prior to launch. The FMA and instrument schedules are provided in the response to Question 15.

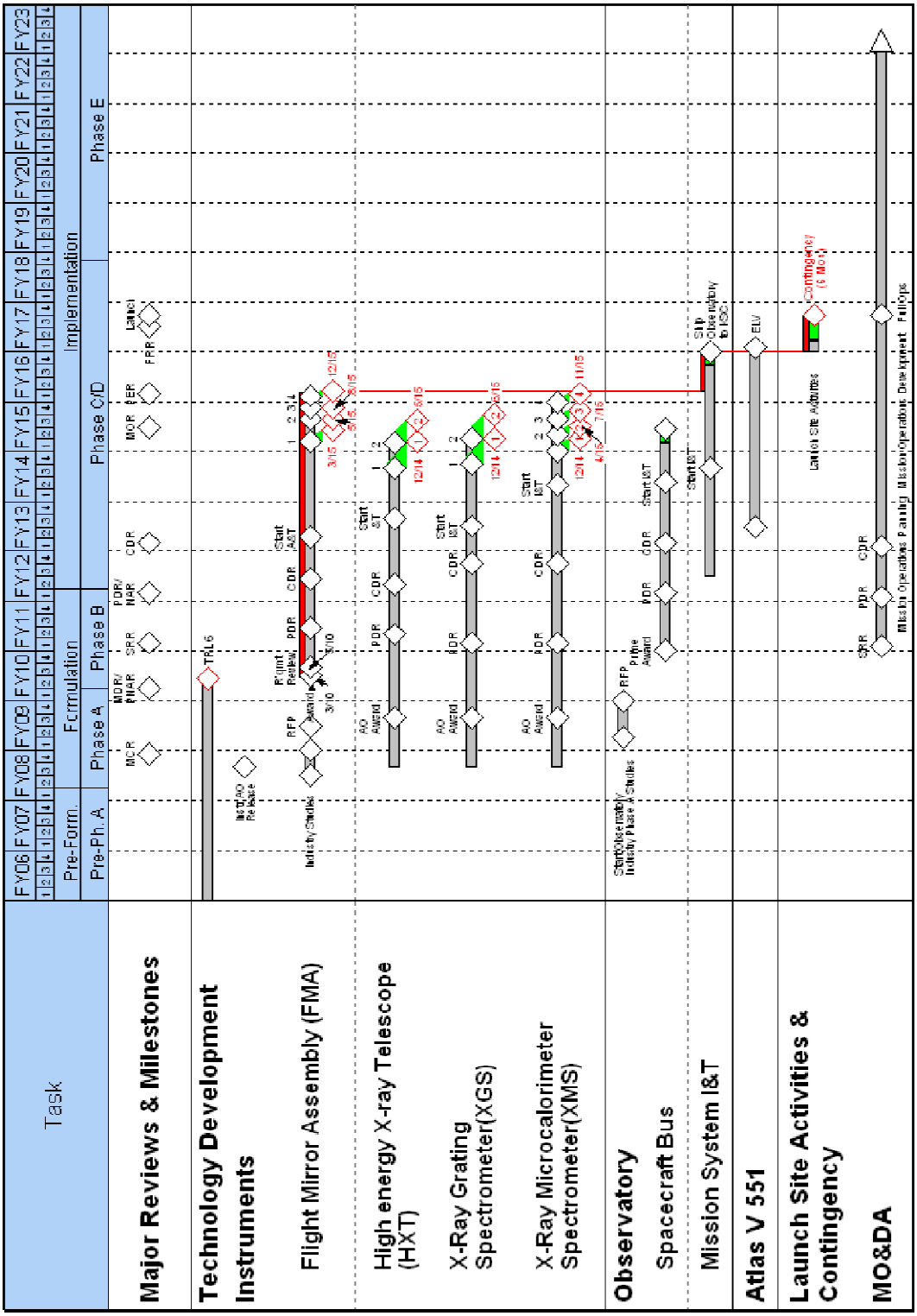

Figure 33-1. Con-X Mission Master Schedule

34. SPACECRAFT CHARACTERISTICS TABLE

Question: Spacecraft Characteristics Table (Optional – fill out any known entries if you have selected an implementation).

RESPONSE

Table 34-1. Spacecraft Characteristics

Spacecraft Bus	
Structure	**Value/Summary, Units**
Structures material (aluminum, exotic, composite, etc.)	Isogrid metering structure with optical bench quality low outgassing composite material ▪ High or ultra-high modulus graphite fiber composite layup with a cyanate-ester resin. Precise composite system determination studies to be performed. Present baseline is M54J/954-3 (extensive flight heritage at GSFC, is well understood and available).
Number of articulated structures	▪ One: high gain antenna with two axes of articulation – pointed at Earth
Number of deployed structures	Total: 12, all low precision ▪ 1 high gain antenna – deploy ▪ 2 solar array wings – deploy ▪ 1 mirror bench sunshade – deploy ▪ 4 external flight mirror assembly covers – jettison ▪ 4 internal flight mirror assembly covers – open once
Thermal Control	**Value/Summary, Units**
S/C Type of thermal control used	▪ Passive thermal control design system for the spacecraft bus. ▪ Single fault tolerant thermal subsystem. Redundant (series/parallel) in prime and redundant heaters, thermostats and thermistors. Details: ▪ External MLI, 15 layers; the outer layer is conductive Germanium Black Kapton ▪ Radiators (e.g., NS43G White Paint) ▪ Back side of solar array panels painted (e.g., NS43G white paint) ▪ Internal surface coatings of spacecraft bus high emittance surfaces (e.g., Aeroglaze Z306 Black Paint) except for the battery (possibly internal closeout MLI for isolation) ▪ ChoSeal interface material for box to panel interfaces (electrically and thermally conductive) ▪ Kapton film heaters mounted on box-to-panel interfaces ▪ Heaters are thermostatically controlled ▪ Thermistors for temperature telemetry ▪ Payload cryocooler cold head thermal control via loop-heat pipes connected to dedicated radiator panels

Spacecraft Bus					
Propulsion	**Value/Summary, Units**				
Estimated delta-v budget, m/s		**CBE**	**ACS Tax**	**Contingency**	**Subtotal**
	Launch Window	10 m/s	5%	0%	11 m/s
	ELV Dispersion Correction	40 m/s	5%	0%	42 m/s
	Mid-Course Correction	10 m/s	5%	10%	12 m/s
	Halo Adjust	25 m/s	5%	10%	29 m/s
	L2 station keeping 10 yrs	40 m/s	5%	10%	46 m/s
	Momentum Management	2 m/s	5%	10%	2 m/s
	Disposal	1 m/s	5%	10%	1 m/s
	Total Equivalent delta-v				**143 m/s**
Propulsion type(s) and associated propellant(s)/oxidizer(s)	Pressure regulated NTO (Nitrogen TetraOxide)/Hydrazine bipropellant propulsion system				
Number of thrusters and tanks	Thrusters: ▪ Twelve single string 22N Biprop thrusters used for orbital maneuvers and momentum unloading. Single fault tolerant with respect to thrust vectors and forceless pure momentum couples. Tanks: ▪ Two: monolithic titanium NTO ▪ Two: monolithic titanimu hydrazine tanks ▪ One: composite overlay titanium helium (pressurant) tank				
Specific impulse of each propulsion mode, seconds	▪ Specific impulse for major burns (launch vehicle dispersion correction, mid-course corrections, orbit insertion/orbit amplitude lowering and stationkeeping): 285 seconds ▪ Specific impulse for momentum management burns (~ 100 msec impulses): 150 seconds ▪ Composite average specific impulse over a 10 year mission: 274.8 seconds				

Spacecraft Bus	
Attitude Control	**Value/Summary, Units**
Control method (3-axis, spinner, grav-gradient, etc.).	3 axis stabilized
Control reference (solar, inertial, Earth-nadir, Earth-limb, etc.)	Inertial reference with Sun constraint (Earth-Sun L2 lagrangian libration point)
Attitude control capability, degrees	Attitude Control (3σ): ▪ Pitch: 10 arcsec ▪ Yaw: 10 arcsec ▪ Roll: 30 arcsec
Attitude knowledge limit, degrees	Attitude Knowledge (3σ): ▪ Pitch: 5 arcsec ▪ Yaw: 5 arcsec ▪ Roll: 20 arcsec
Agility requirements (maneuvers, scanning, etc.)	▪ Perform a 60 degree slew in 1 hour, including settling time
Articulation/#–axes (solar arrays, antennas, gimbals, etc.)	▪ High gain antenna articulated in two axes within a 45° cone to point at Earth
Sensor and actuator information (precision/errors, torque, momentum storage capabilities, etc.)	▪ Star trackers (3): noise equivalent angle: 2.5 arcsec (1σ); e.g., Ball Aerospace CT-602; ▪ IRUs (1): drift rate: 0.015 deg/hr, drift stability: 0.0006 deg/rt-hr; e.g., Northrop-Grumman SIRU; ▪ 2 Axis Fine Sun Sensor (2): +/- 32 deg field of view, accuracy: 1 arcmin; e.g., Adcole Model 20910; ▪ Coarse Sun Sensors (6): combined coverage: 4π steradian; e.g., Adcole coarse sun sensor; ▪ Reaction Wheels (4): momentum: 75 Nms each, torque: 0.2 Nm each; e.g., Honeywell HR14 (75); ▪ Thrusters (12): 22N Hydrazine/NTO biprop matched to within 5%, ~10 ms minimum pulse duration

<table>
<tr><th colspan="4">Spacecraft Bus</th></tr>
<tr><th>Command & Data Handling</th><th colspan="3">Value/Summary, Units</th></tr>
<tr><td>Data storage capacity, Mbits</td><td colspan="3">▪ Storage capacity is 144 Gbit (18 GByte).
▪ Sized for two days, each with 6 hours of peak science data rate and 18 hours of nominal science data rate
▪ SDRAM size includes Reed Solomon protection</td></tr>
<tr><td>Spacecraft housekeeping data rate, kbps</td><td colspan="3">4 kbps</td></tr>
<tr><td rowspan="7">Maximum storage record rate, kbps</td><td>Data Source</td><td>Nominal (kbps)</td><td>Peak (kbps)</td></tr>
<tr><td>XMS</td><td>38</td><td>300</td></tr>
<tr><td>HXT</td><td>17</td><td>150</td></tr>
<tr><td>XGS</td><td>87</td><td>867</td></tr>
<tr><td>H/K Instrument</td><td>4</td><td>4</td></tr>
<tr><td>H/K Spacecraft</td><td>4</td><td>4</td></tr>
<tr><td>Total</td><td>150</td><td>1,325</td></tr>
<tr><td>Maximum storage playback rate, kbps</td><td colspan="3">14 Mbps (maximum downlink rate)</td></tr>
<tr><th>Power</th><th colspan="3">Value/Summary, Units</th></tr>
<tr><td>Type of array structure (rigid, flexible, body mounted, deployed, articulated)</td><td colspan="3"><u>Solar Array:</u>
▪ Rigid: two deployable non-articulated solar array wings, 3 panels each</td></tr>
<tr><td>Array size, meters x meters</td><td colspan="3">2.1 x 5.2 square meters, each wing (21.8 square meters total area)</td></tr>
<tr><td>Solar cell type (Si, GaAs, Multi-junction GaAs, concentrators)</td><td colspan="3">Triple-junction GaAs (28% efficiency)</td></tr>
<tr><td>Expected power generation at Beginning of Life (BOL) and End of Life (EOL), watts</td><td colspan="3">5330 W BOL, 4710 EOL (10 yrs, comprising string redundancy)</td></tr>
<tr><td>On-orbit average power consumption, watts</td><td colspan="3">4140 W, incl. 30 % Contingency</td></tr>
<tr><td>Battery type (NiCd, NiH, Li-ion)</td><td colspan="3">Li-ion, 18 cells with cell by-pass switches</td></tr>
<tr><td>Battery storage capacity, amp-hours</td><td colspan="3">20 amp-hours, max 50% depth of discharge after Launch</td></tr>
</table>

35. DESCRIPTION OF MISSION OPERATIONS

Question: Provide a brief description of mission operations, aimed at communicating the overall complexity of the ground operations (frequency of contacts, reorientations, complexity of mission planning, etc). Analogies with currently operating or recent missions are helpful.

RESPONSE

Constellation-X (*Con-X*) is launched from the Kennedy Space Center directly to a 800,000 km radius halo orbit around the Sun-Earth Lagrangian L2 Libration point following a direct insertion path (without lunar gravity assist or phasing loops). The cruise duration to L2 is approximately 100 days, during which time the science instruments will remain off and the mirror covers closed. Upon arrival at L2, a maneuver to lower the diameter of the orbit to 700,000 km radius will be performed. This will ensure that Con-X stays within the Earth's magnetosheath the majority of the time, thus taking advantage of the beneficial radiation shielding effects of the Earth. The baseline L2 orbit provides few observing constraints and a stable thermal environment, leading to a high observing efficiency.

Normal science operations begin after L2 Orbit Insertion (LOI). Forceless pure torque momentum dumps and routine station-keeping maneuvers for orbit maintenance will be conducted periodically during the mission.

During launch and the initial insertion into the drift trajectory, communications will occur through the Tracking Data Relay Satellite System (TDRSS) and/or the Deep Space Network (DSN). During cruise and L2 operations, communications will be provided by the Deep Space Network (DSN).

Mission Operations will be conducted from the *Con-X* Science and Operations Center (CXSOC) in Cambridge, MA, with communications supported by real-time direct links with White Sands (for TDRSS) and JPL (for DSN).

The Con-X ground data system consists of three principal data processing elements: the Ground Stations (DSN, TDRSS), the Mission Data System (MDS) and the Science Data System (SDS). The MDS and SDS are collocated at the CXSOC and reuse existing mission operations data systems and facilities currently supporting the *Chandra* X-ray Observatory.

The CXSOC consists of the facilities, data systems and staff required to conduct the mission operations and all aspects of the science program including science instrument operations, calibration, mission planning, data system development, operations and maintenance, public education and outreach and grants programs. The MDS performs the mission data processing functions for the spacecraft including commanding, real-time safety and health monitoring, trending, anomaly resolution, mission planning, flight dynamics and science instrument health and safety monitoring. The CXSOC also houses the Con-X spacecraft simulator used to verify flight software patches, and interfaces with the Science Instrument team facilities for instrument flight software maintenance. The SDS provides for all science processing functions including pipeline processing, management and distribution of data, archiving and provision of analysis software to the user community, and support for dissemination of images and data to the public. These activities are conducted from a single facility in order to reduce operations costs and maximize team integration and synergy.

The CXSOC is staffed with the Flight Operations Team (FOT), ground operations staff and science staff. The FOT team coordinates the space/ground contacts with the ground stations, generates

commands, monitors spacecraft telemetry and critical safety parameters from the instrument engineering data, and monitors the performance of the each spacecraft. The Ground team operates and maintains the MDS. The CXSOC science staff conducts the annual review of observing proposals, performs science mission planning, develops science analysis software, conducts science data processing, archiving, dissemination of data to the observers, calibration, science trending, education and public outreach, and administers the *Con-X* grants programs.

The operations concept for *Con-X* has been developed around a 'primary operations thread', the end-to-end sequence of steps needed to accomplish a science observation. The thread provides a structure to develop detailed operational scenarios, and allows for the development of a complete set of processes, appropriate ground data system architecture, staff organization and staff functions. The *Con-X* primary operations thread is based on the *Chandra* operations concept and includes the annual proposal cycle, mission planning cycle, weekly scheduling, routine pass activity (uplink, downlink, monitoring and trends), science data processing, science data archiving and distribution, and science data analysis. Other functions include anomaly resolution, training and simulation, calibration, science monitoring and trends. The *Con-X* ground architecture, the CXCSOC data system design and operations processes have been developed from the primary thread.

It is anticipated that the annual *Con-X* observing program will consist of ~100 targets from ~250 peer reviewed programs, as well as required calibration targets. An annual long-term schedule is developed that incorporates time constraints and long-term pointing constraints. During routine operations, a weekly observation list is extracted from the long-term schedule and a weekly mission schedule generated that includes science instrument mode selection and commanding, star field selection for each target, slew sequence optimization, and incorporates engineering and spacecraft constraints. The weekly schedule and resulting command loads are generated by the FOT mission planners using the MDS.

Command loads are uplinked every 2-3 days and the observing sequence executes autonomously onboard the spacecraft with science and engineering data stored on the solid state recorder. A single ~30 minute ground contact per day is sufficient for checking the safety and health of the vehicle, downloading the last 24 hours of data and uplinking the next command load as needed. During the contact, MDS software checks the real-time data automatically for limit violations and controllers take action for out-of limit conditions. Following receipt of the dump data from DSN, tools are run to check limits and trend data from the last 24 hours, and the data are provided to the SDS for science processing, archiving and distribution to observers. The *Con-X* archive will be a component of the High Energy Astrophysics Science Archive Research Center (HEASARC) ensuring that the data products, software and calibration files follow the standards developed for other high energy missions, and that the data will be available to the community over the long term.

Con-X will support Targets of Opportunity (TOO) requests from observers in order to respond to unexpected, high priority science events such as a supernova, gamma ray burst or a sudden change in state in variable objects. Based on our *Chandra* experience, we expect to support 1-2 TOOs per month with response times of 1-3 days. Table 35-1 summarizes the key operations metrics and parameters for both Con-X and *Chandra*.

Table 35-1. A Comparison of Key Operational Metrics for Con-X and Chandra

Parameter	Chandra	Con-X
Mission duration	5 year (10 goal)	5 year (10 consumables)
Number of instruments	2 focal plane	3 focal plane
Sky Access	95% over a year	100% over six months
Observing Efficiency averaged over mission life	65%	85%
Slews per day (average over mission life)	2-3	2-3
Station Keeping Maneuvers	0	Once every 21 days
Pointing accuracy	Knowledge: 0.707 arcsec (pitch/yaw)	Knowledge: 4 arcsec (pitch and yaw), 20 arcsec (roll) 3-sigma
	Control: 4 arcsec (pitch and yaw)	Control: 10 arcsec (pitch and yaw), 30 arcsec (roll) 3-sigma
Aspect determination	0.707 arcsec RMS	5 arcsec
Timing	10 μs capability	100 μs to UTC
Onboard Telemetry rate	32 kbps	150 kbps (avg.), 1.33 Mbps (max.)
Onboard Data Storage	2.6 GBit	144 Gbit
Recorded Volume per day	2.8 GBit	19.4 Gbit (avg.), 57.3 Gbit (max, assuming 6 hours of peak rate)
Number of contacts per day	3	1
Time to downlink 1 day data	45 min 1 Mbps	23 min (avg.), 68 min (max.) at 14 Mbps
Data uplink rate (DSN)	2 kbps	2 kbps
Frequency of command loads	Once every 2-3 days	Once every 2-3 days
Data Latency	72 hours	72 hours
TOO Frequency	1-2/month	1-2/month
TOO Response Time	1 day	1 day
Shifts per day	2	1
Science and Telemetry Archive Storage	0.5 TB/year	20 TB/year

Table 35-1 shows the high degree of operations commonality between the two missions and indicates a relatively low overall mission operations complexity. Factors that contribute to the low complexity for Con-X include the relatively long average observation time per target ($\geq$8-10 hours), corresponding small number of targets ($\leq$20 per week), benign orbit (L2 with 1 station keeping maneuver every 3 weeks), simple science instrument operation modes and data formats, and lack of complex mechanisms. This assessment is supported by a recent (Dec 06) study of *Con-X* by the GSFC Integrated Mission Design Center (IMDC) who concluded that the mission has a “Relatively simple mission operations concept [that] allows [an] 8x7 operations approach to be employed”, “Technology readiness at TRL 8-9”, “Technology complexity: minimal”, and that there were "no risk/issues of concern.”

36. UNUSUAL CONSTRAINTS OR SPECIAL COMMUNICATIONS

Question: Identify any unusual constraints or special communications, tracking, or near real-time ground support requirements.

RESPONSE

Constellation-X has no unusual constraints or requirements in these areas.

Planned communications and tracking is as follows:

- DSN ranging is required for orbit determination. Our present baseline, using a Batch Least Squares orbit solution, is two 30 minute ranging periods per day required during the transfer orbit, and one 30 minute period per day required at L2, to be performed simultaneously with the daily data dumps. In order to determine the orbit to the required accuracy, the orbit disturbances from momentum unloading must be less than 0.5 mm/s per day over a three week interval. (This is a requirement on the attitude control system, not ground system). A future trade will be performed to assess the feasibility of an orbit solution using Kalman filters, which would allow relaxing the orbit disturbance requirements (see Question 24).

All mission critical operations (delta-v burns, opening of doors and other deployments, stationkeeping maneuvers) will be performed with real-time live telemetry coverage. Real-time live telemetry coverage is available 100% of the time during the entire mission, but will only be used during scheduled data dumps and mission critical operations.

37. UNUSUAL OR ESPECIALLY CHALLENGING OPERATIONAL CONSTRAINTS

Question: Identify any unusual or especially challenging operational constraints (i.e. viewing or pointing requirements).

RESPONSE

There are no unusual or challenging operational constraints during the entire Con-X Mission. The nearly constant thermal and viewing conditions afforded by the L2 orbit remove the viewing constraints experienced by observatories in Earth orbits, like *Chandra* and *Suzaku*. Stationkeeping burns are performed at elective times, no more frequently than once every 21 days.

38. MISSION OPERATIONS AND GROUND DATA SYSTEMS

Question: Mission Operations and Ground Data Systems Table (Optional – provide only if you have selected a S/C and operations implementation).

RESPONSE

Table 38-1. Mission Operations and Ground Data Systems

Downlink Information	Value, Units
Number of data dumps per day	▪ One ~30 min data dump per day (avg) at 14 Mbps ▪ Once a month an 111 minute contact is required for the downlink of peak data at 14 Mbps
Downlink frequency band, GHz	▪ Ka-band for science data downlink, 26 GHz ▪ S-band for TT&C, 2250 MHz (notional) downlink - Use omnis: 2 kbps telemetry - Use HGA: 8 kbps telemetry - Use TDRSS for launch and LEO critical events: 1 kbps telemetry
Telemetry data rate(s), bps	▪ Nominal science data rate is 142 kbps. ▪ Peak science collection rates up to 6 hours at 1.3 Mbps during bright object observations at random intervals (assume once a month)
Spacecraft transmitting antenna type(s) and gain(s), dBi	▪ 0.5 m high gain dish antenna for Ka-band and S-band, 18.7 dBi ▪ Omnidirectional antennas (2) for S-band, -3 dBi
Spacecraft transmitter peak power, watts.	▪ Ka-band: 10 watts RF (use TWTAs) ▪ S-band: 5 watts RF to omnis or the HGA ▪ (95% rain availability is considered)
Downlink receiving antenna gain, dBi	▪ DSN 34 m antenna, ~73.5 dBi
Transmitting power amplifier output, watts	▪ Ka-band: 10 Watts RF ▪ S-band: 5 Watts RF
Uplink Information	**Value, Units**
Number of uplinks per day	▪ ~2 command load uplinks per week
Uplink frequency gand, GHz	▪ S-Band uplink at 2.0718 Ghz (notional), 200W to HGA, 2 kW to Omni
Telecommand data rate, bps	▪ DSN 34 to omnis: 1 kbps command ▪ DSN 34 to HGA: 2 kbps command ▪ TDRSS to omnis for launch and LEO critical events: 1 kbps command
Spacecraft receiving antenna type(s) and gain(s), dBi	▪ 0.5 m high gain dish antenna for S-band, 18.7 dBi ▪ Omnidirectional antennas for S-band, -3 dBi

39. TOTAL MISSION COST FUNDING PROFILE

Question: Total Mission Cost Funding Profile Template.

RESPONSE

The overall mission funding requirement for Con-X is provided in Table 39-1. The total mission cost estimate for all phases is $2, 162M in real year dollars ($1,739M fixed year FY07) including prior year funding of $51M. The cost to complete is $2,111M real year ($1,688M in fixed year dollars). Costs by fiscal year are also provided in real year dollars. An inflation rate of 3.1% per year has been assumed.

Table 39-1 provides costs broken down into elements as defined in the BEPAC Request For Information (RFI). In addition to the elements defined in the RFI, the Con-X budget also includes separate line items for Project Management, Systems Engineering, Safety and Mission Assurance, and Technology Development. Separate lines are shown for the Flight Mirror Assembly as well as for each of the instruments: the X-ray Microcalorimeter Spectrometer (XMS), the X-ray Grating Spectrometer (XGS) and the Hard X-ray Telescope (HXT). The contents of each element are defined in Appendix D.

39.1 Basis of Cost Estimate

The majority of the cost estimates are based on grass roots estimates and supported by vendor estimates, where appropriate. Grass roots and parametric cost modeling (PRICE-H) have been performed for the spacecraft, FMA and instruments. The PRICE-H modeling provided very good agreement with the grass roots. Atlas V 551 launch vehicle cost estimates were provided by Kennedy Space Center (KSC). Project management, Systems Engineering, Safety and Mission Assurance, and Mission Integration and Test were generated by grass roots and bases on substantial GSFC experience on similar missions. Reserves are included, using a percentage formula, based on experience with similar space flight missions (see also section 39.2 below.) Science, Mission Operations and Data Analysis costs have been generated by grass roots, using *Chandra* and other heritage mission experience as a basis. Budget for Education and Outreach is allocated at an overall level of 0.4% of the total mission cost.

39.1 Budget Reserves

The funding profile includes cost reserves at a level of 17% for Phase A, 25% for Phase B, 30% for Phase C/D (exclusive of launch vehicle) and 5% for Phase E. The reserves are currently without lien and are held at the Project Management level for distribution as required.

39.2 Budget Phasing

Of the total cost through phase C/D (in fixed year ’07 dollars, exclusive of launch vehicle), ~11% is planned through Phase A (including prior costs), ~23% through Phase B and ~49% through mission CDR.

Figure 39-1. Total Mission Cost Funding Profile

(FY Costs[1] Real Year Dollars, Totals in Real Year and 2007 Dollars)

$M (RY)	Prior	FY07	FY08	FY09	FY10	FY11	FY12	FY13	FY14	FY15	FY16	FY17	FY18	FY19	FY20	FY21	FY22	Total Real Year	Total FY07
Concept Study	20.1	3.0	6.8	21.9														51.9	50.9
Project Management*					5.2	6.1	7.3	6.8	7.1	6.9	6.3	3.7						49.4	40.7
Systems Engineering*					5.9	7.0	7.4	7.6	7.5	7.2	6.4	3.2						52.1	43.1
Safety & Mission Assurance*					2.8	3.4	3.6	3.7	3.8	3.6	3.5	2.1						26.4	21.7
Technology Development*	30.9	3.2	7.8	13.1	7.3													62.3	60.6
Science					6.6	7.8	9.3	10.8	14.7	19.8	19.6	21.7						110.4	88.3
Flight Mirror Assembly*					14.3	37.1	38.7	40.8	40.4	15.3	0.9							187.5	158.4
XMS (Instrument)				3.7	16.0	18.1	33.0	41.6	32.7	25.5								170.6	143.4
XGS (Instrument)				1.7	13.0	15.1	19.2	17.9	14.8	4.9								86.6	74.0
HXT (instrument)				1.0	5.8	7.3	8.7	7.7	4.2	1.5								36.1	31.1
Spacecraft					5.3	37.1	65.1	59.8	49.7	17.7								234.7	197.4
Ground Data System Dev					0.6	0.8	3.6	4.5	7.1	11.9	12.8	13.3						54.6	42.7
MSI&T[2]					0.0	0.0	1.4	2.2	4.2	17.3	28.8	18.0						71.8	55.1
Launch services					0.0	1.0	1.0	1.9	40.6	81.8	97.5	53.9						277.6	213.9
MO&DA[3]					0.1	0.1	0.1	0.2	0.3	0.3	3.7	8.7	70.4	71.7	71.0	65.4	50.6	342.7	232.6
EPO					0.4	0.6	0.6	0.6	0.6	0.6	0.7	0.8	0.8	0.9	0.9	0.9	0.9	9.4	7.0
Reserves	0.0	0.0	1.5	8.3	20.8	35.1	59.4	61.3	56.1	39.7	24.8	14.3	3.6	3.6	3.6	3.3	2.6	338.0	278.4
TOTAL	**51.0**	**6.2**	**16.1**	**49.7**	**104.1**	**176.7**	**258.5**	**267.3**	**283.6**	**254.0**	**204.9**	**139.9**	**74.8**	**76.2**	**75.4**	**69.6**	**54.1**	**2162.1**	**1739.3**

1 Costs should include all costs including any fee

2 MSI&T - Mission System Integration and Test and preparation for operations

3 MO&DA - Mission Operations and Data Analysis

** "Other" cost elements, in addition to those specfically defined in Question 39 of the BEPAC RFI*

APPENDIX A – NUMBERED LIST OF QUESTIONS

Numbered List of Questions Mapped to RFI	
Science and Instrumentation	
1	Describe the scientific objectives and the measurements required to fulfill these objectives.
2	Describe the technical implementation you have selected, and how it performs the required measurements.
3	Of the required measurements, which are the most demanding? Why?
4	Present the performance requirements (e.g. spatial and spectral resolution, sensitivity, timing accuracy) and their relation to the science measurements.
5	Describe the proposed science instrumentation, and briefly state the rationale for its selection.
6	For each performance requirement, present as quantitatively as possible the sensitivity of your science goals to achieving the requirement. For example, if you fail to meet a key requirement, what will the impact be on achievement of your science objectives?
7	Indicate the technical maturity level of the major elements of the proposed instrumentation, along with the rationale for the assessment (i.e. examples of flight heritage, existence of breadboards, prototypes, etc)
8	Briefly describe the overall complexity level of instrument operations, and the data type (e.g. bits, images) and estimate of the total volume returned.
9	If you have identified any descope options that could provide significant cost savings, describe them, and at what level they put performance requirements and associated science objectives at risk.
10	In the area of science and instrumentation, what are the three primary technical issues or risks?
11	Fill in entries in the Instrument Table to the extent possible. If you have allocated contingency please include as indicated, if not, provide just the current best estimate (CBE).
Science and Instrumentation (Optional)	
12	For the science instrumentation, describe any concept, feasibility, or definition studies already performed (to respond you may provide copies of concept study reports, technology implementation plans, etc).
13	For instrument operations, provide a functional description of operational modes, and ground and on-orbit calibration schemes.
14	Describe the level of complexity associated with analyzing the data to achieve the scientific objectives of the investigation.
15	Provide an instrument development schedule if available.
16	Provide a schedule and plans for addressing any required technology developments, and the associated risks.
17	Describe the complexity of the instrument flight software, including estimate of the number of lines of code.
18	Compare the scientific reach of your mission with that of other planned space and ground-based missions.
Mission Design	
19	Provide a brief descriptive overview of the mission design (launch, orbit, pointing strategy) and how it achieves the science requirements (e.g. if you need to cover the entire sky, how is it achieved?)
20	Provide entries in the mission design table to the extent possible. Those entries in italics are optional. For mass and power, provide contingency if it has been allocated, if not – provide just your current best estimate (CBE). To calculate margin, take the difference between the maximum possible value (e.g. launch vehicle capability) and the maximum expected value (CBE plus contingency).
21	Provide diagrams or drawings (if you have them) showing the observatory (payload and s/c) with the components labeled and a descriptive caption. If you have a diagram of the observatory in the launch vehicle fairing indicating clearance, please provide it.
22	Overall (including science, mission, instrument and S/C), what are the three primary risks?
Mission Design (Optional)	
23	If you have investigated a range of possible launch options, describe them, as well as the range of acceptable orbit parameters.
24	If you have identified key mission tradeoffs and options to be investigated describe them.

Numbered List of Questions Mapped to RFI	
Spacecraft Implementation	
25	Describe the spacecraft characteristics and requirements. Include, if available, a preliminary description of the spacecraft design and a summary of the estimated performance of the spacecraft.
26	Provide an overall assessment of the technical maturity of the subsystems and critical components. In particular, identify any required new technologies or developments or open implementation issues.
27	What are the three greatest risks with the S/C?
Spacecraft Implementation (Optional)	
28	If you have required new S/C technologies, developments or open issues and you have identified plans to address them, please describe (to answer you may provide technology implementation plan reports or concept study reports).
29	Describe subsystem characteristics and requirements to the extent possible. Such characteristics include: mass, volume, and power; pointing knowledge and accuracy; data rates; and a summary of margins.
30	Describe the flight heritage of the spacecraft and its subsystems. Indicate items that are to be developed, as well as any existing instrumentation or design/flight heritage. Discuss the steps needed for space qualification.
31	Address to the extent possible the accommodation of the science instruments by the spacecraft. In particular, identify any challenging or non-standard requirements (i.e. Jitter/momentum considerations, thermal environment/temperature limits etc).
32	Define the technology readiness level of critical S/C items along with a rationale for the assigned rating.
33	Provide a preliminary schedule for the spacecraft development.
34	Spacecraft Characteristics Table (Optional – fill out any known entries if you have selected an implementation.)
Mission Operations	
35	Provide a brief description of mission operations, aimed at communicating the overall complexity of the ground operations (frequency of contacts, reorientations, complexity of mission planning, etc). Analogies with currently operating or recent missions are helpful.
36	Identify any unusual constraints or special communications, tracking, or near real-time ground support requirements.
37	Identify any unusual or especially challenging operational constraints (i.e. viewing or pointing requirements).
38	Mission Operations and Ground Data Systems Table (Optional – provide only if you have selected a S/C and operations implementation)
39	Total Mission Cost Funding Profile Template

APPENDIX B – LIST OF ACRONYMS AND ABBREVIATIONS

Å..... Angstrom
AANM ..... New Millennium Survey
ACIS ..... AXAF CCD Imaging Spectrometer
ACS ..... Attitude Control System
ACTDP..... Advanced Cryocooler Technology Development Program
ADR ..... Adiabatic Demagnetization Refrigerator
AETD ..... Applied Engineering Technology Directorate
AGN ..... Active Galactic Nucleus
AH..... Ampere-hour
Al..... Aluminum
ALMA ..... Atacama Large Millimeter Array
AO..... Announcement of Opportunity
arcmin ..... arc minutes
arcsec ..... arc seconds
ASCA ..... Advanced Satellite for Cosmology and Astrophysics
Au..... Gold
BEPAC..... NRC Beyond Einstein Program Assessment Committee
BH..... Black Hole
BHFP ..... Black Hole Finder Probe
BI..... Back-Illuminated
Bi..... Bismuth
bps ..... bits per second
C ..... Carbon
C ..... Celsius
C&DH..... Command and Data Handling
CAA ..... Committee on Astronomy & Astrophysics
CADR..... Continuous Adiabatic Demagnetization Refrigerator
CalDB ..... Calibration Database
CBE ..... Current Best Estimate
cc ..... cubic centimeters
CCD ..... Charge-Coupled Device
CCSDS ..... Consultative Committee for Space Data Systems
Cd ..... Cadmium
CDA ..... Centroid Detector Assembly
CdZnTe..... Cadmium Zinc Telluride
ChIPS ..... Chandra Imaging and Plotting System
CIAO ..... Chandra Interactive Analysis of Observations
CIT ..... California Institute of Technology
cm ..... centimeter
CP/CM ..... Center of Pressure/Center of Mass
cps ..... counts per second
CPU ..... Central Processing Unit
Cs..... Cesium
CTE..... Coefficient of Thermal Expansion
CTI ..... Charge Transfer in Efficiency
cts ..... counts
Cu ..... Copper
CXC ..... Chandra X-ray Center
CXSOC ..... Constellation-X Science and Operations Center
C_t..... Critical Temperature
CZT ..... Cadmium Zinc Telluride
DC..... Direct Current
DE..... Dark Energy
DETF ..... Dark Energy Task Force
DM ..... Dark Matter
DOF ..... Degree-of-Freedom
DSN ..... Deep-Space Network
E..... Energy
EELV..... Evolved Expendable Launch Vehicle
EEPROM ..... Electronically Erasable Programmable Read-Only Memory
EGSE..... Electrical Ground Support Equipment
ELV ..... Expendable Launch Vehicle
EMI/EMC..... Electromagnetic Interference/Compatibility
EOL..... End of Life
EOS ..... Earth Observing System
ESA..... European Space Agency
ETU..... Engineering Test Unit
EU ..... Engineering Unit
eV..... electron Volts
Fe..... Iron
FFT ..... Fast Fourier Transform
FITS ..... Flexible Image Transport System
FMA ..... Flight Mirror Assembly
FOM..... Figure of Merit
FOV..... Field of View
FPC..... Focal Plane Camera
FPM ..... Focal Plane Module
FRR..... Flight Readiness Review
FSW..... Flight Software
FY ..... Fiscal Year
G ..... Gravitational Constant
Gbit ..... Gibabit
Gbytes..... Gigabytes
Ge ..... Germanium
gm ..... gram
GMST..... Greenwich Mean Sidereal Time
GN&C..... Guidance, Navigation & Control
GR..... General Relativity
GS..... Ground System
GSE ..... Ground Support Equipment
GSFC..... Goddard Space Flight Center
GUI..... Graphical User Interface
H ..... hyperbolic
H/K..... Housekeeping

He ..... Helium
HEFT ..... High Energy Focusing Telescope
HEO ..... High Earth Orbit
HERO ..... High Energy Replicated Optics
HETE ..... High Energy Transient Experiment
HETG(S) ..... High Energy Transmission Grating (Spectrometer)
HEW ..... Half Energy Width
HGA ..... High Gain Antenna
HPB ..... High-Pressure Bridgeman
HPD ..... Half Power Diameter
HQ..... Headquarters
HRC ..... High Resolution Camera
HV..... High Voltage
HXT..... Hard X-ray Telescope
Hz..... Hertz
I ..... Iodine
I&T ..... Integration and Test
I/F ..... Interface
ID ..... Inner Diameter
IMDC..... Integrated Mission Design Center
InFOCμS..... International Focusing Optics Collaboration for μCrab Sensitivity
IR ..... Infrared
IRU..... Inertial Reference Unit
ISS ..... International Space Station
JDEM ..... Joint Dark Energy Mission
JWST ..... James Webb Space Telescope
J/T ..... Joule/Thompson
K..... Kelvin
kbps ..... kilobits per second
kByte..... Kilobyte
keV..... Kilo Electron Volt
kg ..... Kilogram
kHz..... KiloHertz
KOH ..... Potassium Hydroxide
KSC ..... Kennedy Space Center
ksec ..... kilosecond
LCC..... Life Cycle Cost
LEO..... Low Earth Orbit
LETG(S)..... Low Energy Transmission Grating (spectrometer)
LISA ..... Laser Interferometer Space Antenna
LL ..... Lincoln Labs
LLNL ..... Lawrence Livermore National Labs
LRF ..... Line Response Function
LRR..... Launch Readiness Review
LST ..... Large Survey Telescope
LV..... Launch Vehicle
LV..... Low Voltage
LVPC ..... Low Voltage Power Converter
LVPS..... Low Voltage Power Supply
LZP ..... Level Zero Processing
m..... meter
m/s ..... meters per second
MBE ..... Molecular Beam Epitaxy
MHz..... Megahertz
MIT..... Massachusetts Institute of Technology
mK..... milliKelvin
MLI ..... Multilayer Insulation
mm ..... millimeter
Mo ..... Molybednium
MO&DA..... Mission Operations and Data Analysis
MOC..... Mission Operations Center
ms ..... millisecond
MSE ..... Mission Systems Engineer
MSFC..... Marshall Space Flight Center
MUX..... Multiplexer
mW..... milliWatt
N ..... Neutron
NASA ..... National Aeronautics and Space Administration
Nb ..... Niobium
NeXT..... Non-thermal Energy eXploration Telescope
NIST..... National Institute of Standards and Technology
nm ..... nanometers
NRAO..... National Radio AstronomyObservatory
NS ..... Neutron Star
NSF..... National Science Foundation
NTO ..... Nitrogen tetroxide (or dinitrogen tetroxide), rocket fuel
OAP ..... Optical Alignment Pathfinder
OB..... Optical Bench
OBC ..... On-Board Computer
OCC/SOC ..... Operations Control Center/Single Operations Center
OD..... Orbit Determination
OD..... Outside Diameter
ODRM..... Observation Design Reference Mission
OGS..... Objective Grating Spectrometer
OS..... Operating System
OSS ..... Office of Space Science
OSSMA..... Office of Systems Safety and Mission Assurance
PHA..... Pulse Height Amplitude
PMD..... Propellant Management Device
PoST ..... Position Sensitive TES
PSE..... Power Supply Electronics
PSF ..... Point Spread Function
psia ..... pounds per square inch, absolute
QPO..... Quasi-Periodic Oscillation
RF ..... Radio Frequency
RFI ..... Request for Information
RGS ..... Reflection Grating Spectrometer
RMS..... Root Mean Square
ROM..... Rough Order of Magnitude
ROSAT..... Roentgen-Satellite

RSDO ..... Rapid Spacecraft Development Office
RXTE ..... Rossi X-ray Timing Explore
SAO ..... Smithsonian Astrophysical Observatory
S/A ..... Solar Array
SBIR ..... Small Business Innovative Research
S/C ..... Spacecraft
SDO ..... Solar Dynamics Observatory
SDRAM ..... Synchronous Dynamic Random Access Memory
sec ..... second
SEP ..... Science Enhancement Package
Si ..... Silicon
SMBH ..... SuperMassive Black Hole
Sn ..... Tin
SNL ..... Space Nanotechnology Laboratory
SPT ..... South Pole Telescope
SQUID ..... Superconducting Quantum Interference Device
SXT ..... Spectroscopy X-ray Telescope
Ta ..... Tantalum
TB ..... Thermal Balance
TBD ..... To Be Determined
TBR ..... To Be Resolved
Tbyte ..... Terrabyte
TCP/IP ..... Transmission Control Protocol/ Internet Protocol
TDRSS ..... Tracking and Data Relay Satellite System
Te ..... Tellurium
TES ..... Transition-Edge Spectrometer
Ti ..... Titanium
TLM ..... Telemetry
TLRD ..... Top-Level Requirements
TM ..... Telescope Module
TOO ..... Target of Opportunity
TPF ..... Terrestrial Planet Finder
TRIP ..... Technology Readiness and Implementation Plan
TRL ..... Technology Readiness Level
TT&C ..... Tracking, Telemetry and Command
TV ..... Thermal Vacuum
TWTA ..... travelling wave tube amplifiers
μsec ..... microsecond
μm ..... micrometer
UTC ..... Universal Time Coordinated
ULX ..... UltraLuminous X-ray source
VLT ..... Very Large Telescope
W ..... Watt
WHIM ..... Warm-Hot Intergalactic Medium
XEUS ..... X-ray Evolving Universe Spectroscopy Mission
XGS ..... X-ray Grating Spectrometer
XIS ..... X-ray Imaging Spectrometer (on ..... Japanese Mission Suzaku)
XMM ..... X-ray Multi-Mirror Mission
XMS ..... X-ray Microcalorimeter Spectrometer
z ..... red shift
Zn ..... Zinc
ZOC ..... Zero Order Camera

APPENDIX C – RISK CONVENTIONS

The conventions defined in Tables C-1 and C-2 are used for risk ratings assigned in responses to Questions 10, 22 and 27. This convention is being standardized at GSFC.

Table C-1. Risk Consequence Categories

Consequence Categories					
Risk Type	**1 Very Low**	**2 Low**	**3 Moderate**	**4 High**	**5 Very High**
Safety	Negligible or No impact.	Could cause the need for only minor first aid treatment .	May cause minor injury or occupational illness or minor property damage.	May cause severe injury or occupational illness or major property damage.	May cause death or permanently disabling injury or destruction of property.
Technical	No impact to full mission success criteria	Minor impact to full mission success criteria	Moderate impact to full mission success criteria. Minimum mission success criteria is achievable with margin	Major impact to full mission success criteria. Minimum mission success criteria is achievable	Minimum mission success criteria is not achievable
Schedule	Negligible or no schedule impact	Minor impact to schedule milestones; accommodates within reserves; no impact to critical path	Impact to schedule milestones; accommodates within reserves; moderate impact to critical path	Major impact to schedule milestones; major impact to critical path	Cannot meet schedule and program milestones
Cost	<2% increase over allocated and negligible impact on reserve	Between 2% and 5% increase over allocated and can handle with reserve	Between 5% and 7% increase over allocated and can not handle with reserve	Between 7% and 10% increase over allocated, and/or exceeds proper reserves	>10% increase over allocated, and/or can't handle with reserves

Table C-2. Risk Likelihood Categories

Likelihood Bins	**Safety** (Likelihood of safety event occurrences)	**Technical** (Estimated Likelihood of not meeting mission technical performance requirements)	**Cost/Schedule** (Estimated Likelihood of not meeting allocated Cost/Schedule requirement or margin)
5 Very High	($P_S > 10^{-1}$)	($P_T > 50\%$)	($P_{CS} > 75\%$)
4 High	($10^{-2} < P_S < 10^{-1}$)	($25\% < P_T < 50\%$)	($50\% < P_{CS} \leq 75\%$)
3 Moderate	($10^{-3} < P_S < 10^{-2}$)	($15\% < P_T < 25\%$)	($25\% < P_{CS} \leq 50\%$)
2 Low	($10^{-6} < P_S < 10^{-3}$)	($2\% < P_T < 15\%$)	($10\% < P_{CS} \leq 25\%$)
1 Very Low	($P_S < 10^{-6}$)	($0.1\% < P_T < 2\%$)	($P_{CS} \leq 10\%$)

APPENDIX D – DEFINITION OF COST ELEMENTS FOR TABLE 39-1

The costs provided in Table 39-1 are grouped as defined in the BEPAC Request For Information (RFI). Additional elements have been added where necessary (see Table 39-1). The contents of each element in the table are defined as follows:

Concept Study: Includes all pre-formulation and formulation studies, including industry phase A studies for the observatory and flight mirror assembly, and all associated management, science support, etc. This does not include technology development and reserves as well as funding for the instruments and Flight Mirror Assembly (FMA) which are awarded near the end of Phase A

Project Management: The business and administrative planning, organizing, directing, coordinating, controlling, and approval processes used to accomplish overall Project objectives, which are not associated with specific hardware or software elements. This element includes project reviews and documentation.

Systems Engineering: The technical and management efforts of directing and controlling an integrated engineering effort for the project. This element includes the efforts to define the observatory and ground system, conducting trade studies; the integrated planning and control of the technical program efforts of design engineering, software engineering, specialty engineering, system architecture development, and integrated test planning, system requirements writing, configuration control, technical oversight, control and monitoring of the technical program, and risk management activities.

Safety and Mission Assurance: The technical and management efforts of directing and controlling the safety and mission assurance elements of the project. This element includes design, development, safety assessment, review, and verification of practices and procedures and mission success criteria intended to assure that the delivered spacecraft, ground systems, mission operations, and payloads meet performance requirements and function for their intended lifetimes. This element does not include mission and product assurance efforts at partners/ subcontractors other than a review/oversight function, and the direct costs of environmental testing. Product assurance efforts should be distributed to each separate product/deliverable WBS element.

Technology Development: This element includes the leading, managing, and performing technology demonstration for the Project. This element does not include hardware and software for flight hardware. This element does not include instrument developmental models, such as prototypes or engineering units that occur after award of instrument contracts.

Science: This element includes the managing, directing, and controlling of the science investigation aspects of the Project including the Project Scientist and science team members. Responsibilities include defining the science requirements; ensuring the integration of these requirements with the flight system; ground systems, mission operations; providing the algorithms for data processing and analyses. All science activities that occur beyond on-orbit commissioning of the observatory are included in the MO&DA element.

Flight Mirror Assembly (FMA): This includes leading, managing, and implementing the FMA hardware. This element also includes all design, development, production, assembly, test efforts and associated GSE to deliver the completed system for integration with the spacecraft.

X-ray Microcalorimeter Spectrometer (XMS): This includes leading, managing, and implementing the XMS hardware and software. This element also includes all design, development, production, assembly, test efforts and associated GSE to deliver the completed system for integration with the spacecraft.

X-ray Grating Spectrometer (XGS): This includes leading, managing, and implementing the XGS hardware and software. This element also includes all design, development, production, assembly, test efforts and associated GSE to deliver the completed system for integration with the spacecraft.

Hard X-ray Telescope (HXT): This includes leading, managing, and implementing the HXT hardware and software. This element also includes all design, development, production, assembly, test efforts and associated GSE to deliver the completed system for integration with the spacecraft.

Spacecraft: The spacecraft that serves as the platform for carrying Flight Mirror Assembly (FMA) and instrument. It includes the following subsystems as appropriate: Power, Command & Data Handling, Telecommunications, Structure and Mechanical, Thermal, Propulsion, Guidance Navigation and Control, Wiring Harness, and Flight Software. This element also includes all design, development, production, assembly, test efforts and associated GSE to deliver the completed spacecraft for integration with the payload.

Ground Data System Development: The complex of equipment, hardware, software, networks, and mission-unique facilities required to conduct mission operations of the spacecraft and payloads. This complex includes the computers, communications, operating systems, and networking equipment needed to interconnect and host the Mission Operations software. This element includes the design, development, implementation, integration, test and the associated support equipment of the ground system, including the hardware and software needed for processing, archiving and distributing telemetry and radiometric data and for commanding the spacecraft. Also includes ground hardware and software associated with science data processing.

Mission Systems Integration and Testing (and prep for ops): This element includes the hardware, software, procedures and project-owned facilities required to perform the integration and testing of the project's systems, payloads, spacecraft, launch vehicle, ground system, and mission operations.

Launch Vehicle / Services: The management and implementation of activities required to place the spacecraft directly into its operational environment, or on a trajectory towards its intended target. This element includes launch vehicle; launch vehicle integration; launch operations; any other associated launch services and associated ground support equipment.

Mission Operations and Data Analysis: The management of the development and implementation of personnel, procedures, documentation and training required to conduct mission operations. This element includes tracking, commanding, receiving/processing telemetry, analyses of system status, trajectory analysis, orbit determination, maneuver analysis, target body orbit/ephemeris updates, logistics, and disposal of remaining mission resources at end-of-mission.

Education and Public Outreach: Provides for the education and public outreach (EPO) responsibilities of NASA's missions, projects, and programs in alignment with the Strategic plan for Education (Includes management and coordinated activities, formal education, informal education, public outreach, media support, and web site development).

Reserves: Unallocated budget held at the Project Management level.